ARS JOURNAL

A PUBLICATION OF THE AMERICAN ROCKET SOCIETY

FORMERLY JET PROPULSION

January 1959 Volume 29 Number 1

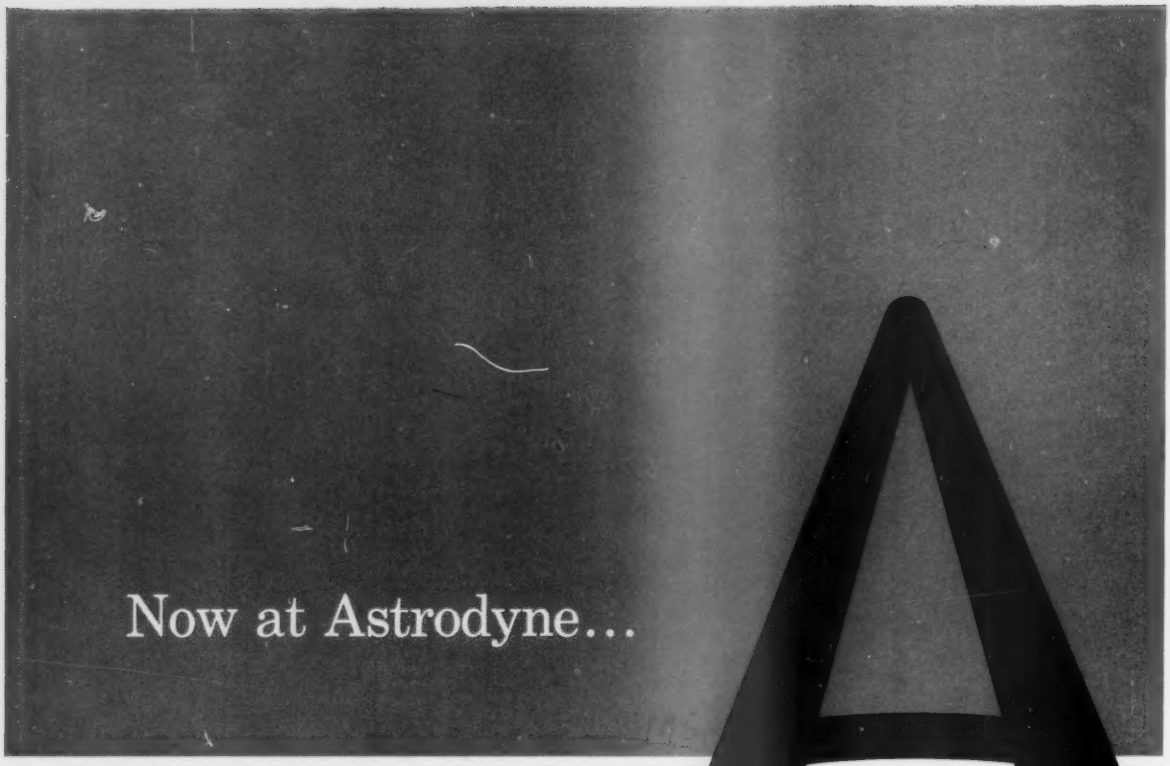

THE CAPABILITY TO DESIGN AND DEVELOP THE MOST ADVANCED SOLID PROPELLANT PROPULSION SYSTEMS

ASTRODYNE

Astrodyne has the capability and experience to design, develop, and manufacture complete solid propellant rocket propulsion systems, extruded and cast propellants, rocket motors and boosters, and gas generator charges for auxiliary power units.

Astrodyne built this capability by bringing together in one productive group an elite corps of scientists, engineers, and technicians. Men with experience in research, design, and manufacture of superior solid propellants for JATO units, gas generator charges, and large boosters were teamed with others who had pioneered in the development of the largest rocket engines in use today.

This experienced team now is at work on the development of large-scale cast propellant motors, the design of advanced lightweight rocket hardware, and the formulation and testing of high-energy propellants with optimum physical properties for ballistic missile applications.

Inquiries are welcomed on all phases of the solid propellant field—from preliminary design to quantity production.

ASTRODYNE, INC. McGREGOR, TEXAS

Able-One... a new apogee in scientific teamwork!

Preparation and execution of an undertaking such as the United States' IGY space probe demanded the participation and exceptional efforts of 52 scientific and industrial firms and the Armed Forces. The Advanced Research Projects Agency and the AFBMD assigned Space Technology Laboratories the responsibility for the project which was carried out under the overall direction of the National Aeronautics and Space Agency. One measure of this teamwork is the spectacular success of the Able-One flight into outer space.

Members of **STL's** senior technical staff will be available for personal interviews at the Institute's 27th Annual Meeting, Hotel Astor, New York City, January 26-29, 1959.

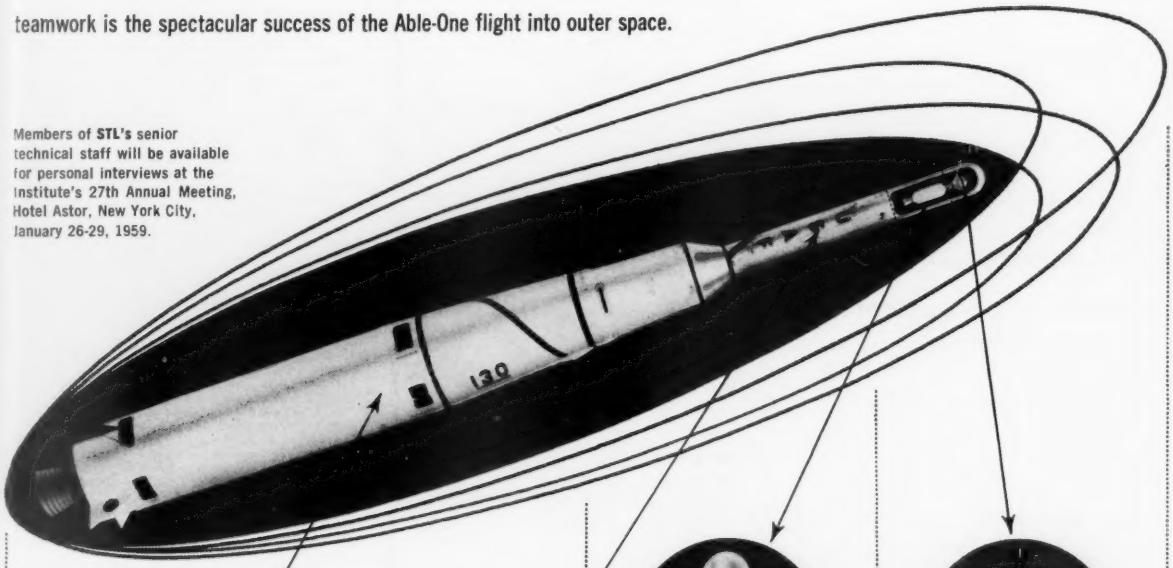

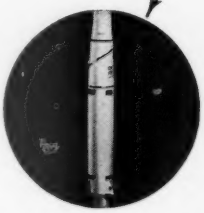

1st stage: Vehicle, Douglas Aircraft **Thor** IRBM; propulsion, Rocketdyne; airframe, control, electrical and instrumentation, Douglas Aircraft; assembly, integration, and checkout, Douglas Aircraft.

2nd stage: Propulsion system and tanks, Aerojet-General; control, electrical, instrumentation, accelerometer shutoff, and spin rocket systems, STL; assembly integration, and checkout, STL.

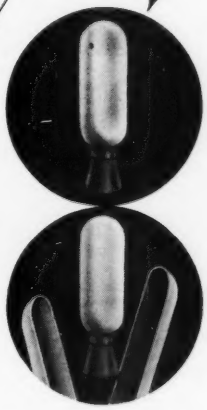

3rd stage: Rocket motor, U. S. Navy Bureau of Ordnance and Allegheny Ballistic Laboratory; structure and electrical, STL; assembly, integration, and checkout, STL; ground testing, USAF's Arnold Engineering Development Center.

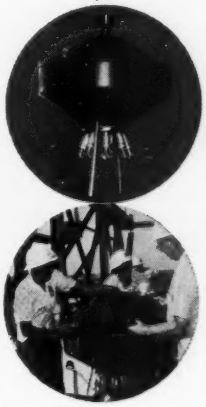

Payload: Design and production of **Pioneer**, the payload of the Able-One vehicle, was conducted by STL in addition to its overall technical direction and systems engineering responsibility of the Air Force Ballistic Missile Division project. This highly sophisticated package included a NOTS TV camera and transmitter and Thiokol rocket motor.

Inquiries concerning openings on our staff will be welcomed by

Space Technology Laboratories, Inc.
5730 Arbor Vitae Street, Los Angeles 45, California.

ARS JOURNAL

A PUBLICATION OF THE AMERICAN ROCKET SOCIETY

FORMERLY JET PROPULSION

Scope of ARS JOURNAL

This Journal is devoted to the advancement of astronautics through the dissemination of original papers disclosing new scientific knowledge and basic applications of such knowledge. The sciences of astronautics are understood here to embrace selected aspects of jet and rocket propulsion, space flight mechanics, high-speed aerodynamics, flight guidance, space communications, atmospheric and outer space physics, materials and structures, human engineering, overall system analysis, and possibly certain other scientific areas. The selection of papers to be printed will be governed by the pertinence of the topic to the field of astronautics, by the current or probable future significance of the research, and by the importance of distributing the information to the members of the Society and to the profession at large.

Information for Authors

Manuscripts must be as brief as the proper presentation of the ideas will allow. Exclusion of dispensable material and conciseness of expression will influence the Editors' acceptance of a manuscript. In terms of standard-size double-spaced typed pages, a typical maximum length is 22 pages of text (including equations), 1 page of references, 1 page of abstract and 12 illustrations. Fewer illustrations permit more text, and vice versa. Greater length will be acceptable only in exceptional cases.

Short manuscripts, not more than one quarter of the maximum length stated for full articles, may qualify for publication as Technical Notes or Technical Comments. They may be devoted to new developments requiring prompt disclosure or to comments on previously published papers. Such manuscripts are usually published within two months of the date of receipt.

Sponsored manuscripts are published occasionally as an ARS service to the industry. A manuscript that does not qualify for publication, according to the above-stated requirements as to subject, scope or length, but which nevertheless deserves widespread distribution among jet propulsion engineers, may be printed as an extra part of the Journal or as a special supplement, if the author or his sponsor will reimburse the Society for actual publication costs. Estimates are available on request. Acknowledgment of such financial sponsorship appears as a footnote on the first page of the article. Publication is prompt since such papers are not in the ordinary backlog.

Manuscripts must be double spaced on one side of paper only with wide margins to allow for instructions to printer. Include a 100 to 200 word abstract. State the authors' positions and affiliations in a footnote on the first page. Equations and symbols may be handwritten or typewritten; clarity for the printer is essential. Greek letters and unusual symbols should be identified in the margin. If handwritten, distinguish between capital and lower case letters, and indicate subscripts and superscripts. References are to be grouped at the end of the manuscript and are to be given as follows: For journal articles: authors first, then title, journal, volume, year, page numbers; for books: authors first, then title, publisher, city, edition and page or chapter numbers. Line drawings must be clear and sharp to make clear engravings. Use black ink on white paper or tracing cloth. Lettering should be large enough to be legible after reduction. Photographs should be glossy prints, not matte or semi-matte. Each illustration must have a legend; legends should be listed in order on a separate sheet.

Manuscripts must be accompanied by written assurance as to security clearance in the event the subject matter lies in a classified area or if the paper originates under government sponsorship. Full responsibility rests with the author.

Submit manuscripts in duplicate (original plus first carbon, with two sets of illustrations) to the Editor, Martin Summerfield, Professor of Aeronautical Engineering, Princeton University, Princeton, N. J. Preprints of papers presented at ARS national meetings are automatically considered for publication.

ARS JOURNAL is published monthly by the American Rocket Society, Inc. and the American Interplanetary Society at 20th & Northampton Sts., Easton, Pa., U. S. A. Editorial offices: 500 Fifth Ave., New York 36, N. Y. Price: $12.50 per year, $2.00 per single copy. Second-class mail privileges authorized at Easton, Pa. Notice of change of address should be sent to the Secretary, ARS, at least 30 days prior to publication. Opinions expressed herein are the authors and do not necessarily reflect the views of the Editors or of the Society.

(right) Part of giant capacitor bank used to fire "hotshot" tunnel. Bank is capable of 5 million kilowatt jolt.

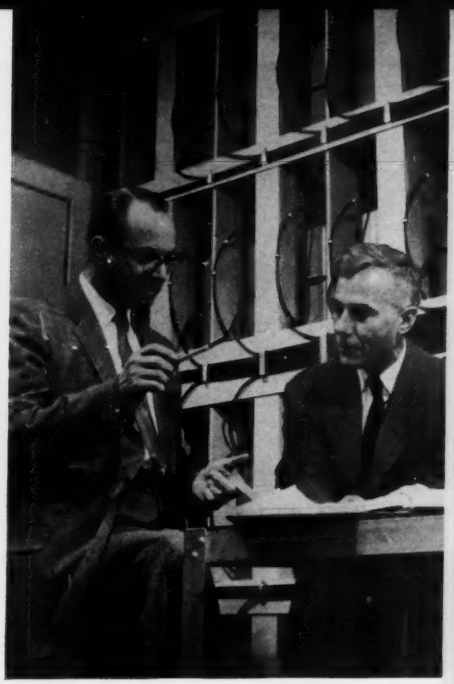

(above) Lockheed's "hotshot" tunnel – only one in private industry.

(right) Research and Development facilities in the Stanford Industrial Park at Palo Alto, California, provide the latest in technical equipment.

EXPANDING THE FRONTIERS OF SPACE TECHNOLOGY

Lockheed capabilities in thermodynamics and gas dynamics are unsurpassed in private industry. Basic work is being performed on problems relating to missiles and spacecraft under simulated conditions of upper atmosphere and outer space. Studies include: boundary layer flow and heat transfer; cooling and insulation; thermodynamic instrumentation for flight test; design of rocket motor controls and nozzle structures; re-entry thermal protection; materials specification; and thermal environments of electronic, mechanical and hydraulic equipment. Also under study are new methods and improved techniques of thin film thermometry, measurements of dissociation and combination of nitric oxide and high-speed shock wave flows.

Equipment includes the fastest wind tunnel in industry, fired by 20 million kilowatts; a hydromagnetic tube which produces velocities of over Mach 250 and temperatures approaching 500,000°K; a "hotshot" tunnel for shock wave, gas and heat studies, capable of velocities of 16,500 mph and temperatures above 12,000°F; and a ballistic range on which projectiles are fired at speeds up to 20,000 ft/sec.

Scientists and engineers of outstanding talent and inquiring mind are invited to join us in the nation's most interesting and challenging basic research programs. Write: Research and Development Staff, Dept. A-25, 962 W. El Camino Real, Sunnyvale, California, or 7701 Woodley Ave., Van Nuys, California. For the convenience of those living in the East and Midwest, offices are maintained at Suite 745, 405 Lexington Ave., New York 17, New York, and Suite 300, 840 No. Michigan Ave., Chicago 11, Illinois.

"The organization that contributed most in the past year to the advancement of the art of missiles and astronautics." NATIONAL MISSILE INDUSTRY CONFERENCE AWARD

Lockheed / MISSILE SYSTEMS DIVISION / SUNNYVALE, PALO ALTO, VAN NUYS, SANTA CRUZ, SANTA MARIA, CALIFORNIA CAPE CANAVERAL, FLORIDA ALAMOGORDO, NEW MEXICO

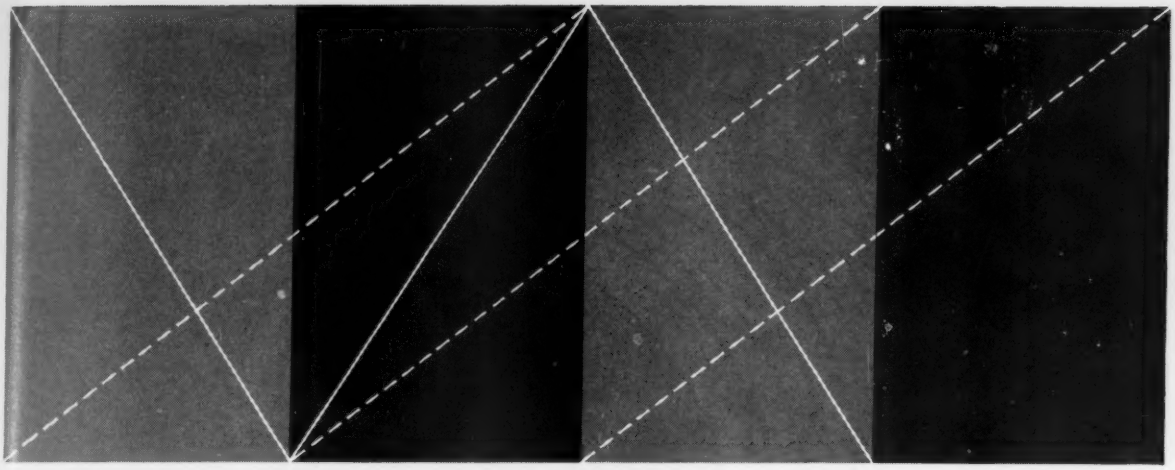

SCIENTISTS AND ENGINEERS

AVCO—PIONEER IN RE-ENTRY—IS EXPLORING NEW APPROACHES TO SPACE AND MISSILE TECHNOLOGY

Re-entry work on the Air Force *Titan* and *Minuteman* ICBMs—plus other new, advanced projects—creates an exciting atmosphere for both basic and applied work at Avco's Research and Advanced Development Division. Positions are open at all levels for creative scientists and engineers—both theoretical and experimental.

Unusual and challenging openings exist for:

Physicists
Metallurgists
Organic Analytical Chemists
Heat Transfer Engineers
Numerical Analysts
Physical Chemists
Ceramists
Aerodynamicists
Stress Analysts
Programmers and Applied Mathematicians

Mechanical Engineers—Components and Systems
Electrical and Electronic Engineers—Components and Systems
Operations Research Engineers
Specifications Engineers
Primary Laboratory Standards Engineers
Calibration Engineers
Statisticians
Project Staff and Program Planning Engineers

The Division's new suburban location provides an unusually attractive working environment outside of metropolitan Boston. The large, fully equipped, modern laboratory is in pleasant surroundings, yet close to Boston educational institutions and cultural events. Publications and professional development are encouraged, and the division offers a liberal educational assistance program for advanced study.

Avco

Research and Advanced Development division

Address all inquiries to:
Dr. R. W. Johnston,
Scientific and Technical Relations,
Avco Research and Advanced Development Division,
201 Lowell Street, Wilmington, Massachusetts

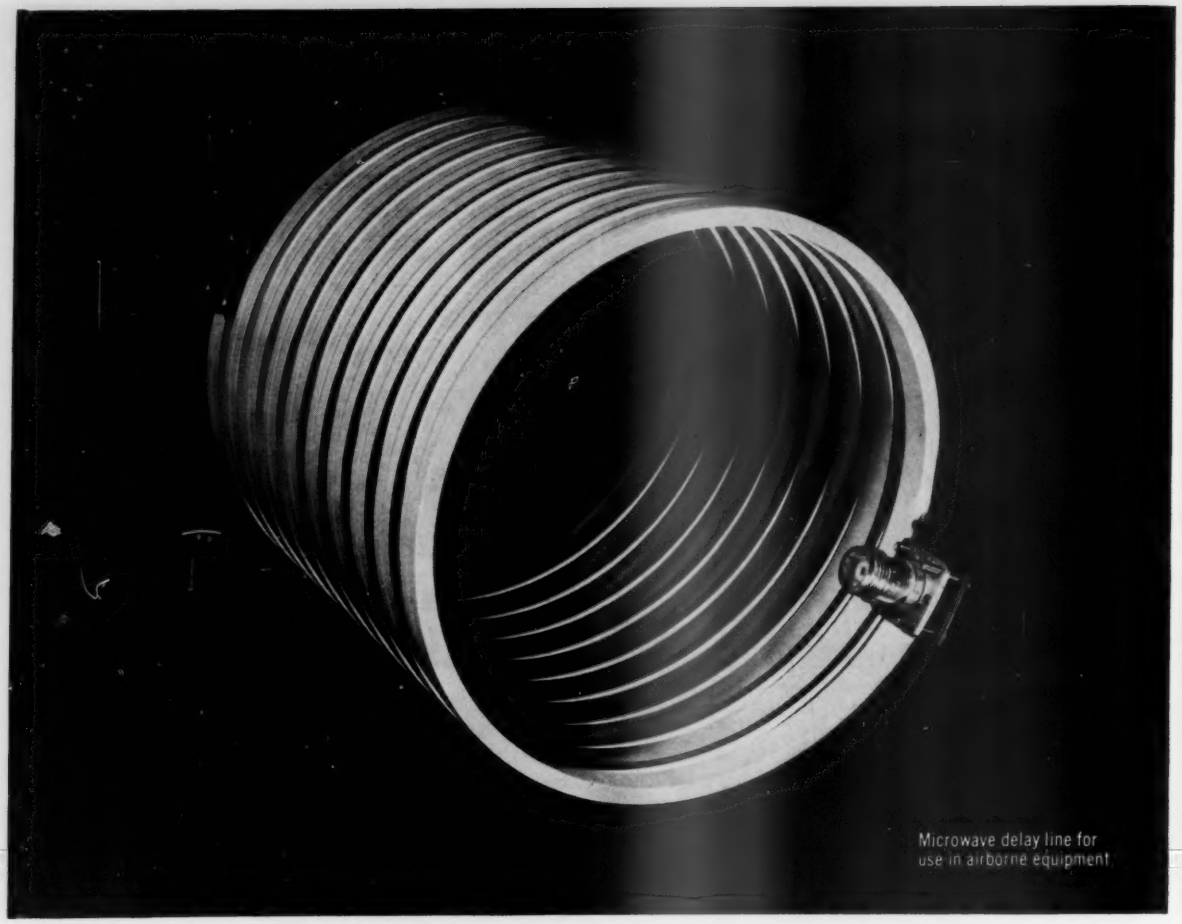

Microwave delay line for use in airborne equipment

MICROWAVE RESEARCH

The expanding role of electronic equipment in modern military operations has given high priority to microwave research. No field today offers greater challenge to the scientist and engineer.

In support of current electronic countermeasures programs and in anticipation of future systems requirements, Ramo-Wooldridge Division is engaged in microwave research to develop new techniques and to refine conventional components.

Research is under way at Ramo-Wooldridge for new methods and new designs to reduce substantially the over-all size, weight and complexity of electronic equipment for both airborne and ground-based uses.

For example, the low-loss delay line in the photograph above was designed, developed and manufactured by Ramo-Wooldridge for use in airborne equipment. Packaged for use in the system for which it was designed, this miniature ceramic unit weighs less than two pounds. It replaces a component which weighed more than twenty pounds and occupied more than five times as much volume.

Special opportunities exist for those with qualified experience in microwave research—in technique evaluation, component development, and design of such systems equipment—at Ramo-Wooldridge.

Engineers and scientists are invited to explore openings at Ramo-Wooldridge in:

- Electronic Reconnaissance and Countermeasure Systems
- Infrared Systems
- Analog and Digital Computers
- Air Navigation and Traffic Control
- Antisubmarine Warfare
- Electronic Language Translation
- Information Processing Systems
- Advanced Radio and Wireline Communications
- Missile Electronics Systems

RAMO-WOOLDRIDGE

P. O. BOX 90534, AIRPORT STATION • LOS ANGELES 45, CALIFORNIA

a division of ***Thompson Ramo Wooldridge Inc.***

Editorial

We Change Our Name

Starting with this issue, JET PROPULSION will be known by the simple title ARS JOURNAL. When the publishers of an established periodical decide to change its name, there must be a reason. We feel it is our obligation to explain this action to the 12,000 members of the American Rocket Society and to our readers and contributors all around the world.

Let it be understood at the outset that a change of name has some temporary disadvantages. There will undoubtedly be some confusion among our subscribers and members who may look for the familiar magazine in January and will not find it. Librarians will have to introduce the new name in their catalogue files and still keep alive the old name. Authors of articles in this and other magazines might make mistakes in their reference lists.

Why then did the ARS Board of Directors authorize the change? The answer is that it is part of the growth pattern of the American Rocket Society. The old name has outlived its usefulness: It no longer indicates properly the ever-broadening field of interest of the Society and of its Journal.

Your Society is an explosive phenomenon among technical organizations on the American scene. It is no longer the baby of 1200 members that it was in 1951; it is now a vigorous youth of 12,000 members and is growing at the impressive rate of 50 per cent per year. From 3 Sections in 1951, we have grown to 42 Sections, and more groups are asking for charters. Instead of a pocket-size quarterly magazine, our publishing program now provides each member with two full-size monthly magazines, and plans are being developed for further expansion of this program.

The most striking aspect of our growth, however, is the broad scope of our scientific interest. Not long ago, this Journal was known mainly for its coverage of rocket propulsion. When, a few years later, the Society found among its active members many engineers in the ramjet field and scientists concerned with fundamentals of propulsion that could not be identified solely with the rocket engine, the less restrictive name JET PROPULSION was adopted. But the Journal does not limit itself any longer to the propulsion field; it has for some time fully accepted the responsibility to serve the general field of astronautics.

A glance at the cover of this issue of ARS JOURNAL will show articles on guidance, attitude control, orbital mechanics, supersonic aerodynamics, high temperature materials and multistaging of rockets, in addition to the traditional subjects of propellants, combustion and rocket propulsion. In January 1958 we inaugurated a monthly series of survey articles by experts in various areas of astronautics, a series that has been highly successful as an attempt to weld together our membership. Through this series, a specialist in one field can learn something about the scientific advances that have been made in other fields. Survey articles have appeared on nuclear propulsion, rocket reliability, high strength materials, flight mechanics, aerodynamic heating, pressure and temperature instrumentation, and other topics.

As we continue this broadened program under the less restrictive name, we will be aided by the Society's new technical committees, 22 in all, which are staffed by persons of recognized high competence drawn from industry, government and universities. In addition, a small panel of editorial consultants is being formed to aid us in the selection of the most important papers to publish.

The new ARS JOURNAL will be faced with an important challenge. That challenge is to become a coherent balanced periodical in the entire area of astronautical science and not merely a collection of individual research articles. The editors' approach to this task will be through the publication of the most significant and the best written articles available. We will continue to rely on the many expert reviewers in laboratories and research centers around the country who have guided us in the past, to arrive at the proper decision on each submitted manuscript.

Martin Summerfield
Editor

Recent Advances in Boron Technology

RICHARD A. CARPENTER[1]

Midwest Research Institute
Kansas City, Mo.

The author has directed the boron fuels program at Midwest Research Institute under a subcontract to Callery Chemical Company for the past six years. He received a B.S. degree from the University of Missouri in 1948 and his M.A. in Chemistry in 1949. He has written several technical papers in the areas of boron chemistry, organic synthesis and high temperature reactions of hydrocarbons. Mr. Carpenter was Assistant Manager of the Chemistry and Chemical Engineering Division at Midwest Research Institute until recently. He is now Manager of the Washington office of the Callery Chemical Company.

TEN YEARS ago Pauling's General Chemistry text had nothing more interesting to report on boron chemistry than the familiar "borax bead" test. Today the school boy is quite aware, albeit from gasoline additive advertising, of the utility of the fifth element in the periodic table.

This rapid growth in our knowledge started early in World War II and was accelerated by various defense interests. The Signal Corps desired a new source of hydrogen for balloons, and sodium borohydride provided a compact, reliable generation system. The Atomic Energy Commission looked for volatile uranium compounds, and uranium borohydride seemed a likely possibility. The high thermal neutron cross section of boron was of importance to nuclear applications, but the extreme range of this value between the two isotopes (B^{10} - 4010 barns, B^{11} - 50 millibarns) made their separation necessary. This required studies of complexes, such as boron trifluoride etherate. Torpedo propulsion systems based on water reactive chemicals further intensified the work on alkali metal borohydrides.

Jet propulsion was also advancing rapidly in this same period. It was soon obvious that increased performance could be achieved by using fuels with greater heating values per unit weight. The heat of combustion for a chemical compound depends principally on its atomic composition, and, to a lesser extent, on energy contained in strained bonds. Of the light metals, boron has a high heat of combustion, is available in quantity and forms a wide variety of compounds with carbon and hydrogen (13).[2] Beginning in 1952, the Bureau of Aeronautics sponsored Project Zip to prepare boron compounds with high heats of combustion and physical properties similar to conventional hydrocarbon aircraft fuels. Callery Chemical Co. (a division of Mine Safety Appliances Co.) and Olin-Mathieson Chemical Corp. were designated prime contractors.

Project Zip required the development of practicable, economic syntheses of boron hydrides and their derivatives. Therefore, a broad fundamental program in boron chemistry was undertaken by the prime contractors and over 50 subcontractors at universities, research institutes and government laboratories. Many classes of compounds other than hydrides were studied, and the recent advances in boron technology have been largely due to this impetus.

A brief historical review of previous boron chemistry shows the roots of American interest dating to the appointment of Alfred Stock of Germany as the George Fisher Baker Non-Resident Lecturer in Chemistry at Cornell University in 1932. His book "Hydrides of Boron and Silicon" was a primary literature source up to about 1930 (69). A review article by Professor H. I. Schlesinger of the University of Chicago, the leader of the American work in this field, was published in 1942 (65). A useful source of general information is the series of articles in the "Encyclopedia of Chemical Technology" published in 1948 (36). An excellent treatment of the organic compounds of boron was prepared by Lappert in 1956 (42). Developments in the chemistry of diborane and borohydrides were covered by Schlesinger and Brown in 1953 (64). Complete coverage of the open literature from 1953 to date has been provided by the Current Literature Abstracts Bulletin (2) which comprises monthly reports compiled by the High Energy Fuels Division of Olin-Mathieson Chemical Corp. under contract with the U. S. Air Force. These are available to qualified laboratories. A comprehensive review of molecular addition compounds of boron was published in 1958 by Stone (71). Most recently, April 1958, a symposium was held, entitled "From Borax to Boranes" which presented new work on all phases of boron chemistry (48).

This paper primarily covers the period from January 1955 to August 1958. Unfortunately, some of the chemistry remains classified and thus is not included here, but the main investigative paths are well indicated, and future trends can be anticipated with some certainty. The bibliography is not claimed to be comprehensive, but will lead the interested reader to the principal workers in the field and to developments which the writer considers to be most significant, currently and in the immediate future.

The Chemistry of Boron

Ore Processing

Although boron is not abundant in the Earth's crust, geochemical processes have concentrated the element due to the volatility of boric acid in steam. The western coast of North America has several significant deposits both as ores and brines. Searles Lake, Calif., produces a crude borax, on fractional crystallization from partially evaporated brine. Refining yields $Na_2B_4O_7 \cdot 10H_2O$ and $Na_2B_4O_7 \cdot 5H_2O$, and anhydrous borax is produced at the fusion temperature. Boric acid is obtained by treating borax with sulfuric acid or carbon dioxide under high pressure. Boric oxide is the result of fusing and heating boric acid (9). Recently, open pit mining of 91 per cent borax has been started near Boron, Calif.

Anhydrous borax and boric oxide must be shipped in closed hopper cars because of deliquescence; hence, most large-scale processors, not located adjacent to the ores, receive the hydrated borax or boric acid. Calcium and other borates occur to a significant extent, but are not processed in large tonnages at present (74).

Received Nov. 28, 1958.

[1] Present address: Callery Chemical Co., 1346 Connecticut Ave. N. W., Washington 6, D. C. Member ARS.

[2] Numbers in parentheses indicate References at end of paper.

Boron Metal and Refractory Compounds

Boron metal is prepared by reducing boric oxide with magnesium, aluminum or sodium, by electrolysis of borates or boric oxide in molten salt electrolyte with a graphite anode, by decomposition of volatile hydrides on a hot wire, or by reduction of boron halides with hydrogen at high temperatures. High quality requires careful processing, but 99.999 per cent purity can be achieved. An amorphous powder is the usual product. Ninety-five per cent pure crystalline boron is produced by passing boron trichloride and hydrogen over electrically heated graphite rods (20). Boron is added to steel up to 1.5 per cent to increase hardenability and mechanical properties.

Boron metal may be fabricated by consolidation of the powder with unreactive bonding agents (lead, boric oxide, sulfur, cements) or with metals. Boron may be fused by induction heating but not by resistance heating. The metal may be evaporated by resistance heating, electron bombardment or radiation. Size reduction of boron is difficult because of its hardness, but it can be pulverized in a mortar and pestle made of boron carbide with the introduction of less than 1 per cent B_4C.

Boron burns rather slowly, 2 cm/min at 2000 C, in pure oxygen. At lower temperatures, the transport of B_2O_3 from the reaction zone is limiting, and at higher temperatures the collision rate of oxygen with the burning surface may be rate controlling (72). The extreme difficulty of obtaining complete combustion may be due to deposition of B_2O_3 on momentarily cool surfaces during ignition or convective conditions. The stability of borides as combustion products has been studied by Grosse (28).

Borides may find utility in thermoelectric power conversion. The Hall effect has been studied for transition metal borides (32). Boron forms p-type semiconductors, and, if ideally pure, would have a resistivity of 2×10^7 ohm-cm at room temperature. Boron greatly improves the conductivity of aluminum.

Borides produced by light metal reduction of B_2O_3 are lithium, sodium, potassium, beryllium, calcium and aluminum. Only calcium (CaB_6) and aluminum (AlB_{12} and AlB_2) give constant compositions (51). Magnesium boride may be hydrolyzed by strong base to yield borohydrides (KBH_4, $(CH_3)_4NBH_4$) directly (35). Magnesium is removed from magnesium boride by heating in a vacuum. Nickel boride is precipitated from borohydrides and nickel salts in organic solvents and used to coat steel. Zirconium and chromium boride cermets show promise in jet engine applications at 1800 F. Boron carbide reacts with metals in cermets (cobalt, chromium, iron, titanium and nickel) to form borides (12). The Borolites (e.g., Cr_2B + Cr−Mo alloy) show good characteristics in heat-shock resistance, oxidation resistance and stress-to-rupture strength through 2000 F.

Boron carbide (B_4C or $B_{12}C_3$ and other ratios) is a hard, stable, lightweight material useful as a reactor moderator, fuel and refractory. It is made from boric oxide and carbon. Treatment with chlorine or bromine yields the boron halide.

Boron nitride is made by pyrolysis of $BCl_3 \cdot NH_3$ or $B(OCH_3)_3 \cdot NH_3$. Articles useful to 1600 C may be molded at high temperature and pressure, and one modification of boron nitride ("borazon") is similar to diamond in hardness and stability (79).

Isotope Separation

Boron^{10} has a thermal neutron capture cross section of 4010 barns, while that of B^{11} is 50 millibarns. Natural boron contains about 19 per cent B^{10}, but the percentage varies as to origin. The low weight of the atoms and consequent large mass ratio of the isotopes makes separation occur fairly readily in geochemical processes. Mass spectrographic analyses are often in error, due to exchange between the volatile boron compound and the boron in glass apparatus.

A large-scale separation plant has been constructed by Hooker Electrochemical Co. It is based on the countercurrent distillation of a dissociable complex, as $BF_3 \cdot O(CH_3)_2$, in a 300-plate column. The boron trifluoride is liberated as $CaF_2 \cdot BF_3$ and converted to the metal (30,37). The price of amorphous B^{10} as metal is estimated at $57 per lb. A reactor using borax solution as moderator has been in operation for some time.

B^{10}-enriched BF_3 has been suggested as a reactor poison. Contained in a fusible vessel, it would rapidly diffuse through the reactor core if an excursion occurred. Control elements of enriched boron metal and thin coatings of the metal on steel as shielding are reported. High burnup of B^{10} to lithium and helium can be obtained. Boron carbide has been employed embedded in plastic sheets, rolled into aluminum (Boral), hot pressed, as a bonded block or as granular fill. Neutron counters employ enriched BF_3 gas.

Although present processes separate only B^{10} in high purity, B^{11} may have usage as a refractory material with low cross section in borides, boron carbide and boron nitride.

Boron compounds may be used for "neutron capture" tumor therapy in the brain. The alpha particle released on bombardment could kill a cell near a stable organoboron compound, which had been preferentially absorbed previously in the tumor tissue.

Borate Salts

The Group I and II metals form boric acid salts. These can be prepared in aqueous solution and precipitated by pH adjustment. Aluminum borates result from the addition of Al_2O_3 to a B_2O_3 melt. Sodium and potassium oxyfluoborates ($4NaF \cdot 5B_2O_3$) are prepared from the alkali fluoride and boric oxide. Sodium fluoborate is a by-product of diborane manufacture from NaH and BF_3 etherate, and its recycle to recover both sodium and fluorine values is rather difficult. Due partially to this fact, present diborane processes are based on other boron sources. Ammonium pentaborate is produced in good yields by treating borax with aqueous ammonium chloride. $(NH_4)_2B_{10}O_{16}$ may then be thermally decomposed to give boric oxide (81).

Sodium tetramethoxyborate, $NaB(OCH_3)_4$, is a by-product of sodium borohydride production. It may be converted to sodium methyl carbonate and methyl borate by carbon dioxide. Other tetra alkoxyborates are known.

Sodium perborate, formed from hydrogen peroxide and sodium metaborate, is used as a "dry bleach" for household laundering.

Boron-Oxygen-Carbon Compounds

The esters of boric acid $B(OR)_3$ are perhaps the single class of boron compounds studied most extensively in the past few years. The preparative methods include reaction of boric acid with alcohols and the azeotropic removal of the ester formed, the use of boric oxide as both the boron source and dehydrating agent, and the formation of a higher boiling ester from a lower one by alcoholysis. The rate of hydrolysis of esters depends on the steric hindrance of the nucleophilic attack of water on the central boron atom (68).

The most important ester is methyl borate, an intermediate to sodium borohydride and many other organoboron compounds. Its preparation is peculiar, in that methanol and methyl borate form an azeotrope which is the lowest boiling component in the system. Complete conversion of methanol and boric acid to methyl borate can be achieved on a continuous basis. The azeotrope is separated by solvent extraction and the methanol recycled. Methyl borate is the cheapest source of boron for organic reactions and will be widely exploited in the future.

Aryl borate esters may be converted to aryl borondichlorides with PCl_5 (50). Alcohols are dehydrated to olefins by

the pyrolysis of their borate esters. The esters are alkylating agents in the Friedel Crafts reaction.

The boroxines are six-membered rings of alternate boron and oxygen atoms. Trimethoxyboroxine is but one member in the system boric oxide-methyl borate. Syrupy liquids containing up to 2.5 mols B_2O_3 to 1 $B(OCH_3)_3$ may be obtained (14). Various boron substituted alkyl and alkoxy boroxines have been prepared. Reaction with chlorine or metal chlorides usually produces alkyl halides or alkyl borondichlorides (34). Substituted anilines react to link two boroxine rings through a B—N—B bond.

Mixed alkoxy boron halides are formed from the boron trihalide and alcohols but disproportionate readily. Dimethoxy chloroborane is produced by treating methyl borate with CCl_4, $SiCl_4$,PCl_3, $COCl_2$ or SO_2Cl_2. Boron peroxides, $Bu(OOR)_3$, are formed from boron halides and alkyl peroxides or by autoxidation of trialkyl boranes.

Mixed anhydrides of boric acid and fatty acids have been shown to have the structure $(RCOO)_2$ B—O—$B(OOCR)_2$ rather than $B(OOCR)_3$ probably due to steric hindrance (25).

Boron Halides

Boron halides, and particularly boron trichloride, are useful intermediates in boron chemistry. BCl_3 is produced by countercurrently contacting boric oxide with carbon and chlorine. The by-product phosgene is thus also used as a chlorinating agent. Carbon with $SiCl_4$, PCl_3 or SCl will also produce BCl_3 from boric oxide (56). Subchlorides B_2Cl_4 and B_4Cl_4 have been prepared recently, and diboron tetrachloride is the subject of intensive study as a precursor of organoboron compounds (73). Diboron tetrachloride reacts immediately with hydrogen at room temperature to yield $HBCl_3$, which disproportionates to diborane and boron trichloride.

Boron trifluoride is widely used as a catalyst in alkylations and isomerization of aromatic hydrocarbons. The boron trifluoride dinitrogen tetroxide complex is used as nitrating agent. Boron trichloride splits carboxylic acid esters to acylchloride and alkoxyborondichloride (24).

Reaction between diazomethane and boron trifluoride yields fluoromethylene borondifluoride (F_2BCH_2F) (27).

Boron-Nitrogen-Carbon Compounds

The electron deficiency of the boron atom makes possible the formation of strong coordination compounds with nitrogen containing molecules. The B—N bond generally is hydrolytically and thermally stable. Methyl borate or boron trichloride reacts with ammonia to give $BX_3 \cdot NH_3$, then splits out HX to BX_2-NH_2, BX=NH, and finally boron nitride.

Borazine (a six-member ring of alternate B and N atoms, $B_3H_3N_3H_3$) has been studied extensively since its discovery in 1926. Improved syntheses from $LiBH_4$ and NH_4Cl, alkylamine hydrochlorides and alkyl borondichlorides have led to the preparation of many B- and N-substituted derivatives.

The borazanes ($H_3B \cdot NR_3$) may be prepared by hydrogenating alkyl diboranes in the presence of tertiary amines (39). Ethylene diamine and diborane yield $BH_3 \cdot NH_2CH_2CH_2NH_2 \cdot BH_3$ which loses hydrogen to give solid polymers.

Pyridine and its homologs react readily with boric acid to form white, nonhygroscopic solids. Aniline and boric acid split out water to yield the "boranilide" $C_6H_5NHB(OH)_2$.

Amine boranes are becoming commercially available for the first time. Primary amine boranes ($RNH_2 \cdot BH_3$) tend to eliminate hydrogen. Burg and his co-workers have extensively studied the boron hydride derivatives of nitrogen and phosphorus compounds (12).

Dibutoxyboron chloride and diethylamine form dibutyl diethylaminoboronate $(C_4H_9O)_2BN(C_2H_5)_2$. The amino chloroboronite $C_4H_9(Cl)BN(C_2H_5)_2$ is formed similarly. These compounds are easily hydrolyzable liquids (23).

Polymers

Much hope for utility is expressed for inorganic polymers containing boron. The B—N bond is isoelectronic with the C—C bond, but analogs of polyolefins tend toward the monomeric state on methylation. A $[(CH_3)_2NBH_2]_n$ chain can exist if supported by an electron donor end group. The much more stable $(R_2PBH_2)_n$ system has resulted in moisture and oxygen resistant, resilient polymers. Pentaborane and trialkyl phosphines give resins which remain light colored and transparent to 500 C (11).

Another approach has involved the preparation of borate esters, in which the tendency for hydrolysis of the B—O bond is decreased by electron-rich atoms in the alkoxy radical. The diethanolamine ester of phenylboronic acid is hydrolytically stable and may be recrystallized from water (58). Glycol borates have been incorporated in polyurethanes and silicones, but moisture resistance has not been achieved. Organosilicon boranes, RB $[CH_2$ Si $(R)_2OSi(OR)_3]_2$ are reported (67).

An interesting possibility is the use of secondary amine borondichlorides which have a remarkable resistance to hydrolysis. The dimer of dimethylamine borondichloride is stable in moist air at 25 C. A four-membered ring of alternating B and N atoms is postulated (52). If piperazine and boron trichloride split out HCl and form a similar ring, a chain polymer is possible

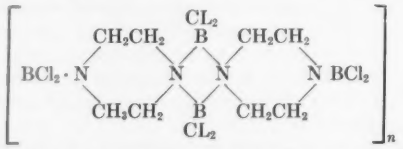

Effort is being directed toward forming linear polymers from B-substituted borazines (tri-β-chloro vinyl-B-borazine) (58). A yellow nonvolatile resin of empirical formula $BCl_3 \cdot 2CO$ has been formed by an 11,000-v silent discharge through a mixture of BCl_3 and CO (76).

Boric acid-glycol polymers do not resist hydrolysis. The B—O—Si linkage shows some promise for hydrolytic stability insofar as it has been investigated. Heating boric acid and dimethyldichlorosilane yields a colorless polymer which hardens in air (67). Boron trichloride and dialkylsiloxanes yield tris-(dialkylchlorosiloxy)-boranes, $B(OSiR_2Cl)_3$ (49).

Boron Hydrides

An excellent reference book, "Boron Hydrides and Related Compounds," has been assembled by the Callery Chemical Co. under the Bureau of Aeronautics' sponsorship (62). A similar review was published in 1955 by Stone (70).

The boron hydrides form two homologous series B_nH_{n+4} and B_nH_{n+6}. Polymeric hydrides of the formula $(BH_n)_x$ are produced as pyrolysis products of the lower hydrides. The hydrogen atoms in boron hydrides may be bonded to one boron, or may exist in a bridge structure

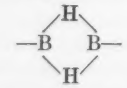

Since diborane is a precursor of nearly all the other hydrides, it has received the most attention recently. Major (47) and Adams (1) have reviewed methods of preparation of diborane.

The synthesis of diborane on a large scale is being accomplished by Callery Chemical Co. at Lawrence, Kas. and at Muskogee, Okla., and by Olin-Mathieson Chemical Corp. at Niagara Falls and at Model City, N. Y. Exact processes and conditions are still classified information. Approximately 90 per cent of present facility and production costs of high energy fuels is in the preparation of diborane.

An intriguing possibility is the formation of diborane from boron halides and nascent hydrogen (26). An interesting compound (dimethoxyborane, $HB(OCH_3)_2$) is produced from the

pyrolysis of sodium trimethoxyborohydride ($NaBH(OCH_3)_3$). Dimethoxyborane equilibrates to diborane and methyl borate. Ziegler has suggested a cyclic process using aluminum as the active metal with boron trifluoride (40). However, the large-scale production of diborane requires the minimum number of processing steps and recycles, thus emphasizing syntheses which are as direct as possible.

The higher boranes are made almost exclusively by the pyrolysis of diborane. The gas is usually passed between a hot and a cold surface for a short time. The products are always mixtures and are separated by solvent extraction or careful low pressure distillation. Tetraborane-10 (B_4H_{10}), pentaborane-9 (B_5H_9), pentaborane-11 (B_5H_{11}) and decaborane ($B_{10}H_{14}$) are prepared in this way (61). Catalysts have been used to permit conversion at lower temperatures, thus avoiding somewhat the formation of undesired nonvolatile high molecular weight boranes (80,8). Decaborane may be further polymerized to higher hydrides. The terminal hydrogens react first, and products resembling dimers of decaborane are obtained (7). No products more volatile than decaborane are found. Exchange of both hydrogen and boron atoms occurs when boron hydrides are mixed, indicating the lability of these compounds (38).

The reactions of boron hydrides depend on the structure type (18). A symmetrical cleavage of a double bridge bond by amines, ethers, etc., yields BH_3 coordination compounds. Tetraborane is cleaved by ether to form $(C_2H_5)_2O{\cdot}B_3H_7$ and B_2H_6.

A second reaction type involves unsymmetrical cleavage of a bridge bond to yield H_2B^+ and BH_4^- or $B_3H_6^-$. The reaction of sodium amalgam with diborane in ether yields an equimolar mixture of $NaBH_4$ and NaB_3H_8. Decaborane yields an intermediate $Na_2B_{10}H_{14}$ which reacts further to $NaB_{10}H_{13}$. The "diammoniate" of diborane has the structure $[H_2B(NH_3)_2]^+(BH_4)^-$(55). The existence of both positive and negative ions suggests pure ionic hydrides which could be prepared by reactions of salts of these ions with one another (43).

A third reaction type is the loss of hydrogen from the boron hydride, as in the pyrolyses previously discussed. The last reaction type is the loss of protons, as in the ionization of decaborane in dioxane-water.

The use of boron hydrides in solid propellants will depend primarily on combustion product behavior, but the form in which the compounds can be incorporated in the grain is also important. Composite propellants normally contain about 20 per cent polymeric fuel binder and 80 per cent crystalline oxidizer, which imparts no mechanical strength to the system. If more fuel is added, not chemically attached to the binder (i.e., aluminum, lithium borohydride), more oxidizer is required. The proportion of the propellant holding the mixture together decreases to the point where satisfactory mechanical properties cannot be obtained.

The possibility exists of copolymerizing boron hydride with diamines or hydrazines to produce chain polymers.

$$B_{10}H_{14} + N_2H_4 \rightarrow [-NH-NH_2{\cdot}B_{10}H_{12}{\cdot}NH_2-NH_2{\cdot}B_{10}H_{12}-]_n$$

Hydrazine and diborane form an adduct melting at 2 C (66). Decaborane reacts with acetonitrile to form $B_{10}H_{12}{\cdot}2CH_3CN$ (60). Boranes add to olefins and acetylenes. These substituted boranes present opportunities for "grafting" on to conventional polymers. The simple mixing of boron hydrides into the composite propellant is hampered by their moisture sensitivity.

Metal Borohydrides

Complex hydrides have been the subject of much study recently. Many double hydrides of Group 1 and Group 3 metals are known ($NaBH_4$, $LiAlH_4$, etc.). Triple hydrides are formed by

$$NaBH_4 + Al(BH_4)_3 \rightarrow Na^+[Al(BH_4)_4]^-$$

These compounds may have utility as fuels when more is known about them. Stable borohydrides are formed with lithium, sodium, potassium, rubidium, cesium, beryllium magnesium, calcium, strontium, barium, aluminum, copper, silver, zinc, cadmium, scandium, titanium, yttrium, zirconium, hafnium, manganese and iron.

Sodium borohydride is produced on a tonnage basis as an intermediate for diborane by Metal Hydrides, Inc. The process involves a mineral oil dispersion of sodium hydride reacted with methyl borate (15).

The complexes of sodium hydride and borate esters, sodium trialkoxyborohydrides $NaBH(OR)_3$ are somewhat unstable. Disproportionation to sodium borohydride and sodium tetraalkoxyborate occurs readily. This reaction can be driven to completion by the precipitation of borate from tetrahydrofuran solution.

Potassium borohydride is made by metathesis of sodium borohydride and potassium hydroxide (19). The borohydrides are widely used as reducing agents in organic synthesis (22). The activity of sodium borohydride can be greatly increased by aluminum chloride (10). Aluminum borohydride may be an intermediate. The borohydrides are alkaline whereas diborane is an acidic reducing agent.

Boron-Carbon Compounds

Boron may be attached to as many as four organic radicals: The boronic acids ($RB(OR)_2$), borinic acids (R_2BOR), trialkyl boranes (R_3B) and the tetra aryl boron salts ($NaBAr_4$). Recognition of the tetra coordinate boronate ion $[ArB(OR)_3]^-$ has led to quantitative yields of aryl boronic acids from Grignard reagents and methyl borate (77). Alkyls of other active metals react with tricovalent boron compounds to yield boron—carbon bonds. Diborane and boron subhalides add to unsaturated hydrocarbons. Other methods of forming boron—carbon bonds include the reaction of BCl_3 with acetylene yielding chlorovinyl borondichloride, and the reaction of borohydrides with olefinic halides HCN or CO.

The boronic acids dehydrate and trimerize to substituted boroxines $(RBO)_3$. Boronic acids form anhydrides $(R_2B)_2O$. Alkyl boronic acid esters can disproportionate to trialkyl borates and trialkyl boranes at elevated temperatures. The alkynyl boronic acids are sensitive to B—C bond rupture on hydrolysis, but in general the boronic acids are moisture stable.

Surprisingly, benzene diboronic acid $(HO)_2BC_6H_4B(OH)_2$, is hydrolytically and thermally stable (mp 420 C) possibly because of a shift of electrons from the ring to the two deficient boron atoms (53).

$NH_4[B(C{\equiv}CC_6H_5)_4]$ may be derived from BF_3 and $C_6H_5C{\equiv}CMgBr$ (41). Triacetylenic boranes are prepared from sodium acetylides and boron halides and are stabilized as the amine or sodium acetylide complex salt (21). Triallyl borane is prepared from the Grignard and ethyl borate, trivinyl borane from vinyl sodium.

Sodium tetraphenylboron is used for the gravimetric determination of potassium and organic bases (5).

A recent report concerns the preparation of simple boron-carbon ring compounds, 1-n-butyl boracyclopentane and 1-n-butyl boracyclohexane (16). The synthesis of boracyclohexatriene would be most interesting. This would permit the study of electron distribution in this compound compared with benzene and pyridine

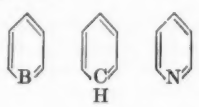

Alkyl Boranes

The boron hydrides have high heats of combustion but are not suitable for high energy fuels because of handling difficul-

ties. Therefore, modifications incorporating hydrocarbon radicals are necessary.

Effort has centered about the alkyl penta- and decaboranes. Two synthetic routes are possible. The borane may be prepared and then alkylated with an alkyl halide and a catalyst. Alternatively an olefin and diborane may yield the desired product (29). Diethyl diborane results from the reaction of sodium borohydride and vinyl bromide. Alkyl boranes are fairly stable toward hydrolysis but are usually spontaneously flammable. They react with themselves to form resinous products. This tendency is accelerated by impurities.

The trialkyl boranes (R_3B) are under investigation as flame-out preventers, when added to jet fuel and also as catalysts for olefin polymerization. Trimethyl, triethyl, tripropyl and tributyl borane are available. They may be formed from the appropriate olefin and diborane or by alkylating boron halides with aluminum alkyls. Cyclopropane reacts with diborane to yield tripropyl borane. The trialkyl boranes react with hydrogen under pressure to yield alkyl diboranes, and equilibrate with boron halides to yield alkyl haloboranes. Unsymmetrical triaryl boranes are stable as complex salts but tend to disproportionate to symmetrical compounds.

Propulsion Applications

The use of boron compounds in air-breathing propulsion systems centers on alkyl boranes which combine the desirable physical and handling properties with heats of combustion greater than 25,000 Btu/lb (78). A number of specific compounds are now available in experimental quantities. The present fuel HEF is reported to have a density of 0.82, an order of magnitude increase in flame speed over JP6, and thermal stability which limits residence time to a maximum of 1 min at 500 F. Utilization of these fuels will be on a special mission concept because of their cost, optimistically estimated at $0.65 to $1 per lb (29). Slurries of boron metal in hydrocarbon have also been developed (54). The application at present appears to be restricted to afterburners and ramjets, because of the problems imposed by boric oxide and boric acid deposits when these fuels are burned ahead of a turbine. The alkyl boranes are not as thermally stable as hydrocarbons and tend to deposit solid polymerization products in fuel lines and nozzles. Additives can overcome this deficiency to some extent. Engine operation may be limited to temperatures below 3000 F because of the considerable heat of vaporization of boric oxide.

The use of boron compounds in rocket engines requires a somewhat different analysis than in air-breathing systems. The compounds considered as fuels may be similar, but the much higher exhaust temperatures make the behavior of combustion products quite important. Any endothermic process involving boric oxide will detract from the total energy available. Research is in progress to provide reliable data on the heat of vaporization of boric oxide, the extent and heat of dissociation to B_2O_2, the extent and heat of reaction with hydrogen and water, and the problems of condensing boric oxide vapors.

The heat of sublimation of B_2O_3 is 78 kcal/mol, and it is monomeric all the way to the boiling point, 2500 K. The extent of dissociation to B_2O_2 and BO is small, less than 5 per cent at 2500 K. When water is present, $H_2B_2O_4$ is formed rather than HBO_2. Boric oxide reacts with carbon to give carbon monoxide and boron or boron carbide at 1900 K (44, 45,46).

When fluorine or chlorine is used in the oxidizer, the products are monomeric BF_3 and BCl_3. Data are available on these compounds but must be estimated for BF_2, BF, BCl_2 and BCl, the possible dissociation products (57).

The disparity of thermodynamic information gives calculated values of specific impulse and flame temperature for the reaction of decaborane and ammonium perchlorate which vary considerably. The actually realizable values will dictate the future interest in boron compounds as rocket fuels.

Analytical

Methods of analyzing for boron and its compounds have necessarily received increased study as the technology has developed. The older wet methods have been refined and several new techniques adapted.

Neutron absorptiometry has been widely applied to the determination of boron compounds in mixtures. The method is nondestructive; the state of chemical combination is immaterial, and there are few interferences (17). The capture cross section of natural boron is 781 ± 10 barns in a neutron beam of 2200 m/sec.

Gas phase chromatography may be used to separate volatile boranes. Mineral oil and tricresyl phosphate are used as coatings on celite (33). Soluble borates are analyzed for boron content by flame photometry using the characteristic green band. Extensive infrared spectroscopic work has resulted in many band assignments.

Handling Problems

Spontaneous ignition of borane-oxygen mixtures may take place at temperatures and pressures lower than those expected for thermal explosion limits. Diborane-oxygen shows an explosion peninsula at 10 to 15 mm Hg and 150 to 170 C, pentaborane-oxygen, 10 to 130 mm Hg and 30 to 60 C, and decaborane-oxygen, 80 to 110 mm Hg and 80 to 120 C (6). The flammability limits of diborane in dry air are 0.9 to 98 mol per cent. The alkyl boranes are much less hazardous, and the high energy fuels are not spontaneously flammable.

Boron compounds other than the boron halides are not corrosive, and do not affect most structural metals. Boron hydrides and alkyl boranes are damaging to all organic resins, rubbers, plastics and adhesives. Teflon, Kel-F and asbestos are satisfactory for gasket service.

Areas of manufacture or handling should be designed so that spills or leakage can be deluged with water and thoroughly washed away.

Fire extinguishment of boron hydrides and their derivatives is not yet well worked out. The best current approach is water-fog or mechanical foam. Halogenated hydrocarbons may react violently and should never be used to fight fire (3).

Physiological Properties of Boron Compounds

The toxicity of boron compounds has been studied extensively to provide clinical history when high energy fuels and other materials become more widely used. Many false impressions have been created, but in fact, no fatality due to boron poisoning has resulted from the thousands of man-years so far spent on Project Zip. The key to the danger in any particular situation is the vapor pressure of the compounds used. The hazard index (vapor pressure/LC_{50}) of some boron compounds is: Diborane, 25,000, pentaborane, 40,300, decaborane, 1.4, alkyl borane, 11.5; compared with hydrazine, 33, CCl_4, 6, benzene, 7.8 (63).

Decaborane in toxic quantities causes a slow, progressive decrease in heart force. Breathing diborane causes mainly lung damage, whereas more slowly hydrolyzed compounds accumulate and cause central nervous system effects, liver and kidney damage. The maximum allowable concentration for alkyl boranes has not been established, but will probably be less than one part per million.

The major precautions are good ventilation, protective clothing to prevent contact with skin and regular physical examinations for those who have long time exposure (3).

Gas mask protection against diborane, pentaborane and decaborane is assured by a cartridge of Hopcalite, silica gel and activated charcoal.

Monitoring devices for boron hydrides sensitive to 10 parts per billion are available commercially from Mine Safety Appliances Co. The color producing reaction of triphenyl

tetrazolium chloride with diborane, pentaborane and decaborane is employed for spot checks. An amperometric, continuously recording system is also available.

Treatment of boron poisoning consists of an injection of barbiturates or Robaxin followed by rest and treatment of the symptoms. Affected areas of the body may be decontaminated by a 1 per cent aqueous triethanolamine solution followed by washing with soap and water.

Boron is an important and necessary trace element in plant growth. When needed, it is added as borax. However, too high a concentration in the soil acts as an herbicide. Studies have shown that no adverse effects should occur from "fall out" of boric acid from boron fueled aircraft or in the vicinity of processing plants.

Conclusion

The rapidly expanding chemistry of boron can be expected to bear fruit in the next few years in a wide variety of applications. As an example of the diversity already reported: Trialkyl boranes catalyze olefin polymerizations, boric oxide cross links hydroxy polymers, trimethoxyboroxine extinguishes magnesium metal fires, sodium borohydride is used in permanent hair wave compositions, borates are both trace element fertilizers and herbicides, methyl borate in carbon dioxide suppresses the generation of electrostatic charges on discharge, nuclear applications include B^{10} and boron carbide, borides find service as refractories, and the ubiquitous motor fuel additives consist of polyol borates or boronic acids.

Broad basic knowledge has been obtained in the various government agency sponsored programs during the last 10 years. The "tailor making" of boron compounds to any specific role is now possible.

References

1 Adams, R. M., "Preparation of Diborane," presented at the American Chemical Society meeting, San Francisco, Calif., April 13–18, 1958.

2 Anon., "Current Literature Abstracts Bulletin," Olin-Mathieson Chemical Corp. (Contract AF 33(600)-33920), 1953 to present.

3 Anon, "HiCal-3 Handling Bulletin, C-1100," Callery Chemical Co., Aug. 1, 1958.

4 Anon., "Refractory Uses of Boron and Titanium Carbides Bonded with Metals," *Ceramics*, vol. 8, 1956, pp. 184–187.

5 Barnard, A. J. and Buechl, H., "Sodium Tetraphenylboron, 1956: A Bibliography," *Chemist-Analyst*, vol. 46, 1957, pp. 16–17.

6 Bauer, W. H. and Wiberley, S. E. "Explosive Oxidation of the Boranes," presented at the American Chemical Society meeting, San Francisco, Calif., April 13–18, 1958.

7 Beachell, H. C. and Haugh, J. F., "The Pyrolysis of Decaborane," *J. Amer. Chem. Soc.*, June 26, 1958.

8 Beckman, R. B., "Catalytic Pyrolysis of Diborane," CCC–1024–TR-272, Nucl. Sci. Abstrs., vol. 12, no. 6, 4070, 1958, p. 455.

9 Bixler, G. H. and Sawyer, D. L., "Boron Chemicals from Searles Lake Brines," *Ind. and Engng. Chem.*, vol. 49, 1957, pp. 322–333.

10 Brown, H. C. and Rao, B. C. S., "A New Powerful Reducing Agent," *J. Amer. Chem. Soc.*, vol. 78, 1956, pp. 2582–2588.

11 Burg, A. B., "Polymer Systems Derived From Boron Hydrides," presented at the American Chemical Society meeting, San Francisco, Calif., April 13–18, 1958.

12 Burg, A. B., "Studies on Boron Hydrides. Final Technical Report of Investigations on Water Reactive Chemical Compounds," USAEC NP-6366, Nucl. Sci. Abstrs., vol. 11, no. 20, 11058, 1957, p. 1222.

13 Carpenter, R. A., "Liquid Rocket Propellants," *Ind. and Engng. Chem.*, vol. 49, no. 4, 1957, p. 48A.

14 Carpenter, R. A., Hughes, R. L. and Bergman, F. J., "Preparation Properties and Structure of Methoxy Boroxines," presented at the American Chemical Society meeting, Miami, Fla., March 1957.

15 Chilton, C. H., "First Tonnage Production of Sodium Borohydride: Vital Link to High Energy Fuels," *Chem. Engng.* vol. 64, no. 12, 1957, p. 146.

16 Clark, S. L. and Jones, J. R., "Synthesis of Boron-Carbon Ring Compounds," presented at the American Chemical Society meeting, San Francisco, Calif., April 13–18, 1958.

17 DeFord, D. D. and Braman, R. S., "A Study of Neutron Absorbtiometry and its Application to the Determination of Boron," CCC-1024-TR-243, Nucl. Sci. Abstrs. vol., 11, no. 20, 11078, 1957, p. 1224.

18 Edwards, L. J. and Perry, R. W., "Systematics in the Chemistry of the Boron Hydrides," presented at the American Chemical Society meeting, San Francisco, Calif., April 13–18, 1958.

19 Fedor, W. S., Banus, M. D. and Ingalls, D. P., "Potassium Borohydride Manufacture," *Ind. and Engng. Chem.*, vol. 49, 1957, pp. 1664–1672.

20 Fetterley, G. H. and Hazel, W. M., "The Development on a Commercial Scale of a Process for the Manufacture of Crystalline Boron and Analytical Methods," USAEC A-2191, Nucl. Sci. Abstrs. vol. 11, no. 175, 9668, 1957, p. 1063.

21 Foster, W. E., "Preparation and Stabilization of Acetylenic Boranes," presented at the American Chemical Society meeting, San Francisco, Calif., April 13–18, 1958.

22 Gaylord, N. G., "Reduction with Complex Metal Hydrides," Interscience Publishers, New York, 1956.

23 Gerrard, W., Lappert, M. F. and Pearce, C. A., "Chemistry of Certain Novel Organic Boron Compounds," *Chem. and Ind.*, 1958, pp. 292–293.

24 Gerrard, W. and Wheelans, M. A., "Fission of Esters of Carboxylic Acids by Boron Trichloride," *J. Amer. Chem. Soc.*, 1956, pp. 4296–4300.

25 Gerrard, W. and Wheelans, M. A., "The Constitution of Boron Acetate," *Chem. and Ind.*, 1954, pp. 758–759.

26 Glemser, O., "Formation of Diborane by Treating Boron Tribromide with Formaldehyde in Presence of Activated Copper," German Patent 949,943, Sept. 27, 1956.

27 Goubeau, J. and Rohwedder, K. H., "Reaction of Diazomethane and Boron Trifluoride in the Gas Phase," *Annalen*, vol. 604, 1957, pp. 168–178.

28 Grosse, A. V., "The Production of Temperatures above 4000°K by Chemical Means and Chemistry above 4000°K," Résumés of Communications, 16th Int. Congress Pure and Applied Chemistry, Paris, 1957.

29 Heaston, R. J., "The Future of Aircraft Fuels," presented at Society of Automotive Engineers meeting, New York, N. Y., April 8, 1958.

30 Hooker Electrochemical Co., "Boron and Its Isotopes," USAEC U-3548, Nucl. Sci. Abstrs. vol. 11, no. 21, 11912, 1957, p. 1323.

31 Hough, W. V. and Edwards, L. J., "Metal Boron Hydrides," presented at the American Chemical Society meeting, San Francisco, Calif., April 13–18, 1958.

32 Juretsche, H. J. and Steinitz, R., "Hall Effect and Electrical Conductivity of Transition Metal Diborides," *J. Phys. Chem. Solids*, vol. 4, 1958, pp. 118–127.

33 Daufman, J. J., Todd, J. E. and Koski, W. S., "Application of Gas Phase Chromatography to the Boron Hydrides," *Analytical Chemistry*, vol. 29, 1957, pp. 1032–1035.

34 Keller, R. N. and Vander Wall, E. M., "Boroxine Derivatives," presented at the American Chemical Society meeting, San Francisco, Calif., April 13–18, 1958.

35 King, A. J. et al., "A New Method for the Preparation of Borohydrides," *J. Amer. Chem. Soc.*, vol. 78, 1956, p. 4176.

36 Kirk–Othmer (ed.), "Encyclopedia of Chemical Technology, Volume II," The Interscience Encyclopedia, Inc., N. Y., pp. 584–622.

37 Kirshenbaum, I., Sabi, N. and Schutz, P. W., "The Separation of the Boron Isotopes," USAECA-2120, Nucl. Sci. Abstrs., vol. 12, no. 3784, 1958, p. 426.

38 Koski, W. S., "Mechanisms of Isotopic Exchange in the Boron Hydrides," presented at the American Chemical Society meeting, San Francisco, Calif., April 13–18, 1958.

39 Koster, R., "A Simple Synthesis of N-Trialkylborazanes," *Angewandte Chemie*, vol. 69, 1957, p. 94.

40 Koster, R. and Ziegler, K., "Preparation of Diborane," *Angewandte Chemie*, vol. 69, 1957, pp. 94–95.

41 Kruerka, U., "New Organoboron Compounds," *F. Naturforsch*, vol. 116, 1956, pp. 606–607, 676–677.

42 Lappert, M. F., "Organic Compounds of Boron," *Chem. Rev.*, vol. 56, 1956, pp. 959–1064.

43 Lipscomb, W. N., "Possible Boron Hydride Ions," *J. Phys. Chem.*, vol. 62, 1958, p. 381.

44 Margrave, J. L., private communication.

45 Margrave, J. L. and Soulen, J. R., "Vaporization of Boric Oxide and Thermodynamic Data for the Gaseous Molecules B_2O_3, B_2O_2 and BO," *J. Amer. Chem. Soc.*, vol. 78, 1956, p. 2911.

46 Margrave, J. L. et al., "Structures and Thermodynamic Properties of High Temperature Gaseous Species in the B_2O_3-H_2O System," Résumés of Communications, 16th Int. Congress Pure and Applied Chemistry, Paris, 1957.

47 Major, C. J., "Technology of Boron Hydrides," *Chem. Eng. Prog.* vol., 54, no. 3, 1958, p. 49.

48 Martin, D. R. (chairman), "Symposium on From Borax to Boranes," Abstracts of papers presented at American Chemical Society meeting, San Francisco, Calif., April 13–18, 1958.

49 McCusker, P. A. and Ostdick, T., "Reactions of Haloboranes with Organocyclosiloxanes," *J. Amer. Chem. Soc.*, vol. 80, 1958, pp. 1103–1106.

50 Mikhailov, B. M. and Kostrama, T. V., "Synthesis of Arylboron Dichlorides," *Izvest. Akad. Nauk SSSR, Otdel. Khim. Nauk*, 1956, pp. 1144–1146.

51 Mikheeva, V. I. et al., "Preparation of Amorphous Boron of a High Degree of Purity," *Zhur. Neorg. Khim.* vol. 2, 1957, pp. 1223–1253.

52 Musgrave, O. C., "The Preparation of Some Dimeric Sec-Amino Boron Dihalides," *J. Amer. Chem. Soc.*, 1956, pp. 4305–4307.

53 Nielsen, D. R. and McEwen, W. E., "Benzene Diboronic Acids," *J. Amer. Chem. Soc.*, vol. 79, 1957, pp. 3081–3084.

54 Olson, W. T., "Possibilities and Problems of Some High Energy Fuels for Aircraft," presented at Society of Automotive Engineers meeting, New York, April 8, 1958.

55 Parry, R. W. et al., "Chemistry of Boron Hydrides and Related Hydrides," WADC-TR-56-318, Nucl. Science Abstrs. vol. 11, no. 1, 80, 1957, p. 8.

56 Pearson, R. K. et al., "Conversion of Boric Oxide to Boron Trichloride," Nucl. Sci. Abstrs., vol. 11, no. 12A, 6232, 1957, p. 670.

57 Potocki, R. M. and Mann, D. E., Nat. Bur. Standards Report no. 1561, May 1952.

58 Ruigh, W. L., "Research on Boron Polymers. Final Report," Nucl. Sci. Abstrs., vol. 10, no. 23, 11694, 1956, p. 1351.

59 Ruigh, W. L. et al., "Research on Boron Polymers," presented at the American Chemical Society meeting, San Francisco, Calif., April 13–18, 1958.

60 Schaeffer, R., "A New Type of Substituted Borane," *J. Amer. Chem. Soc.* vol. 79, 1957, p. 1006.

61 Schaeffer, R., "Interconversion Reactions of Boranes," presented at the American Chemical Society meeting, San Francisco, Calif., April 13–18, 1958.

62 Schechter, W. H., Jackson, C. B. and Adams, Roy, M., "Boron Hydrides and Related Compounds," 2nd ed., Callery Chemical Co., May 1954.

63 Schechter, W. H., "Toxicity of High-Energy Fuels Poses Hazards for Handlers," *Missiles and Rockets*, vol. 3, April 1958, pp. 85–86.

64 Schlesinger, H. I. and Brown, H. C., "New Developments in the Chemistry of Diborane and the Borohydrides," *J. Amer. Chem. Soc.* vol. 75, 1953, pp. 186–224.

65. Schlesinger, H. I. and Burg, Anton B., "Recent Developments in the Chemistry of the Boron Hydrides," *Chem. Rev.*, vol. 31, 1942, pp. 1–41.

66 Schlesinger, H. I., "Hydrides and Borohydrides of the Light Weight Elements and Related Compounds," Nucl. Sci. Abstrs., vol. 10, no. 23, 11690, 1956, p. 1350.

67 Seyforth, D., "Organosilicon Boranes," U. S. Patent 2,831,009, April 15, 1958.

68 Steinberg, H. and Hunter, D L., "Preparation and Rate of Hydrolysis of Boric Acid Esters," *Ind. and Engng. Chem.*, vol. 49, 1957, pp. 174–181.

69 Stock, Alfred, "Hydrides of Boron and Silicon," Cornell University Press, Ithaca, N. Y., 1933.

70 Stone, F. G. A., "Chemistry of the Boron Hydrides," Quarterly Rev., London, vol. 9, 1955, pp. 174–201.

71 Stone, F. G. A., "Stability Relationships Among Analogous Molecular Addition Compounds of Group III Elements," *Chem. Rev.*, vol. 58, 1958, pp. 101–129.

72 Talley, C. P., "Combustion of Elemental Boron," AD-135080, ASTIA, T.A.B., U57-4, p. 344.

73 Urry, G., Kerrigan, J., Parsons, T. D. and Schlesinger, H. I., "Diboron Tetrachloride, B_2Cl_4, as a Reagent for the Synthesis of Organoboron Compounds," *J. Amer. Chem. Soc.* vol. 76, 1954, pp. 5299–5301.

74 Ver Planck, W. E., "History of Borax Production in the United States," *Calif. J. Mines Geol.*, vol. 52, 1956, pp. 273–291.

75 Voronkov, M. G. and Zgonnik, V. N., "Organosilicon Derivatives of Boric Acid-Tris (Trialkylsilyl) Borates and Polyboronorgano Siloxanes," *Zhur. Obshchei. Khim.*, vol. 27, 1957, pp. 1476–1483.

76 Wartik, T. and Rosenberg, R. M., "Discharge Induced Formation of Boron Polymers," *J. Inorg. Nucl. Chem.*, vol. 3, 1957, p. 388.

77 Washburn, R. M. et al., "Organoboron Compounds. Aromatic Compounds," presented at the American Chemical Society meeting, San Francisco, Calif., April 13-18, 1958.

78 Weilmuenster, E. A., "New Power From the Desert," presented at the Annual Meeting of the San Francisco Chapter of the Armed Forces Chemical Association, San Francisco, Calif., Sept. 26, 1957.

79 Wentorf, R. H., "Cubic Form of Boron Nitride (Borazon)," *J. Chem. Phys.*, vol. 26, 1957, p. 956.

80 Whitney, E. D., "Conversion of Diborane to Higher Molecular Weight Boranes in the Presence of Certain Heterogeneous Catalysts," presented at the American Chemical Society meeting, San Francisco, Calif., April 13–18, 1958.

81 Wilson, C. O. et al., "The Production of Ammonium Pentaborate and Boric Oxide from Borax," presented at the American Chemical Society meeting, San Francisco, Calif., April 13–18, 1958.

A Ballistic Bomb Method for Determining the Experimental Performance of Rocket Propellants

DONALD N. GRIFFIN[1]
CHARLES F. TURNER[2]
and GEORGE T. ANGELOFF[3]

Olin Mathieson Chemical Corp.
New Haven, Conn.

A method has been devised for the determination of measured performance values of rocket propellants without the requirement of actual rocket motor operation. Constant-volume combustion in a ballistic bomb will provide accurate data on the impetus $(nRT)_v$ of a propellant system. By an approximation method $(nRT)_v$ is converted to $(nRT)_p$, from which term characteristic velocity (C^*), and hence specific impulse (I_{sp}), can be derived. Since an impetus value can be obtained with as little as 50 to 100 gm of propellant, the ballistic bomb method allows performance evaluation at an early stage when only limited quantities of a new propellant are available.

AS GREATER emphasis has been placed on the development of new and higher energy rocket propellants, both solid and liquid, it has become increasingly apparent that there is an urgent need for rapid and relatively simple methods of obtaining a measure of specific performance at a stage as early as possible in the development process. Propellant evaluation cannot depend solely on calculated performance, since this only represents maximum theoretical performance, and not necessarily that which can be achieved in practice. Furthermore, calculated performance is often inaccurate and misleading in cases where gross assumptions have been made in the thermodynamic constants used or the product gas composition.

As one step in the evaluation of new propellants, it has been standard practice to determine experimentally their specific impulse by means of small scale rocket motor tests. This type of test usually involves a minimum of several pounds of propellant, and the use of test cell facilities with extensive instrumentation for dynamic measurement of thrust, chamber pressure and propellant consumption rate. With solid propellants, rocket motor testing also requires the prior development of propellant charges of proper burning rate and geometry. Because of these factors, unfortunately, motor testing is usually not carried out until months, or even years, after the synthesis of a new propellent system is first considered.

In the gun field it has been standard practice for many years to measure the "force constant" or "impetus" of powder propellants simply by measuring the maximum pressure obtained by the explosion of a given weight of propellant in a closed vessel of known volume. The closed bomb involves a constant volume reaction at pressures in the range of 10,000 to 50,000 psi, whereas rocket combustion is a constant-pressure process normally carried out at pressures not greater than 1000 psi. In spite of this fact, we have developed a method whereby the high-pressure, constant-volume thermodynamic data can be converted to low-pressure, constant-pressure values with sufficient accuracy to make the ballistic bomb a promising tool for preliminary experimental evaluation of propellants for rocket application. The closed bomb method is particularly attractive because of its low cost and simplicity which allow rapid testing in the laboratory without the need for extensive facilities or equipment. Also, only small quantities of propellants are required ($\sim$5 gm per test).

The impetus of a propellant is a measure of the quantity nRT from the perfect gas equation and represents energy per unit mass. In gun terminology this term is normally expressed as ft-lb/lb, or cal/gm. In rocket application, the term characteristic velocity (C^* = ft/sec) is also an expression of nRT. Therefore, a value of characteristic velocity, and hence specific impulse, for a given propellant can be determined directly in the laboratory by means of a closed bomb measurement, provided that the value of nRT measured under high-pressure, constant-volume conditions can be related to the low-pressure, constant-pressure conditions encountered in a rocket motor.

In connection with liquid propellant gun development at Olin Mathieson Chemical Corporation (OMCC) a closed bomb apparatus has been developed for use in the ballistic evaluation of liquid monopropellants. This bomb procedure represents a simplification of typical rocket testing methods for the following reasons. No injection problem is present, and since high pressure accelerates the decomposition reaction, the use of catalysts is obviated. Furthermore, in the bomb a vigorous ignition process is used which should make this one standard test satisfactory for most monopropellant systems.

While this test was originally developed for liquid monopropellant evaluation, its applicability to other propellant systems is apparent. Burning rate is not critical in the closed bomb, provided that it is fast enough to allow the overall combustion process to occur under conditions approaching adiabatic. Therefore, solid propellants may be tested without prior knowledge of linear burning rate since the propellant sample is burned in a granulated state.

Liquid bipropellant systems present a more complex problem in that the fuel and oxidizer components should be mixed uniformly before reaction occurs, or at least before the combustion reaction is completed. Certain bipropellant systems are miscible and nonhypergolic, in which case they

Received June 23, 1958.

[1] Associate Director, Military Chemicals Research, Energy Division. Member ARS.

[2] Manager, Liquid Propellant Application Research, Energy Division. Member ARS.

[3] Technical Specialist, Energy Division.

can be mixed and handled as monopropellants in the described apparatus. Hypergolic systems would require a special means of charging fuel and oxidizer components to the bomb, followed by suitable mixing before or during the combustion reaction. This latter case has not yet been investigated in the work described in this paper.

Thermodynamic Relationships

Review of Ballistic Terms and Correction Factors

The ideal gas equation of state is

$$PV = nRT \qquad [1]$$

where

P = pressure
V = volume
n = no. of moles of gas
R = universal gas constant
T = absolute temperature

At high pressures, gases do not behave in accordance with the ideal case, and we must distinguish between ideal and real gas behavior. For example, at 1000 psi the difference between ideal and real gas is very small, while at pressures of 50,000 to 100,000 psi the difference can be greater than 30 per cent. Therefore, in the calculation of maximum pressures and temperatures under gun conditions, corrections must be made to take into account the departure of gas properties from the ideal case.

The best known equation of state which conforms to the behavior of real gases at high pressures is the Noble-Abel equation

$$PV = a + bP$$

or

$$P(V - b) = a \qquad [2]$$

where a and b are constants.

Impetus (F) or force constant is a measure of the work potential of a propellant burned under constant-volume conditions, and is expressed in terms of energy per unit mass. For ideal gases, then

$$F = PV = nRT \qquad [3]$$

If we let a in Equation [2] correspond to nRT in the ideal Equation [1], we can set up the following expression for real gases

$$P(V - b) = nRT \qquad [4]$$

where b is the "covolume" with the dimensions of volume per unit mass. Covolume is a property of real gases which is very nearly a constant independent of pressure, and which accounts for the difference between real and ideal behavior. Thus, covolume is an essential term in ballistic calculations, and its value must be determined experimentally for any propellant under consideration.

Determination of Impetus and Covolume

Impetus is determined readily in a closed bomb by measuring maximum pressure (P_{max}) obtained at a given propellant loading density (Δ). Since loading density is a measure of mass per unit volume, then

$$V \text{ (per unit mass)} = \frac{1}{\Delta}$$

or

$$PV = \frac{P_{max}}{\Delta} \qquad [5]$$

Because of the covolume effect, at high pressures, measured values of PV vary with pressure. Therefore, in order to obtain a measured value of impetus, the value of PV must be determined at zero pressure, since the relationships in Equation [3] hold only under ideal conditions, and the properties of real gases approach the ideal case as pressure approaches zero.

To obtain the value of PV at zero pressure (i.e., impetus), PV must be determined at several pressures by varying propellant loading density. A linear plot can then be made of PV vs. P and extrapolated to zero pressure.

Impetus is usually expressed as ft-lb of work per lb of mass. To obtain impetus in these terms from ballistic bomb measurements Equation [5] may be used as

$$F \text{ (ft-lb/lb)} = 2.307 \frac{P_{max}(\text{psi})}{\Delta(\text{gm/cc})}$$

To obtain a measured value of covolume, Equation [4] can be rearranged as

$$b = \frac{PV - nRT}{P} \qquad [6]$$

where

PV = measured at pressure (P)
P = measured pressure
nRT = impetus (either calculated or determined by extrapolation of measured PV values to zero pressure)

Covolume is normally expressed as in.^{3} per lb. Therefore, to obtain a measured value in those units Equation [6] may be used as

$$b(\text{in.}^3/\text{lb}) = 12 \frac{PV - nRT(\text{ft-lb/lb})}{P(\text{lb/in.}^2)}$$

Conversion of Constant-Volume to Constant-Pressure Terms

Determination of Characteristic Velocity Characteristic exhaust velocity (C^* = ft/sec) is a function of the combustion product gas properties in a rocket combustion chamber, and can be expressed thermodynamically as

$$C^* = \frac{\sqrt{gkRT_c}}{k\sqrt{\left(\frac{2}{k+1}\right)^{(k+1)/(k-1)}}} \qquad [7]$$

where

k = specific heat ratio
R = gas constant
T_c = chamber temperature

Thus both characteristic velocity and impetus are functions of nRT. However, it has already been stated that F (impetus) is a constant-volume term, whereas combustion in a rocket motor is under constant-pressure conditions. Therefore, in order to relate impetus to characteristic velocity, $(nRT)_v$ must be converted to $(nRT)_p$.

Gas composition and heat release vary between constant-volume and constant-pressure conditions. Accordingly both n and T will vary. In the determination of impetus in the ballistic bomb, only the product of n and T is obtained. Thus an exact conversion of $(nRT)_v$ to $(nRT)_p$ cannot be made since actual gas composition and temperature are not known. However the following approximation has been made which appears to be sufficiently accurate for the purposes of the test.

Let

Q_p = heat change at constant pressure

Q_v = heat change at constant volume
T_p = constant-pressure flame temperature
T_v = constant-volume flame temperature
k = C_p/C_v = specific heat ratio

The relationship between the heat change at constant pressure (Q_p) and constant volume (Q_v) may be expressed as

$$Q_p = Q_v + P\Delta V \quad [8]$$

where $P\Delta V$ represents the external work done by the system for a reaction carried out at constant pressure.

For a combustion reaction where the total heat release is very large, $P\Delta V$ is negligible with respect to Q_v, and we may set

$$Q_p = Q_v$$

in which case

$$C_pT_p = C_vT_v \quad [9]$$

or

$$T_v = kT_p \quad [10]$$

If then we assume that n is constant in going from products at T_v to product at T_p, then

$$nRT_v = knRT_p \quad [11]$$

and substituting in Equation [3]

$$F = knRT_p \quad [12]$$

We may now express characteristic velocity (C^*) in terms of impetus (F) as follows

$$C^* = \frac{\sqrt{gF}}{k\sqrt{\left(\frac{2}{k+1}\right)^{(k+1)/(k-1)}}} \quad [13]$$

For most propellants the value of k is 1.25 ± 0.03. Therefore, if we assume a constant value (namely 1.25) for k, the C^* Equation [13] can be reduced to the following relationship

$$C^* = 7.72\sqrt{F(\text{ft-lb/lb})}$$

Obviously Equation [13] will only apply if n does not vary with temperature in the range from T_p to T_v. For propellants containing only carbon, hydrogen, oxygen and nitrogen, n is invariant. For other cases, the closed bomb method of determining C^* values will be in error by the degree that n varies with temperature. The theoretical C^* Equation [7] is independent of chamber pressure, neglecting second order pressure effects on dissociation. In cases where the effect of pressure on dissociation is significant, the measured value of C^* may also be in error by the degree that n varies with pressure.

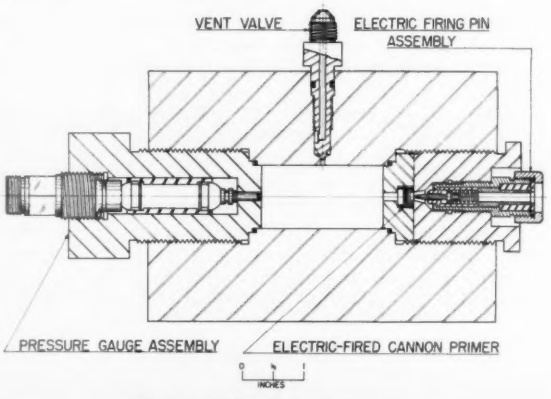

Fig. 1 Ballistic bomb assembly

DETERMINATION OF SPECIFIC IMPULSE The specific impulse of a propellant is given by the following equation

$$I_{sp} = \frac{C^*C_F}{g} \quad [14]$$

where

I_{sp} = specific impulse (sec)
g = acceleration of gravity (32.2 ft/sec²)
C_F = nozzle coefficient

Therefore, in terms of impetus, specific impulse is given by the following equation

$$I_{sp} = 0.240\,C_F\sqrt{F} \quad [15]$$

For the conversion of impetus to characteristic velocity a constant value of 1.25 has already been assumed for k, and hence the following values of nozzle coefficient (C_F) can be used

$$C_F = 1.41\ (P_c = 315\ \text{psia})$$
$$C_F = 1.58\ (P_c = 1000\ \text{psia})$$

Therefore, the following factors may be used to obtain specific impulse directly from impetus

$$I_{sp}(P_c = 315\ \text{psia}) = 0.338\sqrt{F(\text{ft-lb/lb})}$$
$$I_{sp}(P_c = 1000\ \text{psia}) = 0.379\sqrt{F(\text{ft-lb/lb})}$$

Description of Apparatus

A simple ballistic bomb apparatus has been developed at OMCC for liquid monopropellant evaluation (see Fig. 1). This bomb consists of a small cylindrical chamber, horizontally positioned, with a pressure gage holder in one end, and an electrically-fired 20-mm cannon primer held in an assembly at the opposite end for use as the igniter. A vent valve is located on the top of the bomb for venting pressure after a test, and the liquid propellant sample is charged to the bomb through the vent-valve port by means of a hypodermic syringe.

Any suitable pressure gage could be utilized provided it is capable of measuring pressures in the range of 15,000 to 60,000 psi. Only maximum pressure is required for the determination of impetus. However, if pressure vs. time is measured, then the rate of pressure rise may be utilized as a measure of the bulk burning rate of the propellant charge.

In the present apparatus a piezo-electric crystal gage is used with the output of the crystal element being recorded by means of an oscilloscope and camera combination, and pressure vs. time is measured during propellant burning. A typical pressure record for a liquid monopropellant test is shown in Fig. 2. After burning is completed, and maxi-

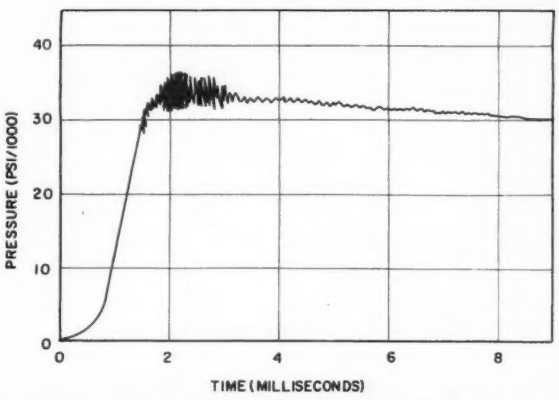

Fig. 2 Typical pressure vs. time record for a liquid monopropellant

mum pressure has been reached, the pressure trace decays because of the decrease in pressure due to cooling of the hot gases, and also because of leakage of the electrical charge built up in the crystal gage element which functions as a capacitor.

Accurate measurement of maximum pressure is essential in the determination of the impetus value of a propellant. Therefore, a straight line extrapolation is made of the rise and decay portions of the pressure record, and the intersection of these lines is taken as the maximum pressure. For maximum accuracy the pressure should be corrected for heat losses during burning and for the igniter energy. These corrections are of opposite value, and in the present apparatus they are estimated to be approximately equal in magnitude (approximately 1 per cent). Therefore, no correction has been applied.

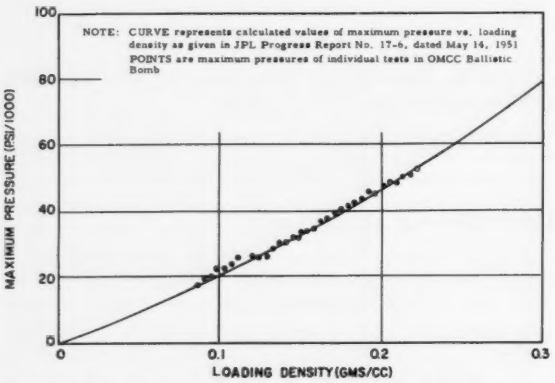

Fig. 3 A comparison of calculated and measured values of maximum pressure vs. loading density for nitromethane

Determination of Accuracy

Accuracy of Impetus Measurement

In order to determine the accuracy of the present ballistic bomb for the determination of the impetus values of liquid monopropellants, a series of individual tests was made with nitromethane at different loading densities. A plot of maximum pressure vs. loading density was compared with calculated values for this propellant system, and agreement was obtained within the limits of accuracy of the method of measuring pressure (see Fig. 3). Therefore, it is assumed that for those propellants which can be ignited and burned satisfactorily, accurate values for impetus and covolume can be obtained. Where necessary, additional ignition energy could be supplied with the recorded pressures corrected accordingly.

Accuracy of Conversion to Constant-Pressure Terms

In order to determine the accuracy of the method of conversion of impetus to characteristic velocity and specific impulse, several different monopropellant systems were tested. Measured pressures vs. loading densities for nitromethane, hydrazine and ethylene oxide are shown in Fig. 4. From these data the plots of PV vs. P for each propellant were derived as shown in Fig. 5, with the impetus values obtained by extrapolation to zero pressure.

Conversion of impetus to specific impulse was then carried out in accordance with the method described in the section, Thermodynamic Relationships. These values are summarized in Table 1, and are compared with theoretical specific impulse. With both nitromethane and hydrazine, measured values approached theoretical. In the case of ethylene oxide, measured performance was about 10 per cent low; however, this is in reasonable agreement with the measured performance obtained in an actual rocket com-

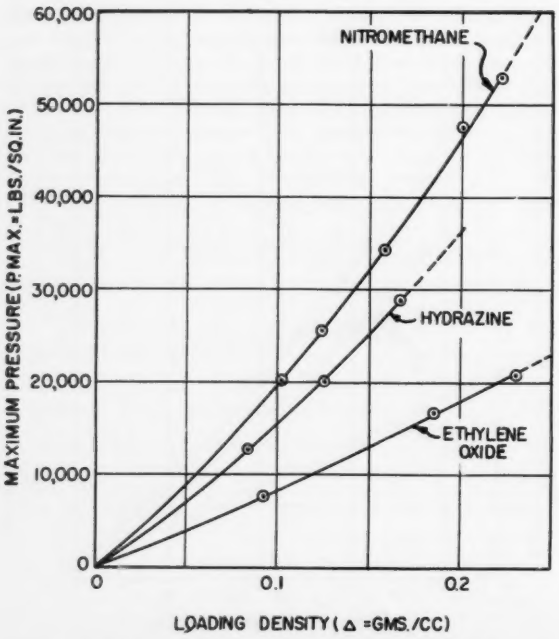

Fig. 4 Maximum pressure vs. loading density for selected liquid monopropellants in the ballistic bomb

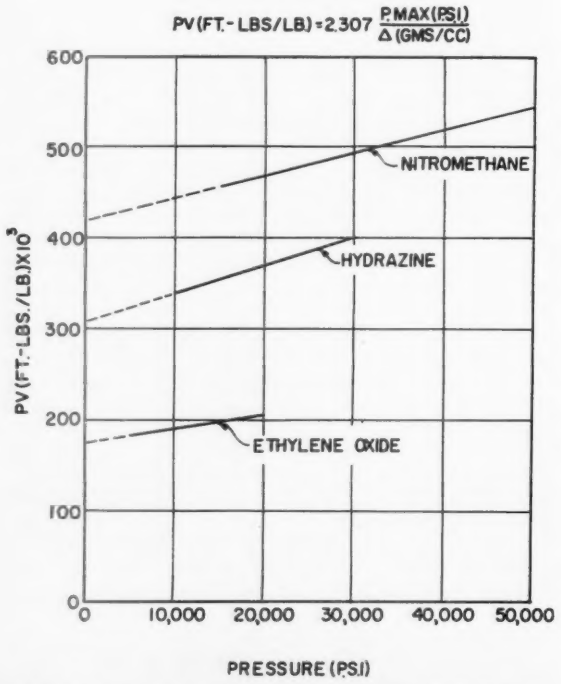

Fig. 5 PV vs. P for selected liquid monopropellants as determined in the ballistic bomb

Table 1 A comparison of theoretical specific impulse with values obtained by the ballistic bomb method

Propellant	Specific impulse (P_c = 315 psia) Calculated (I_{sp} = sec)	Measured (I_{sp} = sec)	Per cent of theor.
nitromethane	220	219	99
hydrazine	188–192	188	98–99
ethylene oxide	159–162	142	88–89

bustion chamber with ethylene oxide monopropellant.

On the basis of these preliminary tests, it can be concluded that the ballistic bomb is a useful method of determining the specific performance of rocket propellants. The method of conversion of the constant-volume performance value to a constant-pressure term is apparently valid within limits of accuracy which are sufficient for propellant evaluation purposes. However, further verification should be obtained by testing as wide a range as possible of both liquid and solid propellants before the method could be adopted universally.

New Aspects in Ceramic Coatings

PAUL A. HUPPERT[1]

Gulton Industries, Inc.
Metuchen, N. J.

Requirements and problems created by ultra-high speed and space flight conditions with emphasis on newly developed metal alloys and high energy fuels call for special high temperature resistant protective coatings. Recent achievements in modifying conventional ceramic coatings and application techniques are described, and lithium compounds as prime modifying constituents are discussed.

REQUIREMENTS and problems created by ultra high speed and space flight conditions, with emphasis on utilizing super metal alloys, refractory metals and high energy fuels call for new types of ceramic coatings and for new application techniques. Conventional refractory ceramic coatings have been modified by introducing superrefractory materials in combination with highly powerful fluxing agents, such as lithium compounds.

While in the past ceramic coatings were developed to withstand long duration counted in hundreds and thousands of hours, new applications, especially in the missile field, require protection at extremely high temperatures for very short duration, in some cases only of microseconds.

Often, metallic elements, used as alloying materials in order to improve structural strength, are chemically attacked by the combustion products deriving from high energy fuels, leading to formation of eutectics that cause embrittlement of the base metal and destroy its strength properties. Blanket- or barrier-type protective coatings have to serve in two ways: To increase heat resistance performance, and to protect the base metal against corrosion.

Studies have been initiated for using ceramic coatings as dry film lubricants. Converted ceramic coatings serve as ceramic adhesives or brazing compounds, are used for electrical insulation and in the field of instrumentation.

Modified Ceramic Coatings

Conventional ceramic coatings consist of a two-phase system whereby refractory particles are embedded in a glass matrix. The amounts and types of these refractories are limited. It was found that by changing the original two-phase system into a three-phase system, consisting of glass, refractory particles and added fluxing agents, higher heat resistance ranges result. Among the materials selected for fluxing purposes are vanadium pentoxide, tungstic oxide, molybdenum trioxide and lithium compounds. Lithia, known in the field of ceramics as the most powerful fluxing and wetting agent at elevated temperatures, gave the best results so far. It permits not only incorporation of higher quantities of refractory materials into the coatings without being forced to raise the application firing temperature, but also incorporation of superrefractories, such as borides, carbides, nitrides and zirconates, typical examples of which are quoted in the following table.

Table 1 List of superrefractory materials (deg C) (with melting points above 2500 C)

	MP		MP
Elements			
carbon	3500	rhenium	3000
molybdenum	2650	tantalum	2850
osmium	2700	tungsten	3350
Oxides			
beryllium	2500	magnesium	2500
calcium	2550	thorium	2800
hafnium	2800	zirconium	2950
Borides			
hafnium	3050	zirconium	2900
tungsten	2900		
Carbides			
hafnium	4150	thorium	2800
molybdenum	2550	titanium	3100
niobium	3500	tungsten	2850
silicon	2550	zirconium	3550
tantalum	4150	zirconium-tantalum	3900
Nitrides			
boron	2750	tantalum	3300
hafnium	3300	titanium	3200
scandium	2650	zirconium	3000
Zirconates			
barium	2700	strontium	2700
calcium	2550	thorium	2800

Presented at the ASME-ARS Aviation Conference, Dallas, Texas, March 17-20, 1958. Revised Oct. 1958.

[1] Director, Ceramic Coating Department. Member ARS.

An excellent material is boron nitride (1),[2] a good heat insulator at high temperatures, superior to calcia, alumina, magnesia and even thoria. The crystal structure of boron nitride is similar to graphite, which accounts for its greasy feel, and it also has led to the development of elevated temperature resistant dry film lubricants. Its low electrical conductivity at elevated temperatures makes its application useful as an ingredient in electrically insulating ceramic coatings. If utilized in the form of a ceramic coating (2), its lack of mechanical strength becomes unimportant, and its oxidation resistance is increased by the surrounding glass particles.

A very interesting feature of boron nitride bearing coatings is their tendency toward self-healing under elevated temperature exposure. This is important for coating molybdenum, serving as a remedy against "catastrophic" oxidation. It also leads to the idea of constructing coatings with highest possible film strength in the unfired bisque, which can mature by the developed frictional heat during actual flight conditions.

In very recent work, the three-phase system was reconverted into a new type of a two-phase system in which glass and fluxing compounds are combined by applying those types of complex lithium compounds, which by their nature are of a glassy structure. Examples are lithium borosilicate, lithium fluoborosilicate, lithium barium-strontium borosilicate, lithium zirconium silicate.

Ceramic coatings are applied by standard methods in thin layers of a maximum thickness up to 0.001 in., either as single coats, as multiple coats, or in sandwich-type combinations of different types of coatings for special purposes, such as for thermal shock resistance, heat insulation, chemical corrosion resistance, erosion resistance.

New types of coatings have been obtained by modifying conventional ceramic coating compositions by increasing the refractory additions in such a magnitude that the heat corrosion resistance range is improved by almost 800 F, as proved by extended heat endurance testing. At short time heating exposure, these coatings withstand up to approximately 6500 F under actual test conditions. Adherence, elasticity, impact and thermal shock as well as vibration resistance are excellent.

Application Techniques

The most important methods of applying ceramic protective surfaces over metals are: Standard applications of ceramic coating, flame spray techniques, solution ceramics and surface layer depositions, a novel approach.

Conventional ceramic coatings and their modifications are applied by the customary porcelain enameling techniques of preparing a coating slip, with water or organics as vehicles; applying it on a precleaned metal surface by such standard methods as spraying (including automatic and electrostatic spraying), dipping, draining, slush coating, etc.; drying, and firing. A modification has been reported for low melting coatings by spraying the coating slip on a preheated metal surface, thus eliminating the subsequent firing (3).

The most important rivals of conventional ceramic coating techniques are the *flame spray applications*, adapting the flame spray metalizing process to ceramic materials. The method consists of melting ceramic particles deriving either from a powderized mixture or from a presintered rod in a high temperature flame, and ejecting the atomized particles under force onto clean metal surfaces on which they immediately solidify. Materials used for this purpose are standard refractories, such as alumina, zirconia, zircon, titania and also cermets. Depending on the base metal, on the refractory materials and on the number and thickness of layers applied, these coatings withstand very high temperature ranges. They have, however, a number of disadvantages; the adherence is only mechanical and must be closely controlled. This is especially important since many features, such as elasticity, impact, thermal shock and vibration resistance are functions of the adherence. The coating is porous and permeable and has insufficient erosion resistance. Although the equipment is not too expensive and can easily be transported to the place of operation, the cost of application is high.

The process called *Solution Ceramics* (4) has not become popular. It is accomplished by spraying atomized solutions of appropriate chemicals on clean, preheated metal surfaces. Its adherence is also mechanical and not chemical.

Great prospects are offered by the new technique of *surface layer depositions*. This method consists of layers of refractory materials adhering either to the base metal directly or to an intermediary layer by a means of suitable glasses or ceramic coatings.

It is produced by applying over a bisque layer of coating a layer of refractory particles and firing both layers simultaneously. It can be applied over the complete range of metals by using low melting glasses for light metal alloys, and low or high melting glasses for high alloys, super alloys and refractory metals. By this method, one can introduce high amounts of standard refractory materials, as well as the full line of "super" refractories, including cermets. One of its advantages is its resemblance to flame spray applications in appearance, performance and thickness of coating, preserving high adherence, continuity of coating and economy of application.

Modified ceramic coatings can be combined with the newly developed surface layer techniques. Thus, the refractory particles which are responsible for the final performance of the coating can be introduced by embedding them into the glass matrix or by applying them on the surface of the glass layer, by combining both systems, or finally, by using different types of refractory and superrefractory materials individually or combined in each layer. These many possible combinations widen the field of application for ceramic coatings and increase their potential performance.

Considerations of Lithia Bearing Coatings

The favorable influence of lithia on porcelain enamels and ceramic coatings has frequently been discussed. It is herewith summarized as follows:

Several properties of ceramic coatings depend on two main features: The amounts and types of interface metal oxides (5) deriving from the base metal and going into solution in the coating during the firing process, and the amounts and types of bubbles produced in the coating. Both factors depend on the composition of the coating, are especially influenced by the amounts and types of lithium compounds introduced, and on the firing cycles in respect to both time and temperature.

The *adherence* of coating to metal is affected by both the interface metal oxide layer and the bubble structure. Lithia acts as an adherence promoter in two ways: Because of its fluxing power, it widens the firing range thus helping the development of the oxide from the base metal; and because of its wetting power, it aids the penetration of the generated metal oxide into the coating. Figs. 1, 2 and 3 represent photomicrographs which demonstrate the interface oxide layers on coated stainless steel, aluminum and magnesium, respectively.

The *impact resistance* is a function of the adherence and of the thinness of the coating; lithia bearing coatings can be applied in thinner layers as explained by their effect as network modifiers (6). Also indirectly influenced by the high degree of adherence is the excellent resistance of lithia bearing ceramic coatings against *vibration*, a feature becoming increasingly important.

Thermal shock resistance is a function of several properties, such as adherence, thinness of coating and compatability of the coefficients of thermal expansion of the coatings and the base metals.

[2] Numbers in parentheses indicate References at end of paper.

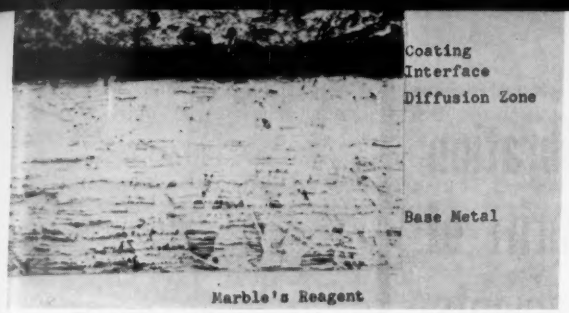

Fig. 1 Photomicrograph of a typical ceramic coating applied on stainless steel type 321

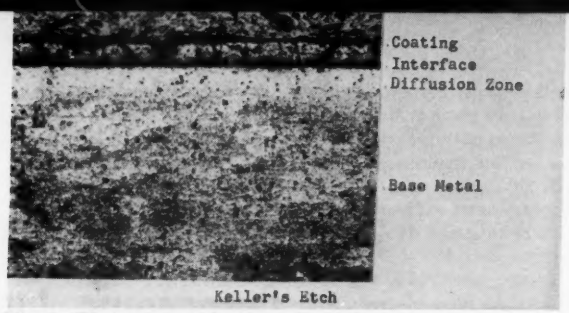

Fig. 2 Photomicrograph of an elevated temperature corrosion resistant ceramic coating applied on 3003 type aluminum

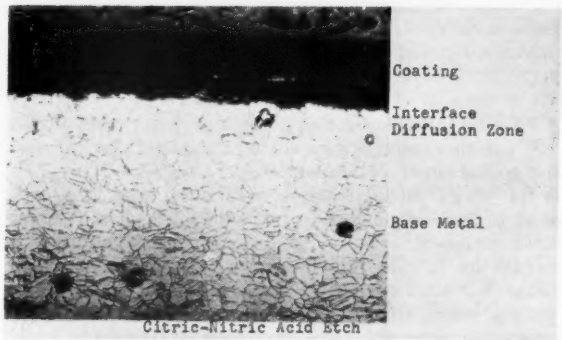

Fig. 3 Photomicrograph of a boron nitride bearing ceramic coating applied on magthorium HK21M

Investigations in recent years have proved that lithia has the highest thermal expansion coefficient, as compared to all commonly used ingredients of glasses. Its cubical coefficient of expansion is quoted (7) as 18×10^{-7} (per deg C), as compared to soda with 10×10^{-7}, which has become quite important for the development of coatings on different metals with wide variations of thermal expansion properties.

An explanation can be offered for the long prevailing belief that lithia reduces and not increases thermal expansion. It has been found that in the presence of even minute amounts of lithia, highly increased quantities of SiO_2 can be dissolved in glasses; silica having an extremely low coefficient of expansion thus reduces the total actual coefficient of expansion of the resulting glass.

With the introduction of space technology, the thermal shock resistance is not only important at ultra-high temperatures, but also at ultra-low temperatures. Lithia-based coatings perfectly resist repeated *freezing and thawing* action.

The extremely low *viscosity* of the lithia bearing glasses (8) readily permits the oxide-metal diffusion process. This low degree of viscosity is simultaneously responsible for the improvement in the continuity of the coating. The density factor of lithia is higher than that of the other alkalis and of many important constituents of glasses, such as silica, alumina, boric oxide and magnesia. The effect of lithium as a network modifier, giving rise to "contracted" or "condensed" glasses because of its small ionic radius, has become well-known (6); thus, lithium tends to reduce the number and sizes of voids in a system and creates a high continuity of the coating with an extreme degree of freedom of pores and pinholes. When replacing clay by lithium compounds (9) for the purpose of suspension of the slip, the bubble structure, an inherent characteristic of porcelain enamels, is very favorably influenced by reducing sizes and amounts of the bubbles.

The *hardness* of a ceramic coating depends to a great extent on the density of the glass and on the bubble structure. Moreover, hardness is an additive characteristic that can be calculated by using factors; these hardness factors show that lithia again ranges very highly and is superior to the other alkalis (10). *Surface hardness* is another additive characteristic of glasses, can equally be calculated and is also favorably influenced by lithia.

The *chemical resistance*, including *weather resistance*, of glasses or ceramic coatings also depends on refractory constituents, especially silica and titania. Additions of lithia do not influence chemical resistance directly, but are helpful in counterbalancing higher additions of such refractory ingredients, thus promoting the chemical resistance. The high continuity of the coatings due to lithia aids equally to prevent chemical attack through pores and pinholes. Lithium compounds are *nontoxic*.

Outlook for the Future

Conditions dictated by space flight and space technology are opening a new wide field for application of ceramic coatings. Refractory metals are becoming commercially available in many ways; new super alloys are being developed continuously, and light metal alloys which maintain tensile strength at elevated temperatures have surpassed the stage of pilot production. These materials, however, need protection against corrosion. The rapid development of new high energy fuels creates new problems. Ceramics by themselves have high heat resistance but show lack of structural strength. The ideal solution to many of the newly created problems seems to be offered by the combination of heat resistant ceramics with metals of high structural strength. This combination is offered solely by ceramic coatings. The art is rapidly advancing.

Acknowledgment

The writer expresses his appreciation for the valuable cooperation of his assistant, Gerald Geltman, and his thanks to Walter M. Fenton, Vice-President, Product Research & Development, Lithium Corporation of America, Inc., for his continuous assistance. The program of developing modified types of high temperature resistant ceramic coatings was initiated by the Lithium Corporation of America, Inc.

References

1 Taylor, K. M., "Boron Nitride," *Mat. and Methods*, Jan. 1956, *also* Tech. Bull., Carborundum Co.

2 Huppert, P. A., "Ceramic Coatings Raise Heat Resistance of Super Alloys," *Iron Age*, Nov. 14, 1957.

3 Frazer, R. F. and Cianchi, A. L., "Application of Protective Coating such as Enamel Compositions to Metal Surfaces," Brit. Pat. 642,105, July 12, 1950.

4 "Solution Ceramics—A New Development in Protective Coatings," *Ind. Heating*, vol. 21, no. 10, 1954, pp. 2097–2098.

5 King, B. W., Tripp, H. P. and Duckworth, W. H., "The Nature of Adherence of Porcelain Enamels to Metal," *Ceramic Ind.*, vol. 69, no. 3, 1957, p. 101.

6 Huppert, P. A., "Lithia in Porcelain Enamels—An Analysis of its Behavior," paper presented at the American Ceramic Society Convention, Dallas, Texas, May 8, 1957.

7 Vielhaber, L., "Emailtechnik," *Deutscher Ingenieur-Verlag*, Düsseldorf, 1953.

8 "Lithium Metals & Salts, Handbook," Hans-Heinrich-Huette ed., Frankfurt a/Main, Germany.

9 Fenton, W. M., "Mill Addition Agent for Enamel Slips," U. S. Pat. 2,662,028, Dec. 8, 1953.

10 Petzold, A., "Email," VEB Verlag Technik, Berlin, 1955.

Some Effects of Vibration and Rotation on the Drift of Gyroscopic Instruments[1]

R. M. STEWART[2]
Space Electronics Corp.
Glendale, Calif.

GYROSCOPIC instruments are now being used in the guidance and control systems of virtually every aircraft and guided missile of current design. Great care is exercised in the design, production and operation of these devices in order to minimize random or unpredictable drift of the indicated stable directions. Such things as bearing friction, torques due to interconnecting wires and mass unbalance are given close attention and have, through painstaking and ingenious instrument design, fabrication and assembly techniques and system planning, been reduced to suitable levels. However, it has become increasingly apparent that other sources of drift may occur which are aggravated by the high vibration levels and fast rotational response to disturbances characteristic of modern aircraft and missiles.

First of all we might ask, what are the fundamental causes of vibrations and oscillations of a rocket, which is our primary interest. There are basically four: 1 Motor combustion, 2 ignition and staging transients, 3 aerodynamically-generated sound and associated structural vibration, and 4 air turbulence and wind shear.

There are some important differences and similarities in these various factors. The first two, which are strictly propulsion problems, will always be present, whereas 3 and 4 are problems only within the atmosphere (ordinarily at altitudes of about 50,000 ft or less).

From another point of view, items 1 and 3 are the things ordinarily associated with vibration (mostly in the frequency range of about 20 to 2000 cps), while 2 and 4 are the things that give control system designers headaches and result in oscillations of somewhat lower frequencies (mostly within about 0.2 to 20 cps). Lack of structural rigidity, liquid fuel sloshing and control system idiosyncrasies aggravate this problem and should be considered as secondary causes of the oscillations. These factors may even have some bearing (however inconclusive) on the perennial solid vs. liquid propulsion debate in somewhat the following ways:

1 Optimum performance considerations for rockets have tended to result in higher thrust-to-weight ratios for solids than for liquids. The resulting higher accelerations often lead to higher maximum dynamic pressure.

2 Combustion induced vibration seems to be a more controllable and predictable factor in liquids than in solids. This is not necessarily a fundamental limitation for solids but is partially connected with the relative stage of development of the engines and the fact that in a solid propellant engine, the size and shape of the combustion chamber are continually changing during flight.

3 From the standpoint of structural stiffness, the solid propellant advocates claim the advantage.

4 Fuel sloshing is not a problem in a solid propellant rocket.

It would be presumptuous and somewhat foolish to try to draw any conclusion from these comments other than that there is an intimate connection between rocket design and guidance and control design which cannot be left entirely up to the judgment of specialists in either field. In a complete missile system preliminary design, it becomes apparent that the effects of missile environment on instrument reliability and accuracy may affect somewhat such system decisions as best type of propulsion system, optimum burning times and the ballistics and control scheme.

It is the purpose of this paper to describe and indicate possible analytical approaches to *some* of the most significant mechanisms by which vibration induced drifts may occur, and to indicate, where possible, some means of alleviating them. In all cases we will not consider gimbal bearing friction, mass unbalance or other sources of steady extraneous torques on the gyro rotor. The mechanisms to be discussed are: Non-Newtonian viscosity in single degree of freedom (SDF) integrating-rate gyros (1),[3] nonisoelasticity in SDF gyros, noncommutative effects for SDF stabilized platform, gimbal inertia effects, 2 DF gyros, and spin axis torque coupling in 2 DF gyros. High-frequency elastic resonances are not discussed explicitly in detail, because they are a more familiar problem and one which depends strongly on the details of each particular gyro design.

Non-Newtonian Viscosity in Platform Stabilizing SDF Integrating-Rate Gyros

Three SDF gyros may be used to stabilize a three-gimbal-axis platform. In the floated gyro, the rotor assembly is supported in an inner housing by a spin-axis bearing suspension. The inner housing is buoyantly supported by a high density liquid between the inner and outer housings, and is held in place by a low friction jeweled bearing.

The stable platform is provided with a servo system for each gyro, which detects and compensates for disturbing torques about the gimbal axes. The basic operation of the platform is such that only torques about the precession axes of the gyros affect the drift performance of the platform, and the corresponding drift of the platform is always around the input axis of the gyro in question.

To describe the drift performance of the stable platform, it will be convenient to introduce the following notation: Let p_n, s_n, h_n be an orthogonal set of unit vectors directed along the precession (output), spin and input axes of the nth gyro. These vectors are oriented so that $h_n \times p_n = s_n$. Let $\phi_n(t)$ denote the angle through which the stable platform drifts because of a torque $L_n(t)$ applied about the precession axis of

Presented at the ARS Semi-Annual Meeting, Los Angeles, Calif., June 9–12, 1958.

[1] This paper presents the results of one phase of research performed at the Jet Propulsion Laboratory, California Institute of Technology, Pasadena, Calif., under Contract no. DA-04-495-Ord 18, U. S. Army Ordnance Corps.

[2] R. M. Stewart was formerly a Staff Engineer at the Jet Propulsion Laboratory, California Institute of Technology, and Member of the Senior Staff, Ramo-Wooldridge Corp.

[3] Numbers in parentheses indicate References at end of paper.

the nth gyro. This angle is measured in the counterclockwise direction about the particular input axis with which it is associated.

It may be shown that if the natural nutational frequency or any structural resonance frequencies of the gyro in question are large compared to the significant frequency components of $L(t)$, then $\phi_n(t)$ is given by the simple expression

$$\phi_n(t) = -\frac{1}{H_n}\int_0^t L_n(\tau)d\tau = -\frac{1}{H_n}\int_0^t (L_n \cdot p_n)d\tau \qquad [1]$$

where H_n is the spin-angular momentum of the nth gyro, and L_n is the total vector torque in the gyro.

When a single degree of freedom integrating-rate gyro precesses, there is a viscous restraining torque about the precession axis. Ideally, the viscous torque is proportional to angular rate (Newtonian viscosity)

$$L_{v_n} = -K_v\dot{\xi} \qquad [2]$$

where ξ is the angular rotation of the gimbal relative to the outer case. Then, for low frequency inputs, Equation [1] can be used with the understanding that $\phi(t)$ is a proper input angle

$$\phi_n(t) = \frac{1}{H_n}\int_0^t K_v\dot{\xi}dt = \left(\frac{K_v}{H_n}\right)\xi(t) \qquad [3]$$

or, as desired, angular rotation about the input axis is proportional to the precession angle. (Gyros of this type are frequently constructed so that the constant of proportionality is unity.) Frictional or viscous effects, however, which give rise to torques other than this type (Eq. [2]) may cause cumulative errors since then the integration of Equation [3] cannot be carried out to give $\phi_n(t)$ as a unique function of ξ. The fact that they are linearly related is not so important as the requirement that they be merely uniquely related. There is a larger class of viscous-type torques than that given by Equation [2] which satisfy this requirement, namely

$$L_{v_n} = K_v f(\xi)\dot{\xi} \qquad [4]$$

where $f(\xi)$ is a single-valued function of ξ. Then

$$\begin{aligned}\phi_n(t) &= -\frac{1}{H_n}\int_0^t K_v f(\xi)\dot{\xi}dt \\ &= -\frac{K_v}{H_n}\int_0^{\xi(t)} f(\xi)d\xi = \frac{K_v}{H_n}g(\xi)\end{aligned} \qquad [5]$$

where $g(\xi)$ is a single-valued function of ξ. In other words, input and output are still uniquely related if the constant angular velocity coefficient characteristic of Newtonian-type viscosity is replaced by any single-valued function of the precession angle ξ.

If the viscous torque is a function of $\dot{\xi}$ only, but a nonlinear one, then, even though no unique relation will exist between ξ and ϕ, no cumulative drift will occur so long as

1 ξ (and, hence $\dot{\xi}$) may be reasonably represented as stationary time-series having zero mean value due to the action of the platform gyro feedback circuits.

2 The curve of torque vs. $\dot{\xi}$ has odd symmetry.

3 All probability distribution functions of ξ and $\dot{\xi}$ have even symmetry (plus and minus values occur with equal frequency, etc.). It is possible to elaborate on this point in a number of ways, but it appears to be virtually self-evident and will not be considered further in this paper.

These conditions will tend to be satisfied as long as the gyro, feedback circuits, torquers and the excitation all have symmetrical characteristics. Lack of symmetry in any of these respects may be expected to produce a drift of the platform which is roughly linear with time.

Other types of anomalous frictional and viscous effects may result in cumulative drift of the platform, but there will be a tendency for the effect to average out somewhat in a statistical fashion during the period of a single flight. For example, it may be easily shown from Equation [1] that stationary random contributions to anomalous precession-axis torques of zero mean value would cause drifts of the platform such that the rms drift angle would increase, for times somewhat longer than the significant correlation time, only as $1\sqrt{n}$ times the drift due to a steady torque of the same magnitude, where n is the number of significant correlation intervals. Furthermore, the magnitude of such effects is highly correlated with the magnitude of angular deviations and rates of the platform, and hence can be minimized by good design of the servo loop around the platform. Similar effects occur due to rotations of the outer case of the gyro about the precession axis. For example, if the gyro is suddenly turned about this axis from one position to another and then back again, a net error may result from the inner can's (gimbal) not returning to its original position, but, again, the magnitude of this type of error in flight is highly correlated with the tightness of the platform servo loop.

Drifts Due to Nonisoelastic Displacements of the SDF Gyro Gimbal

Let the acceleration to which the platform is subjected due to thrust and drag be represented by a. The vector a may be projected along the p, h and s directions of each gyro.

$$a = (a\cdot p_n)p_n + (a\cdot s_n)s_n + (a\cdot h_n)h_n \qquad [6]$$

It may be assumed that the displacement of the center of mass of the gyro rotor in each of these directions is proportional to the acceleration but opposite in direction

$$d_n = -k_p(a\cdot p_n)p_n - k_s(a\cdot s_n)s_n - k_h(a\cdot h_n)h_n \qquad [7]$$

where k_p, k_s and k_h are "compliance coefficients" that depend on the construction of the gyros. The resultant torque on the nth gyro due to the displacement d_n is given by

$$L_n = -(d_n \times Ma) \qquad [8]$$

where M is the mass of the gyro rotor and axle. Only the component of L_n along p_n results in a drift. The torque in this direction is given by

$$\begin{aligned}L_n\cdot p_n &= -(d_n \times Ma)\cdot p_n \\ &= M(k_s - k_h)(a\cdot s_n)(a\cdot h_n)\end{aligned} \qquad [9]$$

The drift angle ϕ_n due to this torque is calculated from Equation [1]

$$\phi_n(t) = \frac{M(k_s - k_h)}{H_n}\int_0^t (a\cdot s_n)(a\cdot h_n)dt \qquad [10]$$

In a ballistic missile, by choosing a set of gyro orientations such that, in every case, either the spin or input axis is perpendicular to the azimuth plane, it is apparent from the preceding expression that most of the effect of steady thrust and drag forces can be eliminated.[4] The effect of vibration, however, is not eliminated by this means and probably requires that considerable effort be employed to make the gimbal structure isoelastic along the spin and input axes, i.e., to make $k_s = k_h$ in Equation [10].

In order for vibration to cause a serious cumulative effect, it is necessary that, over an extended period of time, the vibrations along the two significant axes should be highly correlated or, roughly, maintain a fixed phase relation. The usual analytical treatment of this effect considers a sinusoidal oscillation along a fixed but skewed axis, and the result indicated is a drift which increases approxi-

[4] This conclusion is contingent, of course, on the validity of [7], which implies that the principal elastic axes coincide with the geometric axes of symmetry of the gyro structure and assembly.

mately linearly with time. A similar result is obtained for a stationary random vibration along a fixed skewed axis. If the vibration components are considered to be independent stationary random variables, then the bandwidth and relative frequency location of these vibrations may be seen to be important in determining the severity of effect; sharp resonances (narrow bandwidths) which give rise to long-term coherent vibration must be avoided.

The following analysis illustrates this effect more exactly. Equation [10] which, it should be remembered, holds at frequencies below the gyro nutational frequency may be written

$$\phi(t) = \frac{M(k_s - k_h)}{H} \int_0^t a_s a_h dt \qquad [11]$$

If a_s and a_h are considered to be stationary random variables, then it may easily be shown that the mean square drift angle $\sigma_\phi^2(t)$ is given by

$$\sigma_\phi^2(t) = \frac{2M^2(k_s - k_h)^2 t}{H^2} \int_0^t \left[1 - \frac{\tau}{t}\right] \phi_{sh}(\tau) d\tau \qquad [12]$$

where $\phi_{sh}(\tau)$ is the autocorrelation function of the product $a_s a_h$. If a_s and a_h are independent, then

$$\phi_{sh}(\tau) = \phi_s(\tau)\phi_h(\tau) \qquad [13]$$

where ϕ_s and ϕ_h are the autocorrelation functions of a_s and a_h, respectively. Making this substitution and considering times t somewhat longer than the significant correlation time (roughly inverse of bandwidth) the integral above becomes

$$\sigma_\phi^2(t) \approx \frac{2M^2(k_s - k_h)^2}{H^2} t \int_0^\infty \phi_s(\tau)\phi_h(\tau) d\tau \qquad [14]$$

This last integral is proportional to the low frequency spectral density of the product $a_s a_h$. If the vibrations along the two axes are statistically similar, differing only in magnitude, then

$$\begin{aligned} \phi_s(\tau) &= \sigma_s^2 R(\tau) \\ \phi_h(\tau) &= \sigma_h^2 R(\tau) \end{aligned} \qquad [15]$$

where $R(\tau)$ is the normalized autocorrelation function of a_s, and a_h ($R(0) = 1$, and σ_s and σ_h are the mean square values of a_s and a_h, respectively). Thus if we define the "effective correlation time" T as

$$T = \int_0^\infty R^2(\tau) d\tau$$

and the "bandwidth" as

$$\begin{aligned} B &= \frac{1}{T} \\ \sigma_\phi^2(t) &= \frac{2M^2(k_s - k_h)^2 \sigma_s^2 \sigma_h^2 t}{H^2 B} \end{aligned} \qquad [16]$$

Thus the root mean square drift angle increases with the square root of time and decreases in the same way with increasing bandwidth. Thus, it is important, in connection with nonisoelastic effects, to avoid sharp vibration resonances.

Noncommutative Effects for SDF Stabilized Platform

The following analysis is intended to illustrate a frequently neglected phenomenon which will produce drift of an SDF gyro-stabilized platform. This phenomenon will be called the "noncommutative" effect because of the close analogy to the well-known fact that angles are noncommutative, i.e., that the final orientation of a rigid body which undergoes a sequence of finite rotations about body-fixed axes is not a unique function of the angles alone, but depends on the order in which the rotations occur. A simple consequence of this is that a sequence $(A, B, -A, -B)$, where A and B are rotations around two different axes, will ordinarily not result in a return to original orientation in spite of the fact that the net rotation about each axis ($A - B$ and $B - B$) is zero.

The drift due to nutation described in (2) is a special case related to this effect, and, owing to the phase coherent oscillating nature of the transient errors, produces a serious cumulative drift, which increases approximately linearly with time.

What this analysis is intended to show, however, is that even if nutation is completely eliminated there will still be a "random walk" type of drift. This random drift depends on the magnitude of transient errors due to all causes.

As a simple example of noncommutativity, and one which gives a preliminary feeling for the effect, the following situation has been considered. Assume that a platform rotates with angular velocities ω_x, ω_y, ω_z around three mutually perpendicular axes (x, y, z) attached to the platform. For simplicity, consider $\omega_z = 0$ and ω_x and ω_y square waves of arbitrary phase

$$\omega_x = \begin{cases} a, & 0 \le t \le T_1 + T_2 \\ -a, & T_1 + T_2 \le t \le 2(T_1 + T_2) \end{cases}$$

$$\omega_y = \begin{cases} b, & 0 \le t \le T_1 \\ -b, & T_1 \le t \le 2T_1 + T_2 \\ b, & 2T_1 + T_2 \le t \le 2(T_1 + T_2) \end{cases}$$

Then consider the position of the platform, relative to its initial rest position, at time $2(T_1 + T_2)$. At this time, the integrals of the rates

$$\int_0^t \omega_x dt, \int_0^t \omega_y dt, \int_0^t \omega_z dt$$

are all zero. But a straightforward (and somewhat tedious) calculation shows that the platform will have rotated through an angle ϕ given by

$$\cos\frac{\phi}{2} = 1 - \frac{2a^2b^2}{(a^2 + b^2)^2}\left(1 - \cos\sqrt{a^2 + b^2}T_1\right)\left(1 - \cos\sqrt{a^2 + b^2}T_2\right)$$

For small angles this reduces approximately to

$$\phi = 2\epsilon_x\epsilon_y\theta$$

where

$\epsilon_x = aT$ = "amplitude" of $\int \omega_x dt$
$\epsilon_y = bT_1$ = "amplitude" of $\omega_y dt$
$\theta = T_2/T$ = "phase" between x and y oscillations, and $T = T_1 + T_2$

This equation can also be used to give a rough idea of what to expect if ϵ_x and ϵ_y are independent stationary random processes of zero mean value having a narrow-band but distributed continuous spectrum. A simple model of such errors is one in which the above cycle is repeated coherently for n cycles, then again coherently for another n cycles with new independent values of ϵ_x, ϵ_y and θ, etc. At the end of n cycles[5]

$$\phi_n \approx n\phi = n(2\epsilon_x\epsilon_y\theta)$$

or, averaging over θ and assuming root mean square ϵ_x and ϵ_y both equal to σ_ϵ

$$\sigma_{\phi_n} \approx n\sigma_\epsilon^2$$

If B is called the effective bandwidth and is made equal to the reciprocal of the time required for n coherent cycles, then

[5] This might be called the "coning" equation, since it indicates the approximately linear drift with time due to sinusoidal coherent coning which has been noted by various persons.

$n = f_o/B$, where f_o is the frequency of oscillation (or "center frequency") and hence

$$\sigma_{\phi_n} \approx \frac{f_o}{B}\sigma_\epsilon^2$$

Since subsequent intervals of n cycles are considered to be independent, after a long time t, there will have occurred about $m = Bt$ independent coherent periods, and, according to the well-known theory of random walks

$$\sigma_{\phi_m} = \sqrt{m}\sigma_{\phi_n}$$

Therefore

$$\sigma_\phi(t) \approx \frac{f_o}{B}\sigma_\epsilon^2\sqrt{m} = \sigma_\epsilon^2 f_o\sqrt{\frac{t}{B}}$$

This final expression indicates then a drift whose magnitude increases as the square of the amplitude of transient errors, is proportional to the center frequency, increases with a random walk-type dependence on time and increases with decreasing bandwidth.

The following portions of this report deal with a more refined analysis of this problem which, however, leads to a similar result. Before launching into such an analysis, it is well to examine a few possible numbers in order to justify further attention to this problem.

Assuming

$$\begin{aligned} \sigma_\epsilon &= 10 \text{ mils} \\ f_o &= 15 \text{ cps} \\ B &= 2 \text{ cps} \\ t &= 60 \text{ sec} \end{aligned}$$

the equation above gives $\sigma_\phi \approx 0.5$ deg.

As a next step in the statistical analysis of this effect we propose the following problem: Assume that the motion of the platform under the influence of various disturbances and the correcting action of the servo loops is such that the integrals of angular rates about three mutually perpendicular axes attached to the platform are *independent stationary* random variables having *zero mean value*. This is approximately what would be expected using perfect HIG-type integrating-rate gyros with high viscosity and simple output-nulling feedback, since each output is ideally the integral of the corresponding input angular rate. Calculation of the mean square drift to be expected will then be attempted, and it will be shown that it does, in fact, tend to increase with time approximately as indicated in the previous section.

It should be noted that the assumption of stationary integrated rate implies not only statistically stationary angular rates but also a certain restrictive condition on allowable autocorrelation functions for the angular rates ω_x, ω_y, ω_z. Consider the output of the x gyro

$$\epsilon_x(t) = \int_0^t \omega_x dt$$

If ω_x is assumed stationary, then it may be easily shown that, unless the spectral density of ω_x at low frequencies, say $\Phi_{\omega x}(0)$, is zero, ϵ_x will not be stationary but instead will have a mean square value which increases approximately linearly with time. Since the normal action of the platform feedback loops is such as to prevent ϵ from increasing without bound, choices of ω must be limited to those for which

$$\Phi_\omega(0) = 0$$

Since Φ must also go to zero at high frequencies, the allowable spectral distributions for ω must be of the type shown in Fig. 1.

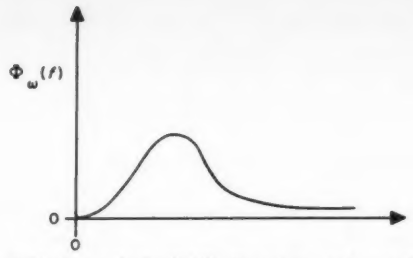

Fig. 1 Typical spectral distribution for each angular rate component

Because of the mutual Fourier transform relation between spectral density and autocorrelation function, this requirement is equivalent to the requirement that the integral of the autocorrelation function of each ω over all time should also be zero

$$\int_0^\infty \phi_\omega(\tau)d\tau = 0$$

Let x_0, y_0, z_0 be the components of a vector fixed in the platform at time $t = 0$, relative to some fixed coordinate system. Then if the platform is rotated at subsequent times, the vector will have new components $x(t)$, $y(t)$, $z(t)$, and for each time t there will be an orthogonal matrix $A(t)$ such that $X = AX_0$ where $X_0 = (x_0, y_0, z_0)$, and $X = (x, y, z)$. The problem is that of finding $A(t)$ given only statistical information about the angular velocity components. Let $\Omega = (\omega_x, \omega_y, \omega_z)$ be the angular velocity vector. Then

$$\dot{X} = \frac{d}{dt}X = \omega \times X = \omega \times AX_0$$

and also

$$\dot{X} = \frac{d}{dt}AX_0 = \dot{A}X_0$$

so that

$$\dot{A}X_0 = \omega \times AX_0$$

But

$$\omega \times X = (\omega_y z - \omega_z y, \omega_z x - \omega_x z, \omega_x y - \omega_y x) = MX$$

where M is the matrix

$$M = \begin{pmatrix} 0 & -\omega_z & \omega_y \\ \omega_z & 0 & -\omega_y \\ -\omega_y & \omega_x & 0 \end{pmatrix}$$

so that $\dot{A}X_0 = MAX_0$. But this must be true for all X_0; hence

$$\dot{A} = MA$$

The example worked out above corresponds to the exact solution of these differential equations for the case where M is a constant matrix over each of three ranges whose sum is the whole interval. Exact solution of the equations is impossible, however, except in certain such specific cases. As long as M is a continuous matrix the equations can be solved approximately by an iteration procedure which will converge.

Let

$$A_{n+1} = A_0 + \int_0^t MA_n dt$$

where A_0 is the identity matrix (corresponding to no rotation at $t = 0$ as an initial condition). Then a Lipschitz condition is fulfilled by the equation which guarantees the convergence of

$\lim_{n\to\infty} A_n$, and clearly this limit satisfies the differential equations. Thus

$$A(t) = A_0 \int_0^t M(\tau_1)A_0 d\tau_1 + \int_0^t M(\tau_1)\int_0^{\tau_1} M(\tau_2)A_0 d\tau_2 d\tau_1 + \int_0^t M(\tau_1)\int_0^{\tau_1} M(\tau_2)\cdots\int_0^{\tau_{n-1}} M(\tau_n)A_0 d\tau_n d\tau_{n-1}\cdots d\tau_2 d\tau_1$$

The first three terms in this expansion are

$$A(t) \sim \begin{matrix}100\\010\\001\end{matrix} + \begin{pmatrix} 0 & -\int_0^t \omega_z dt & \int_0^t \omega_y dt \\ \int_0 \omega_z dt & 0 & -\int_0^t \omega_x dt \\ -\int_0^t \omega_y dt & \int_0^t \omega_x dt & 0 \end{pmatrix} + \begin{pmatrix} -\int z \int z - \int y \int y & \int y \int z & \int z \int x \\ \int x \int y & -\int x \int x - \int z \int z & \int z \int y \\ \int x \int z & \int y \int z & -\int y \int y - \int x \int x \end{pmatrix}$$

where $\int z \int z$ means

$$\int_0^t \omega_z(\tau_1)\int_0^{\tau_1} \omega_z(\tau_2)d\tau_2 d\tau_1$$

and $\int x \int y$ means

$$\int_0^{t^+} \omega_x(\tau_1)\int_0^{\tau_1} \omega_y(\tau_2)d\tau_2 d\tau_1$$

The first term above is the original matrix A_0; the second gives the stationary component of jitter corresponding directly to the gyro transient errors, and the third represents the first order uncorrected effect.

One of the quantities of interest is the component of an accelerometer axis along a direction initially perpendicular to it; for example, what fraction of the y accelerations is picked up by the x direction accelerometer. The result is easily seen to be $x \cdot y_0$

$$\begin{aligned} x \cdot y_0 &= (a_{11}, a_{21}, a_{31})(0, 1, 0) \\ &= \int_0^t \omega_x dt + \int_0^t \omega_x(\tau_1)\int_0^{\tau_1} \omega_y(\tau_2)d\tau_2 d\tau_1 \end{aligned}$$

If ω_x and ω_y are stationary random variables of mean zero, then

$$\sigma^2 \int_x \int_y (t) = \overbrace{\left[\int_0^t \omega_x(\tau_1)\int_0^{\tau_1} \omega_y(\tau_2)d\tau_2 d\tau_1\right]\left[\int_0^t \omega_x(\tau_3)\int_0^{\tau_3} \omega_y(\tau_4)d\tau_4 d\tau_3\right]}$$

where $\overbrace{\quad}$ denotes ensemble average. Then

$$\begin{aligned} \sigma^2 \int_x \int_y (t) &= \overbrace{\int_0^t\int_0^t \omega_x(\tau_1)\omega_x(\tau_3)\int_0^{\tau_1}\int_0^{\tau_3} \omega_y(\tau_2)\omega_y(\tau_4)d\tau_4 d\tau_2 d\tau_3 d\tau_1} \\ &= \int_0^t\int_0^t \overbrace{\omega_x(\tau_1)\omega_x(\tau_3)}\int_0^{\tau_1}\int_0^{\tau_3} \overbrace{\omega_y(\tau_2)\omega_y(\tau_4)}d\tau_4 d\tau_2 d\tau_3 d\tau_1 \\ &= \int_0^t\int_0^t \phi_{\omega_x}(\tau_3 - \tau_1)\int_0^{\tau_1}\int_0^{\tau_3} \phi_{\omega_y}(\tau_2 - \tau_4)d\tau_4 d\tau_2 d\tau_3 d\tau_1 \end{aligned}$$

where $\phi_{\omega_x}(\tau)$ is the autocorrelation function for ω_x.

In order to evaluate this integral in a fairly general way, it is necessary to choose a typical form of autocorrelation function. In general, autocorrelation functions must have the following properties

$$\phi_\omega(-\tau) = \phi_\omega(\tau)$$

$\phi_\omega(0) = \sigma_\omega^2$. (Thus if we let $\phi_\omega(\tau) = \sigma_\omega^2 R_\omega(\tau)$ then $R_\omega(0) = 1$.)

$$\phi_\omega(\infty) = 0, \text{ if the mean value of } \omega \text{ is zero}$$

$$|\phi_\omega(\tau)| \leq \phi_\omega(0) \text{ for all } \tau$$

In addition, as discussed in the first section, it is essential to choose for this problem,

$$\int_0^\infty \phi_\omega(\tau)d\tau = 0$$

in order that the gyro outputs do not increase in magnitude with time.

Many functions satisfying these requirements were tried, but the only one for which the integral has been successfully evaluated is the function

$$R_\omega(\tau) = \begin{cases} \cos \omega_0\tau, & |\tau| \leq \dfrac{2\pi n}{\omega_0} \\ 0, & |\tau| > \dfrac{2\pi n}{\omega_0} \end{cases}$$

where n is any integer.

Unfortunately, this is an impossible autocorrelation function because of another requirement for such functions, namely, their Fourier transforms should be everywhere positive, since that is the power spectrum which must be the square of an absolute value. This requirement is not satisfied by the above function, but it is felt that this will not cause any significant difference in the final result.

The integral to be evaluated then is of the form

$$\sigma_\omega^4 \int_0^t\int_0^t R_\omega(\tau_3 - \tau_1)\int_0^{\tau_1}\int_0^{\tau_3} R_\omega(\tau_4 - \tau_2)d\tau_4 d\tau_2 d\tau_3 d\tau_1$$

The inner integral pair is symmetric in τ_3 and τ_1, as is the outer integrand. Thus, in the final integration only $\tau_3 \geq \tau_1$ will need to be considered. And since $R(\tau) = 0$ for $\tau \geq 2\pi n/\omega_0$, the integration can be performed over several regions and then added.

The result of this integration for $t \geq 4n\pi/\omega_0$ is

$$\sigma^2 \int_x \int_y (t) \approx \frac{2n\pi\sigma_\omega^4}{\omega_0^3} t$$

By the Schwarz inequality, it can be shown easily that in general $\sigma^2 \int_x \int_y$ is proportional to t, but the universal bounding constant so obtained is so large that it is of no value. This is due to the fact that the inequality takes no account of oscillation in $R(\tau)$.

If it is noted that the "bandwidth" B corresponding to the autocorrelation function assumed is about $B = f_0/n$. Then

$$\sigma^2(t) \approx \frac{\sigma_\omega^4}{\omega_0^2}\frac{t}{B}$$

or

$$\sigma(t) \approx \frac{\sigma_\omega^2}{\omega_0}\frac{t}{B}$$

In order to compare this with the result given in the first section, note that

$$\phi_\omega(\tau) = -\frac{d^2}{d\tau^2}\phi_\epsilon(\tau)$$

Thus, for this case,

$$\phi_s(\tau) = \begin{cases} \frac{\sigma_\omega^2}{\omega_0^2} \cos \omega_0 \tau, & |\tau| \leq \frac{2\pi n}{\omega_0} \\ 0, & |\tau| > \frac{2\pi n}{\omega_0} \end{cases}$$

and hence

$$\sigma_\epsilon^2 = \phi_s(0) = \frac{\sigma_\omega^2}{\omega_0^2}$$

and

$$\sigma(t) = 2\pi\sigma_\epsilon^2 f_o \sqrt{\frac{t}{B}}$$

Except for a factor of 2π, this is the same result as obtained in the first section. Using this formula and the same numbers used in that section, $\sigma \approx 3$ deg. An analysis which takes into consideration the gyro dynamics in more detail leads to similar results for similar amplitudes of vibration of the spin axis.

2 DF Free Gyro, Effect of Gimbal Inertia

Anisoelasticity is also a potential problem with the two degree of freedom gyro, but there are other more unique mechanisms, particularly those associated with airframe oscillations if the gyro is attached directly to the airframe.

One aspect of this problem is treated in (2), where it is shown that spin axis nutations may be induced which cause a quasi-steady drift by sudden movement of the outer case of the gyro. This is true even in the absence of bearing friction, and is brought about by inertial coupling through the gimbal when the spin axis is not orthogonal to the two gimbal axes.

Similar effects occur if the case of the gyro is oscillating due to oscillations of the vehicle, but these will not be treated further in this paper due to the similarity to the effects described in (2).

2 DF Gyro Spin Axis Torque Coupling

Another possible source of drift in a 2 DF gyro, somewhat similar to the preceding one in that it is induced by rotational oscillations of the gyro case when the spin axis is not orthogonal to the two gimbal axes, is the excess torque characteristic of the spin motor when it "slips" out of the stable synchronous running condition.

It is frequently overlooked that a perfect 2 DF gyro should really have three degrees of freedom, the third one being the spin axis. Neglecting gimbal inertia as well as gimbal bearing friction, the spinner could certainly not be caused to wobble if it were freely coasting on perfect spin axis bearings. An extreme opposite assumption concerning the spin axis (which is frequently made to expedite analytic studies) is that the speed of the rotor is constant, relative to the motor case attached to the inner gimbal frame. This would be the case for an extremely "tight" synchronous motor. Such a response would, however, suggest extremely large amounts of wobble which, through a type of noncommutative effect, might lead to serious cumulative drift. The actual circumstances lie somewhere between these extremes, and the following analysis is intended to give a better approximation to a realistic situation.

Consider the 2 DF gyro schematic shown in Fig. 2. The angle α is the angle between the spin axis and the normal to the two gimbal axes. We assume that the vehicle within which the gyroscope is attached is oscillating around the normal to the gimbal axes with angular velocity Ω_v or, at any time, it has rotated from the nominal position shown through an angle β_v.

Then, assuming a near-perfect gyro which produces only

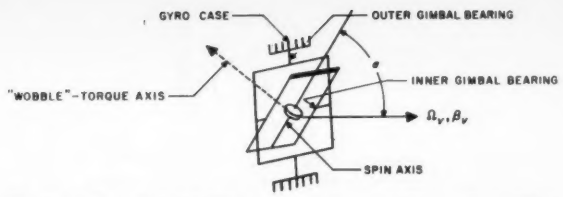

Fig. 2 Schematic of 2 DF gyroscope in nonorthogonal condition

negligible spin axis torques, the angular spin axis "slip" δ_S must be approximately given by

$$\delta_S \approx \left(\frac{1}{\cos \alpha}\right) \beta_v$$

and, assuming an excess motor torque proportional to this slip angle

$$L_{\text{spin}} \approx K_M \delta_S = K_M \left(\frac{1}{\cos \alpha}\right) \beta_v$$

However, the net vector torque on the spinner must also lie along the line normal to the two (assumed perfect) gimbal axes, and hence must include a component, in addition to that around the spin axis, around the line indicated as the "wobble"-torque axis. Clearly, then

$$(\sin \alpha) L_{\text{spin}} - (\cos \alpha) L_{\text{wobble}} = 0$$

or

$$L_{\text{wobble}} = (\tan \alpha) L_{\text{spin}}$$

Hence

$$L_{\text{wobble}} = K_{\text{motor}} \left(\frac{\tan \alpha}{\cos \alpha}\right) \beta_v$$

In terms of two Eulerian angles[6] θ and ϕ which indicate the amount of wobble of the spin axis, the approximate equations of motion, assuming small θ and ϕ, are

$$I_x \ddot{\phi} - I_s \omega_s \dot{\theta} = 0$$

$$I_x \ddot{\theta} + I_s \omega_s \dot{\phi} = L_{\text{wobble}}$$

where I_x is the spinner transverse moment of inertia, and $I_s\omega_s$ is the spinner angular momentum (see (3)).

For frequencies of oscillation ω well below the gyro spin frequency, since

$$|\phi| = \frac{I_s \omega_s}{I_x \omega} |\theta|$$

then

$$|\phi| \gg |\theta|$$

and these ϕ-oscillations correspond to wobble of the spinner around the inner gimbal axis. Solving these equations simultaneously for the steady-slide amplitudes associated with sinusoidal oscillations gives

$$\left[-\frac{I_x^2 \omega^2}{I_s^2 \omega_s^2} + 1 \right] |\phi| = \frac{|L_{\text{wobble}}|}{I_s \omega_s}$$

Or, for low frequencies

$$|\phi| \approx \frac{|L_{\text{wobble}}|}{I_s \omega_s \omega}$$

[6] θ in these equations differs by 90 deg from θ as defined in (3).

or

$$|\phi| \approx K_{\text{motor}} \frac{\left(\frac{\tan \alpha}{\cos \alpha}\right) |\beta_v|}{I_s \omega_s \omega}$$

In order to estimate roughly the magnitude of this effect, let us suppose that the peak excess spinner torque

$$|L_{\text{spin}}| = K_M \left(\frac{1}{\cos \alpha}\right) |\beta_v|$$

equals the peak torque available to start the gyro from rest and bring it up to running speed. Then

$$|\phi|_{\max} \cong \frac{\tan \alpha}{I_s \omega_s \omega} |L_{\text{start}}|$$

But, approximately

$$\frac{L_{\text{start}}}{I_s \omega_s} = \frac{1}{T_{\text{start}}}$$

where T_{start} is the "run-up" time of the gyro. Then

$$|\phi|_{\max} \approx \frac{\tan \alpha}{\omega T_{\text{start}}}$$

and for $\alpha = 45$ deg

$$|\phi(45 \text{ deg})|_{\max} \approx \frac{1}{\omega T_{\text{start}}}$$

If ω corresponds to $\frac{1}{2}$ cps, and $T_{\text{start}} \approx 30$ sec, this gives

$$|\phi\ (45 \text{ deg})|_{\max} \approx \frac{1}{(2\pi)(0.5)(30)} \cong 10^{-2} \text{ rad}$$

$$\approx \tfrac{1}{2} \text{ deg}$$

This wobble by itself might not be serious, but, coupled with a θ-wobble, due perhaps to gimbal inertia effects of the same magnitude, it would be expected, through a noncommutative-type effect such as described previously, to cause a cumulative drift of order of magnitude

$$\epsilon_{\max} \approx |\phi|^2_{\max} \approx 10^{-4} \text{ rad/cycle}$$

or

$$\dot{\epsilon}_{\max} \approx \omega \epsilon_{\max} = \pi \times 10^{-4} \text{ rad/sec}$$

$$\approx 65 \text{ deg/hr}$$

Such a drift rate is easily detected and frequently objectionable.

If the gyro were closer to "gimbal-lock" (where the axis becomes parallel to the outer gimbal axis) then the error increases rapidly.

For example, let $\alpha = 80$ deg with all other conditions as before. Then, $\dot{\epsilon}_{\max} \approx 2100$ deg/hr! Statistical treatment of this problem indicates, as in the other cases, that a random walk type of drift is to be expected.

Conclusion

A number of theoretical models of gyro drift induced by vibration, transient errors and rotational oscillations of the carrier have been discussed. In a sense, each is an idealized abstraction of the actual situation intended to indicate the requirements for some of the simplest nontrivial mechanisms of drift. In practice, all these, and others not so amenable to analysis, occur simultaneously and may interact strongly. One of the most challenging contemporary problems in this field is that of devising tests suitable for detecting, isolating and correcting the causes of drift due to random excitation. In striving for this goal, extensive theoretical analysis appears to be an indispensable companion to experimental work.

In the field of engineering design, efforts applied along the following general lines will all contribute to a program for improved inertial systems:

1 Reduce level of vibration by improved motor design, aerodynamic design and ballistics and control schemes.

2 Attempt to attain tighter attitude control of missiles; this effort will be aided by better structural rigidity and alignment.

3 In all of the mechanisms of drift that have been discussed, asymmetries, lack of orthogonality or wobbling in preferred directions appear to be particularly serious offenders. Thus, these situations should be avoided whenever possible by avoiding asymmetries in rigidity of supporting structures and deleterious platform control system cross-coupling.

4 Lastly, is the field of gyro and platform design in itself. Indications here again are for increased symmetry, lighter gimbals, higher structural resonant frequencies, stiffer structures and decreased gimbal bearing and spin axis torques.

Acknowledgment

This paper is a condensation of work done sporadically at the Jet Propulsion Laboratory over the last four years. The author wishes to acknowledge contributions by and helpful discussions with some of the present and former members of the Laboratory staff: Robert Parks, for general information, suggestions and encouragement; John Scull, for advice on the experimental facts of life; and Tom Layton, Lee Sonneborn and Charles Miller for analytical contributions.

References

1 Draper, C. S., Wrigley, W. and Grohe, L. R., "The Floating Integrating Gyro and its Application to Geometrical Stabilization Problems on Moving Bases," *Aeron. Engng. Rev.*, vol.1 5, no. 6, June 1956, pp. 46–62.

2. Plymale, B. T. and Goodstein, R., "Nutation of a Free Gyro Subjected to an Impulse," *Trans. ASME*, vol. 77, 1955, *also J. Appl. Mech.*, vol. 22, Sept. 1955, pp. 365–366.

3. Houston, W. V., "Principles of Mathematical Physics," McGraw-Hill Book Co., New York, 1934, 1st ed., pp. 117–122.

Improvements in the Operating Characteristics of n-Propyl Nitrate

R. W. LAWRENCE[1] and W. P. KNIGHT[2]

Aerojet-General Corp.
Azusa, Calif.

This paper summarizes chemical aspects of the work done at the Aerojet-General Corp. in the development of a gas generator using n-propyl nitrate. The methods employed to reduce the chamber temperature and carbon formation are described. This work led to the use of the additive ferrocene, which successfully reduced carbon deposition. Attempts to reduce the chamber temperature were only partially successful. Attempts to propagate a detonation through tubes containing n-propyl nitrate and tests to determine the minimum amount of an inert gas required to prevent the burning of n-propyl nitrate in air are also described.

A MONOPROPELLANT used for power generation possesses, in theory, an advantage over bipropellants because of the saving of weight. A monopropellant satisfactory for this purpose should operate over a wide range of chamber pressures at a chamber temperature that is sufficiently low to minimize problems of materials of construction and yet high enough to sustain combustion. In addition, the products of decomposition should contain as few solids as possible, to prevent the clogging of small nozzles. The principal monopropellants that have been considered are nitromethane, ethyl nitrate, n-propyl nitrate, hydrazine, ethylene oxide, nitroethane and hydrogen peroxide. For ethylene oxide and organic nitrates, thermochemical calculations show that a considerable amount of carbon can be expected if the dwell time in the chamber is long.

It was found in the course of the work on n-propyl nitrate that the observed adiabatic chamber temperature is considerably higher than that calculated by thermochemical methods, the observed temperature being approximately 2350 F. Furthermore, sufficient carbon was formed to cause partial clogging of the exhaust nozzle and consequent erratic operation. An experimental program was carried out to find some additive or additives that would result in either a decrease in the amount of carbon decomposition or in a decrease in the gas temperature.

These two tasks, which are not necessarily distinct problems, are discussed in the paragraphs that follow. Finally, tests concerning the safe handling of n-propyl nitrate are described:

1 Attempts to initiate a detonation wave in tubes filled with the liquid.

2 Attempts to determine the amount of an inerting atmosphere required to prevent ignition of n-propyl nitrate-air mixtures by a hot surface.

3 Adiabatic compression tests.

Composition of Combustion Products

Theoretical Composition

The chamber temperature which will be attained when a monopropellant decomposes under adiabatic conditions can be calculated, provided that there is ample time for the propellant gases to come to equilibrium. Such calculations have been made for n-propyl nitrate assuming that the products are only CO, CO_2, H_2, H_2O, N_2, CH_4 and graphite. A typical calculation (1)[3] shows that at 800 psia and 1300 K (1880 F) the gas consists of carbon monoxide and hydrogen and has the following composition:

	Moles per mole of n-propyl nitrate
CO	2.18
CO_2	0.207
H_2	2.32
H_2O	0.403
N_2	0.500
CH_4	0.386
C (graphite)	0.223

A heat balance, assuming these products, yields an adiabatic chamber temperature of 1350 K (1970 F), whereas the measured chamber temperature is in the range from 2300 to 2400 F.

Flame temperatures higher than the theoretical value can be calculated if one assumes methane to be present in the gas mixture in amounts greater than the theoretical amount. In fact, a higher flame temperature will result if other hydrocarbons are present.

Experimental Analysis

Because the adiabatic chamber temperature was considerably higher than the calculated value, attempts were made to obtain a representative product composition by a combination of gas analyses and a material balance on carbon, hydrogen and oxygen. The gas analyses were made by the vapor-phase chromatographic method.

The following gases were identified and their concentrations measured: H_2, CO, CO_2, CH_4, C_2H_6 and C_2H_4. In addition, N_2, H_2O, HCN and NH_3 were identified in the gaseous product. The results were somewhat unsatisfactory because of the difficulty in obtaining a good material balance and because of clogging of the water-cooled probes with carbon. One of several gas analyses available is given in Table 1, where the concentrations of nitrogen, water, ammonia, hydrogen cyanide and solid carbon were obtained by a material balance.

A heat balance, using this particular composition, will yield an adiabatic chamber temperature close to the observed value of 2200 F. It should be noted that the experimental product composition contains much less carbon monoxide and hydrogen but more water and methane than that based on equi-

Received Feb. 10, 1958.

[1] Senior Chemist. Member ARS.

[2] Principal Chemist.

[3] Numbers in parentheses indicate References at end of paper.

Table 1 Experimental analysis of the products of decomposition of n-propyl nitrate at 2200 F, 600 psia

Compound	Approximate gas composition volume per cent
H_2	15.1
CO	33.5
CO_2	0.8
N_2	5.5
CH_4	10.7
C_2H_6	1.0
C_2H_4	3.4
H_2O	21.8*
NH_3	4.1*
HCN	4.1*
	100.0

* Calculated

librium, and, in addition, hydrogen cyanide and ammonia are present. The experiments indicated that gas compositions should be obtained experimentally rather than by calculation, so that realistic values for the characteristic velocity C^* and for the specific heat ratio can be obtained.

As an example of the complexity of the decomposition process, some of the reactions that have been studied kinetically are shown in Fig. 1, starting with n-propyl nitrate vapor. At relatively low temperatures (191 C) the decomposition products from n-propyl nitrate are mainly n-propyl nitrite and nitroethane (2). The kinetics of the decomposition of n-propyl nitrite (3) and of propylene (4) have also been studied; the final products from propylene are hydrogen, methane, ethylene, acetaldehyde, acetylene, benzene and toluene. The illustrated steps in Fig. 1 are obviously not the only ones possible. For example, nitrogen dioxide and nitroethane can oxidize any of the hydrocarbons present, and the aldehydes would further decompose to simpler species.

Carbon Formation

The carbon formation can occur through any one of a series of steps, the simplest being the disproportionation of carbon monoxide at approximately 1300 F

$$2CO \rightleftharpoons C + CO_2$$

or carbon may be formed by the cracking of methane, ethylene

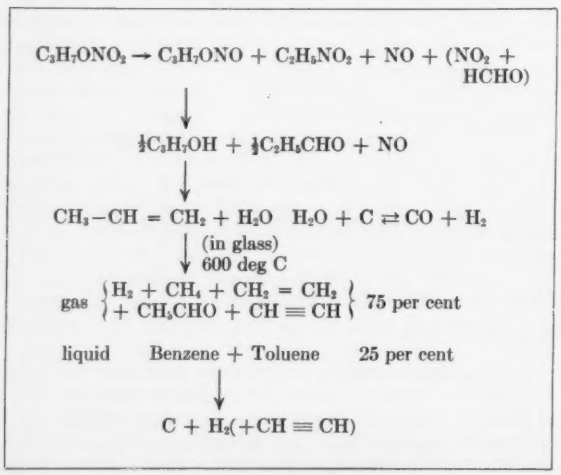

Fig. 1 Some possible decomposition products of n-propyl nitrate at progressively higher temperatures

or cyclic hydrocarbons. In fact, the carbon may come from a multitude of different reactions (5). The picture is further complicated by the fact that many of these reactions are influenced by catalysts and yield different products depending on the influence of the container walls. In summary, the two problems of reducing the amount of coking and simultaneously reducing the adiabatic chamber temperature are intimately related, but the solution of one will not necessarily solve the other. Furthermore, the complexity of the thermal decomposition process makes it extremely difficult to predict the effect of any specific scheme to solve the problem.

Experimental Method

The equipment used was a cylindrical gas generator with a spray injector and with an 800-in. characteristic length L^*. No major changes in the chamber configuration were made during this program, and the flow rate was held constant during the tests. The gas temperature and the outside wall temperature were taken during the run by means of thermocouples. The chamber pressure during the tests ranged from 800 to 1200 psig. The weight and character of the carbon remaining in the chamber were also noted after the completion of each run.

Reduction of Chamber Temperatures

In order to lower the chamber temperature, various substances were added which should absorb heat by endothermic decomposition, such as diethyl oxalate and diethyl carbonate. In addition to the high heat of vaporization of water, which should lower the temperature, Groll (6) has reported that steam reduces the amount of coke formation during the cracking of hydrocarbons in an iron tube. Therefore water, a low-freezing emulsion of ethylene glycol plus water in n-propyl nitrate, and various alcohols were also tried. Another suggestion for lowering the flame temperature comes from the reported inhibition by halogen compounds of the oxidation of carbon monoxide during the combustion of the carbon in air. Concentrations varying from 0.1 to 2 per cent of compounds, as $POCl_3$, PCl_3, Cl_2, CCl_4, $CHCl_3$, $SnCl_4$, CH_2Cl_2, HCl and I_2 were reported to be very effective (7). If carbon monoxide oxidation could be inhibited in the gas generator, the chamber temperature should be decreased. Therefore, some of these halogen compounds were tried as additives in concentrations up to 5 weight per cent.

Nearly all of the trials resulted in carbon formation, so that accurate thermocouple readings were not always obtained. Nevertheless, no really satisfactory reduction in chamber temperature was obtained unless a large amount of additive was used.

Reduction of Carbon Formation

Attempts were also made to find additives to reduce the amount of carbon deposition. The program plan for the reduction of the coking problem was first to search the available literature for the solution of analogous problems. For example, there is an enormous amount of literature on the thermal cracking of hydrocarbons. The effect of steam in preventing coking has already been mentioned. Combustion catalysts, such as the acetylacetonates of iron, copper and manganese, were used to determine whether this would result in a reduction of the carbon deposits. Additives have been found useful in reducing carbon deposits in turbojet engines. For example, Jonash and Cook have tested additives, such as commercial fuel oil additives, lead additives, cadmium naphthenate and ferrocene (dicyclopentadienyl iron II) to prevent coking of the burners (8). The authors state that there is probably an optimum concentration for each of these additives and that ferrocene was the best additive found when used at a concentration of 0.05 weight per cent.

A partial list of the additives tried at Aerojet-General is

shown in Table 2. The results of these tests can be summarized as follows: None of the compounds listed resulted in a substantial reduction in carbon deposition, with the exception of carbon tetrachloride, ferric acetylacetonate and ferrocene. In the case of carbon tetrachloride, short runs gave no carbon, but considerable carbon was formed in longer runs. In this instance, it appears that the rate of carbon deposition accelerates with time. The results obtained with ferrocene were completely satisfactory for the required duration, the only carbon formed being a thin dust on the chamber walls.

Because the hydrocarbon dicyclopentadiene used as an additive did not prevent carbon deposition, the behavior of ferrocene must be attributed in some way to the iron. The ferrocene does not alter the chamber temperature, which would be expected if the ferrocene altered the gas composition markedly. It is not known whether the ferrocene prevents the initial formation of carbon or merely prevents it from forming agglomerates that can stick to a metal surface, because no reliable values for the total amount of carbon produced were obtained during the program. In the hope that other effective additives containing iron could be found, ferric acetonylacetate was reinvestigated over a wider concentration range than previously used. The best concentration found was between 0.05 and 0.10 per cent, but the results were inferior to those obtained with ferrocene.

In summary, a method of successfully preventing carbon deposition was achieved by the use of ferrocene for this particular gas generator configuration, but no method of reducing the chamber temperature by using additives was satisfactory. In the future, it would be desirable to obtain chamber gas analyses over a range of operating pressures with and without ferrocene and at various values of the characteristic length L^*, in order to obtain a better insight into the mechanism of carbon deposition.

Propellant Safety

Several types of tests have been made to evaluate the safety of handling n-propyl nitrate. These are: (a) Adiabatic compression, (b) attempts to propagate a detonation wave through liquid n-propyl nitrate, and (c) measurements of the amount of inert gas, such as nitrogen, carbon dioxide or Freon 13B1, required to prevent the ignition of n-propyl nitrate and air mixtures by a hot surface or by an electric spark. The detonation propagation tests, adiabatic compression tests and the ignition tests are described briefly below.

Adiabatic Compression Tests

Adiabatic compression tests are made to evaluate the sensitivity of a monopropellant vapor to sudden compression, which could occur in the event of a sudden pressure rise in a system containing both liquid and vapor. If this compression of the vapor raises its temperature until a self-sustaining exothermic chemical decomposition can start at one point in the system, then the decomposition can spread through the whole system and result in rupture of the apparatus.

At Aerojet-General, a simple adiabatic compression tester is used as a screening test. It consists of a $\frac{3}{8}$-in. or $\frac{1}{4}$-in. U-tube about 18 in. long, closed at one end and partly filled with a given weight of monopropellant at a known temperature. The other end of the U-tube is connected through a quick opening valve to a source of high pressure nitrogen. Opening the valve results in compression of the vapor at the closed end of the U-tube. The rate of pressurization required to initiate a reaction violent enough to rupture the tube is a measure of the sensitivity of the monopropellant.

A sufficient number of tests are performed at each rate of pressurization to determine the rate of pressurization that results in rupture of the tube in 50 per cent of the tests. For n-propyl nitrate this value is 80,000 to 100,000 psi/sec. The absolute values of the pressurization rate are not the criteria ordinarily used to determine the relative safety of a monopropellant. Usually another monopropellant is also run as a control, so that the monopropellants may be rated in the order of their increasing sensitivity toward adiabatic compression. As a comparison, the value of the 50 per cent point for ethyl nitrate is about 10,000 psi/sec, so that the hazard involved in compressing ethyl nitrate containing bubbles of vapor is much higher than for n-propyl nitrate.

Detonation Propagation

In order to determine the ease of propagation of a detonation in liquid n-propyl nitrate at 300 F, the ability of a detonation wave to pass two right-angled bends in stainless steel tubing was measured. The apparatus in which the tests were run consists of an annular reservoir filled with n-propyl nitrate. In the center of this reservoir is a separate container which can be filled with a liquid explosive. The reservoir containing the n-propyl nitrate is connected to a length of $\frac{1}{4}$-in. stainless steel tubing, in which two right-angled bends were made about 4 in. apart. The outer reservoir and tubing were filled with n-propyl nitrate. The apparatus was then sealed and heated to 300 F. A test tube containing a quantity of Aerex (a proprietary Aerojet liquid explosive) and an initiator were lowered into the inner reservoir and detonated.

Table 2 The effect of additives on carbon formation in an n-propyl nitrate gas generator

Additive	Weight per cent	Carbon formation
carbon disulfide	2.0	moderate
tetraethyl lead	2.0	small
carbon tetrachloride	0.10	none
iodine	0.75	large
dicyclopentadiene	0.05	large
ferrocene	0.05	none
ferrocene	0.01	none
ferric acetylacetonate	0.005	moderate
ferric acetylacetonate	0.01	moderate
ferric acetylacetonate	0.05	small
ferric acetylacetonate	0.10	small
ferric acetylacetonate	2.0	large
manganese acetylacetonate	0.20	large

In the tests conducted in this manner, no propagation of the detonation wave occurred in the n-propyl nitrate. The $\frac{1}{4}$-in. tubing was recovered intact in each case, and liquid was found remaining in the $\frac{1}{4}$-in. tubing.

For comparison, the $\frac{1}{4}$-in. tubing and the outer reservoir were filled with Aerex explosive, which is known to propagate a detonation wave, and initiated in a similar manner. Only shreds of the $\frac{1}{4}$-in. stainless steel tubing were found after the test. Therefore it was concluded that liquid n-propyl nitrate at 300 F does not propagate a detonation wave in a $\frac{1}{4}$-in. tube. These tests were extended to tubes of larger diameter, $\frac{1}{2}$ in. and $1\frac{1}{4}$ in., and again no detonation propagation was observed. However, confinement in a heavier tube may result in detonation (9).

Ignition Tests

Another possible hazard that was investigated is the behavior of n-propyl nitrate sprayed against a hot metal surface in an atmosphere consisting of air mixed with either nitrogen, carbon dioxide or Freon 13B1 (bromotrifluoromethane). It

Table 3 Incidence of ignition for n-propyl nitrate injected against a metal plate in various atmospheres

Gas temp, deg F	Plate temp, deg F	Vol per cent air	Vol per cent N_2	n-PN, ml	Total tests	Combustion
275–325	800–940	25	75	2.0	14	3
415–450	900–910	25	75	2.0	5	5
415–450	800–900	12.5	87.5	1.0	11	0
			Vol per cent Freon 13B1			
415–455	875–900	25	75	2.0	5	0
430–440	850–865	50	50	2.0	5	3
425–435	815–850	37.5	62.5	2.0	5	4
415–440	795–780	25	75	2.0	3	0
415–440	745–780	25	75	1.0	3	0
430–440	770–790	32	68	1.0	5	0
			Vol per cent CO_2			
420–450	890–900	25	75	2.0	5	0
420–450	900–925	37.5	62.5	2.0	5	0
425–450	925	50	50	2.0	3	3

has been reported that the minimum ignition temperature of n-propyl nitrate vapor in air is about 350 F (9), so that it is of interest to determine whether inert diluents can afford protection. The original apparatus consisted of a 230-ml glass tube containing a heated stainless steel target against which liquid n-propyl nitrate was injected with a hypodermic needle. Later, a larger apparatus of 12.8 liters was constructed with a window in one end.

In order to ensure conditions that would always yield combustion for air and n-propyl nitrate mixtures, the temperature of the target was set arbitrarily at 800 to 940 F. The parameters studied were the composition of the gas mixture, the amount of n-propyl nitrate injected against the plate and the incidence of flame. The total pressure before injection of the liquid n-propyl nitrate was 14.7 psia. The results of some of these tests in the 12.8-liter apparatus are shown in Table 3. These tests indicate that for a plate temperature of 800 to 940 F and a gas temperature of 400 to 500 F, the following concentration of inert gas must be used to prevent inflammation: Nitrogen—75 to 87 vol per cent, Carbon dioxide—50 to 63 vol per cent and Freon 13B1—50 to 75 vol per cent. However, it is known that if the gas temperature were equal to the plate temperature the amount of inerting gas should be increased to prevent combustion.

In addition to the tests shown in Table 3, some tests were also made on the ease of ignition of these mixtures with a continuous spark from a 14-mm automobile spark plug, the power being supplied by a Model T Ford spark coil activated by 25 v a-c. In those experiments where combustion failed to occur, this spark was used. In all of those cases where ignition failed to occur on the heated surface, the use of a spark was also unsuccessful in igniting the gas mixture.

Acknowledgment

The authors wish to acknowledge the support of D. G. Burdick, director of the program; C. P. Chalfant who was responsible for the testing program, and Dr. S. Witz who suggested many of the additives that were tried. C. C. Cook and G. B. Shoemaker performed most of the work on propellant safety.

References

1 Ethyl Corporation, "Technical Information Concerning Normal Propyl Nitrate," RM-118, May 28, 1954.

2 Levy, J. B. et al., "The Thermal Decomposition of Nitrate Esters," *J. Amer. Chem. Soc.*, vol. 77, 1955, p. 2015.

3 Steacie, E. W. R. and Shaw, G. T., "The Homogeneous Unimolecular Decomposition of Gaseous Alhyl Nitrites, III The Decomposition of Propyl Nitrite," *J. Chem. Phys.*, vol. 3, 1935, p. 344.

4 Hurd, C. D., and Meinert, R. N., "The Pyrolysis of Propylene," *J. Amer. Chem. Soc.*, vol. 52, 1930, p. 4978.

5 Ubbelohde, A. R., "Status of the Theory of the Kinetics of Combustion Reactions," Fifth Symposium on Combustion, Reinhold Publ. Co., New York, 1955, p. 799.

6 Groll, H. P. A., "Vapor-Phase Cracking," *Ind. and Engng. Chem.*, vol. 25, 1933, pp. 787–798.

7 Arthur, J. R., Bingham, D. H. and Bowring, J., "Kinetic Aspects of the Combustion of Solid Fuels," Third Symposium on Combustion and Flame and Explosion Phenomena, Williams and Wilkins Co., Baltimore, 1949, p. 466.

8 Jonash, E. R. and Cook, W. P., "Effect of Fuel Additives on Carbon Deposition in a J-33 Single Combustor," NACA RM E-55-F-30a, Lewis Flight Propulsion Laboratory, Sept. 8, 1955.

9 U. S. Bureau Mines and Naval Ordnance Laboratory, "The Safety Characteristics of Normal Propyl Nitrate," Feb. 11, 1957.

The Ignition Behavior of Various Amines With White Fuming Nitric Acid

ROSE L. SCHALLA[1] and EDWARD A. FLETCHER[2]

Lewis Research Center, NASA
Cleveland, Ohio

Spontaneous ignitibility depends on synergetic behavior of several reactions, each of which exerts its greatest independent influence at a different time during the ignition period. The most important of these reactions are a liquid phase neutralization reaction for aliphatic amines, a liquid phase nitration reaction for aromatic amines, and a slower, rate determining oxidation reaction which follows the others. Mixing which is too rapid can quench ignition if the mixture ratios, favoring the various reactions leading to ignition, are too widely separated.

THE IGNITION of amines with nitric acid has been a subject of considerable interest for many years. In the past, a number of authors have studied the phenomenon and have attempted to explain it with generalizations which could be applied to all such systems. A commonly used technique was to measure ignition delays for a large number of amines under a constant controlled set of conditions and then to try to explain the observed orders of the ignition delays in terms of the various physical or chemical properties of the amines.

An example of this treatment is the work of Rapp and Strier (1).[3] Using a drop-test method, these authors established a set of axioms for predicting relative ignitibility based on the structural properties of the amines. Their treatment ignored the effect of fuel-oxidant ratio, ambient atmosphere and mixing rate; however, the axioms obtained are useful within their limitations.

Mixing has been shown to be a variable which can affect the ignition delay (2) and was even shown, with some systems, to be the rate determining step (3).

In none of these studies, however, was the fuel-oxidant ratio in a well-mixed system or the ambient atmosphere considered important variables. In previous work from this laboratory, the ignition behavior under conditions of very rapid mixing was reported for the propellant system triethylamine, WFNA (4). The behavior of this system was studied by measuring the rate of pressure rise resulting from rapid mixing and injection of the propellants into a constant-volume bomb. Ignition delays were determined as a function of several variables including fuel-oxidant ratio, the bomb volume and the nature of the atmosphere in the bomb before injection. The processes associated with ignition were separated into three well-defined steps, and from the nature of these steps ignition was postulated to consist of:

1 A fast, liquid phase reaction which yields some gaseous products, followed by

2 an induction period, the length of which determines the ignition delay, and then

3 ignition and combustion.

The rates of the reactions in step 2 were found to be quite sensitive to the temperature achieved by neutralization, the charge density and the composition of the reactants in the gas phase. These rates were found to be especially sensitive to the presence of gas phase oxidants; ignition was completely suppressed by inert gases.

The importance of neutralization with this particular combination appeared quite firmly established. Ignition delays reported in the literature, however, cannot be correlated with the base strengths of the amines. In addition, a few preliminary experiments at this laboratory revealed that the order of ignition delays was not constant but changed and could even be reversed by varying the fuel-oxidant ratio in a given homologous series of amines, or by enriching the ambient atmosphere with oxygen. Consequently attempts to generalize the behavior of amines and correlate it with any single variable, such as base strength or physical structure are a gross oversimplification of the problem.

The present investigation was undertaken to study the effects of fuel-oxidant ratio, charge density and ambient atmosphere in the hope that such a study would shed more light on amine-acid ignitions. A number of amines similar to those reported in (1) were studied.

Experimental

The apparatus and techniques used were described in detail in (4). The apparatus was essentially a device which permitted the reactants to be rapidly mixed and injected into a constant-volume bomb in less than 1 millisec, and a device for observing and recording the pressure rise inside the bomb as a function of time.

The white fuming nitric acid contained 97.38 per cent HNO_3, 0.60 per cent NO_2 and 2.02 per cent H_2O. One batch of HNO_3, which was used only with aniline, contained 97.0 per cent HNO_3, 1.0 per cent H_2SO_4, 1.7 per cent H_2O and 0.3 per cent NO_2. The amines were obtained from various commercial sources and were used without further purification.

Time-Pressure Curves

The time-pressure curves obtained with the fuels studied in this investigation were similar to those reported for triethylamine (4). Ignition consisted of three well-defined steps. The pressure rise in the first step was about 25 lb/in.^{2} for dipropylamine and varied from 15 to 40 lb/in.^{2} for the other fuels. The time associated with this pressure rise averaged about 3 millisec. The first slope (rate of initial pressure rise) remained essentially constant over the fuel-oxidant range reported. There was little or no pressure rise in the second step. This was typical of all fuels studied except triethyl- and

Received June 24, 1958.

[1] Aeronautical Power Plant Research Engineer (Combustion).

[2] Head, Propellant Chemistry Section. Member ARS.

[3] Numbers in parentheses indicate References at end of paper.

tripropylamine which showed a maximum near $m = 0.37$.

For diethyl-, dipropyl- and dibutylamine, studies were also made with oxygen in the bomb and at reduced bomb volumes. The first slope was not affected by substitution of oxygen for air in the bomb, but reduction of the bomb volume increased the first slope and caused the expected variation with fuel-oxidant ratio. The second slope was again very small.

Results and Discussion

Trialkylamines

Fig. 1 shows the variation of ignition delay with mixture composition for three trialkylamines, triethylamine, tripropylamine and tributylamine. In addition, there is a dashed portion of the triethylamine curve which shows delays obtained with oxygen instead of air initially in the bomb. The effect of oxygen is to shorten delays when the fuel-oxidant ratio is higher than that which gives the minimum delay with air in the bomb. With leaner mixtures, the delay is not affected by added oxygen. Oxygen broadens the spontaneous ignition region by displacing the rich limit to the right.

It is also quite interesting to note that the delays are in the order $Bu_3N > Pr_3N > Et_3N$ over most of the ignitible region. The order obtained by Rapp and Strier is $Bu_3N > Et_3N$ slightly $> Pr_3N$. If one extrapolates the curves to leaner mixtures than those shown in Fig. 1, the order obtained by Rapp and Strier is suggested. For example, if the curves are extrapolated to an amine mole fraction of 0.1, the values for Et_3N, Pr_3N and Bu_3N are about 15.5, 12.5 and 37 millisec, respectively. The values reported by Rapp and Strier are 70, 50 and 240 millisec. The drop-test values are thus all in qualitative agreement with the present values. The delays in the two experiments even show a crude proportionality. The significance of this is that the mechanism which ultimately brings about ignition is probably the same for both experimental techniques, but that it takes place after a longer interval in the drop test. An additional observation that might be made at this point is that, as the delays grow longer, the discrepancy between the rapidly mixed delays and the drop tests increases. Well-mixed delays are probably truer measures of the chemistry involved than the drop tests. In drop tests, ignition depends on the formation of a critical region whose composition lies somewhere between pure fuel and pure oxidant, where the rate of heat and/or radical production by chemical reaction is sufficient to render the reaction self-sustaining. The longer ignition takes, the greater will be the extent to which heat and active species can diffuse away from this region, and the greater will be the departure of the system from what one might expect from the adiabatic chemistry alone. In well-mixed systems, a particular mixture either is critical or it is not. The delay will be more nearly representative of the chemistry involved in the reactions leading to ignition. The closeness of the minima to the fuel-

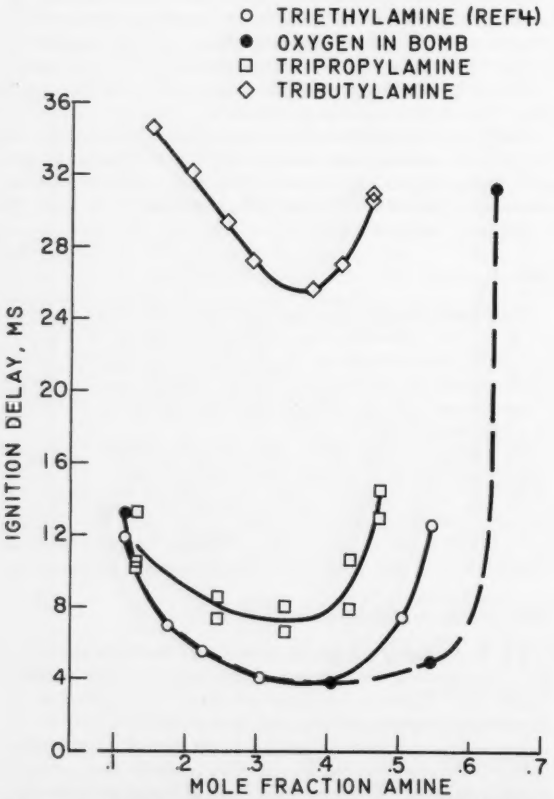

Fig. 1 Variation of ignition delay with mixture ratio of trialkylamines in 430 ml bomb containing air initially. The dashed curve is for triethylamine with oxygen initially in the bomb

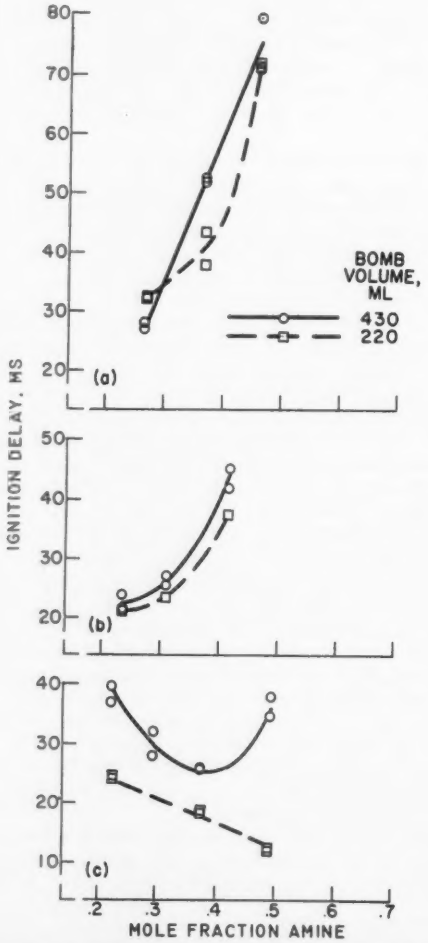

Fig. 2 Variation of ignition delay with mixture ratio and with bomb volume of dialkylamines. The bomb initially contained air. (a) Di-n-butylamine, (b) dipropylamine, (c) diethylamine

oxidant ratio for complete neutralization ($m = 0.5$) implies that with trialkylamines, neutralization plays the important role suggested in (4). The mole fraction of amine required for oxidation to CO_2, H_2O and N_2 is in the range 0.0625 to 0.11.

Dialkylamines

With dialkylamines, the behavior is different. Dialkylamines would be expected to react, after neutralization, by a mechanism which is chemically quite different from that which characterizes trialkylamines. The importance of neutralization, as evidenced by the positions of the minima, is not easily demonstrated, because the induction periods associated with secondary amines are longer than those of the corresponding tertiary amines. This is evidenced by the longer delays obtained in both this work and the work of Rapp and Strier. With secondary amines, especially those containing larger hydrocarbon groups, the chemistry during the induction period is by far the most dominant factor. It produces a great deal of variation in the results from amine to amine. This masks the effects of the neutralization reaction, as illustrated in Figs. 2 to 5.

In Fig. 2, the effect of increasing the charge density by decreasing the bomb volume is shown. The bomb initially contained air. Ignition delays are reduced somewhat with Bu_2NH and Pr_2NH, and somewhat more with Et_2NH and in such a way as to suggest that, when the second step reaction rate is speeded by increasing the concentration of reactants, neutralization plays a correspondingly more important role in the overall reaction.

When a similar comparison is made with oxygen in the bomb (Fig. 3), the effect of the bomb volume is obscured, especially with the higher homologs, possibly because a decrease in

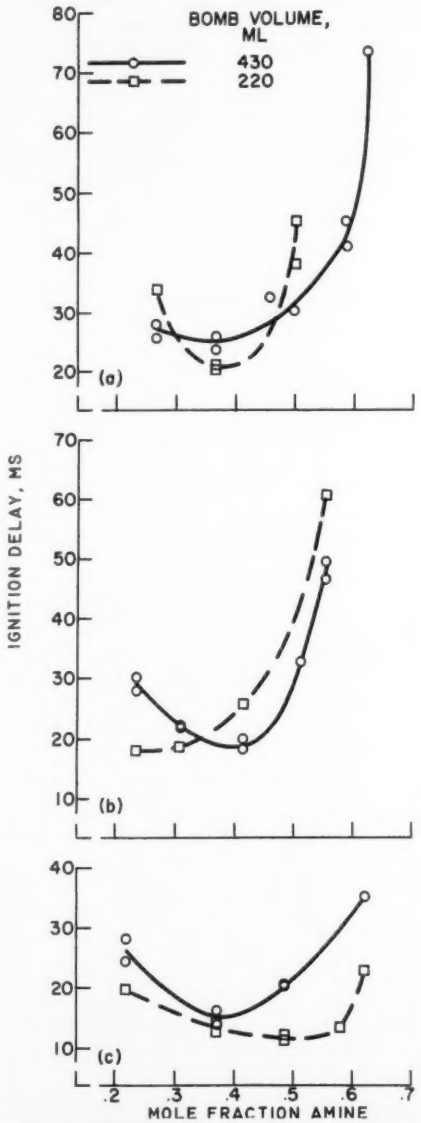

Fig. 3 Variation of ignition delay with mixture ratio and with bomb volume of dialkylamines. The bomb initially contained oxygen. (a) Di-n-butylamine, (b) dipropylamine. (c) diethylamine

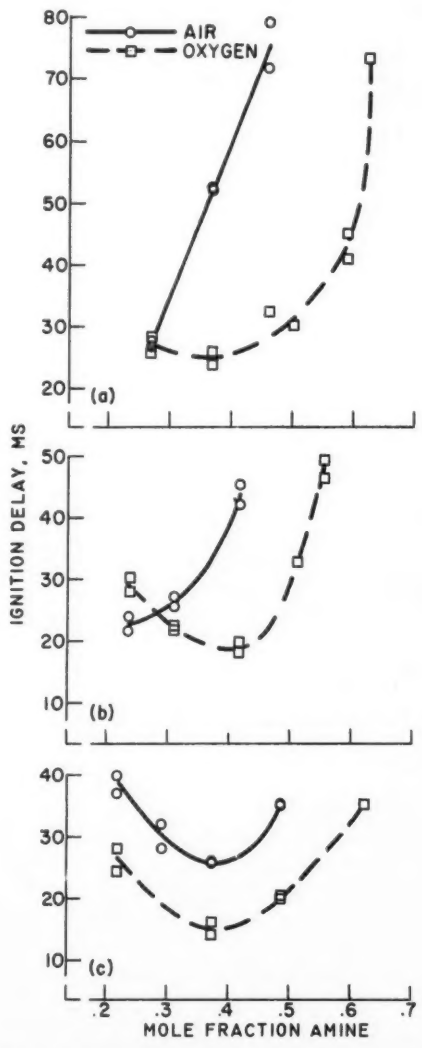

Fig. 4 Effect of composition of initial atmosphere on the ignition delays of dialkylamines in the large bomb. (a) Di-n-butylamine, (b) dipropylamine, (c) diethylamine

bomb volume also results in a decrease in the total amount of oxygen available for the induction period reaction. With diethylamine, there is a hint of the importance of neutralization.

The role of neutralization is shown more dramatically in Figs. 4 and 5, where the effect of enriching the ambient air with oxygen is shown at two constant charge densities. When the ambient atmosphere was oxygen instead of air, the second, rate determining step was greatly speeded, giving shorter delays for all of the amines over most of the ignitible range. The optimum fuel-oxidant ratio for ignition also shifted markedly toward that for neutralization. The shift was most pronounced with the larger molecules, where the effect of second step chemistry had been to make ignition so slow as to render neutralization relatively unimportant.

Another interesting facet of the behavior of these systems is shown in Fig. 6 where the ignition delays of the three secondary amines are plotted as a function of the fuel-oxidant ratio for ordinary conditions, i.e., full-size air filled bomb. Over much of the range where ignitions were obtained, the relative reactivities were $Et_2NH > Pr_2NH > Bu_2NH$, which favors the view that the neutralization reaction is important, since the heats of neutralization per gram of mixture are also in that order. The order is exactly opposite to that obtained by Rapp and Strier. As the mixture is made leaner, the order changes, and an extrapolation into regions where ignition could not be achieved in the rapid mixing reactor will give the order obtained by Rapp and Strier, $Bu_2NH > Pr_2NH > Et_2NH$. This again suggests that the drop test studies gave

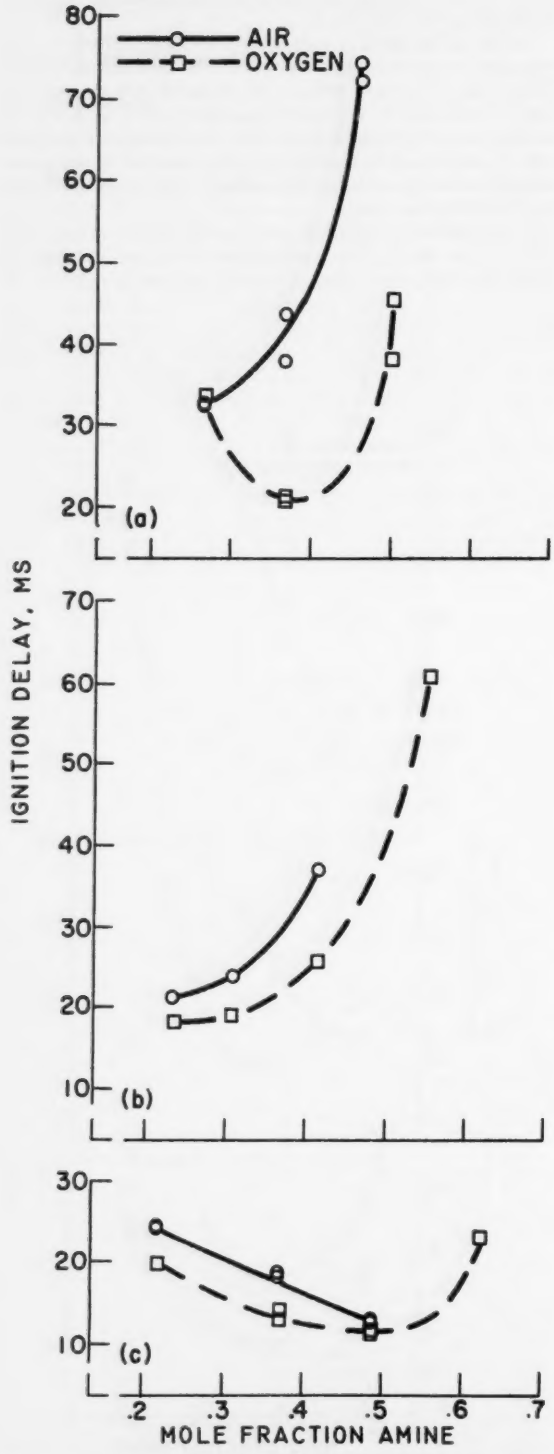

Fig. 5 Effect of composition of initial atmosphere on the ignition delays of dialkylamines in the small bomb. (a) Di-n-butylamine, (b) dipropylamine, (c) diethylamine

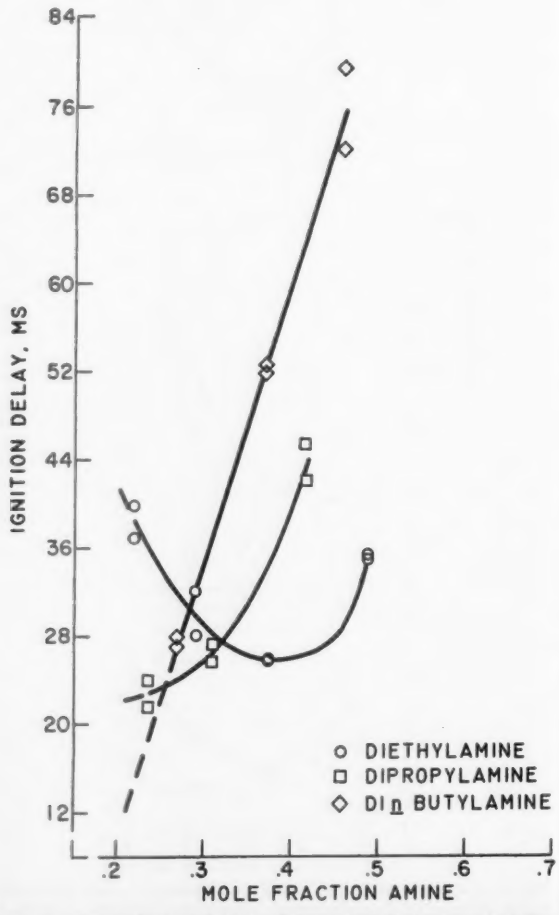

Fig. 6 Comparison of ignition delays of dialkylamines in large air-filled bomb, showing extrapolation to drop-test conditions

results which are peculiar to a mixture which is leaner than those which will give a minimum delay when mixing is rapid.

In addition to the work reported with the straight chain amines, it seemed of interest to study the behavior of di-secondarybutylamine, which did not behave according to the rules set by Rapp and Strier in their study. This amine violates the rule that substitution of a methyl group for a secondary hydrogen at the α carbon position is conducive to ignitibility, since it had a delay (300 millisec) which was longer than that of either dipropylamine (170 millisec) or dibutylamine (150 millisec). These amines were of particular interest, because it appeared that, in general, the rules of Rapp and Strier were applicable to the chemistry involved in the second step, and the reason for these amines' exceptional behavior was unclear. Fig. 7 compares the behavior of disecbutyl and dibutyl amines and shows that the former is, in fact, more ignitible than the latter over most of the composition range, and that the order reverses as the favored fuel-oxidant ratio in the drop test is approached. The behavior of methyl n-butylamine and methyl sec-butylamine is also shown in Fig. 7(b). The delays are shorter for the latter, as they should be, except at the rich limit where they coincide.

Monoalkylamines

The only monoalkylamine studied in the present work was n-butylamine. No ignitions were obtained with this system in the rapid mixing reactor, although Rapp and Strier report that the combination is spontaneously ignitible. If reference is made to the differences in behavior of the more reactive di- and trialkylamines in these two apparatuses, the behavior is again consistent with a model which makes use of both neutralization and a subsequent oxidation reaction as factors which determine ignition delays. The interpretation is simply that, when the reactants are well-mixed, compositions which give a high temperature due to neutralization are beyond a rich limit for ignition, and leaner compositions are also outside the spontaneous ignition region simply because the temperature is too low. In the drop test, where there is a steep concentration gradient, a high temperature (neutralization) region is quite close to a somewhat leaner region. Transport of heat from the neutralization region can raise the temperature in the leaner region to above its spontaneous ignition temperature. Thus, mixing which is too efficient may sometimes prevent a spontaneous ignition. This phenomenon is not unique with this system. Somewhat similar behavior has been observed with gaseous diffusion flames (5). The mechanics of the processes which lead to quenching of a diffusion flame by rapid mixing of the reactants are probably somewhat similar, although the chemical reactions involved are vastly different.

General Discussion of Aliphatic Amines

The experimental results described previously suggest that ignition of amines with nitric acid is not a simple phenomenon which can be correlated with any single physical, chemical or structural property of the amine. It suggests instead that ignition is a complex function of many parameters.

Even if mixing is excluded as a variable by making the mixing rate very high, the relative reactivities of amines change with fuel-oxidant ratio. With trialkylamines, the relative reactivity of triethylamine and tripropylamine appears to reverse as the fuel-oxidant ratio is changed. With dialkylamines, the order is completely reversed for the three amines in the sequence diethyl-, dipropyl-, dibutylamine. It is hard to suggest any single property which would explain the reversal. Instead, we must call upon at least two factors which can vary with fuel-oxidant ratio in such a way as to cause the reversal.

It has already been shown that the nature of the amine has the greatest effect in determining the relative magnitudes of the ignition delay (1), i.e., the length of the induction period. It has also been shown that the heat evolved during neutralization is important in determining ignition delay. How are these effects interrelated?

The ignition process can be envisioned as follows

$$\text{reactants} \xrightarrow[\text{some thermal decomposition}]{\text{mixing, neutralization}} \text{products} + \text{heat} \quad [1]$$

very fast

products of [1] +

$$\text{added oxidants} \xrightarrow[\text{slow}]{\text{elevated temperature}} \text{ignition} \quad [2]$$

The rate of reaction [2] determines the ignition delay. This rate will vary with the particular amine, amount of added oxidant present, pressure and temperature. The effect of reaction [1] is to provide the initial environment in which the reactants of reaction [2] find themselves.

Neutralization in itself does not appear to be a sufficiently potent factor to bring about ignition. In a system which contains no extraneous oxidizing agents, such as atmospheric oxygen, well-mixed triethylamine-nitric acid will not ignite at any fuel-oxidant ratio (4). The heat of neutralization can,

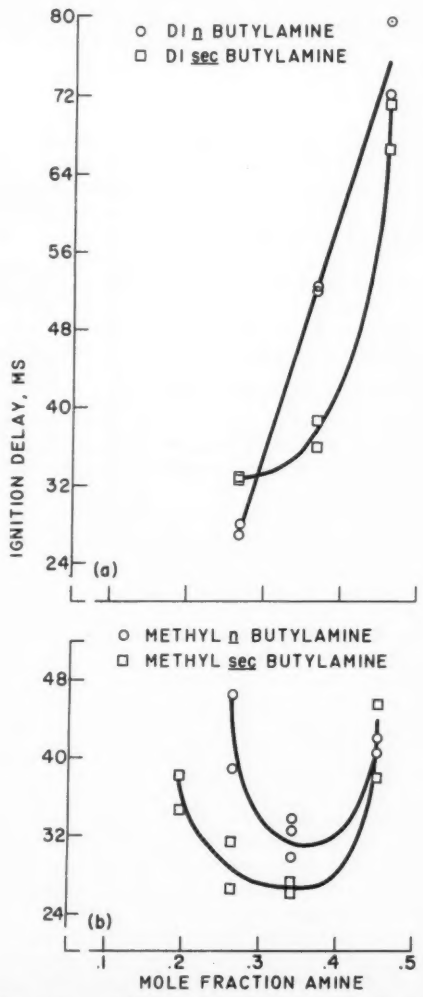

Fig. 7 Comparison of ignition delays of branched chain amines with straight chain amines

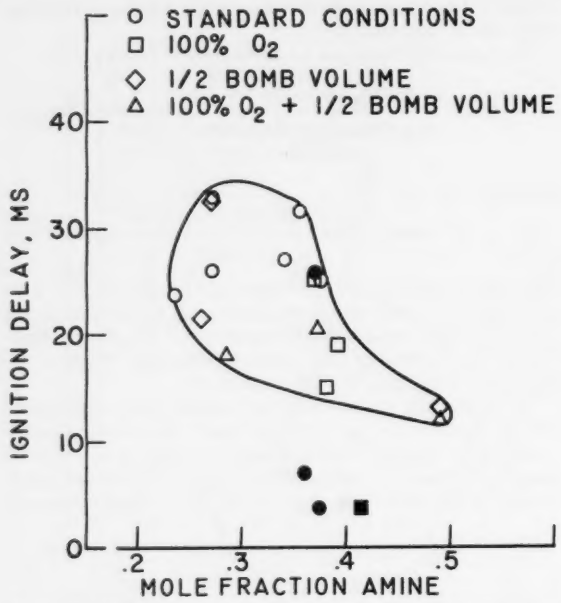

Fig. 8 Variation of minimum ignition delays of all the amines at all conditions studied with mixture ratio

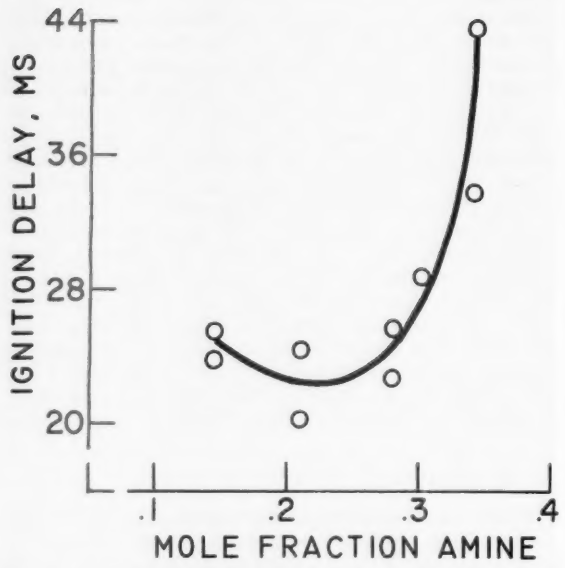

Fig. 9 Variation of ignition delay of diethylaniline with mixture ratio using sulfuric acid-free nitric acid

and does, however, greatly increase the rate of reaction during the induction period by raising the temperature. Just as mixing rate is eliminated as a variable which determines ignition delay by rapid mixing, it might be anticipated that ignition delay variations associated with reaction [2] might be reduced by increasing its rate. Unfortunately, in the present experiment the rate cannot be made high enough to eliminate its effects completely. By a decrease of the bomb volume which raises the pressure and by the presence of pure oxygen in the ambient atmosphere, the rate can usually be increased somewhat.

As this rate is increased, the effect of the heat of neutralization becomes observable. In other words, as the second step oxidation reaction becomes less and less rate determining, the heat of neutralization has a greater and greater effect in reducing the ignition delay.

When the other chemical reactions leading to ignition (step [2]) are very fast, the shortest delays should occur at a fuel-oxidant ratio which gives the greatest temperature rise due to neutralization. The short delays should be similar in magnitude, since the temperature rise associated with neutralization, which takes place at the same rate regardless of other variables, becomes rate determining to a greater degree.

Conversely, when the secondary reactions (step [2]) are slow, they are more rate determining; in addition to being longer, the delays will be more variable. The greater variation will be due to the different chemical behavior of the various amines because of differences in structure and chemical properties. As the *minimum* ignition delay for any amine-acid system grows shorter, as a result of a variation of the charge density or ambient atmosphere, the fuel-oxidant ratio which produced that delay should be closer to stoichiometric for neutralization. As the delays grow longer, the variation in minimum ignition delay should increase.

The minimum ignition delay obtained with each amine at each condition of charge density and initial oxygen concentration is plotted in Fig. 8 as a function of the mole fraction of the amine which produced that delay. Secondary amines are plotted as open symbols and tertiary amines are plotted as solid symbols. The data points for the tertiary amines suggest that, with the lower amines, the effects of neutralization have already been felt, as was suggested in (4). The subsequent oxidation reactions are fast. The delays are low, and the concentration which produced these delays is near that for neutralization. The distribution of the points for the secondary amines is more informative. With these amines, the step [2] reactions appear to be slower, and the ignition delays have, therefore, more variance with respect to fuel-oxidant ratio. On the figure, these data points are enclosed in an envelope which is quite broad at low fuel oxidant ratios and becomes narrow as the fuel-oxidant ratio for neutralization is approached.

Aromatic Amines

In a previous paper, it was also suggested that, whereas neutralization appeared to be an important first step with aliphatic amines such as triethylamine, nitration might well be of great importance with aromatic amines (4). Accordingly, a study was made of diethylaniline with the results shown in Fig. 9. The minimum did indeed occur at a fuel-oxidant ratio which was lower than that for other tertiary amines, but the high values of the ignition delays were somewhat surprising, in view of the low values obtained by Kilpatrick and Baker for aniline and the present values for triethylamine. More surprising was the observation that aniline and methylaniline would not ignite. The explanation for this behavior was discovered when it was observed that a batch of nitric acid, which analyzed to 99.05 per cent HNO_3, gave results in good agreement with those of Kilpatrick and Baker. Subsequent chemical analysis of this batch disclosed that it contained 0.969 per cent H_2SO_4. The work of Hughes, Ingold et al. (6) shows that concentrations of sulfuric acid much lower than this have a very marked effect in increasing the rates of nitration of aromatic compounds in nitromethane solution. For example, the rate of nitration of benzene by nitric acid in nitromethane is increased by a factor of 10 by the addition of about 0.05 per cent H_2SO_4, and the increase

of reaction rate is almost linear with H_2SO_4 concentration. With just a few per cent added H_2SO_4, therefore, it is reasonable to expect that the rate of nitration in the liquid phase should increase by a factor of several hundred. The greatly increased rate of nitration with sulfuric acid present would, therefore, be expected to lead to ignition, and it does. In the absence of small amounts of sulfuric acid, the nitration reaction is quite slow, and the heat of reaction is dissipated fast enough so that the mixture does not ignite.

Concluding Remarks

In view of what has been said about the importance of the second step in determining the magnitude of the ignition delay, one might reasonably question whether the neutralization concept has any practical significance, since the overall mole fractions of amines in rocket engines will usually be much lower than those which give a high neutralization temperature. The answer is that the concept provides means of controlling or minimizing ignition or combustion time lag by means of propellant staging. Propellants might be staged in such a way that fullest advantage is taken of any exothermic liquid phase reaction which may occur. The rate of combustion in a rocket engine is said to be limited by the rate of vaporization of the propellants (7,8). This suggests that if the amine and part of the acid were premixed, for example, in a swirl cup in the injector at a mole fraction of about 0.5 and the excess acid injected through separate holes, the effect on the premixed propellants would be equivalent to preheating them about 100 to 200 C. The rate of vaporization or decomposition of the amine and part of the acid would be increased over the rate obtained with more conventional injector configurations, leading to greater combustion efficiency or smaller thrust chambers.

References

1 Rapp, Louis R. and Strier, Murray P., "The Effect of Chemical Structure on the Hypergolic Ignition of Amine Fuels," JET PROPULSION, vol. 27, no. 4, 1957, pp. 401–404; *see also* "Chemical Aspects of Hypergolic Ignition for Liquid Propellant Rocket Engines," Second AGARD Combustion Colloquium, Univ. of Leige, Belgium, Dec. 5–9, 1955.

2 Pino, M. A., "A Versatile Ignition Delay Tester for Self-Igniting Rocket Propellants," JET PROPULSION, vol 25, no. 9, pt. 1, 1955, pp. 463–466.

3 Kilpatrick, M. and Baker, Louis L., Jr., "A Study of Fast Reactions in Fuel-Oxidant Systems," Fifth Symposium (Int.) on Combustion, Reinhold Publishing Corp., 1955, pp. 196–205.

4 Schalla, Rose L. and Fletcher, E. A., "The Behavior of the System Triethylamine-White Fuming Nitric Acid under Conditions of Rapid Mixing," Sixth Symposium (Int.) on Combustion, Reinhold Publishing Corp., 1957, pp. 911–917.

5 Potter, A. E., NACA Lewis Laboratory, private communication.

6 Hughes, E. D., Ingold, C. K. and Reed, R. I., "Kinetics and Mechanism of Aromatic Nitration. Pt. II—Nitration by the Nitronium Ion, NO_2^+, Derived from Nitric Acid," *J. Chemical Society*, London, 1950, pp. 2413–2414.

7 Priem, Richard J., "Propellant Vaporization as a Criterion for Rocket Engine Design; Calculations of Chamber Length to Vaporize a Single *n*-Heptane Drop," NACA TN 3985, 1957.

8 Priem, Richard J., "Propellant Vaporization as a Criterion for Rocket Engine Design; Calculations Using Various Log-Probability Distributions of Heptane Drops," NACA TN 4098, 1957.

Transport and Thermodynamic Properties in a Hypersonic Laminar Boundary Layer[1]

Part I Properties of the Pure Species

SINCLAIRE M. SCALA[2] and CHARLES W. BAULKNIGHT[3]

General Electric Co.
Philadelphia, Pa.

An accurate determination of the heat transfer and surface shear forces in a hypersonic laminar boundary layer depends upon the solution of the boundary layer equations at the surface of the vehicle. This requires, as auxiliary data, the transport and thermodynamic properties of the fluid medium. For the temperatures normally encountered in hypersonic flight, there is a paucity of experimental data. These properties, therefore, must be established by using empirical models for the potential energy function which represents the molecular interactions between the chemical species present in the gas. Calculations have been made of the transport and thermodynamic properties of the components of dissociated air by the use of the formulae of statistical mechanics, the Lennard-Jones 6:12 model for the molecular species where appropriate, and the rigid sphere model for the atomic species, and are presented here.

COMPRESSIBILITY effects have usually been included in the analysis of boundary layers on vehicles in high speed flight; however, the following approximations have frequently been made:

1 The specific heat of air is constant.

2 The product of density and viscosity is constant.

3 The Lewis number is unity, and, hence, the diffusion terms do not appear explicitly in the energy equation for a binary mixture.

4 The Prandtl number is constant.

Received May 20, 1958.

[1] Based on work performed under the auspices of the U. S. Air Force, Ballistic Missiles Division, Contract no. AF 04(645)-24.

[2] Research Engineer, Aerosciences Laboratory, Missile and Space Vehicle Department. Member ARS.

[3] Physical Chemist, Aerosciences Laboratory, Missile and Space Vehicle Department.

At hypersonic flight speeds, the fluid enveloping the body is dissociated air, which is produced by shock waves preceding the body. The boundary layer at the surface of the body then contains gradients of species concentration as well as gradients of temperature and velocity.

Consequently, it must be stated in contradistinction to the above assumptions, that:

1 The specific heat of air is not constant.

2 The product of density and viscosity is variable.

3 Ordinary diffusion is present, and the Lewis numbers are not constant.

4 The Prandtl number is not constant.

5 Thermal diffusion is present and may be important when homogeneous reaction rates are slow.

In order to assess the characteristics of a hypersonic boundary layer, it is therefore necessary that the transport and thermodynamic properties of the gas be known accurately. Calculations have been made of these properties of the components of dissociated air. The formulae of statistical mechanics, the Lennard-Jones 6:12 model for the molecular species where appropriate, and the rigid sphere model for the atomic species have all been employed in this study. The determination of these properties constitutes a major problem in its own right; the inclusion of temperature- and composition-dependent properties contributes considerably to the complexity of boundary layer analyses. Perusal of the latest published work on the status of transport and thermodynamic property data (1, 2 and 3),[4] reveals that the data presented here are not available elsewhere. The data will be useful in the study of hypersonic phenomena at the surface of space vehicles, which will be considered in future publications.

Transport Properties

According to the kinetic theory of gases, the transport of energy, mass and momentum occurs because of collisions between gaseous particles, and the conservation laws of thermodynamics and mechanics are obeyed during the collision processes. Macroscopic transport properties can then be defined in terms of these processes.

If we assume that a temperature can be defined, we can state that energy is transferred from a high temperature region to one at lower temperature by means of a mechanism known as thermal conductivity. It is noted that the existence of this mechanism does not, of course, preclude the transport of energy by diffusion and radiation processes. The transport of mass is effected by driving forces, such as concentration gradients, pressure gradients, temperature gradients and force fields, which define the process of diffusion. Finally, due to the presence of pressure gradients, viscous stresses and force fields, momentum is transported through the system.

The computation of the transport properties of the molecular species discussed here is based upon the rigorous theory of Chapman and Enskog (4) which includes the following assumptions:

1 Only binary collisions between molecules are considered.

2 Binary collisons are elastic.

3 The intermolecular force field is spherically symmetrical.

4 Molecular collisions are adequately described by the equations of classical mechanics.

5 The velocity distribution function is assumed to be Maxwellian in order that a temperature can be defined.

Despite these limitations, calculations based upon this theory yield results comparable to experimental data at low temperatures and densities (5, 6).

In order to obtain numerical results utilizing the theory of Chapman and Enskog, a potential energy function is required which represents the molecular interactions between a pair of species present in the gas. The earliest theoretical models which were developed for the potential function included only the repulsive forces between particles, such as, for example, the rigid sphere model.

$$\varphi(r) = \infty \quad r < \sigma$$
$$\varphi(r) = 0 \quad r > \sigma \qquad \ldots\ldots\ldots\ldots\ldots\ldots\ldots\ldots\ldots\ldots [1]$$

where r is the intermolecular separation distance, and σ is the collision diameter. A more realistic model was developed by Lennard-Jones; his model is the 6:12 potential energy function. This energy function includes the forces of long range attraction and short range repulsion between the two species involved in a collison. This function may be written

$$\varphi(r) = 4\epsilon[(\sigma/r)^{12} - (\sigma/r)^{6}] \qquad [2]$$

where ϵ is the maximum attractive energy.

For nonpolar molecules, the intermolecular force may be expressed as $F(r) = -d\varphi/dr$. This expression implies that the molecules are attracted to each other by an induced dipole-induced dipole force which is inversely proportional to the seventh power of the separation distance and repelled by a force which is empirically assumed to be inversely proportional to the thirteenth power of the separation distance (7).

The use of the Lennard-Jones 6:12 potential for the calculation of transport properties in gases at moderate temperatures is fairly widespread, and it is assumed here that similar calculation procedures can be applied to purely molecular encounters at high temperatures. However, at these higher temperatures, dissociation occurs, and atomic species are then present in the gas. Although scattering cross sections and collision integrals have been computed for the noble monatomic gases which have closed outer electron shells, i.e., Ne, A, Kr, He and Xe, none are available for monatomic gases which are the products of dissociation and have low lying excited states. (The present status of atomic species is discussed in (8).)

Values of the collision diameter (8) can be estimated for binary collisions between atomic and molecular species. However, the theory of interaction processes between excited atomic and molecular species is not fully developed, and thus no computations of the scattering cross sections have been made yet. Consequently, the necessary collision integrals cannot be calculated, and, hence, approximations must be introduced. It has been suggested (9) that a good approximate treatment of atom-molecule interactions would involve the use of a "suitably adjusted" potential energy function. For simplicity, however, the atomic species are treated here as rigid elastic spheres.

In performing the calculations in accordance with the theory, the coefficients of the transport properties may be expressed in terms of omega integrals, $\Omega^{(1,s)}$, which take into account the dynamics of the collision process. These integrals have been computed for a large number of nonpolar gases using the Lennard-Jones 6:12 potential. Various investigators have independently computed values for these integrals which show excellent agreement with each other. Tabulated values of these integrals (as a function of T^*) are available in many references, e.g. (10). It must be remembered, however, the $\Omega^{(1,s)}$ integrals are defined so that they reduce to unity for rigid elastic spheres.

The equations for the calculations of the transport properties to the first approximation are listed below.

Binary diffusion (11) (at a pressure of 1 atm)

$$[\mathfrak{D}_{12}]_1 = 1.145 \times 10^{-4}\, T^{3/2}\left[\frac{m_1 + m_2}{2m_1m_2}\right]^{1/2}\sigma_{12}^{-2}\,\frac{\text{ft}^2}{\text{sec}} \qquad [3]$$

Viscosity (12)

$$[\mu_4]_1 = 1.3369 \times 10^{-4}\sqrt{m_iT}/\sigma_i^2\Omega^{(2,2)}(T^*)\,\frac{\text{lb}}{\text{ft sec}} \qquad [4]$$

[4] Numbers in parentheses indicate References at end of paper

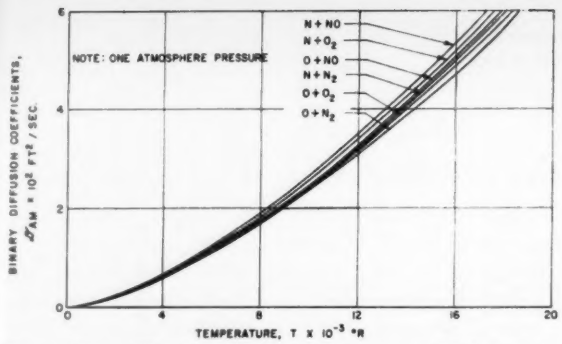

Fig. 1 Binary diffusion coefficients of components of air at 1 atm pressure

Viscosity of mixture (13)

$$\mu = \sum_{i=1} \frac{X_i^2}{\frac{X_i^2}{[\mu_i]_1} + 1.385 \sum_{k \neq i} \frac{X_i X_k RT}{p m_i [\mathfrak{D}_{ik}]_1}} \qquad [5]$$

Thermal conductivity of a binary mixture (14)

$$K = \frac{1 + \bar{Z}_K}{\bar{X}_K + \bar{Y}_K} \qquad [6]$$

where

$$\bar{X}_K = \frac{X_1^2}{[K_1]_1} + \frac{2X_1X_2}{[K_{12}]_1} + \frac{X_2^2}{[K_2]_1}$$

$$\bar{Y}_K = \frac{X_1^2}{[K_1]_1} U^{(1)} + \frac{2X_1X_2}{[K_{12}]_1} U^{(y)} + \frac{X_2^2}{[K_2]_1} U^{(2)}$$

$$\bar{Z}_K = X_1^2 U^{(1)} + 2X_1X_2U^{(z)} + X_2^2U^{(2)} \qquad [7]$$

in which X_1 and X_2 are the mole fractions of species 1 and 2, and $U^{(1)}$, $U^{(2)}$, $U^{(y)}$ and $U^{(z)}$ are a unique function of K_1, K_{12}, K_2, m_1, m_2, ϵ_{12}/k and the temperature (see Table 7).

According to kinetic theory, the thermal conductivity of a gas may be computed from the relationship

$$K = \frac{\delta}{3} \rho \lambda \bar{c}_v = \delta \mu c_v \qquad [8]$$

where δ has a minor dependence (15) on the form of the potential energy function. For rigid elastic spheres, $\delta = 2.522$, whereas for Maxwellian molecules (i.e., when $F(r) \sim (1/r)^5$) $\delta = 5/2$. In these calculations for the atomic species, δ was taken as 5/2. For polyatomic species, a further correction is necessary to take into account the internal degrees of freedom. This led Eucken (16) to propose the expression

$$K_i = \frac{9\gamma_i - 5}{4} \mu_i c_{v_i} = \frac{15}{4} \frac{R_i}{J} \mu_i \left(\frac{4}{15} \frac{c_{v_i} J}{R_i} + \frac{3}{5} \right) \qquad [9]$$

It is interesting to observe that, although Chapman and Cowling object to Eucken's explanation and offer a rigorously derived equation (17)

$$K_{ice} = \left[\frac{15}{4} (\gamma_i - 1) + \frac{u_{11}}{2} (5 - 3\gamma_i) \right] \mu c_{v_i} \qquad [10]$$

their result is not in marked disagreement with Equation [9] since $u_{11} = 1.204$ for smooth elastic spheres; $u_{11} = 1.55$ for Maxwellian molecules, while $K_i = K_{ice}$ when $u_{11} = 1.00$.

In view of the foregoing considerations, the Eucken approximation, Equation [9], has been utilized in the computation of the thermal conductivity of the molecular species, and, arbitrarily, K_{12} was given half of the Eucken correction factor for a binary mixture of atoms and molecules. This was done so that Equation [6], which was derived for a binary mixture of monotomic gases, could be utilized for a binary mixture of atoms and molecules. Thus, the following expression was employed for K_{12}

$$K_{12} = 4.0167 \times 10^{-3} \frac{p\mathfrak{D}_{12}}{A_{12}{}^* T} \left(\frac{2}{15} \frac{c_{v_2} J}{R_2} + \frac{4}{5} \right) \frac{\text{Btu ft}}{\text{ft}^2 \text{ sec deg R}} \qquad [11]$$

In Equation [11] the subscript 2 refers to the molecular species, and p, $\mathfrak{D}_{12}$ and T must be expressed in fps units.

In the light of recent theoretical developments, it is now clear (2) that, although Equation [6] is relatively simple in application, it is not the most realistic expression currently available. The reader is therefore referred to (2) for a complete discussion of the complex but rigorous equation for the computation of multicomponent thermal conductivity.

A comparison between our approximate treatment and the more exact theory is reserved for Part II of this paper.

Curves of six binary diffusion coefficients for the atomic and molecular components of dissociated air are shown in Fig. 1. These curves were calculated by means of Equation [3] and are given explicitly by the data in Table 2; the gas constants are listed in Table 1. The diffusion coefficients are given for a pressure of 1 atm; however, since the diffusion coefficients vary inversely with pressure at constant temperature the following expression is obtained

$$[\mathfrak{D}_{12}]_1 = \frac{[\mathfrak{D}_{12}]_1 \ (p = 1 \text{ atm})}{p(\text{atm})} \qquad [12]$$

The viscosity coefficients of the five components of dissociated air are shown in Fig. 2. These curves were obtained utilizing Equation [4] and the gas constants appearing in Table 1. The data were curve-fitted with fifth degree polynomials for the molecular species, since the omega function $\Omega^{(2,2)}$ varies with temperature; the results appear in Table 3. The viscosity coefficients for the atomic species which were assumed to behave as rigid spheres are also given in Table 3.

Table 1 Gas constants

Species	σ, Å	m_i, $\frac{\text{lb}}{\text{lb mole}}$	R_i, $\frac{\text{ft lb}}{\text{lb deg R}}$	ϵ/k, deg K
N_2	3.749[a]	28.0	55.19	3.749[a]
N	2.88[b]	14.0	110.38	...
O_2	3.541[a]	32.0	48.26	88.0[b]
O	2.96[b]	16.0	96.58	...
NO	3.47[c]	30.0	51.51	119[c]

Note: $\sigma_{12} = \frac{\sigma_1 + \sigma_2}{2}$ (see Eq. [2])

[a] Trautz, M., Melster, A. and Zink, R., *Ann. Physik*, vol. 5, no. 7, 1930, pp. 409–452.

[b] Hirschfelder, J. and Eliason, M., "The Estimation of Transport Properties for Electronically Excited Atoms and Molecules," Technical Report Wis-AF-1; Contract AF 33(616)3414, May 14, 1956.

[c] Johnston, H. and McCloskey, K., *J. Phys. Chem.*, vol. 44, no. 1038, 1940.

Table 2 Binary diffusion coefficients

Atom-molecule pair	Equation
N + NO	$\mathfrak{D}_{AM} = 2.6590 \times 10^{-3} \ T^{3/2}$ ft²/sec
N + O_2	$\mathfrak{D}_{AM} = 2.5680 \times 10^{-3} \ T^{3/2}$ ft²/sec
O + NO	$\mathfrak{D}_{AM} = 2.4798 \times 10^{-3} \ T^{3/2}$ ft²/sec
N + N_2	$\mathfrak{D}_{AM} = 2.4680 \times 10^{-3} \ T^{3/2}$ ft²/sec
O + O_2	$\mathfrak{D}_{AM} = 2.3994 \times 10^{-3} \ T^{3/2}$ ft²/sec
O + N_2	$\mathfrak{D}_{AM} = 2.3075 \times 10^{-3} \ T^{3/2}$ ft²/sec

Table 3 Viscosity of components of air

atomic $\mu_i = aT^{1/2}$ lb/ft-sec

Atomic species (rigid sphere)	N	O
a	6.031×10^{-7}	6.097×10^{-7}

molecular $\mu_i = a + bT + cT^2 + dT^3 + eT^4 + fT^5$ lb/ft-sec

Molecular species (Lennard-Jones 6:12)	N_2	NO	O_2
a	9.3390×10^{-6}	3.9482×10^{-6}	5.0199×10^{-6}
b	1.1306×10^{-8}	1.7830×10^{-8}	1.7901×10^{-8}
c	-6.8452×10^{-13}	-2.2202×10^{-12}	-2.1213×10^{-12}
d	4.1009×10^{-17}	2.2770×10^{-16}	2.1045×10^{-16}
e	-1.3194×10^{-21}	-1.1759×10^{-20}	-1.0688×10^{-20}
f	1.5501×10^{-26}	2.3149×10^{-25}	2.1000×10^{-25}

The thermal conductivity of the atomic species was computed utilizing

$$K_i = \frac{15}{4}\frac{R_i}{J}\mu_i \qquad [13]$$

which assumes Maxwellian atoms. The curve labeled "air atom" in Fig. 3 represents an average for oxygen and nitrogen atoms. As mentioned previously, the thermal conductivity of the air molecules was computed utilizing Equation [9], and the curve labeled "air molecule" in Fig. 3 represents an average for oxygen and nitrogen molecules. The curve marked "hypothetical AM particle" in this figure represents the quantity K_{12} required for the computation of the thermal conductivity of dissociated air, treated as a binary mixture of "air atoms" and "air molecules." The thermal conductivity of dissociated air was calculated using Equation [6]; K_{12}, required for use in Equation [6], was calculated using Equation [11]. These three curves were curve-fitted, using fifth degree polynomials; the coefficients are listed in Table 4.

Thermodynamic Properties

The heat capacity of a gaseous mixture depends upon the contributions of random translation and the internal degrees of freedom of the pure species, such as molecular rotation, molecular vibration and electronic excitation, and the energy required to dissociate or ionize the gas which may be considered as external heat capacity.

If h_i, the enthalpy of a pure species, including chemical, is written

$$h_i = \int_{T_{ref}}^{T} c_{p_i} dT + \Delta h_{f_i}^0 \qquad [14]$$

where $\Delta h_{f_i}^0$ is the heat of formation at the reference temperature, then the enthalpy of a gaseous mixture is

$$h = \sum_i c_i h_i$$

where c_i is the mass fraction of species i, in which case the temperature derivative at constant pressure of the enthalpy becomes

$$c_p = \left(\frac{\partial h}{\partial T}\right)_p = \sum_i \left[c_i \left(\frac{\partial h_i}{\partial T}\right)_p + h_i \left(\frac{\partial c_i}{\partial T}\right)_p\right] \qquad [15]$$

hence

$$c_p = \sum_i c_i c_{p_i} + \sum_i h_i \left(\frac{\partial c_i}{\partial T}\right)_p \qquad [16]$$

or

$$c_p = \bar{c}_p + \sum_i h_i \left(\frac{\partial c_i}{\partial T}\right)_\mu \qquad [17]$$

It is observed that the specific heat of the mixture c_p depends upon two terms. The first term, $\bar{c}_p$, has been given the name "frozen specific heat," because it depends only on the specific heats of the pure species present in the gas, and because it may be evaluated independently of the rate of change of composition of the gas. The second term reflects the chemical heat capacity of a gas and is a measure of the specific heat due to homogeneous chemical reactions, such as dissociation, ionization and combustion. Thus, for a nonreacting gas, the second term on the right-hand side of Equation [17] vanishes, and $c_p = \bar{c}_p$. For a reacting gas, however, the

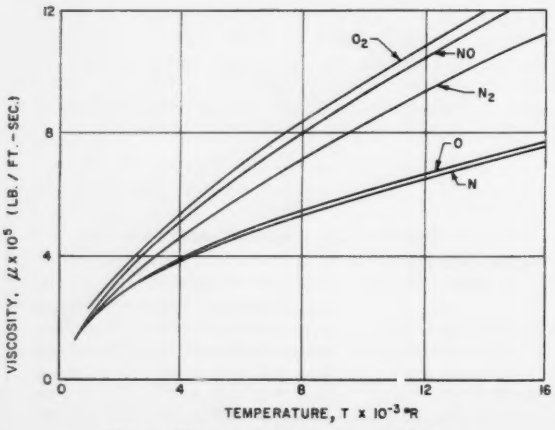

Fig. 2 Viscosities of components of air

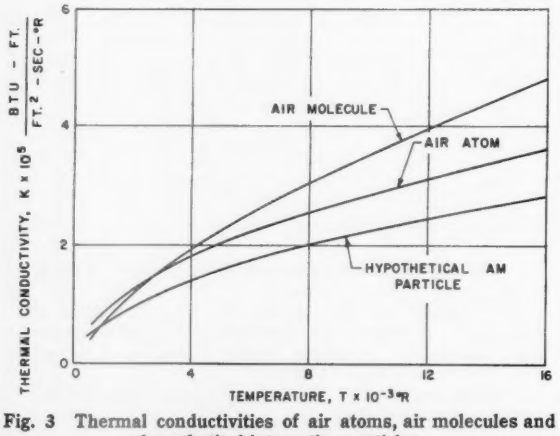

Fig. 3 Thermal conductivities of air atoms, air molecules and hypothetical interaction particles

Table 4 Thermal conductivity

$K_f = a + bT + cT^2 + dT^3 + eT^4 + fT^5$ Btu ft/ft² sec deg R

Species	a	b	c	d	e	f
M	7.3858×10^{-7}	6.6178×10^{-9}	-7.2997×10^{-13}	6.9568×10^{-17}	-3.4594×10^{-21}	6.6743×10^{-26}
A	3.7115×10^{-6}	5.7724×10^{-9}	-8.1325×10^{-13}	8.1610×10^{-17}	-4.1194×10^{-21}	7.9680×10^{-26}
AM	2.5983×10^{-6}	4.3819×10^{-9}	-4.9490×10^{-13}	3.7690×10^{-17}	-1.4371×10^{-21}	2.1073×10^{-26}

derivative $(\partial c_i/\partial T)_p$ is not zero, and can be evaluated only with great difficulty for nonequilibrium mixtures. For the special case of an equilibrium mixture of gases, this derivative can be determined a priori; however, in general, it must be evaluated while solving a particular problem using appropriate reaction rate equations.

The internal specific heat at constant volume c_{v_i} of a pure species may be determined by evaluating the temperature derivative of the partition function q defined in statistical mechanics (for example, (18))

$$c_{v_i} = \left[\frac{\partial}{\partial T}\left(\frac{R_i}{J} T^2 \frac{\partial \ln q}{\partial T}\right)\right]_v \qquad [18]$$

At ordinary temperatures, the contributions of translation and molecular rotation are fully excited. Based upon the assumption that the contributions of the internal degrees of freedom are uncoupled, i.e.

$$q = q_{tr} \times q_{rot} \times q_{vib} \times q_{elec} \qquad [19]$$

and by restricting the maximum temperature so that electronic excitation is negligible, the following equation is obtained for a diatomic molecule (19)

$$c_{v_i} = \frac{3}{2}\frac{R_i}{J} + \frac{R_i}{J} + \frac{R_i\left(\frac{\Theta}{T}\right)^2 e^{\Theta/T}}{J[e^{(\Theta/T)} - 1]^2} \qquad [20]$$

In Equation [20], the three terms represent the contributions of translation, rotation and vibration of the gaseous molecules, respectively. The last term is the Einstein function which depends on Θ, the characteristic temperature.

$$\Theta = \frac{h\nu}{k} = \frac{hc\omega_e}{k} = 1.439\omega_e \text{ cm deg K} \qquad [21]$$

ω_e is the characteristic frequency of vibration of the molecules.

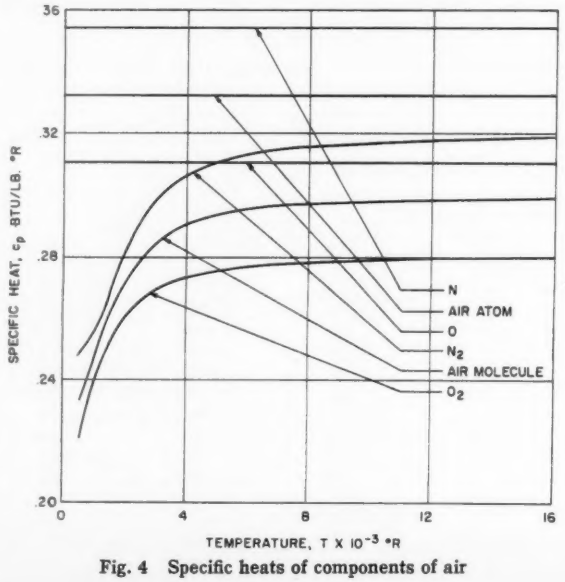

Fig. 4 Specific heats of components of air

If it is assumed further that the gas is a mixture of chemically reacting perfect gases

$$c_{p_i} = c_{v_i} + \frac{R_i}{J} \qquad [22]$$

and, hence, the specific heats at constant pressure of the pure components of dissociated air, atomic and molecular, can be evaluated. Presented below are results obtained for oxygen and nitrogen atoms, and oxygen and nitrogen molecules.

Oxygen atoms and nitrogen atoms have constant specific heats, which depend only upon the contribution of translation, if electronic excitation is neglected.

In fps notation there follows

$$c_{p_O} = \frac{5}{2}\frac{R_O}{J} = 0.3105 \frac{\text{Btu}}{\text{lb deg R}}$$

$$c_{p_N} = \frac{5}{2}\frac{R_N}{J} = 0.3546 \frac{\text{Btu}}{\text{lb deg R}} \qquad [23]$$

Oxygen molecules and nitrogen molecules which are diatomic have variable specific heats defined by Equations [20 and 22]. As indicated in (20)

$$\Theta_{O_2} = 2274 \text{ deg K } (\omega_{e_{O_2}} = 1580.4 \text{ cm}^{-1})$$

$$\Theta_{N_2} = 3395 \text{ deg K } (\omega_{e_{N_2}} = 2359.5 \text{ cm}^{-1}) \qquad [24]$$

The results are presented in Fig. 4; polynomial curve-fits have been obtained which are given in Table 5.

Note that species, such as argon, nitric oxide and other gases, have not been considered here; they are usually present in trace amounts (21) and do not appreciably influence the thermodynamic properties of air. The enthalpies of the pure species follow directly upon integrating the specific heats calculated by means of Equation [22]. The upper limit of integration is, of course, the temperature at which the enthalpy is required. The lower limit of integration must be selected so as to coincide with the reference temperature at which the standard heat of formation, $\Delta h_{f_i}^0$, is evaluated. Common usage is either 0 or 298.15 deg K. $T_{ref} = 298.15\text{K} = 536.7$ R has been accepted for this calculation; hence, there follows

$$\Delta h_{f_O}^0 = 6654 \text{ Btu/lb}$$

$$\Delta h_{f_N}^0 = 14{,}527 \text{ Btu/lb} \qquad [25]$$

where $\Delta h_{f_N}^0$ is based upon the revised dissociation energy (9.758 ev) of nitrogen molecules (22), and the heats of formation of the molecules in standard state are zero by definition.

Then, for the atomic species, oxygen and nitrogen

$$h_O = 6.493 \times 10^3 + 0.3105\ T \text{ Btu/lb}$$

$$h_N = 1.431 \times 10^4 + 0.3546\ T \text{ Btu/lb} \qquad [26]$$

where T is expressed in deg R.

Table 5 Specific heats

$$c_{p_i} = a + bT + cT^2 + dT^3 + eT^4 + fT^5 \text{ Btu/lb deg R}$$

Species	Temperature range, deg R	a	b	c	d	
N_2	$500 \leq T \leq 2700$	2.5262×10^{-1}	-1.5702×10^{-5}	4.1319×10^{-10}	3.3918×10^{-11}	-1.9
	$2700 \leq T \leq 7200$	2.0651×10^{-1}	6.0717×10^{-5}	-1.3814×10^{-8}	1.4488×10^{-11}	-5.3
	$7200 \leq T \leq 16000$	3.8047×10^{-1}	-3.3995×10^{-5}	6.5579×10^{-9}	-5.9304×10^{-11}	2.5
O_2	$500 \leq T \leq 2700$	1.9934×10^{-1}	3.1337×10^{-5}	2.4656×10^{-8}	-2.5372×10^{-11}	8.5
	$2700 \leq T \leq 7200$	1.8820×10^{-1}	7.3482×10^{-5}	-2.7284×10^{-8}	5.3556×10^{-11}	-5.3
	$7200 \leq T \leq 16000$	2.3914×10^{-1}	1.5528×10^{-5}	-2.4641×10^{-9}	1.9518×10^{-11}	-7.6
air molecule	$500 \leq T \leq 2700$	2.7266×10^{-1}	-1.9062×10^{-4}	3.0806×10^{-7}	-1.9307×10^{-10}	5.5
	$2700 \leq T \leq 7200$	2.4530×10^{-1}	1.0725×10^{-5}	4.0440×10^{-9}	-1.6965×10^{-11}	2.1
	$7200 \leq T \leq 16000$	2.8587×10^{-1}	1.9881×10^{-6}	1.8329×10^{-11}	-2.1424×10^{-14}	1.4

Table 6 Enthalpy of air molecule

$$h_M = a + bT + cT^2 + dT^3 + eT^4 + fT^5 + gT^6 \text{ Btu/lb}$$

Temperature range deg R	a	b	c	d	e	
$500 \leq T \leq 2700$	-1.3127×10^2	2.7266×10^{-1}	-9.5310×10^{-5}	1.0269×10^{-7}	-4.8268×10^{-11}	1.1
$2700 \leq T \leq 7200$	-1.4588×10^2	2.4530×10^{-1}	5.3625×10^{-6}	1.3480×10^{-9}	-4.2413×10^{-13}	4.3
$7200 \leq T \leq 16000$	-2.2411×10^2	2.8587×10^{-1}	9.9405×10^{-7}	6.1097×10^{-12}	-5.3560×10^{-16}	2.9

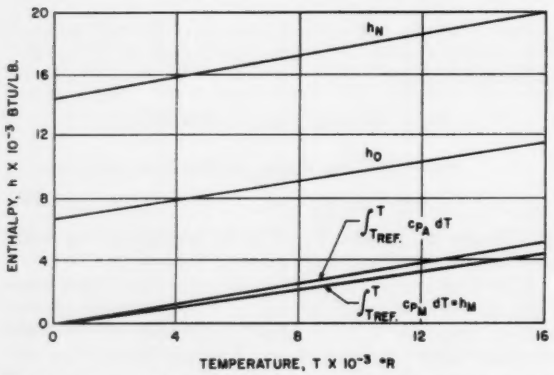

Fig. 5 Enthalpies of air molecules, oxygen and nitrogen atoms and integrated specific heats of air atoms

The enthalpies of the oxygen and nitrogen molecules follow by quadrature from Table 5, utilizing Equation [14] and integrating the fifth degree polynomials term-by-term.

In Fig. 4, the specific heats of the four primary components of dissociated air are presented. In addition, curves labeled "air atom" and "air molecule" are shown, which are simply the arithmetic mean specific heats for the air atoms and molecules, respectively. In Fig. 5 are shown the integrated specific heats for the "air atom" labeled $\int c_{p_A} dT$ and the "air molecule" labeled $\int c_{p_M} dT$. For air molecules, this integral coincides with the enthalpy, because the heat of formation is zero. For convenience, a polynomial curve-fit of the $\int c_{p_M} dT$ is given in Table 6. For the atomic species, the heat of formation, as presented in Equation [25], has been utilized in obtaining the enthalpies which are given in Equation [26] and are also shown plotted in Fig. 5.

Table 7 Temperature dependent variables

T, deg R	$U^{(1)}$	$U^{(3)}$	$U^{(5)}$	$U^{(7)}$	A^*_{12}	B^*_{12}	C^*_{12}
540	0.2804	−0.0761	0.0404	0.2414	1.097	1.095	0.9193
900	...	...	...	...	1.103	1.095	0.9375
1800	...	...	...	...	1.110	1.095	0.9460
2700	0.2860	−0.0701	0.0434	0.2458	1.116	1.095	0.9474
3600	...	...	...	...	1.121	1.095	0.9474
4500	...	...	...	...	1.124	1.095	0.9483
5400	0.2882	−0.0681	0.0443	0.2478	1.126	1.095	0.9483
7200	...	...	...	...	1.129	1.095	0.9483
9000	0.2898	−0.0665	0.0449	0.2491	1.132	1.095	0.9483
10,800	...	...	...	...	1.134	1.095	0.9483
12,600	...	...	...	...	1.135	1.095	0.9483
14,400	0.2906	−0.0657	0.0453	0.2498	1.137	1.095	0.9483
16,200	...	...	...	...	1.138	1.095	0.9483
18,000	0.2919	−0.0644	0.0459	0.2508	1.140	1.095	0.9483

e	f
-1.9330×10^{-14}	3.0776×10^{-18}
-5.3158×10^{-17}	-5.3771×10^{-22}
2.5698×10^{-17}	-4.3095×10^{-22}
8.5378×10^{-15}	-1.0470×10^{-18}
-5.3346×10^{-16}	2.1169×10^{-20}
-7.6374×10^{-18}	1.1759×10^{-22}
5.5255×10^{-14}	-5.9898×10^{-18}
2.1633×10^{-16}	-9.4996×10^{-21}
1.4711×10^{-18}	-3.0737×10^{-23}

f	g
1.1051×10^{-14}	-9.9830×10^{-19}
4.3266×10^{-17}	-1.5833×10^{-21}
2.9422×10^{-19}	-5.1228×10^{-24}

Summary

The investigation described here was undertaken to provide transport and thermodynamic property data, so that the effects of variable properties could be included in analyses of hypersonic viscous flow regimes where dissociation becomes important.

Certain approximations with regard to the interaction of atomic and molecular species have been introduced at this time because of the incomplete state of the theory of such processes.

The transport property coefficients, including ordinary diffusion, viscosity and thermal conductivity, have been calculated for the products of dissociated air; polynomial curve-fits have been obtained. In addition, the specific heat and enthalpies have also been computed.

The precise relationship between the choice of the potential energy function, the force constants and the resultant effect on boundary layer heat transfer has not been considered here; it will form the basis of a future paper. Such an investigation is considered warranted, since it has been estimated that the transport properties calculated may be in error by a factor on the order of 50 per cent at the higher temperatures (23) $T > 10{,}000$ R.

Acknowledgment

The authors wish to express their gratitude to Professors J. Hirschfelder and C. Curtiss (University of Wisconsin) for their helpful suggestions; to Dr. W. Zinman (Aerosciences Laboratory, M&SVD) for his critical review of this work) and to Leon Gilbert and Kathleen Burke for their able assistance in the computations.

References

1 Hilsenrath, J., "Sources of Transport Coefficients and Correlation of Thermodynamic and Transport Data," Selected Combustion Problems, II, AGARD, 1956, pp. 199–244.

2 Curtiss, C. F., Hirschfelder, J. O. and Bird, R. B., "Transport Properties in Gases," Northwestern University Press, Jan. 1958, p. 3.

3 Baulknight, C., "Transport Properties in Gases," Northwestern University Press, Jan. 1958, p. 89.

4 Chapman, S. and Cowling, T. G., "The Mathematical Theory of Non-Uniform Gases," Cambridge Univ. Press, 1953.

5 Johnston, H., McCloskey, K. et al., *J. Chem. Phys.*, vol. 16, no. 968, 1948.

6 Johnston, H. and McCloskey, K., *J. Chem. Phys.*, vol. 44, no. 1038, 1940.

7 Lennard-Jones, J. E., *Proc. Royal Society*, vol. A, no. 106, p. 441, 1924.

8 Hirschfelder, J. O., "Heat Conductivity in Polyatomic, Electronically Excited, or Chemically Reacting Mixtures, III," University of Wisconsin CM-880, Aug. 15, 1956.

9 Hirschfelder, J. O., private communication, Feb. 1958.

10 Hirschfelder, J., Curtiss, C. and Bird, R., "Molecular Theory of Gases and Liquids," John Wiley and Sons, New York, 1954, pp. 1126–1127.

11 *ibid.* p. 539.

12 *ibid.* p. 528.

13 *ibid.* p. 533.

14 *ibid.* p. 535.

15 Jeans, J., "Kinetic Theory of Gases," Cambridge University Press, Cambridge University, 1946, first ed., p. 186.

16 Eucken, A., *Phys. Zeits.* vol. 14, 1913, p. 324.

17 Chapman, S. and Cowling, T. G., (4), pp. 237–238.

18 Glasstone, S., "Thermodynamics for Chemists," Van Nostrand Co., Inc., 1947, sixth ed., p. 102.

19 Dole, M., "Introduction to Statistical Thermodynamics," Prentice Hall, Inc., New York, 1954, p. 132.

20 Herzberg, G., "Spectra of Diatomic Molecules," Van Nostrand Co., Inc., New York, 1950, pp. 553 and 560.

21 Logan, J. and Treanor, C., "Tables of Thermodynamic Properties of Air from 3000–10,000°K.," Cornell Aeronautical Laboratory, Inc., Jan. 1957.

22 Kistiakowsky, G., Knight, H. and Malin, M., "Gaseous Detonations III Dissociation Energies of N_2 and CO," *J. Chem. Phys.*, vol. 20, May 1952, p. 876.

23 Hirschfelder, J. O., private communication, Sept. 1957.

Technical Notes

Calculation of Unsteady Supersonic Flow Past a Circular Cylinder[1]

MARTHA W. EVANS[2] and FRANCIS H. HARLOW[3]

University of California, Los Alamos Scientific Laboratory, Los Alamos, N. Mex.

A numerical calculation method has been used to determine the two-dimensional, transverse flow pattern of air moving at supersonic speeds past an infinite circular cylinder. Details are presented concerning initial flow stages after the cylinder had been impulsively accelerated to a fixed speed. Information is presented in particular about the lateral propagation rate of disturbance, the development of detached shock, stream lines and streak lines, and the drag and isopycnics.

Nomenclature

c = input sound speed
C_D = cylinder drag coefficient
M = Mach number
S = lateral disturbance propagation rate
t = time, measured in units of cell size/c
γ = specific heat ratio for air, taken as 1.4
ρ_0 = input air density
ρ = air density

WE HAVE used a numerical calculation method (1)[4] to study the two-dimensional, transverse flow of air at supersonic speeds past an infinite circular cylinder in a rigid chamber. The approach to steady state was studied in detail for cases in which the cylinder was impulsively accelerated to a fixed speed. Mach numbers studied were 2, 4 and 6. Air was represented by a nonviscous polytropic gas with specific heat ratio $\gamma = 1.4$. The calculations were performed on an IBM Electronic Data Processing Machine, type 704.

An extensive discussion of the general computational technique has been given in (2). The air was represented by Lagrangian mass points called "particles" moving through an Eulerian computational mesh which was fixed, relative to the cylinder. A portion of the region studied, at a late stage in the approach to steady state, is shown in Fig. 1. Particles were inserted at the front of the mesh, and dropped from the computation when they crossed the downstream boundary. Both halves of the system were studied simultaneously in the calculation.

Several computational features differ from those presented in (1 and 2). We did not use the "velocity weighting" procedure for moving particles, thereby eliminating a large amount of computation time. Each particle was moved with its cell-wise velocity, regardless of its position within the cell. The boundary of the cylinder was represented by a set of straight line segments. The treatment of densities, pressures, etc., in the partial cells next to the cylinder was a straightforward extension of the previously reported method. Without the use of velocity weighting, particles could cross into the cylinder or across the chamber wall. These crossings were treated by a simple reflection process.

The Eulerian computational mesh consisted of square cells in a region 42 long by 32 wide. The cylinder diameter was 10 cells. Times are given in units of cell size divided by input sound speed. The Mach number was varied by changing the input velocity.

Results of the Calculations

Growth of the disturbance about the cylinder is shown in Fig. 2 (a to e) for $M = 4$. Approach to the detached shock position of Kim (3) is seen. The sequence of figures shows the shedding of successive undulations along the low-high density boundary. These are caused by the dropping of "velocity weighting." By $t = 9$ (a section of the pattern is shown in Fig. 3), the detached shock is slightly ahead of that of Kim, and the isopycnic at normal density is oscillatory. Kim's isopycnic at $\rho = 1.09\ \rho_0$ is shown. The calculation was not continued to final steady state because of the computation time involved. (The calculation to $t = 9$ required a little more than three hours.) The indication concerning the detached shock position, however, is that it would stand slightly outside of the experimental position. The extent of the discrepancy is not surprising, since the experimental shock lies less than three computational cells in front of the cylinder. The direction of error is the same as in a previous similar calculation (4) for the detached shock in front of a blunt nosed cylinder in supersonic, axially symmetric flow at $M = 5.8$.

Propagation of the disturbance is characterized by the downstream motion of a low density region, and the lateral and forward motion of a compression region.

The low density region should propagate backward with sound speed relative to the air and does so in the computation. A cavity which developed behind the cylinder was a fictitious feature which should not have occurred, because the escape speed was greater than the input velocity. The cavity resulted from the frequent "repartitioning" (2) in the rarefaction region, but its presence had very little effect on the results presented here.

Propagation distance of the lateral compression disturbance is shown as a function of time in Fig. 4 for $M = 4$. The disturbance quickly reaches a steady lateral propagation rate of 2.0 c. Also shown is the distance of backward drift of the position of maximum lateral disturbance. The rate of lateral propagation of disturbance was also calculated for $M = 2$ and $M = 6$, giving, respectively, rates of 1.4 c and 2.5 c. These values tentatively suggest a relation among lateral dis-

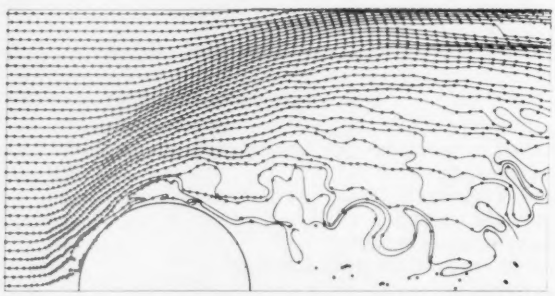

Fig. 1 Instantaneous configuration of particles at a late stage ($t = 9$) in the approach to steady state; $M = 4$

Received June 16, 1958.

[1] Work performed under the auspices of the U. S. Atomic Energy Commission.

[2] Staff member, Theoretical Division.

[3] Staff member, Theoretical Division.

[4] Numbers in parentheses indicate References at end of paper.

EDITOR'S NOTE: The Technical Notes and Technical Comments sections of ARS JOURNAL are open to short manuscripts describing new developments or offering comments on papers previously published. Such manuscripts are published without editorial review, usually within two months of the date of receipt. Requirements as to style are the same as for regular contributions (see masthead page).

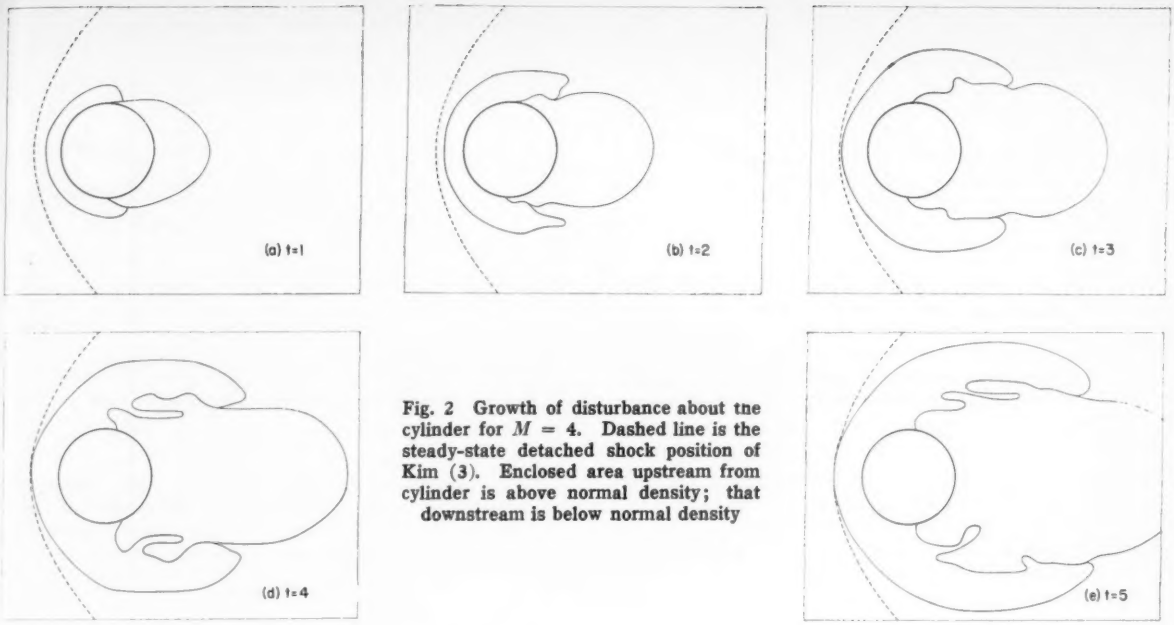

Fig. 2 Growth of disturbance about the cylinder for $M = 4$. Dashed line is the steady-state detached shock position of Kim (3). Enclosed area upstream from cylinder is above normal density; that downstream is below normal density

turbance propagation rate S, input sound speed c and Mach number M

$$S = c\sqrt{M}$$

This same relation has been observed in other calculations for other than cylindrical shapes; it is also consistent with a previous calculation result (4) which showed that approximate steady state is reached near the object in a time given by dividing the diameter by S.

Net force on the cylinder was calculated. Large variations with time are to be expected because of fluctuations of cell-wise particle numbers, but the average calculated force over a long time should correspond closely to experimental results. For $M = 4$, we averaged the force for 21 equal-spaced times from $t = 4$ to $t = 9$, inclusive. From this, the drag coefficient was calculated to be $C_D = 1.15$. We also performed a numerical integration of the pressure coefficient given by Kim (3), obtaining the experimental result $C_D = 1.25$. This latter value appears to agree with the interpolated value given by Hoerner (5).

Fig. 1 shows, for $M = 4$, the configuration of particles at

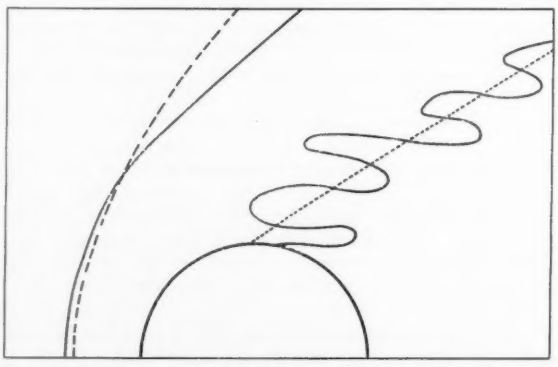

Fig. 3 Part of the disturbance pattern at $t = 9$ for $M = 4$. Symbols are the same as in Fig. 2, with the addition of the dotted line which is the isopycnic $\rho = 1.09\ \rho_0$ of Kim (3)

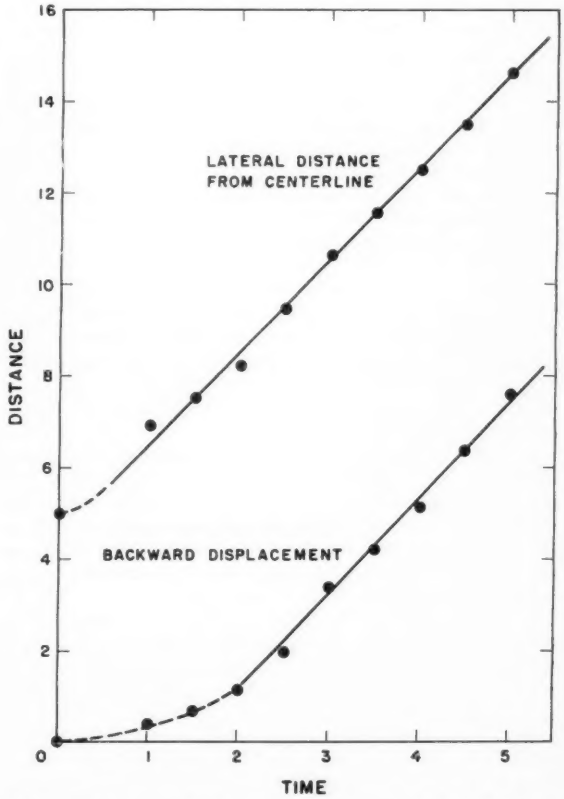

Fig. 4 Distance of maximum lateral compression disturbance from centerline and centerline displacement back from the cylinder center of the position of this maximum disturbance, both as functions of time. $M = 4$

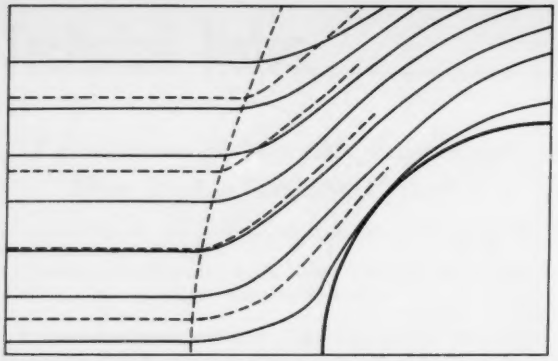

Fig. 5 The stream lines and shock position of Kim (3) (dashed) compared with our streak lines from Fig. 1. $M = 4, t = 9$

Fig. 6 Stream lines behind the cylinder at $t = 9$ for $M = 4$

$t = 9$ for part of the system. Lines connecting the particles have been faired in by referring to detailed sequence listings as printed out by the computer. This information was lost for those unconnected particles near the centerline. The particles marked by "x" were along a line perpendicular to the centerline at input. Reflection of the shock from the rigid chamber wall can be seen in this figure.

The perturbations which grew into large contortions of the streak lines, arose at the cylinder front. They resulted from the irregular cylinder shape, the particle reflection procedure and other causes related to discreteness of the calculational mesh. They correspond roughly to perturbations that might experimentally be produced by roughness of the cylinder or fluctuations in the incoming air.

The shock front had not reached its final position by $t = 9$. Nevertheless, we have compared our streak lines with the stream lines of Kim (3). In Fig. 5, we show Kim's stream lines and shock position (dashed) and our alternate streak lines from Fig. 1. There is close agreement toward the centerline, and the disagreement away from the centerline is as expected from the fact that our shock has not reached its steady position (compare Fig. 3).

Behind the cylinder, the stream and streak lines are considerably different. The stream lines (Fig. 6) were drawn by fairing in lines parallel to the cellwise velocities.

Discussion

The hydrodynamic computing method used in these calculations has now been applied to a rather large number of complicated hydrodynamic problems, and its capabilities and limitations are becoming apparent. The degree to which the results in any problem agree with experiments depends upon several factors, such as:

1 The computational mesh must be fine compared with the dimensions of all features of interest. Thus the shock detachment distance is in error when it should lie only three cells away from the cylinder, whereas it becomes accurate as the mesh fineness increases (4). Individual cell densities at any instant have no real meanings; local densities are meaningful only when averaged over many cells.

2 Certain cellwise quantities can be given meaning by taking time averages. Our isopycnics agree quite well with those of Kim if the local densities are averaged over sufficient time. Likewise, the time-averaged drag coefficient is reasonably good.

3 Certain difficulties persist in spite of these considerations. The flow of gas from a wall, leaving a region of rarefaction, is poorly represented due to repartitioning. In general, the entropy production in a rarefaction is too high if the material moves in the direction of increasing density. Just the opposite difficulty occurs in perturbed stagnation regions (not present in the calculation reported here).

With these considerations in mind, useful information can be obtained by applying this computational method to any of a wide variety of complicated two-dimensional problems involving several materials and generalized boundaries.

References

1 Harlow, F. H., "Hydrodynamic Problems Involving Large Fluid Distortions," *J. Assoc. for Computing Machinery*, vol. 4, April 1957, pp. 137–142.

2 Evans, M. W. and Harlow, F. H., "The Particle-In Cell Method for Hydrodynamic Calculations," Los Alamos Scientific Laboratory Report no. LA-2139, Nov. 1957.

3 Kim, C. S., "Experimental Studies of Supersonic Flow Past a Circular Cylinder," *J. Phy.ical Soc. of Japan*, vol. 11, April 1956, pp. 439–445.

4 Evans, M. W. and Harlow, F. H., "Calculation of Supersonic Flow Past an Axially Symmetric Cylinder," *J. Aeron. Sci.*, vol. 25, April 1958, pp. 269–270.

5 Hoerner, S. F., "Fluid-Dynamic Drag," published by author, 1958, p. 16-16

Characteristic Velocity for Changing the Inclination of a Circular Orbit to the Equator

LEONARD RIDER[1]

Sperry Gyroscope Co., Great Neck, N. Y.

FROM a minimum energy standpoint it is desirable that an impulsive velocity increment applied to a space vehicle for the purpose of changing its direction be effected, if possible, when the velocity of the vehicle is minimal. Use of this principle for the synthesis of a non-coplanar transfer trajectory resulting in the change of inclination of a circular orbit about a circular Earth, leads one to the consideration of a three impulse transfer: The first impulse applied tangentially to the flight path in the sense of travel at the appropriate point of the circular orbit, the second impulse applied at the apogee of the resulting elliptical orbit in the plane perpendicular to the radius vector from the force center and at an angle such that the vehicle velocity at apogee is rotated through the required angle, and the third impulse (retro) applied when the vehicle returns to the point of application of the first impulse and of magnitude equal to the first impulse.

Received Aug. 29, 1958.

[1] Engineer, Weapon System Department. Now Senior Engineer, Convair Astronautics. Member ARS.

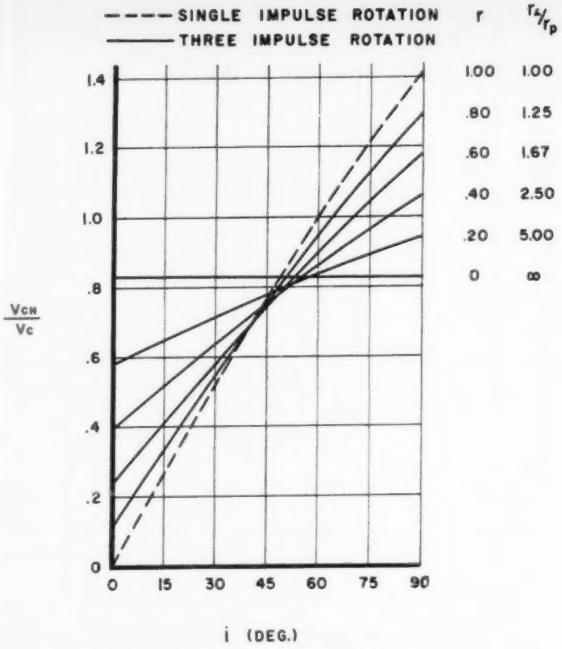

Fig. 1 Characteristic velocity for orbital plane rotation of a circular orbit

The characteristic velocity is of the form

$$V_{CH} = \Delta V_1 + \Delta V_2 + \Delta V_3 = 2\Delta V_1 + \Delta V_2$$
$$= 2V_C \left\{ \sqrt{\frac{2}{r+1}} [r(\sin i/2) + 1] - 1 \right\}$$

where

V_C = vehicle velocity in the original and final circular orbit
i = angle between initial and final orbital planes
r = r_p/r_A = ratio of distance to the force center of perigee and apogee

and is compared in the figure to the characteristic velocity for a single impulsive rotation of the orbital plane whose value is given by

$$V_{CH} = 2V_C \sin i/2$$

It can be seen from the figure that the three impulse mode of orbital plane rotation is more economical than the single impulsive rotation for rotations greater than 49 deg for any r, and results in a maximum theoretical saving of 42 per cent of the required single impulse characteristic velocity for a rotation of 90 deg.

Application of Surface Decomposition Kinetics to Detonation of Ammonium Nitrate[1]

W. H. ANDERSEN[2] and R. F. CHAIKEN[3]

Aerojet-General Corp., Azusa, Calif.

Kinetic rate data for the linear surface gasification (pyrolysis) of ammonium nitrate is used in conjunction with the Eyring grain burning theory to calculate the detonation reaction time for ammonium nitrate. A new grain burning mechanism is postulated which results in a reaction time for detonating ammonium nitrate which is consistent with that calculated by means of the nozzle and curved-front diameter theories. The possible implications of the new model with respect to low velocity detonation in mixtures of granular explosives are discussed.

Received July 7, 1958.
[1] This work was supported by the U. S. Air Force under Contract no. AF18(603)-74 monitored by the Air Force Office of Scientific Research of the Air Research and Development Command.
[2] Research Chemist, Explosive Ordnance Division.
[3] Research Chemist, Chemical Division.

IN THE grain burning detonation theory of Eyring et al. (1)[4] the chemical reaction which propagates the detonation wave is considered to start at the surface of the individual grains of the explosive, where temperatures produced by the shock (detonation) front are sufficient to initiate ordinary chemical reactions at suitable velocities. Each grain of explosive in the reaction zone behind the shock front is considered to undergo a cigarette burning process in which chemical reaction progresses layer by layer inward from the surface, until it reaches the center of the grain; each layer of molecules is not ignited until the previous layer is consumed. The time τ required for complete reaction is then simply the time required for the reaction to traverse the grain radius

$$\tau = \bar{R}_g/\lambda k_r \qquad [1]$$

where $\bar{R}_g$ is the average grain radius of the explosive particles; λ is the diameter of a molecule on the surface of a grain, and k_r is the specific rate constant of the rate controlling reaction. Equation [1] represents the reaction time of detonation.

Eyring et al. have investigated the variation of the steady detonation velocity D in TNT with the diameter d of a cylindrical charge, and have concluded, on the basis of an analysis of reaction times by application of their curved-front theory (1), that the activation energy of the rate controlling surface reaction is lower than that which would normally be expected for first or second order reaction kinetics. Accordingly, they suggested that the rate controlling process was one of diffusion either of heat or matter.

Copp and Ubbelohde (2) made a similar study of the variation in steady-state detonation velocity with explosive cylindrical charge diameter for mixtures of TNT and ammonium nitrate (AN). Their reaction time analysis using Jones' nozzle theory (3) for the diameter effect, $D(d)$, indicated that the detonation reaction times, as defined by Equation [1], were relatively insensitive to the reaction zone temperature. They likewise concluded that the rate controlling process in the detonation decomposition of TNT-AN mixtures and of AN alone has a low activation energy and is not likely to be one of chemical activation.

On the other hand, Cook and co-workers (4,5) describe a grain burning model of detonation in which the decomposition of the surface layer of explosive granules is assumed to follow the kinetics predicted by an extrapolation to detonation temperature of the isothermal bulk decomposition data obtained at relatively low temperatures. In general, detonation reaction times calculated by this method are greater, by a factor of 10 to 100, than those cited by Eyring et al. (1) and by Copp and Ubbelohde (2); they are, however, in agreement with the reaction times predicted by Cook's detonation head theory (4,5) for the diameter effect $D(d)$.

A major source of the discrepancy undoubtedly lies in the fact that it has not been possible to evaluate k_r independently of τ in Equation [1]. Thus, the evaluation of k_r has depended upon detonation reaction times which are calculated by means of the various diameter theories (the curved front, nozzle and detonation head theories).

The purpose of this paper is to indicate how recent work on the kinetics of surface reactions can shed considerable light

[4] Numbers in parentheses indicate References at end of paper.

on the mechanism of low velocity detonation reactions and, in particular, on the mechanism of detonation of ammonium nitrate.

Discussion

A recent paper by Andersen et al. (6) described experiments in which solid ammonium nitrate was made to gasify at temperatures which exceeded the melting point of AN (169.7 C). The gasification reaction took place on the surface of an electrically heated hot plate, and resulted almost exclusively in the formation of NH_3 and HNO_3. The surface pyrolysis process was studied with an apparatus designed to measure directly the linear pyrolysis rate as a function of surface temperature (7).

In these experiments, strands of AN, which were prepared by compressing the powder, were held against an electrically heated hot plate, and the linear rate of regression of the surface was measured as a function of the temperature at which the gasification took place (i.e., the surface temperature).

It was found that the surface gasification of AN, at temperatures above the melting point, occurred so rapidly that for all practical purposes the overall process appeared to be one of sublimation.

The rate data, which were obtained for a range of surface temperatures from about 170 to 300 C, are represented by the following Arrhenius-type rate equation

$$B = 120 \exp(-7100/RT_s) \quad \text{cm/sec} \qquad [2a]$$

At elevated temperatures, an equation with a temperature dependent pre-exponential factor is preferred

$$B = 0.23T_s \exp(-7100/RT_s) \quad \text{cm/sec} \qquad [2b]$$

where B is the linear pyrolysis rate; R is the gas constant (cal/mole-deg), and T_s is the surface temperature (deg K).

A similar endothermic surface gasification reaction under conditions of high heat flux was reported by Schultz and Dekker (8) for ammonium chloride. It is apparent that this type of surface gasification process is the direct result of the surface heating technique.

It would appear that the energy transfer and reaction processes at the AN hot plate interface during linear pyrolysis should be similar to those which occur during burning at a grain surface. For grain burning during AN detonation, we can postulate that the explosive granules gasify by an endothermic process and that the product gases ($NH_3 + HNO_3$) undergo an exothermic redox reaction above the surface. The particles are thus engulfed in the hot flame zone resulting from the redox reaction, and the energy from this reaction supplies the heat flux required to propagate the gasification of the solid. This mechanism is identical with that proposed for the burning of AN in solid composite propellants (9,10). In general, the reaction zone of the detonation wave can be likened to a feedback system, whereby the shock front initiates the chemical reactions which release sufficient energy to maintain the shock front and the reactions. In this manner the reaction time of detonation of AN can be expressed by Equation [1] where the linear pyrolysis rate B replaces λk_r, i.e.

$$\tau = \bar{R}_g/B \qquad [3]$$

As can be seen from Equations [2], the rate controlling process has a relatively small activation energy as postulated by Eyring et al. and by Copp and Ubbelohde. It should be noted that if bulk decomposition of $AN(NH_4NO_3 \rightarrow N_2O + 2H_2O)$ is rate controlling (as Cook has postulated), the linear rate of surface regression would be

$$B = 8.17 \times 10^4 \exp(-38{,}300/RT_s) \quad \text{cm/sec} \qquad [4a]$$

or

$$B = 167T_s \exp(-38{,}300/RT_s) \quad \text{cm/sec} \qquad [4b]$$

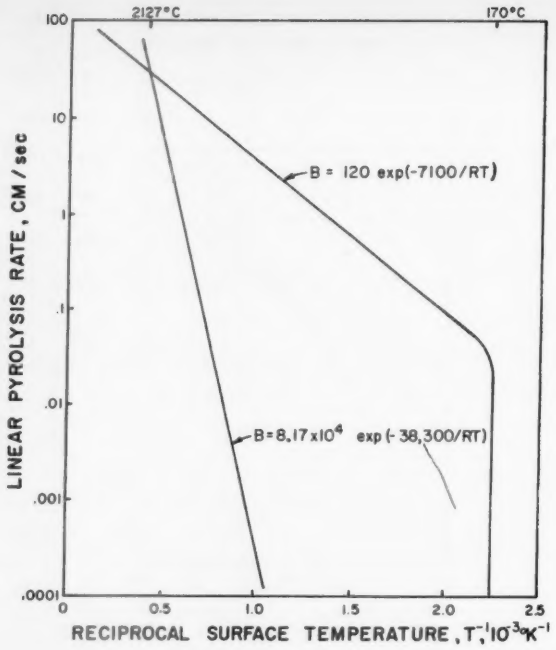

Fig. 1 Comparison of bulk and surface mechanism decomposition rates of a monolayer of ammonium nitrate

The above expressions are obtained by taking $\lambda = 4.18 \times 10^{-8}$ cm,[5] and the rate constant, $k_r = 10^{12.28} \exp(-38{,}300/RT)$ sec^{-1} (11).

A comparison of Equations [2 and 4] (Fig. 1) indicates that the linear surface regression by endothermic gasification (Eq. [2]) is faster than that by exothermic bulk decomposition (Eq. [4]) for all surface temperatures below 2400 K. Reaction zone temperatures for detonating AN have been calculated to be ~1800 K (5); it is therefore reasonable to assume that the surface temperature of the AN grains during detonation would be less than 2400 K, and that the surface reaction will be endothermic with a rate described by Equation [2].

A comparison is given in Table 1 of reaction times calculated from extrapolated kinetic rate data and those calculated by Cook et al. from diameter theories. As can be seen from the table, the reaction time calculated by extrapolation of surface pyrolysis rates to detonation temperatures is in fair agreement with the values from the nozzle and curved-front theories.

In connection with these calculations, it should be mentioned that the grain surface temperature was identified with the detonation gas temperature. Actually, with our grain burning model of the reaction zone, the detonation gas temperature is at the adiabatic flame temperature which results from the reaction between NH_3 (g) and HNO_3 (g). Therefore, the grain surface temperature should be lower than the detonation gas temperature. However, in view of the high pressure in the reaction zone (of the order of 50,000 atm), the flame zone will be quite close to the surface and, hence, the surface and detonation temperatures should be very nearly the same in this case.

It is interesting to examine the consequences of applying surface pyrolysis rate data to detonation reaction times in explosive mixtures (e.g., TNT/AN mixtures). We assume that the gasification of the individual particles proceed by rate processes which are essentially independent of each other. Thus, the faster pyrolyzing component will be consumed at a

[5] λ is considered to be the thickness of a monolayer $(M/N\rho)^{1/3}$, where M is the molecular weight of AN; ρ is the crystal density, and N is Avogadro's number.

Table 1 Comparison of calculated detonation reaction times for pure ammonium nitrate

	Reaction times τ, μ sec				
Grain surface temperature	Nozzle theory	Curved-front theory	Detonation head theory	Bulk decomposition Equations [1 and 4b] *	Surface pyrolysis Equations [1 and 2b] *
1720 K	130	100	3500	5000	350

* $\bar{R}_g$ taken as 175 μ

rate greater than the other constituents. In the case of a two-component mixture with widely differing pyrolysis rates, there will be a drop in the rate of energy release behind the shock front at the point where the faster pyrolyzing component has been completely consumed. It is reasonable to assume that this point corresponds to the Chapman-Jouguet plane, so that the energy release from the slower pyrolyzing constituent occurs in the Taylor expansion region and does not lend support to the detonation front. In terms of the detonation reactions, the slower pyrolyzing component would then behave as an inert material, and the temperature and pressure conditions of the detonation reaction zone would be modified accordingly. However, as the pyrolysis rates of the explosive components in the mixture approach one another, the greater will be their mutual contribution to the energy release in the detonation reaction zone.

Another point of interest concerns the applicability of pyrolysis rate data to high velocity detonations (i.e., RDX, PETN). In these cases, it is quite possible that the rate controlling mechanism is not one of grain burning, but rather a first order decomposition due to shock compression (12). In such cases, surface reaction kinetics would not apply.

Conclusions

The above discussion of the ammonium nitrate detonation reaction strongly suggests that the rate controlling step of grain burning is an endothermic surface gasification process. Low velocity (order) detonation in other granular explosives may involve a grain burning mechanism similar to that postulated for AN. The reaction kinetics of many of these systems should be amenable to elucidation in the laboratory by the linear pyrolysis technique.

Acknowledgment

The authors wish to express their appreciation of the help given by Dr. G. Moe of Aerojet-General Corp. in editing the final draft of this paper.

References

1 Eyring, H., Powell, R. E., Duffy, G. H. and Parlin, R. B., "The Stability of Detonation," *Chemical Reviews*, vol. 45, Aug. 1949, pp. 69–181.

2 Copp, J. L. and Ubbelohde, A. R., "Physico-Chemical Processes Occurring at High Pressures and Temperatures. Parts I and II," *Trans. Faraday Soc.*, vol. 44, 1948, pp. 646–669.

3 Jones, H., "A Theory of the Dependence of the Rate of Detonation of Solid Explosives on the Diameter of the Charge," *Proc. of the Royal Soc.*, vol. 189A, 1947, p. 415.

4 Cook, M. A., Horsley, G. S., Partridge, W. S. and Ursenback, W. O., "Velocity-Diameter and Wave Shape Measurements and the Determination of Reaction Rates in TNT," *J. Chem. Phys.*, vol. 24, 1956, pp. 60–67.

5 Cook, M. A., Mayfield, E. B. and Partridge, W. S., "Reaction Rates of Ammonium Nitrate in Detonation," *J. Phys. Chem.*, vol. 59, 1955, pp. 675–680.

6 Andersen, W. H., Bills, K. W., Dekker, A. O., Mishuck, E., Moe, G. and Schultz, R. D., "The Gasification of Solid Ammonium Nitrate," JET PROPULSION, vol. 28, Dec. 1958, pp. 831–832.

7 Barsh, M. K., Andersen, W. H., Bills, K. W., Moe, G. and Schultz, R. D., "An Improved Instrument for the Measurement of Linear Pyrolysis Rates of Solids," *Rev. Scien. Instrs.*, vol. 29, 1958, pp. 392–396.

8 Schultz, R. D. and Dekker, A. O., "The Absolute Thermal Decomposition Rates of Solids, Part I," Fifth Symposium (Int.) on Combustion, Reinhold Publishing Co., New York, 1955, pp. 260–267.

9 Andersen, W. H., Bills, K. W., Mishuck, E., Moe, G. and Schultz, R. D., "A Model Describing Combustion of Solid Composite Propellants Containing Ammonium Nitrate," Technical Memorandum no. 297, Aerojet-General Corp., Azusa, Calif., Jan. 1958.

10. Chaiken, R. F., "A Thermal Layer Mechanism of Combustion of Solid Composite Propellants: Application to Ammonium Nitrate Propellants," Technical Memorandum no. 290, Aerojet-General Corp., Azusa, Calif., Sept. 1957.

11 Cook, M. A. and Abegg, M. T., "Isothermal Decomposition of Explosives," *Ind. and Engng. Chem.*, vol. 48, 1956, pp. 1090–1095.

12 Chaiken, R. F., "The Kinetic Theory of Detonation of High Explosives," M. S. Thesis, Polytechnic Institute of Brooklyn, June 1958 (submitted to *J. Phys. Chem.*).

A Proposed Kepler Diagram

ROBERT L. SOHN[1]

Space Technology Laboratories, Inc., Los Angeles, Calif.

Nomenclature

a = semimajor axis of the orbit
e = eccentricity of the orbit
E = energy of the body, ft-lb
G = university gravitational constant
h = angular momentum, lb-sec ft
M = mass of the attracting body, slugs
m = mass of the attracted body, slugs
T = period,[2] defined as $2\pi \left(\frac{r_p^{3/2}}{\sqrt{GM}} \right)$
t = flight duration ($t = 0$ at perigee)
v = speed of the attracted body, ft/sec
β = flight path angle with respect to radius vector, rad
λ = twice the ratio of kinetic to potential energy $= v^2 r/GM$
θ = transit angle

Subscripts

a = apogee
p = perigee
See Fig. 1 for coordinate system.

Received Aug. 9, 1958.

[1] Member of the Technical Staff. Member ARS.

[2] It is noted that T would be the period for an ellipse if r_p were replaced by a.

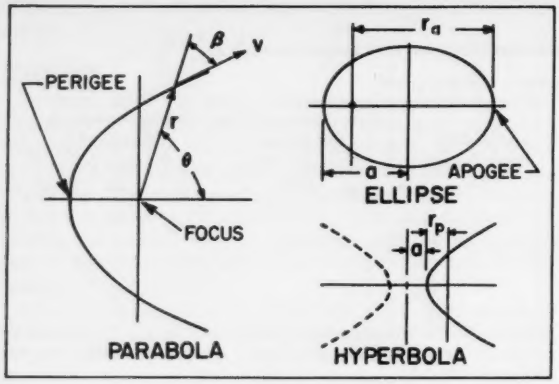

Fig. 1 Coordinate system

A BODY moving in a central force field in the absence of thrust and drag follows a trajectory described by Kepler's laws. If the specific energy of the body is negative, the resulting trajectory will be elliptic in shape, and if the energy is positive, the trajectory will be hyperbolic. A body having zero specific energy will escape the force field along a parabola.

Although Keplerian trajectories are in constant consideration today in connection with space vehicle studies, a simple graphical method does not exist for the rapid computation of vehicle motion along the trajectory.

This note proposes a Kepler diagram which presents the integrated equations of motion in such a manner that the shape of the trajectory as well as the velocity, time, flight path angle and transit angle along the trajectory can be computed quickly and easily. The development of the Kepler diagram and examples illustrating its many uses are presented below.

Development

Kepler's laws and the motion of bodies acting in accordance with them are described in several texts (1,2).[3] These laws are based on conservation of energy and conservation of angular momentum

$$\frac{E}{m} = \tfrac{1}{2} v^2 - \frac{GM}{r} \qquad [1]$$

$$\frac{h}{m} = rv \sin \beta \qquad [2]$$

Through the use of Equations [1 and 2], the trajectories described by bodies operating in the gravitational field can be derived. Of interest are the velocity, time, flight path angle β and transit angle θ, along the path.

Before proceeding, it is desirable to introduce the parameter λ, which is twice the ratio of kinetic to potential energy of the body. Through use of this parameter, it is possible to "normalize" the motion of the body. For example, velocity can be expressed in terms of the velocity at apogee (or perigee), and time can be ratioed to the period T. In this way, the Kepler diagram is made independent of the actual "size" of the trajectory and of the energy associated with it. The quantities of interest are presented in ratio form below

$$a = \frac{r}{2-\lambda} = \frac{r_p}{1-e} = -\left(\frac{GM}{2\frac{E}{m}}\right) \text{ (ellipse)}$$
$$= \frac{r}{\lambda - 2} = \frac{r_p}{e-1} = \left(\frac{GM}{2\frac{E}{m}}\right) \text{ (hyperbola)} \qquad [3]$$

$$\lambda = 2 - \frac{1-e}{\left(\frac{r_p}{r}\right)} \qquad [4]$$

$$\beta = \sin^{-1}\sqrt{\frac{(1+e)\left(\frac{r_p}{r}\right)}{2 - \frac{1-e}{\left(\frac{r_p}{r}\right)}}} \qquad [5]$$

$$\theta = \cos^{-1}\frac{1}{e}\left[1 - (1+e)\left(\frac{r_p}{r}\right)\right] \qquad [6]$$

$$\frac{v}{v_p} = \sqrt{\frac{2\left(\frac{r_p}{r}\right)}{1+e} - \frac{1-e}{1+e}} \qquad [7]$$

$$\frac{t}{T} = \frac{1}{2\pi}\left(\frac{1}{1-e}\right)^{3/2}\left\{\cos^{-1}\frac{1}{e}\left[1 - \frac{1-e}{(r_p/r)}\right] - \sqrt{e^2 - \left(1 - \frac{1-e}{(r_p/r)}\right)^2}\right\} \text{ (ellipse)}$$
$$= \frac{1}{2\pi}\left(\frac{1}{e-1}\right)^{3/2}\left\{\sqrt{\left[\frac{e-1}{(r_p/r)} + 1\right]^2 - e^2} - \cosh^{-1}\frac{1}{e}\left[\frac{e-1}{(r_p/r)} + 1\right]\right\} \text{ (hyperbola)} \qquad [8]$$

The Kepler Diagram

A chart can now be constructed using Equation [4] which relates the radius ratio and λ at given eccentricities. This chart is shown in Fig. 2. The perigee of all orbits lies along the line $r_p/r = 1$, whereas the apogee line is determined by eccentricity (for the ellipses). In the case of hyperbolic trajectories, the body recedes to infinity without reaching an apogee. For hyperbolic paths the line $r_p/r = 0$ gives the flight conditions at infinity. Once a location has been selected on the chart, the eccentricity remains fixed, and the body oscillates along a line of constant eccentricity between perigee and apogee (infinity). Each value of eccentricity, therefore, represents a particular orbit.

A few remarks should be made about the significance of λ. The well-known equations for satellite and escape speed are

$$V_s^2 = \left(\frac{GM}{r}\right) \quad (\lambda = 1)$$
$$V_{ss}^2 = 2\left(\frac{GM}{r}\right) \quad (\lambda = 2)$$

Therefore, the value of λ determines the type of orbit described by the body.

$0 < \lambda < 2$	elliptic
$\lambda = 2$	parabolic (escape)
$\lambda > 2$	hyperbolic speed
$\lambda = 1$, $\beta = 90$ deg	satellite (circular)

The particular areas of operation are noted on Fig. 2. It should be pointed out that, once a point is located on the chart, the requirements for achieving satellite or escape speed can be measured directly (the flight path of the vehicle may have to be redirected also, as will be discussed later).

[3] Numbers in parentheses indicate References at end of paper.

Also of interest are typical operating areas for various types of missiles. ICBM vehicles, for example, approach but do not quite achieve circular speeds, and operate near the apogee portion of the orbit. IRBM vehicles attain even lower speeds. Satellites are usually indicated as having circular orbits. In practice, however, their orbits have a small eccentricity (0 to 0.20) so that they cover a band of altitudes during the orbit. Escape shots are indicated on Fig. 2 as lying close to the parabolic orbit. Lunar shots can be slightly elliptical, whereas interplanetary escapes will be slightly hyperbolic.

Referring to Equations [3 to 8], all quantities are seen to be functions of radius ratio and eccentricity, so that parametric families of velocity ratio, time, etc., overlay the basic grid lines of constant eccentricity. To complete the method these other relations have been plotted on Fig. 2. The resulting Kepler diagram is shown in Fig. 3.

In using the Kepler diagram, velocity, radius and flight path angle are usually specified (as at termination of powered flight). λ and β are thus known, and the orbit can be located on the diagram. Now as the vehicle moves along the orbit (on a line of constant eccentricity) it passes velocity, time and angle lines, so that the motion of the vehicle is described at all points. Some examples of the many types of problems that can be solved with the Kepler diagram are given at the end of this note.

Construction of the Orbit

It will be necessary in some cases to construct the actual orbit. The semimajor axis a is necessary for this purpose. Since radius and λ are usually known, a can be computed from Equation [3]. From the general equation of the conic

$$r = \frac{ep}{1 - e\cos\theta} \qquad \begin{matrix} p = a(1 - e^2) & \text{elliptic} \\ = a\,(e^2 - 1) & \text{hyperbolic} \end{matrix}$$

the complete orbit can now be constructed.

Examples

Velocity That Must Be Added at Apogee to Reach Satellite Condition Presuming that the velocity, flight path angle β and radius are known (at termination of powered flight), λ and β can be used to locate the orbit on the diagram. The orbit can then be traced along a line of constant eccentricity to apogee, where the λ at apogee can be read. Since $\lambda = 1$ is required for a circular orbit, the velocity must be increased by a factor of $1/\sqrt{\lambda}$.

Determining Burnout Conditions for a Required Apogee Altitude Assuming that λ is given, Fig. 3 can be entered at λ and at any arbitrary r_p/r. By tracing the orbit to apogee, r_p/r_a can be read; r/r_a is then equal to $r_p/r_a \div r_p/r$. This procedure can be repeated until the desired apogee radius is found. The required flight path angle β can then be read directly.

Range of a Ballistic Vehicle By entering the chart at the vehicle burnout conditions (λ and β), the missile orbit can be determined. This orbit can be traced from the burnout altitude to apogee, and back to the impact altitude. The transit angle covered during flight can be read directly from the chart. The range traversed is then the radius at the surface times the change in transit angle.

Re-Entry Conditions If λ and β at burnout are known, the orbit can be established on Fig. 3. The orbit can be traced to apogee (along a line of constant eccentricity), and back to the required re-entry altitude, where the new speed and flight path angle can be read directly.

Residual Speeds Residual speed is defined as the speed a body would have after escape from a gravitational force field. Through use of the energy equation, [1], the residual speed is found to be

$$\left(\frac{v_r}{v}\right)^2 = 1 - \frac{2}{\lambda} \qquad \begin{matrix} \theta_r = \cos^{-1}\left(\frac{1}{e}\right) \\ \beta_r = 0 \end{matrix}$$

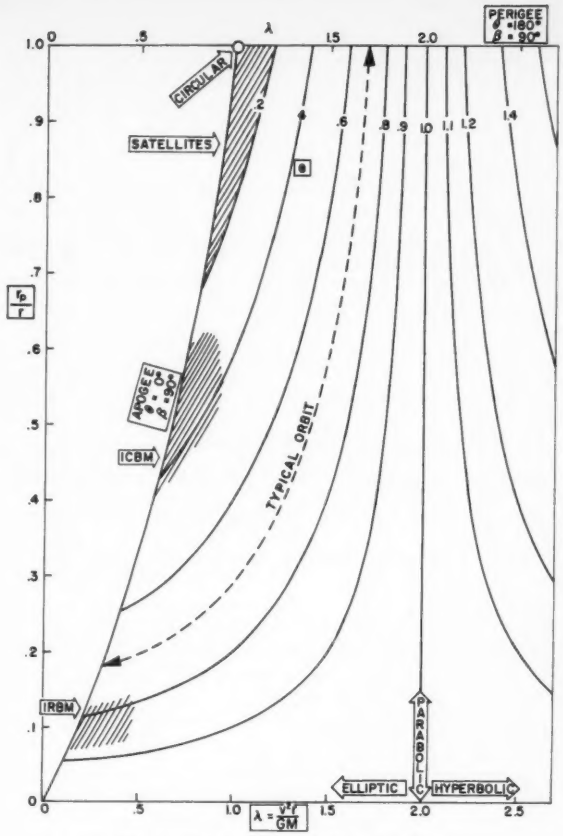

Fig. 2 Basic representation of orbits

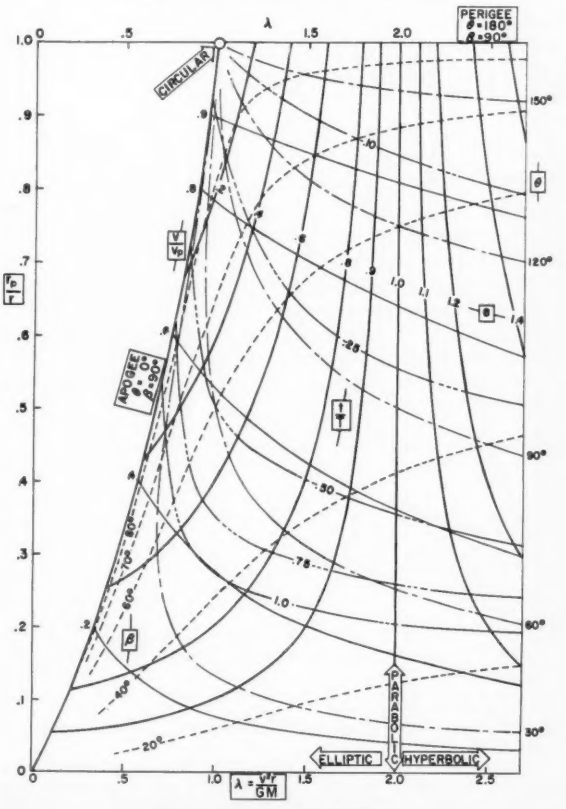

Fig. 3 The Kepler diagram

Auxiliary Charts

Useful nomographs may be prepared to aid in generating λ and T from a knowledge of v, r and GM. This can best be accomplished by plotting λ as a function of r for various values of v (the entire chart being applicable to one value of GM). Since T is a function of r and λ, lines of constant T can be superimposed on the same chart.

References

1 Page, "Introduction to Theoretical Physics," Van Nostrand, New York, third ed., pp. 107–116.

2 MacMillan, "Theoretical Mechanics Statics and the Dynamics of a Particle," McGraw-Hill, first ed., pp. 274–280.

Solution to the Linearized Quasi-Stationary External Diffuser Equations

R. H. EDWARDS[1]

Hughes Aircraft Co., Culver City, Calif.

IN a paper by Chang and Hsu,[2] an approximate solution to the linearized one-dimensional equations of an external diffuser is presented. These equations may be solved exactly in a rather simple fashion.

The equations considered are of the same form as Equations [8 and 9][3] of Chang and Hsu

$$2z\frac{d\sigma}{dz} + 2z\frac{dv}{dz} + \frac{1-z}{1-bz}v = 0 \qquad [1]$$

$$v - \frac{b\sigma}{1-b} + \frac{1-bz}{1-b}\frac{d\sigma}{dz} + \frac{zdv}{dz} = \frac{\epsilon_2}{2} \qquad [2]$$

The integration may be performed by noting that Equation [2] is an exact differential, and may be written

$$\frac{d}{dz}\left[zv + \frac{1-bz}{2b}\epsilon_2 + \frac{1-bz}{1-b}\sigma\right] = 0 \qquad [3]$$

and hence admits the integral

$$zv + \frac{1-bz}{2b}\epsilon_2 + \frac{1-bz}{1-b}\sigma = +\frac{3}{2}\frac{B}{(1-b)b} \qquad [4]$$

This integral corresponds to a quasi-stationary energy integral. The constant on the right-hand side of Equation [4] is chosen so as to correspond to a constant of integration as given in the above mentioned paper.

Substitution of Equation [4] into [1] yields the following first order linear equation in v

$$\frac{dv}{dz} + \left(\frac{1}{z-1} + \frac{b}{1-bz} + \frac{1}{2z}\right)v = -\frac{3}{2}\frac{B}{(1-bz)(1-z)} \qquad [5]$$

and the general solution for v is found to be

$$v = C\frac{1-bz}{\sqrt{z}(z-1)} + \frac{3}{2}\frac{B}{b(z-1)} \times \left(1 + \frac{1-bz}{2\sqrt{bz}}\log\frac{1-\sqrt{bz}}{1+\sqrt{bz}}\right) \qquad [6]$$

Received Aug. 23, 1958.

[1] Member of the Technical Staff, Systems Development Laboratories.

[2] Chang, C. C. and Hsu, C. T., "Solutions to Stoolman's External Diffusion Equation for Instability of a Normal Shock Inlet Diffuser," JET PROPULSION, vol. 28, no. 7, July 1958, pp. 457–460.

[3] The notation used here is identical with that of Chang and Hsu.

The corresponding solution as given in the paper by Chang and Hsu has the form

$$v = C\frac{1-bz}{\sqrt{z}(z-1)} + \frac{Bz}{z-1} \qquad [7]$$

The terms containing C are identical, and those containing B may be shown to be identical to first order in bz.

The solution for σ may be found by solving the integral relation [4], i.e.

$$\sigma = \frac{3}{2}\frac{B}{(1-bz)b} - \frac{1-b}{2b}\epsilon_2 - \frac{z(1-b)}{(1-bz)}v$$

A Novel Combustion Measurement Based on the Extinguishment of Diffusion Flames

A. E. POTTER Jr.[1] and JAMES N. BUTLER[2]

Lewis Research Center, NASA, Cleveland, Ohio

A combustion measurement is described uniquely suited to the study of highly reactive fuel-oxidant combinations.

A NUMBER of combustion measurements, such as burning velocity, quenching distance, ignition energy and flashback boundary velocity gradient, are available for characterizing the combustion process for premixed flames. Unfortunately, a number of fuel-oxidant systems are so reactive that they can be mixed only with difficulty and danger, if at all. For such fuel-oxidant systems, the diffusion flame must provide information about the combustion process. This is especially important when one realizes that in practical combustion systems which use highly reactive fuel-oxidant combinations (e.g., rocket motors), combustion occurs mostly by means of diffusion flames. This note describes a combustion measurement applicable to diffusion flames and hence to highly reactive fuel-oxidant systems.

Zeldovitch (1)[3] and Spalding (2) have shown theoretically that when the flow of fuel and oxidant into a diffusion flame is too great, the chemical reaction cannot keep up, and the flame goes out; Spalding has attributed the extinguishment by forced convection of diffusion flames around burning drops to this effect. In an effort to use this effect as the basis of a measurement of general usefulness, we established a diffusion flame between two opposed gaseous jets, one of fuel and one of oxidant. As the mass flows of fuel and oxidant were increased, a critical flow was reached at which the flame was extinguished in an area surrounding the jet axis. This phenomenon occurred abruptly at a reproducible flow rate. We have called the maximum mass flow rate per unit area at which the flame is extinguished around the jet axis, the flame strength. Spalding has used this same term to mean the maximum fuel (or oxidant) flow which a diffusion flame can support. The experimental flame strength discussed in this note is probably not identical with the quantity that Spalding calls the flame strength in his theory, although the two are certainly closely related.

Apparatus and Procedure

The apparatus is sketched in Fig. 1. Fuel and oxidant were metered by critical flow orifices, and led to two separate opposed jets mounted vertically.

To make a measurement, the fuel and oxidant flows were alternately increased, keeping the flame as well centered as

Received Aug. 8, 1958.

[1] Head, Reaction Kinetics Section.

[2] Aeronautical Research Scientist. Present address, Harvard Univ., Cambridge, Mass.

[3] Numbers in parentheses indicate References at end of paper.

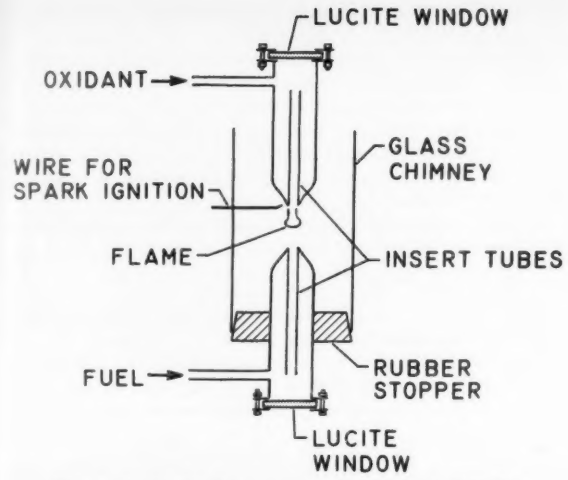

Fig. 1 Apparatus for measurement of flame strength

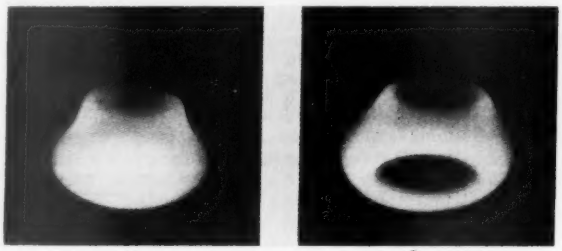

a b

Fig. 2 Diffusion flames stabilized between opposed jets

possible between the two jets, until a hole was observed at the center of the flame. The hole appeared very abruptly at a flow rate reproducible to within ±5 per cent. The flame seemed to break open, so that the phenomenon was called "breaking," and the flame having a hole in its center was called "broken." The "broken" and "unbroken" flames are illustrated by the photographs shown in Fig. 2. The Fig. 2a jet was of an ethylene-nitrogen mixture. The Fig. 2b jet was of air. The flame surrounds the air jet. The flame is seen from below, at an angle of about 45 deg from vertical.

The flame strength was calculated from the experimental results as follows: The mass flows of fuel and oxidant at flame breaking were averaged, and the result divided by the cross-sectional area of the jet to give mean mass flow per unit area. The difference between the two flows ranged from 0 to 10 per cent, with the air flow usually in excess. The mean flow was nearly independent of the difference. Since the flame always broke at the center, it was felt that the mass flow there was the important parameter. Thus, the mean flow was multiplied by the ratio of axial to mean flow velocity to give the mass flow rate per unit area at the jet axis. This factor is 2.0 for laminar (parabolic) flow in straight tubes, and 1.22 for turbulent flow in straight tubes.

All measurements reported are for ambient pressure (about 740 mm) and 40 C.

Geometric Factors

The first parameters studied were geometric ones. Specifically, the effects of flow profile, jet spacing and jet diameter on flame strength were studied.

It was thought at first that the flow profile obtained from a nozzle should be an ideal one for this measurement. This proved not to be the case, as flame strength varied greatly with spacing between the jets. The difficulty apparently was that the velocity profile of the jet stream changed with distance from the exit of the jet tube. When a straight tube, giving a parabolic velocity distribution, was used instead of the nozzle the flame strength was found to be independent of jet spacing over a range of 0.1 to 2.0 cm. Because the straight tubes gave uniform and reproducible values of flame strength, all measurements reported were made with straight tubes.

The effect of jet diameter on the flame strength for ethylene-air and propane-50 per cent O_2, 50 per cent N_2 flames was measured. The variation is small but significant. Flame strength increases linearly with jet diameter, the line having a slope of about 0.24 g/cm³ sec. Because of this, the flame strength must be referred to some standard jet diameter if one wishes to compare different fuel-oxidant systems. A jet diameter of 0.46 cm was chosen as a standard, and all measurements were made with this jet diameter when possible.

Chemical Factors

Flame strength was measured for propane-air, cyclopropane-air, ethylene-air, propane-argon "air," propane-helium "air," acetylene-air, propane-50 per cent O_2, 50 per cent N_2 and propane-oxygen. All combinations except the last two were measured using a jet diameter of 0.46 cm. Propane-50 per cent O_2, 50 per cent N_2 and propane-O_2 were measured using smaller jets and the results extrapolated to 0.46 cm jet diameter. According to Zeldovitch and to Spalding, the maximum mass flow of fuel which a diffusion flame can support without extinguishing is directly proportional to the mass of fuel consumed per second by a unit area of flame front propagating through a fuel-air mixture. This is a very important relation, since it establishes a link between the diffusion and premixed flame. This quantity can be written as $m_f \rho S_u$, where m_f is the mass fraction of fuel in the unburned mixture; ρ is the density of the unburned mixture, and S_u is the burning velocity.

In order to compare $m_f \rho S_u$ with the experimental data, the burning velocity must be known. For this purpose, a choice of fuel-air ratio to which the burning velocity refers must be made. In the theory of Zeldovitch, the stoichiometric mixture is indicated. In the theory of Spalding, the mixture ratio to be used is that with a flame temperature equal to the diffusion flame temperature near extinguishment. For simplicity, burning velocities corresponding to stoichiometric fuel-air mixtures are used.

The flame strength is plotted against $m_f \rho S_u$ in Fig. 3. Here

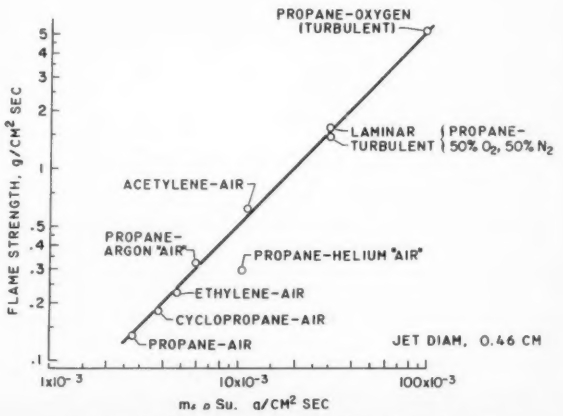

Fig. 3 Relation between flame strength and $m_f \rho S_u$

it is seen that an almost perfect proportionality exists between the measured flame strength and $m_f \rho S_u$, with one exception, that of propane-helium "air." This result establishes beyond a doubt that the flame strength of this research is a measure of combustion reactivity similar to burning velocity. However, the propane-helium "air" datum suggests that some factor has been neglected in the theories of Zeldovitch and of Spalding.

The effect of pressure on flame strength is of interest since $m_f \rho S_u$ should be (approximately) directly proportional to pressure. Preliminary measurements have shown that flame strength is directly proportional to pressure, as expected.

Conclusions

This measurement provides a quantity which appears to characterize the maximum possible combustion rate in a diffusion flame. The measurement should be uniquely suited to highly reactive fuel-oxidant combinations which cannot be premixed.

References

1 Zeldovitch, Y. B., *J. Tech. Phys.*, Moscow, vol. 19, no. 1199, 1949; trans. as NACA Tech. Memo 1296, 1951.

2 Spalding, D. B., *Fuel*, vol. 33, no. 253, 1954; *see also* "Some Fundamentals of Combustion," Academic Press, New York, 1955, p. 215.

Spatial Attitude Control of a Spinning Rocket Cluster

WALTER HAEUSSERMANN[1]

Army Ballistic Missile Agency, Redstone Arsenal, Ala.

Attitude control possibilities and characteristics of a body with high angular momentum about one axis, the roll axis, are discussed. The investigation has been carried out in view of the attitude control requirements for the spinning top of the Jupiter C, carrying Explorer I.

Nomenclature

a_0, a_1 = signal ratios for attitude and angular rate control
C = control torque per unit deflection of control element
I = moment of inertia
c = C/I
T = disturbance torque
t = T/I
k = coupling coefficient in moment equations
β = deflection of control element
ϕ = angular deviation of body from prescribed space fixed attitude
ω = angular velocity
ω_s = angular velocity of spin controlled parts
Dots written above variables denote time derivatives

Subscripts

p = pitch axis
y = yaw axis
r = roll axis
s = spinning part
$*$ = attitude program

THE JUPITER C used the Redstone booster as the first propellent stage to carry three solid propellent stages in order to place the Explorer into its orbit. Shortly after burnout of the first stage, the Redstone booster was expended by separating it from the rocket body containing the instrument compartment of the rocket and the second, third and fourth stages. These three stages were mounted on a rotating launcher to provide spin stabilization during their burning or propellant time.

At the time of separation the rocket had an attitude angle of approximately 52 deg against the vertical. During the following free ballistic flight until ignition of the second stage, the rocket body must be tilted into the horizontal position at apex. A special control system had to be developed to control and align the rocket body with its high angular momentum about the roll axis.

In the following paragraphs the control problem is described and feasible methods for control are discussed.

Missile Attitude Control

Four pairs of control air jet nozzles, providing control torques proportional to their needle displacement are attached to the missile body as indicated in Fig. 1. For such a body with a top, controlled for a constant spin rate, the following moment equilibrium equations can be derived

$$\begin{aligned} I_p\dot{\omega}_p + (I_r - I_y)\omega_r\omega_y + I_{rs}\omega_0\omega_y + C_p\beta_p &= T_p \\ I_y\dot{\omega}_y + (I_p - I_r)\omega_r\omega_p - I_{rs}\omega_0\omega_p + C_y\beta_y &= T_y \\ I_r\dot{\omega}_r + (I_y - I_p)\omega_p\omega_y + C_r\beta_r &= T_r \end{aligned} \quad \ldots\ldots\ldots\ldots\ldots\ldots\ldots\ldots\ldots\ldots [1]$$

The first two terms in each equation correspond to the terms in the well-known Euler equations. The following terms in the pitch and yaw equations describe the coupling torques due to the precession effect of the spinning top, and the last terms on the left side of the equations give the restoring torques due to control effects.

For oscillations with amplitudes expected to be smaller than 0.1 rad and with approximately the same frequency, the terms containing the factors $\omega_r\omega_y$, $\omega_r\omega_p$ and $\omega_p\omega_y$ are negligible. Thus Equations [1] become, after normalizing to a moment of inertia of 1

$$\ddot{\phi}_p + k_y\dot{\phi}_y + c_p\beta_p = t_p \qquad [2a]$$

$$\ddot{\phi}_y - k_y\dot{\phi}_p + c_y\beta_y = t_y \qquad [2b]$$

$$\ddot{\phi}_r + c_r\beta_r = t_r \qquad [2c]$$

with

$$k_p = \frac{I_{rs}}{I_p}\,\omega_0 \qquad [2d]$$

and

$$k_y = \frac{I_{rs}}{I_y}\,\omega_0 \qquad [2e]$$

For pitch and yaw motions, the terms k_y and k_p cause a coupling of Equations [2a and 2b]. The motions about roll are not influenced by either of the two other axes nor do they influence them. Thus roll control can easily be achieved with a control equation of the common form

$$\beta_r = a_{0r}\phi_r + a_{1r}\dot{\phi}_r \qquad [3]$$

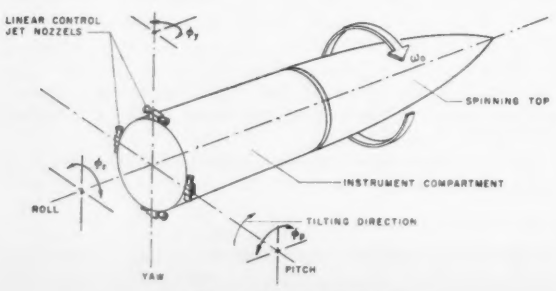

Fig. 1 Body control axes

Received Sept. 6, 1958.

[1] Director, Guidance and Control Laboratory, Development Operations Division. Member ARS.

It may be mentioned here that it is assumed that the controller for the spin rate of the rotating top does not noticeably affect the stability of the roll attitude control system and that it produces only disturbance torques. The correctness of this assumption is not within the scope of this treatment.

The general solution of Equations [2a and 2b], with the assumption of usual control system equations as in Equation [3], leads to a characteristic equation with two pairs of complex roots. If the coupling terms k_y and k_p are large enough to give poor damping of one of the resulting oscillations, terms have to be added in the control equation in order to obtain satisfactory damping. In such a case, it is advantageous to decouple Equations [2a and 2b] by a proper selection of the additional terms in the control equations

$$\beta_p = a_{0p}\phi_p + a_{1p}\dot{\phi}_p - \frac{k_p}{c_p}\dot{\phi}_y \qquad [4a]$$

and

$$\beta_y = a_{0y}\phi_y + a_{1y}\dot{\phi}_y + \frac{k_y}{c_y}\dot{\phi}_p \qquad [4b]$$

The introduction of Equations [4a and 4b] in Equations [2a and 2b] shows the elimination of the coupling terms. Thus the angular motions about the pitch and yaw axes are the same as the motions of the same body without a rotating mass.

The idealized control Equations [4a and 4b] do not contain phase lagging elements with the imperfections of a real control system. Thus in an actual system, small coupling effects between pitch and yaw will remain. In practical cases this coupling effect can be expected to be negligible.

Tilting Program in Pitch

The conventional method to introduce a pitch tilting program is to turn the base of the pickup element of the pitch stabilized axis. The indicated "ϕ_p-error" of the pickup produces a control deflection β_p according to the control equation, and the restoring torque $c_p\beta_p$ causes the actual tilting of the missile. This method requires a transient ϕ_p-error.

For a missile with moment equations according to [2a and 2b] such a common pitch tilting program produces transient ϕ_p- and ϕ_y-errors, both of which have to be reduced to zero by the end of the tilting period.

The quasi-stationary errors due to the tilting program can be avoided by adding terms in the control equation which provide for the proper control deflections during the tilting period. The modified control equations are

for the pitch axis $$\beta_p = a_0\phi_p + a_1\dot{\phi}_p - f_p\dot{\phi}_y + \beta_p^*(t) \qquad [5]$$

for the yaw axis $$\beta_y = a_0\phi_y + a\dot{\phi}_y + f_y\dot{\phi}_p + \beta_y^*(t) \qquad [6]$$

The terms $\beta_p^*(t)$ and $\beta_y^*(t)$ have to produce the torques necessary to achieve the tilting motion. If it is assumed that the attitude derivatives $\dot{\phi}_p$ and $\dot{\phi}_y$ are derived from the attitude information and not independently as, for example, from rate gyros, the pitch control system has to produce according to Equation [2a]

$$\beta_p^* = \frac{-\ddot{\phi}_p^*}{c_p} \qquad [7]$$

and the yaw control system according to Equation [2b]

$$\beta_y^* = \frac{k_y}{c_y}\dot{\phi}_p^* \qquad [8]$$

A simple example for the three tilt programs $\phi^*(t)$, $\beta_p^*(t)$ and $\beta_y^*(t)$ is exhibited in Fig. 2. The relationship of the diagram is easily explained with use of Equations [7 and 8].

The Explorer's Body Control System

In order to average ignition time deviations and unequal thrust of the individual solid propellant rockets due to fabrication tolerances, a high spin rate ω_t was demanded originally, and therefore also relatively high coupling terms k_y and k_p occurred. However, it became possible to reduce the spin rate considerably. Thus the Explorer body control system did not need the decoupling terms of Equations [4a and 4b], nor was it necessary to apply the programs according to Equations [7 and 8].

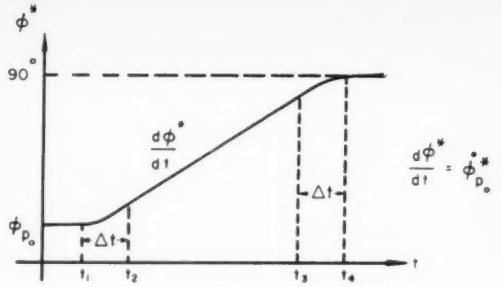

Fig. 2a Pitch attitude program

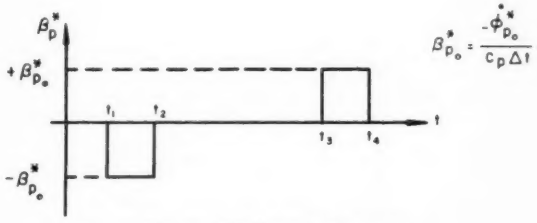

Fig. 2b Pitch control program

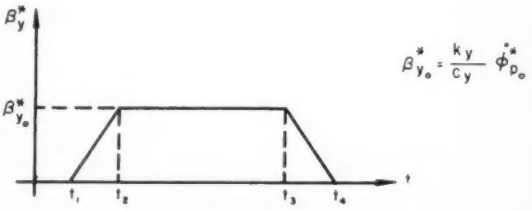

Fig. 2c Yaw control program

Thus the control system had to develop only the necessary torques to produce the tilting in pitch. For reasons of simplicity, the pitch attitude program had a constant turning rate which required certain control deflections during the tilt period. These control deflections can be derived from Equations [2a and 2b] with the following equations

for pitch control $$\beta_p = a_{0p}\phi_p + a_{1p}\dot{\phi}_p \qquad [9]$$

for yaw control $$\beta_y = a_{0y}\phi_y + a_{1y}\dot{\phi}_y \qquad [10]$$

Disregarding transient conditions at the start and end of the tilting period, a constant tilt rate $\dot{\phi}_p^*$ requires the control deflections $\beta_p^* = 0$ and $\beta_y^* = k_y\dot{\phi}_p^*/c_y$ meaning that a yaw torque $c_y\beta^*$ is necessary to maintain the precession rate $\dot{\phi}_p^*$ of the spinning top. This torque can only be produced by a deviation in yaw attitude in the amount of

$$\phi_y^* = \frac{\beta_y^*}{a_{0y}} = \frac{k_y\dot{\phi}_p^*}{a_{0y}c_y}$$

A sufficient decay time for the transients at the end of the tilting program must be provided to allow accurate aligning

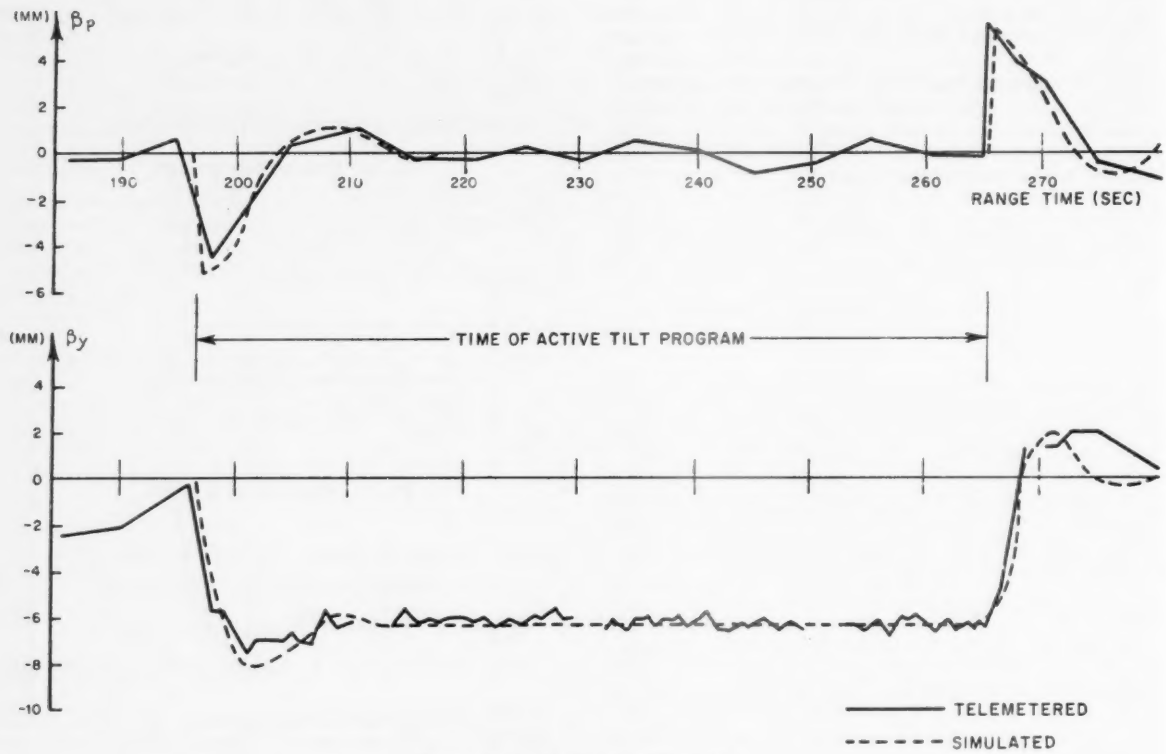

Fig. 3 Control deflection comparison

of the body with its spinning top into the firing position of the first stage of the spinning cluster.

Analog computer investigations revealed satisfactorily small amplitudes and acceptable decay time of transients due to the simplifications and nonlinear imperfections in the control system. Also it was possible to damp satisfactorily the oscillations of both frequencies resulting from the fourth degree characteristic equation by proper selection of the a_1 gain factor. Telemetered flight data show excellent agreement with laboratory results (see Fig. 3).

The author wishes to acknowledge the engineers of his Guidance and Control Laboratory, who contributed to the development of the Jupiter C's spatial attitude control system. Special credit is given to Fritz Mueller, who started analytic investigations, Dieter Teuber, who carried out first digital and analog computations especially in connection with the behavior of the spin rate controller and Fred Digesu, who supported theoretical studies by extensive analog computer investigations.

References

1 Haeussermann, W., "Stability Areas of Missile Control Systems," JET PROPULSION, vol. 27, July 1957.

2 Jasper, N. and Teuber, D. L., "Programmed Rocket Cluster Spin Regulator for Jupiter C Missiles," ABMA Applied Research Branch, Guidance and Control Laboratory, April 1958, *also* ARS JOURNAL (titled "The Cluster Spin Control System for Jupiter C Missiles"), vol. 29, no. 1, pp. 58–61.

3 Stephenson, Reginald J., "Mechanics and Properties of Matter," John Wiley & Sons, New York.

The Cluster Spin Control System for Jupiter C Missiles

NIELS JASPER[1] and DIETER TEUBER[2]

Army Ballistic Missile Agency, Redstone Arsenal, Ala.

A system incorporating modulator and pulsed transistor amplifier is described for controlling the spin rate of the solid propellant stages of the Jupiter C missile. The method fulfills the requirements to avoid an excitation of critical bending modes of the missile and to relieve the spatial attitude control of reaction torques. It also provides the angular momentum for stabilization of the satellite and produces a reduced impulse vector deviation resulting from unsymmetrical burning of the solid propellant rockets.

THE LAUNCHING of the Explorer-type satellites requires that the solid propellant rocket stages have a controlled spin rate In its first flight phase the vehicle is driven by a liquid propellant Redstone engine. In this phase, which lasts until burnout of the liquid engine, the roll movements of the missile are controlled by a powerful rudder control system.

Received Sept. 6, 1958.

[1] Guidance and Control Laboratory, Development Operations Division.

[2] Guidance and Control Laboratory, Development Operations Division.

After burnout the booster is separated from the instrument compartment. On top of the instrument compartment remains the spinning cluster of solid propellant rockets and the satellite. In the next flight phase the missile is gradually tilted into the horizontal position by air nozzles (1).[3] Shortly before reaching apex of the trajectory, the solid propellant rockets are launched from the instrument compartment, and the satellite is brought into the orbit.

The spin of the rocket stages is necessary to cancel unbalanced propulsion forces. The angular velocity has a stabilizing effect and helps to maintain fixed satellite orientation with respect to a spatial coordinate system as the satellite progresses around its orbit.

During the design of the Jupiter C, it became obvious that the spin velocity had to be changed in the first flight phase (takeoff to burnout of the liquid engine) in accordance to a certain program. In the second flight phase (burnout to launching of the rocket cluster) the spin rate has to be kept constant. The reasons are the following:

1 The bending modes of the missile should not be excited by the rotation of the cluster. Due to the fuel consumption in the powered phase of the flight, the missile mode changes, and the cluster has to rotate with a variable speed to avoid a collision with any resonance frequency of the missile configuration (Fig. 1).

2 In the second flight phase, roll control is provided by an air nozzle system. To relieve this system from reaction torques due to speed changes of the cluster, the spin rate has to be regulated within ±1 per cent.

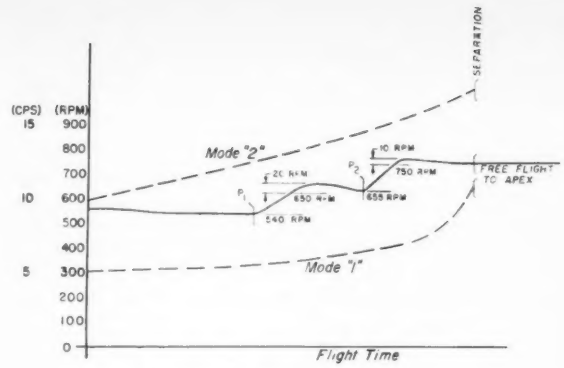

Fig. 1 Speed program of cluster

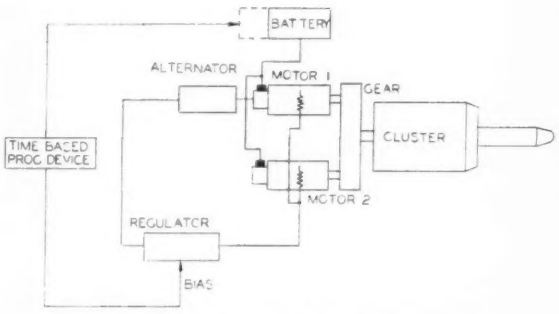

Fig. 2 Functional diagram of spin control system

Cluster Drive System

The cluster is driven by two aircraft d-c shunt motors through a toothed belt from batteries, all mounted in the instrument section. Additionally, the drive system and regulator require RF filters to avoid interference with the missile telemetering. The load on the motors is represented by aerodynamic and bearing friction and by rotational accelerational forces on the system. This load changes during the considered flight phase because:

1 The aerodynamic friction varies with air pressure and missile velocity.

2 The bearing friction depends on the bearing pressure. The latter varies with the linear acceleration of the missile and the aerodynamic pressure.

3 The rotational acceleration changes due to the introduced spin rate program.

This means a load change over a range of 1:5. The battery voltage also changes 30 per cent from its initial value.

An armature voltage regulation system would handle these wide load and supply voltage variations easier than a field control system, but controlling armature currents up to 500 amp would create hardware which by far exceeds the given weight limitations of the satellite carrier. Therefore, it was decided to control the speed of the motors in a closed loop system changing the field excitation. The loop amplification had to be made relatively high, so that the difference between the reference and the actual speed could be kept small over the entire working range. The supply voltage has been increased by a step of about 4 v at the time of the peak load. The system works as shown in Fig. 2.

A small alternator is coupled to the shaft of one drive motor. Its output frequency is compared with a frequency reference. The error is amplified and fed back into the motor field in a direction to minimize this error. The amplifier consists of a magnetic modulator and a transistor power stage. For increasing the speed during flight, the speed reference is changed twice by a stepwise introduction of a bias signal to the magnetic modulator. This signal is derived from a program stored in a missile-borne tape recorder. Since the closed loop always tries to minimize the error between reference and actual speed, the motor changes its speed according to the introduced program.

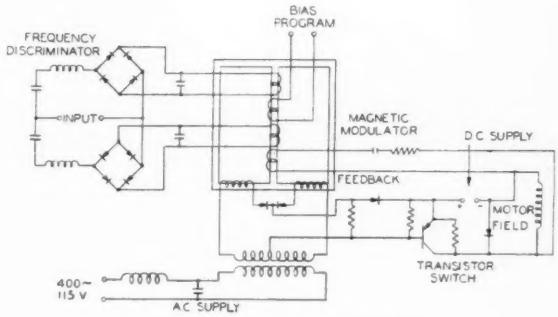

Fig. 3 The regulator (principle)

Fig. 3 shows, in principle, the regulator. The reference is provided by a frequency discriminator consisting of two series tank circuits (2). The tank circuits are tuned to two different resonance frequencies. The crossover point of the two resonance lines represents the frequency or speed reference of the drive motor. The rectified output of these two resonance circuits is fed in opposition in two windings of the following magnetic modulator. This speed reference, and consequently the motor speed, can arbitrarily be shifted to any value between the two resonance points by introducing a variable

[3] Numbers in parentheses indicate References at end of paper.

bias (program) to a third winding of the magnetic modulator.

The field current of each drive motor has to be controlled between 1.2 and 4 amp.

To meet the requirements on the power amplifier in respect to weight, volume and power supply (27 v d-c), a pulsed transistor amplifier was chosen (3).

The magnetic modulator is a magnetic amplifier operated from a square wave supply. It transforms the d-c signal from the frequency discriminator and the programmer into pulse duration modulation to energize the transistor switch on and off in a constant repetition rate of 800 cps. The ratio between "on" and "off" time varies according to the signal. This pulse duration modulation type of operation results in very small power dissipation through the transistor, which has an "on" resistance of about 0.1 ohm and an "off" resistance above 10 k ohm.

For stability, an integral feedback from the output of the transistor amplifier to the magnetic modulator is applied.

Fig. 4 shows the regulation curve (open loop) that is the field current of the drive motors as function of the alternator output. The speed will change from standstill to the regulating range in the closed loop. To avoid overloading of the armature in the starting phase, the transistor switch is bypassed by a resistor, so that the field current will never decrease below a predetermined value. The regulating range can be shifted according to a bias current through the magnetic modulator.

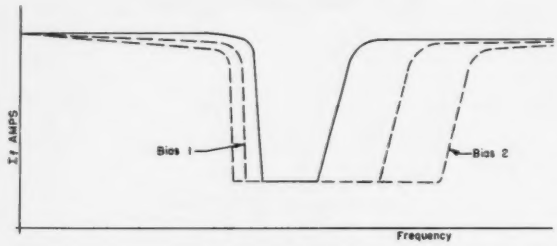

Fig. 4 Regulation curve

Fig. 5 shows the hardware. The drive motor at right is rated for 3.5 hp, 28 v at 7500 rpm with a weight of 25 lb. Coupled to the shaft is the 2-pole alternator shown in the center. Its output frequency changes from 110 to 150 cps during the flight, according to the motor speed. The speed regulator weighs 9.5 lb and is shown uncovered at left. On the front plate are the transistors and diodes mounted on a copper plate serving as heat sink. The components of the tanks are mounted on the top layer for easy adjustment. On the next layer are square wave supply, magnetic modulator and bias adjustment on a board with printed circuits. The relays for introducing the program to increase the speed are below, also resistors for bypassing the transistor switches for minimum field current. The filters for suppressing RF interference with the missile telemetering are covered.

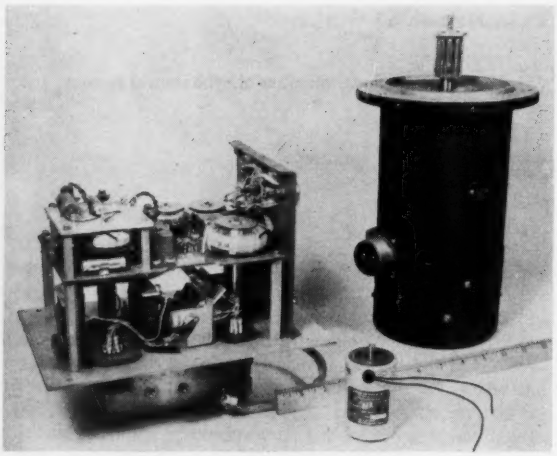

Fig. 5 Flight hardware

The dynamical behavior of the complete system can be sufficiently described by a second order system. The transient response in speed due to a sudden disturbance (battery voltage or load change) indicates an oscillation in speed of 0.1 cps with 70 per cent of critical damping.

Systems Performance Under Actual Flight Conditions

The actual performance of the cluster spin control is shown on Fig. 6 (as indicated by telemetered records from the Explorer 1 launching).

Prior to launching, the cluster is brought up to speed of 550 rpm. After takeoff, the load on the motors increases due to the change in aerodynamic conditions and the increasing missile acceleration. There is a decrease in cluster speed within the accuracy of the regulation. The armature voltage decreases also, since it is a function of the current drawn from the batteries. The reaction torques on the booster roll control system due to the cluster acceleration can be neglected because of the comparably large moment of inertia of the booster and the powerful roll control system.

At peak load, the armature voltage is increased by adding battery cells. Pulse 1 brings the cluster to a speed of 650 rpm by changing the bias on the magnetic modulator. The armature current decreases after reaching a steady state. Pulse 2 accomplishes the final speed of 750 rpm. It is regulated closely after booster cutoff and separation. This is the free flight period where the roll control system has to be relieved from reaction torques due to cluster speed changes. The speed of 750 rpm has been kept with an accuracy of ± 1 rpm during the free coasting period of the upper stages, which lasts several minutes up to apex.

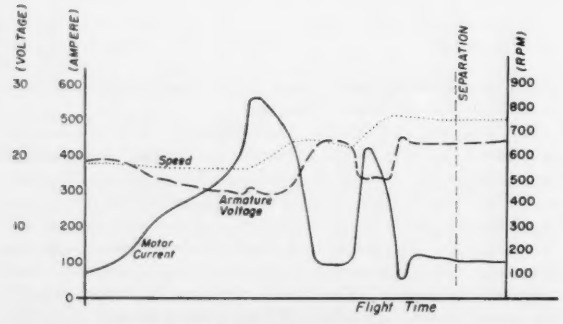

Fig. 6 Flight performance of system

Appendix Interaction With the Roll Control System

It was found that speed deviations and roll response during the flight of the upper stages are satisfactory if the regulator improves the steady state regulation by a factor of 20. The effects on the roll attitude control system are relatively small disturbance torques due to the cluster acceleration $\ddot{\theta}(t)$ resulting in an angular displacement of the instrument compartment

$$\phi(s) = -I_2 \frac{\mathfrak{L}[\ddot{\theta}(t)]}{I_1 s^2 + (c_1 a_1 s + c_1 a_0)(I_1 + I_2)}$$

where

I_1 = moment of inertia of instrument section
I_2 = moment of inertia of cluster
a_0 = gain constant with respect to angular displacement
a_1 = gain time constant with respect to angular rate
c_1 = roll restoring coefficient

Note: Dots above variable denote time derivatives.

Acknowledgment

The contributions of F. W. Wagnon, Guidance and Control Laboratory, to the design of the regulator are greatly appreciated.

References

1 Haeussermann, W., "Spatial Attitude Control of a Spinning Rocket Cluster," JET PROPULSION, vol. 29, no. 1, Jan. 1959.
2 Storm, F., "Magnetic Amplifiers," John Wiley & Sons, New York, 1955, p. 463.
3 Anderson, D. L., Jasper, N., Taylor, J. C., "Pulse Duration Modulated Transistor Switches for DC Amplification," ABMA Research Report no. 1 R 12, 1956.

A Note on Turbulent Boundary Layer Growth in Nozzles[1]

M. SIBULKIN[2]

California Institute of Technology, Pasadena, Calif.

An expression is obtained for the effect of changes in the turbulent boundary layer thickness at the throat of a supersonic nozzle on the boundary layer thickness at the exit of the nozzle. Two limiting cases are considered, and it is found that: 1 If the throat boundary layer is relatively thin, changes in its thickness have a negligible effect on the exit boundary layer thickness; and 2 if the throat boundary layer is relatively thick, changes in its thickness have a proportionate effect on the exit boundary layer thickness.

Nomenclature

h = nozzle height
H = ratio of displacement thickness to momentum thickness
M = Mach number
u = velocity parallel to wall
x = distance parallel to wall
γ = ratio of specific heats
δ = boundary layer thickness
θ = momentum thickness of boundary layer
ν = kinematic viscosity
ρ = density
τ = wall shearing stress

Subscripts

e = nozzle exit station
1 = local value at boundary layer edge
0 = nozzle throat station

IN CALCULATING the boundary layer growth in wind tunnel nozzles, it is sometimes assumed that the boundary layer thickness at the nozzle throat may be neglected (i.e., taken as zero). However, for low speed diffusers, e.g. (1),[3] it has been suggested that the exit boundary layer thickness is directly proportional to the inlet thickness. Since these two approaches appear contradictory, it appeared desirable to attempt a more general analysis of the variation of nozzle exit momentum thickness with nozzle throat momentum thickness. The analysis which follows is limited to the two-dimensional turbulent boundary layer case.

Received Aug. 30, 1958.
[1] This paper presents the results of one phase of research carried out at the Jet Propulsion Laboratory, California Institute of Technology, under joint sponsorship of the Department of the Army, Ordnance Corps (under Contract no. DA-04-495-Ord 18) and the Department of the Air Force.
[2] Formerly Research Engineer, Jet Propulsion Laboratory. Present address: Convair Scientific Research Laboratory, San Diego, Calif.
[3] Numbers in parentheses indicate References at end of paper.

Analysis

For two-dimensional compressible flow the momentum equation can be written as (2)

$$\frac{d\theta}{dx} + \left[\frac{2 + H - M_1^2}{M_1\left(1 + \frac{\gamma - 1}{2} M_1^2\right)} \frac{dM_1}{dx}\right]\theta = \frac{\tau}{\rho_1 u_1^2} \qquad [1]$$

The expression in the brackets is a function only of x, since $H = g(M_1, T_1/T_w)$, and M_1 and T_1/T_w are considered as prescribed functions of x. Equation [1] can therefore be written as

$$\frac{d\theta}{dx} + P(x)\theta = \frac{\tau}{\rho_1 u_1^2} \qquad [1a]$$

For turbulent flow an approximate expression for the wall shearing stress (cf. section II-A of (3)) is

$$\frac{\tau}{\rho_1 u_1^2} = 0.0225\left(\frac{\nu_1}{u_1 \delta}\right)^{1/4} f(M_1, T_1/T_w) \qquad [2]$$

where f contains the effects of compressibility and heat transfer on the wall shearing stress. Combining [1 and 2] gives

$$\frac{d\theta^{5/4}}{dx} + \frac{5}{4} P(x)\theta^{5/4} = Q(x)$$

where

$$P(x) \equiv \frac{2 + H - M_1^2}{M_1\left(1 + \frac{\gamma - 1}{2} M_1^2\right)} \frac{dM_1}{dx}$$

$$Q(x) \equiv \frac{5}{4}\, 0.0225 \left(\frac{\theta}{\delta}\right)^{1/4}\left(\frac{\nu_1}{u_1}\right)^{1/4} f \qquad [3]$$

The expression for Q is a function only of x, since θ/δ, ν_1 and u_1 are functions of M_1 and T_1/T_w. Then, letting $\theta = \theta_0$ at $x = 0$, Equation [3] can be formally integrated to give

$$\theta^{5/4} = e^{-\int_0^x P dx_1}\int_0^x \left(e^{\int_0^{x_1} P dx_2}\right) Q dx_1 + \theta_0^{5/4} e^{-\int_0^x P dx_1} \qquad [4]$$

Equation [4] gives the variation with x of the momentum thickness θ for a given distribution of M_1 and T_1/T_w with x and a given initial momentum thickness θ_0. Thus [4] can be used to calculate the boundary layer growth along the walls of a supersonic nozzle. For a particular nozzle, M_1 and T_1/T_w (and therefore P and Q) are nearly independent of θ_0 so that one can define the constants

$$A \equiv \int_0^e \left(e^{\int_0^x P dx_1}\right) Q dx$$

$$B \equiv e^{-\int_0^e P dx} \qquad [5]$$

where $x = 0$ is the nozzle throat, and $x = e$ is the nozzle exit. Equation [4] then reduces to

$$\theta_e^{5/4} = B(A + \theta_0^{5/4}) \qquad [6]$$

and differentiating [6] gives

$$\frac{d\theta_e}{d\theta_0} = \frac{B^{4/5}\theta_0^{1/4}}{(A + \theta_0^{5/4})^{1/5}} \qquad [7]$$

Equations [6 and 7] are general expressions for the variation of nozzle exit momentum thickness with throat momentum thickness in terms of the nozzle parameters A and B.

In the design of supersonic wind tunnel nozzles one is not, generally, interested in the effect of real changes in θ_0 (e.g., as caused by changes in the nozzle inlet geometry), but in the errors caused by making the simplifying approximation $\theta_0 = 0$. This assumption is based on the belief that the true value of θ_0 is small compared with the true value of θ_e. Thus it is of interest to examine the limiting form of Equation [7] as $\theta_0 \to 0$.

For $\theta_0 \ll A^{4/3}$

$$\frac{d\theta_e}{d\theta_0} = \frac{B^{4/3}}{A^{1/3}}\,\theta_0^{1/3}$$

and

$$\lim_{\theta_0 \to 0} \frac{d\theta_e}{d\theta_0} = 0 \qquad \ldots\ldots\ldots\ldots\ldots\ldots\ldots\ldots\ldots\ldots [8]$$

From Equations [8] one can conclude that the approximation $\theta_0 = 0$ is justified as long as $\theta_0 \ll A^{4/3}$. (A rapid estimation of θ_0 can be made by using Eqs. [35] and [3] of (3).)

If the opposite limiting case is considered, one finds that for $\theta_0 \gg A^{4/3}$

$$\frac{\theta_e}{\theta_0} = \frac{d\theta_e}{d\theta_0} = B^{4/3} \qquad [9]$$

which shows that in this limit θ_e is directly proportional to θ_0 as suggested in (1). (Eq. [9] could be derived directly by assuming $\tau = 0$ in [1a].) Moreover, if [9] is applied to an incompressible flow (which obviously excludes the supersonic nozzle case), it can be shown that the definition of B reduces to

$$B = \left(\frac{u_{1,0}}{u_1}\right)^{5/4(H+2)}$$

which reduces [9] to

$$\frac{\theta}{\theta_0} = \left(\frac{u_{1,0}}{u_1}\right)^{H+2} \qquad [9a]$$

which is similar to the result for incompressible flow given in Equation [7] of (1).

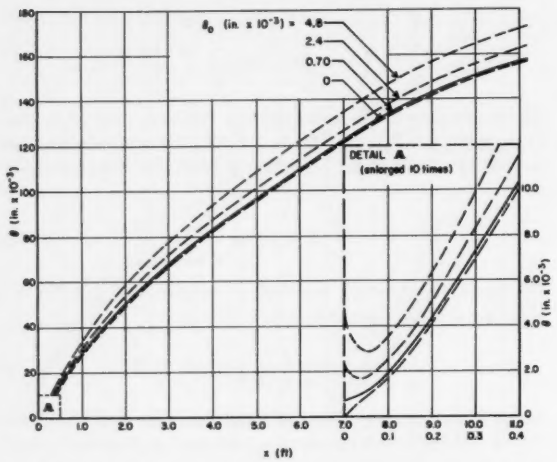

Fig. 1 Growth of boundary layer momentum thickness θ along wall of a supersonic nozzle for several values of throat momentum thickness θ_0. $M_e = 8$, $P_0 = 45$ atm, $T_0 = 1000$ F, $h_0 = 0.084$ in., $h_e = 16$ in.

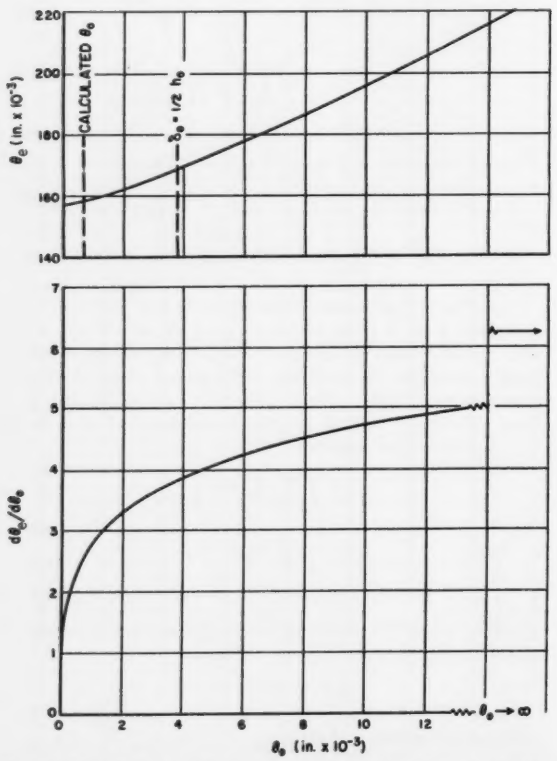

Fig. 2 Variation of exit momentum thickness θ_e and $d\theta_e/d\theta_0$ with throat momentum thickness θ_0

Example of Results

As an example, $\theta(x;\theta_0)$ has been calculated from the throat ($x_0 = 0$) to the exit ($x_e = 11.2$ ft) of a two-dimensional nozzle[4] having an exit Mach number of 8.0 for $P_0 = 45$ atm and $T_0 = 1000$ F. The throat and exit heights of the nozzle are $h_0 = 0.084$ in., and $h_e = 16$ in.

The calculated distributions of θ are shown in Fig. 1 for several assumed values of θ_0 and for the correct value of throat momentum thickness, $\theta_0 = 0.70 \times 10^{-3}$ in. (This value was obtained by integrating [4] from the nozzle inlet, $M = 0.01$, to the nozzle throat.) For this example the constants are

$$A^{4/3} = 25.1 \times 10^{-3} \text{ in.}$$

$$B = 9.90$$

Therefore

$$\frac{\theta_0}{A^{4/3}} = \frac{0.70 \times 10^{-3}}{25.1 \times 10^{-3}} = 0.028$$

and, using the values of θ/δ tabulated in (4)

$$\frac{\delta_0}{h_0/2} = \frac{\theta_0}{(\theta/\delta)_{M=1}}\,\frac{2}{h_0} = \frac{0.70 \times 10^{-3}}{0.091}\,\frac{2}{0.084} = 0.18$$

The corresponding error in θ_e is (using [6])

$$\frac{\theta_{e(\text{true})} - \theta_{e(\theta_0=0)}}{\theta_{e(\text{true})}} = \frac{0.1586 - 0.1568}{0.1586} = 0.011$$

showing that in this case the assumption $\theta_0 = 0$ results in an error of 1 per cent, although the boundary layer at the throat fills about 18 per cent of the nozzle.

To complete the example, the values of θ_e vs. θ_0 and $d\theta_e/d\theta_0$ vs. θ_0 are shown in Fig. 2. However, it may be noted that for

[4] This is the nozzle used in the example given in (3).

a supersonic nozzle, the maximum meaningful value of θ_0 is reached when the boundary layer fills the nozzle throat, i.e., for a two-dimensional nozzle, when $\delta_0 = h_0/2$. For this example

$$\theta_{0(\max)} = \frac{h_0}{2}\left(\frac{\theta}{\delta}\right)_{M=1} = 3.8 \times 10^{-3} \text{ in.}$$

which is still a small value of θ_0 relative to $A^{1/2}$.

References

1 Ross, D. and Robertson, J. M., "An Empirical Method for Calculation of the Growth of a Turbulent Boundary Layer," *J. Aeron. Sci.*, vol. 21, no. 5, May 1954, pp. 355–359.

2 Shapiro, A. H., "The Dynamics and Thermodynamics of Compressible Fluid Flow," vol. II, The Ronald Press, New York, 1954, p. 1092.

3 Sibulkin, M., "Heat Transfer to an Incompressible Turbulent Boundary Layer and Estimation of Heat Transfer Coefficients at Supersonic Nozzle Throats," *J. Aeron. Sci.*, vol. 23, no. 2, Feb. 1956, pp. 162–172.

4 Tucker, M., "Approximate Turbulent Boundary-Layer Development in Plane Compressible Flow along Thermally Insulated Surfaces with Application to Supersonic Tunnel Contour Correction," NACA TN 2045, 1950.

Research on Supersonic Combustion[1]

ROBERT A. GROSS[2]

Fairchild Engine Division, Deer Park, N. Y.

A DETONATION is a wave in which an exothermal chemical reaction takes place and which moves with supersonic velocity with respect to the undetonated (reactant) gas. It is characterized by this supersonic propagation velocity and a large pressure and temperature increase across the wave. A detonation differs from a flame (deflagration) in that a flame moves with subsonic velocity, and its microscopic propagation mechanisms are fundamentally different. A review of the status and recent developments in the field of gaseous detonation is contained in (1).[3]

The only steady detonations that have been previously observed are the so-called "Chapman-Jouguet" detonations. A Chapman-Jouguet detonation is characterized by the fact that the flow immediately behind the wave is sonic ($M_2 = 1$). A Chapman-Jouguet detonation represents the minimum supersonic propagation Mach number for a given fuel-air ratio. It is the type of combustion wave usually found if combustion is initiated in a long tube filled with a combustible mixture. Analytical work (2) has predicted the possibility of other type detonations called "strong" and "weak." A strong detonation has subsonic downstream flow ($M_2 < 1$) whereas for a weak detonation wave $M_2 > 1$. A Chapman-Jouguet detonation represents the merging of the strong and weak detonations in the "singular" solution. Previous failures to find strong or weak detonations in nature have led to the speculation that they might be unstable.

Research Results

Under contract to the Air Force Office of Scientific Research, we began, in October of 1956, to explore means of releasing chemical energy steadily in supersonic flow. A high temperature steady flow supersonic combustion research tunnel was designed, built and put in operation by January 1958. This tunnel produces a steady Mach 3 flow with stagnation temperatures up to 1400 F and a stagnation pressure of approximately 110 psia. Exploratory experiments with hydrogen fuel and air determined that thermal ignition can be obtained at approximately 1250 F (30 psia) and in a chemical reaction time of less than 30 microsec.

During September 1958, a mixture of hydrogen and air was passed through a small normal Mach reflected shock in the Mach 3 section of the tunnel under conditions which our previous research indicated should cause thermal ignition. Combustion did occur resulting in a new, steady detonation wave pattern in the test section. Since then, these test conditions have been repeated numerous times resulting in the same shock to detonation wave transformation. Numerous schlieren photographs, schlieren motion pictures and some centerline probe data have been obtained. All information to date strongly indicates that this supersonic combustion wave is a strong detonation. It is stable, steady, reproducible and obtainable over a wide fuel-air ratio as long as the Mach number of the approach flow is greater than the Chapman-Jouguet Mach number for that fuel-air ratio. It is noteworthy that under these conditions we have burned mixtures of hydrogen-air far leaner than previous experimental ignition, flammability or detonation limit data would have predicted possible (3). Schlieren data indicate that the chemical reactions are completed in less than $\frac{1}{4}$ in., or less than 20 microsec. A schlieren photograph of such a strong detonation is shown in Fig. 1.

Consequences

Steady strong detonation waves have been demonstrated for the first time in the laboratory. They are stable and reproducible. A great deal is analytically known about such waves (2). For a given fuel-air ratio, there is a minimum supersonic Mach number for which steady conditions can be achieved, the Chapman-Jouguet Mach number. For any higher Mach number, a steady strong detonation may be achieved. The domain of such possible stable solutions for hydrogen-air detonations is shown in Fig. 2. There is an additional requirement for the establishment of such detonation waves. The static pressure and temperature behind the initial shock wave system must be such as to cause the particular fuel and oxidizer to react chemically.

Extensive theoretical calculations for hydrogen-air and propane-air strong detonations are contained in (2). It is of interest to note that the total pressure loss across a detonation wave is approximately equal to that of a corresponding shock wave. The high speed of such detonation waves with their corresponding small thickness imply a heat release per unit

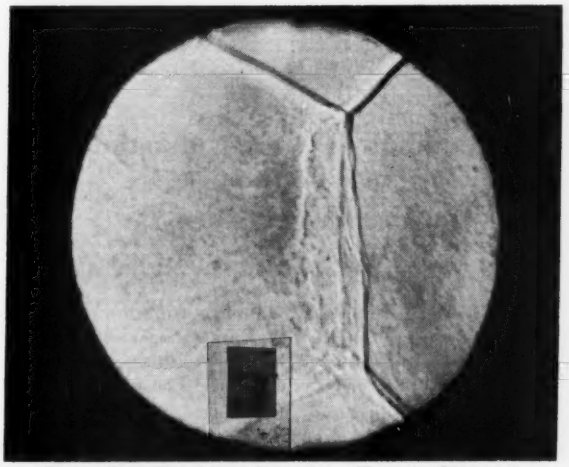

Fig. 1 Standing detonation wave. H_2+ air; $M_1 = 3.0$

Received Nov. 24, 1958.

[1] This research has been supported by the Air Force Office of Scientific Research under contract AF 49(638)-15.

[2] Chief Research Engineer. Member ARS.

[3] Numbers in parentheses indicate References at end of paper.

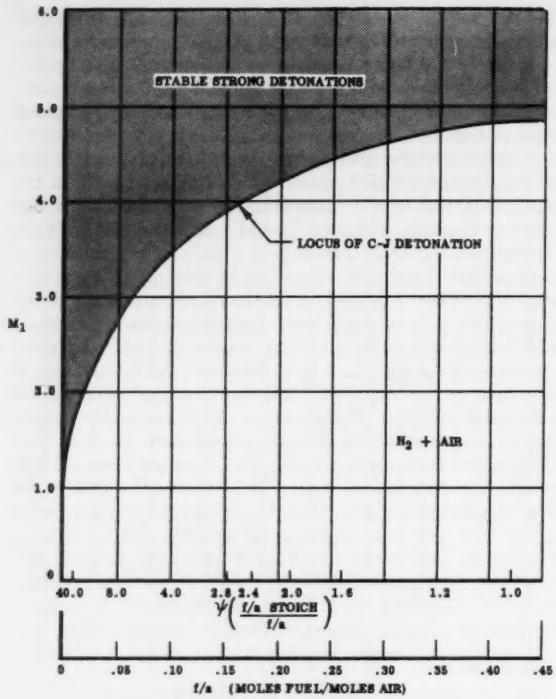

Fig. 2 Stable strong detonations

volume per unit time far exceeding any other previously obtained chemical combustion system.

The physical realization of steady strong detonations in the laboratory has made available a new and powerful research tool. It should provide valuable fundamental data in high temperature chemical kinetics and molecular physics, as well as a rich harvest in aerothermodynamic experiments.

The unusual properties of such strong detonations, such as their very high propagation speed, fast chemical reaction rate, wide fuel-oxidizer combustion capability and high heat release rate, may permit exciting new engineering applications. Consideration of the application of these properties challenge the imagination of creative engineers.

References

1 Gross, R. A. and Oppenheim, T. K., "Recent Advances in Gaseous Detonation," American Rocket Society preprint 688-58, New York, Nov. 1958.

2 See for example, Eisen, Gross and Rivlin, "Theoretical Calculations in Gaseous Detonation," AFOSR TN 58-326; ASTIA no. AD-154230, March 15, 1958.

3 Drell, I. L. and Belles, F. E., "Survey of Hydrogen Combustion Properties," NACA RM E57D24, July 25, 1957.

A Rapid Method for Estimation of Specific Impulse

B. A. FREE[1] and S. F. SARNER[2]

General Electric Co., Cincinnati, Ohio

A semiempirical method for rapid estimation of specific impulse of rocket propellant systems is presented, based on a simplification of standard thermodynamic equations and the use of suitable reference systems. The accuracy of the method is of the order of ±3 per cent in most cases with an extreme range of ±5 per cent. Within this range, systems which produce high flame temperatures, or high degrees of dissociation, and those which involve large amounts of monatomic or tetratomic products deviate, in general, more than the conventional systems.

Received March 1958.

[1] Propellants Chemist, Applied Research Operation. Member ARS.

[2] Physical Chemist, Applied Research Operation. Member ARS.

IN ORDER to estimate the performance of various rocket propellant combinations, a few strict thermodynamic methods have been derived which are capable of extreme accuracy (1,2,3),[3] and a number of short methods have been proposed which considerably reduce the labor and computation requirements inherent in the more exact derivations (4,5,6). The short methods, however, usually involve the preparation of long lists or charts of an empirical nature, a process which in itself is involved and time-consuming. Both of the above methods, moreover, require a degree of familiarization and facility with rocket propellant computations foreign to the average technical engineer whose main interest may lie elsewhere.

The need for a simple and extremely rapid method of estimation of specific impulse was felt by the authors about a year ago, and an extensive investigation into the causes of the complexity of present calculations has led to the following simplification.

One of the most widely used methods of calculating specific impulse of rocket propellant combinations is based on the relationship

$$I = 6.93\varphi \sqrt{\frac{T_c}{M}} \sqrt{\frac{2\gamma}{\gamma - 1}\left[1 - \left(\frac{P_e}{P_c}\right)^{\frac{\gamma - 1}{\gamma}}\right]} \qquad [1]$$

where I is specific impulse, φ an efficiency coefficient, T_c and M the chamber temperature in deg R and the average molecular weight of the combustion products, γ the specific heat ratio C_p/C_v, and P_e and P_c the exit and chamber pressure, respectively. A brief consideration of this equation at once points out that, although the relationship itself is simple, dissociation will seriously affect T_c, M and γ, making the estimation of these essential quantities a tedious process; in addition, this effect will be magnified by increasing temperature. At any given temperature, however, the dissociation effect as well as γ will be about the same for systems involving similar reaction products. Such systems when considered simultaneously in the equation

$$\frac{I_1}{I_2} = \frac{6.93\varphi}{6.93\varphi} \sqrt{\frac{T_{c1}M_2}{T_{c2}M_1}} \sqrt{\frac{x_1}{x_2}} \qquad [2]$$

where

$$x = \sqrt{\frac{2\gamma}{\gamma - 1}\left[1 - \left(\frac{P_e}{P_c}\right)^{\frac{\gamma - 1}{\gamma}}\right]}$$

should simplify without too much loss in accuracy to the approximation

$$\frac{I_1}{I_2} \approx \sqrt{\frac{T_{c1}M_2}{T_{c2}M_1}} \qquad [3]$$

Since the dissociation effect for such similar systems is about the same, Equation [3] may be further simplified to

$$\frac{I_1}{I_2} \approx \sqrt{\frac{t_{c1}m_2}{t_{c2}m_1}} \qquad [4]$$

where t_c and m now mean those values which would be found if no dissociation occurred, values which are very easily obtained by simple calculations. The accuracy of this expression has been found to be roughly in proportion to the similarity between the two systems considered, as would be expected, provided that the calculated values for t_c are not too far apart. Table 1 is a typical example of such comparisons.

[3] Numbers in parentheses indicate References at end of paper.

Table 1 A comparison of similar systems

System	Mole fractions of products: HCl	HF	H_2	N_2	m	t_c deg K	I_{calc}	I_{true}
1 NH_3-1.3F_2 (reference)	...	0.7879	0.0606	0.1515	20.13	5530	...	296
2 N_2H_4-1.67F_2	...	0.7152	0.0707	0.2141	20.45	5851	300	302
3 NH_3-0.7236ClF_3	0.2099	0.6297	0.0153	0.1450	24.35	4108	240	231.5

The loss in accuracy when comparing system 3 with system 1 has been shown to be due to the large change in t_c between the two systems; this trend would seriously limit the application of Equation [4] if it were not for the existence of homologous series which provide a gradually ascending flame temperature with the same oxidizer as one ascends the series. By this means, the performance of all fuels in a class, such as saturated hydrocarbons when used in conjunction with a common oxidizer, are susceptible to very accurate estimation, provided the true impulse values for several members of the class are known. Instead of using many specific known-unknown pairs of systems, it has been found convenient to define an average reference system for which $m = 25$ at all temperatures. Equation [4] then becomes

$$I_{calc} \approx I_{ref} \sqrt{\frac{t_{c\,calc}}{t_{c\,ref}} \frac{25}{m_{calc}}} \qquad [5]$$

For several known systems, since t_c and m may be easily evaluated assuming no dissociation, Equation [5] may be solved for I_{ref}, and the results plotted against the corresponding values for t_c. The result is a reference curve of a hypothetical homologous series, showing the best value of I_{ref} to be used in Equation [5 or 6] for a given value of t_c. Fig. 1 is a typical example obtained by using methane, ethane and methylcyclopentane as reference fuels with liquid oxygen as oxidizer.[4]

In estimating the specific impulse value for an unknown fuel, say octane, the value for t_c is first calculated, and the corresponding value of I_{ref}, obtained from Fig. 1, may be substituted into the further simplified form of Equation [5]

$$I \approx I_{ref} \sqrt{\frac{25}{m}} \qquad [6]$$

Using Fig. 1 and Equation [6], the specific impulse values for the fuels octane, JP-4 and ethylene have been estimated and compared with previously known values in Table 2;

Table 2 Hydrocarbon-LOX comparisons

System	t_c deg K	m	I_{calc}	I_{true}
1 C_8H_{18} + 7.8535O_2	3744	21.49	248	248
2 JP-4 + 9.855O_2	4045	23.09	257	249
3 C_2H_4 + 1.6306O_2	3758	20.06	258	264

these examples are, as before, typical of many similarly calculated systems. The accuracy of the first estimation, made on a member of the homologous series, is excellent; examples 2 and 3, not members of the homologous series, are still within the range of reasonable estimation.

Up to this point, the applications of this method have been somewhat limited in scope. The next step, that of directly applying Equation [6] and an appropriate reference curve to all rocket propulsion systems, may at first seem too hasty and without theoretical significance. However, although this extension naturally involves some further loss in accuracy, there are several compensating factors which limit what otherwise might be extremely large errors in estimation. The first of these factors is that x, as defined in Equation [2], is self-compensating, that is, as C_p changes considerably, the C_p/C_v function, which is x, is subject to much smaller changes. As an example, when C_p undergoes approximately a 50 per cent change, as is the case in comparing a diatomic molecule to a triatomic one, the corresponding change in x is only about 6 per cent when $P_e/P_c = 0.049$. Since normal chemical propulsion systems rarely involve heat capacity deviations greater than this, and since an average reference system will be utilized, the error introduced by the reduction of Equation [1] to Equation [3] should not exceed ±3 per cent in most cases.

Further, it can be shown that diatomic gases like N_2, H_2, HF and CO dissociate, in general, much less than triatomic gases like H_2O and CO_2. Since the present method assumes that dissociation is completely compensated for by compari-

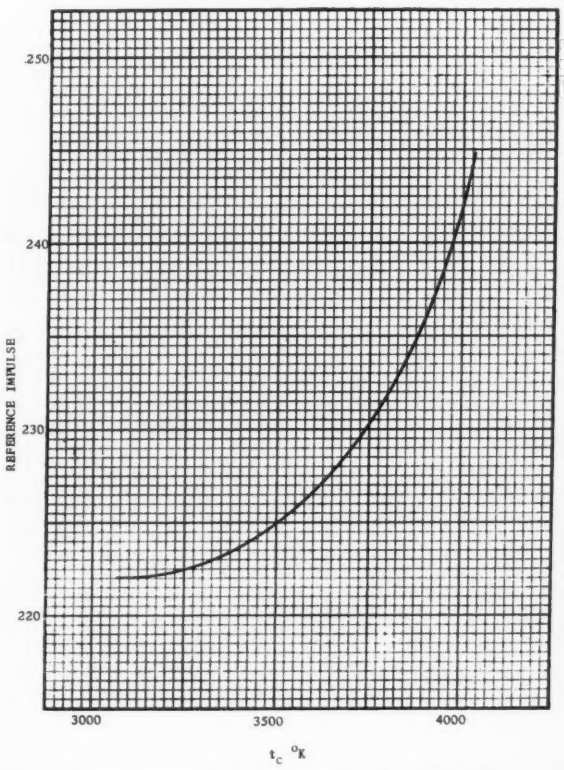

Fig. 1 Reference curve for use with Equation [6] on saturated hydrocarbons

[4] Known values were extracted from numerous sources using a pressure ratio of 300 to 14.7 psi. Similar reference curves could be constructed or suitable conversion factors could be derived for other pressures.

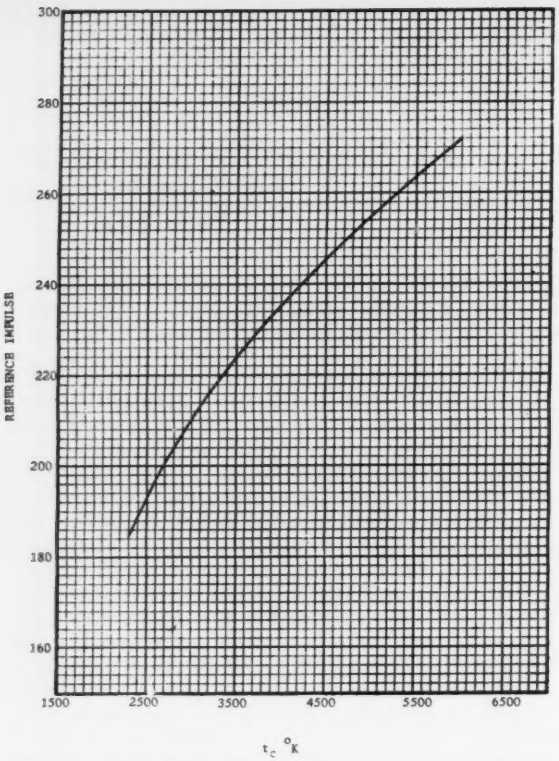

Fig. 2 General reference curve for use with Equation [6]

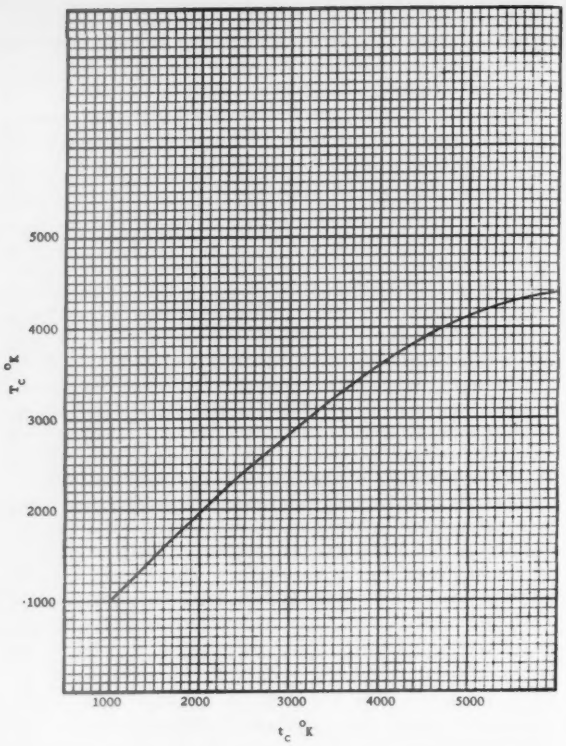

Fig. 3 The relationship between calculated and actual flame temperature

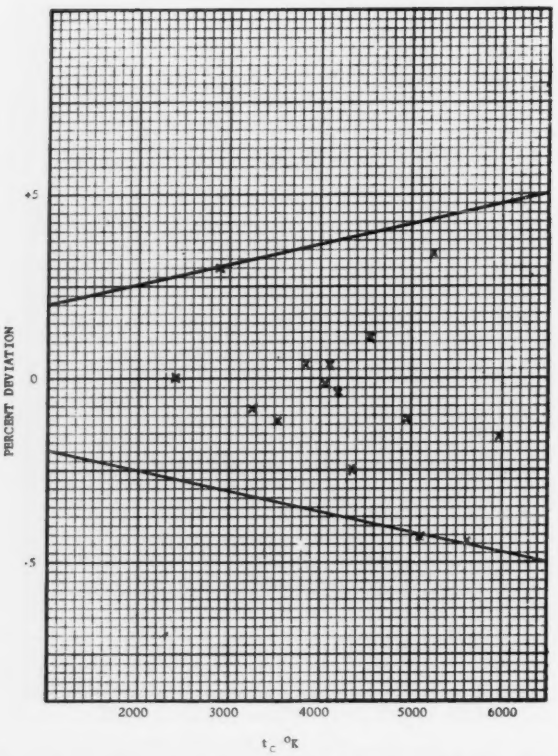

Fig. 4 Performance estimation errors for miscellaneous real systems

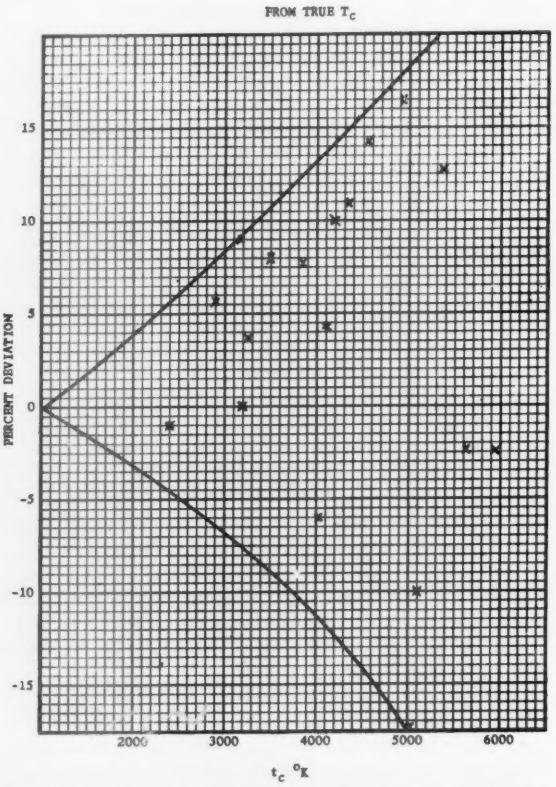

Fig. 5 Flame temperature estimation errors for miscellaneous real systems

Table 3 Miscellaneous performance estimations

	System	O/F ratio	m	Temperature, deg K t_c	$T_{c\,calc}$	$T_{c\,true}$	Impulse I_{calc}	I_{true}
1	hydrogen-LOX	2.89	7.96	2391	2390	2414	345	345
2	hydrogen-ozone	2.65	7.36	2903	2790	2633	384	373
3	methyl alcohol-WFNA	2.36	25.64	3187	3000	2744	212	219
4	ammonia-LOX	1.25	19.16	3255	3050	2941	248	250
5	hydrazine-N_2O_4	1.00	20.71	3501	3220	2981	246	249
6	aniline—WFNA	3.00	25.81	3201	3000	3001	213	222
7	ethyl alcohol—LOX	1.50	23.03	3841	3450	3198	243	242
8	ethylamine-N_2O_4	4.09	27.78	4197	3680	3332	229	230
9	methylamine-LOX	2.06	23.76	4544	3850	3366	255	252
10	hydrogen-N_2O_4	11.50	20.07	4350	3750	3372	272	279
11	ammonia-ClF_3	3.93	24.34	4100	3650	3500	241	240
12	acetylene-N_2O_4	2.98	26.96	4927	4100	3518	246	249
13	atomic hydrogen	60 mole per cent	2.02	5380	4225	3758	919	889
14	JP4-LOX	2.26	23.09	4045	3600	3830	259	260
15	methyl alcohol-fluorine	2.37	21.61	5622	4310	4406	285	298
16	hydrazine-fluorine	1.98	20.45	5963	4420	4529	295	300
17	atomic nitrogen	40 mole per cent	28.02	5106	4125	4594	243	254

son with another system, a positive error is introduced when a system involving a large proportion of triatomic reaction products is considered. Similarly, a negative error is expected from this source (dissociation) when largely diatomic gases are considered. These same systems, however, are subject to a compensating error (±3 per cent) mentioned in the paragraph above, because x is large for triatomic and small for diatomic products. Since this method assumes that x is a constant for all systems, it may be reasoned that the two major sources of error discussed here are always compensating.

Although the degree of this compensation could probably be estimated more accurately by extensive mathematics, more easily obtainable results may be obtained by applying Equation [6] to the large number of propellant systems available which were calculated by more exact methods. As before, an average hypothetical system is defined for which $m = 25$. By the use of a number of known systems (selected for variety) in Equation [5], t_c and I_{ref} have been established for a large number of points.[4] Fig. 2 denotes, as in the previous example, a synthetic average reference curve. Since it is not the aim of this method to provide extreme accuracy but to avoid very large errors, the curve has been drawn through the median of the points.

A by-product of this method of estimation is obtained by plotting all the calculated t_c's from various combinations against true flame temperature T_c. The result, expressed in Fig. 3, provides a convenient way of approximating flame temperatures of unknown systems.

By the use of Figs. 2 and 3 and Equation [6] a number of propellant combinations have been evaluated and compared with previously known listings for specific impulse and flame temperature.[4] Table 3 and Figs. 4 and 5 show the values calculated and the deviations from the values obtained by more exact methods.

Although the data presented here are considered adequate to apply to unknown systems at the present time, there is no doubt that, due to the statistical approach followed in constructing Figs. 2 and 3, the inclusion of more points on the reference curve would make it somewhat more reliable. Future users of the method will find that after a degree of facility is established, the estimation of impulse for a specific mixture will take about 30 minutes, and thus large numbers of systems may be scanned in a relatively short period of time.

Numerous attempts at improving the accuracy of this method further by the addition of the empirical correction factors based on various apparent trends have met with little success. The authors have long abandoned this phase of investigation, and similar efforts are not recommended as being particularly fruitful.

In conclusion, this method, when used within its proper limitations, provides a rapid and convenient tool for estimating the value of new propellants, for scanning large numbers of propellants in a weeding out process, and for any investigation which emphasizes speed rather than extreme accuracy. Although accuracy will suffer when the present data is applied to systems involving high temperatures or large amounts of products other than diatomic and triatomic gases, it is believed that the majority of propellant combinations in use at the present time are sufficiently average to fall within the scope of this investigation.

References

1 Zucrow, M. J., "Principles of Jet Propulsion and Gas Turbines," John Wiley and Sons, New York, 1948, chap. 12.

2 Brinkley, S. R., Jr. and Lewis, B., "The Thermodynamics of Combustion Gases: General Calculations," U. S. Department of Interior, April 1952.

3 Huff, V. N., Gordon S. and Morrell, V. E., "General Method and Thermodynamic Tables for Computation of Equilibrium Composition and Temperature of Chemical Reactions," NACA Report no. 1037, 1951.

4 Johnston, S. A., "Short-cut Method for Calculating the Performance of Fuels Containing C,H,O, and N, with HNO_3, Liquid Oxygen, or NH_4NO_3," C.I.T.-J.P.L. progress Report 20-202, Nov. 1953.

5 Clark, J. D., "The Narts Method of Rocket Performance Calculation," NARTS report no. 71, Nov. 1955.

6 Dekker, A. O., "Rapid Estimation of Specific Impulse of Solid Propellants," JET PROPULSION, vol. 26, July 1956, p. 572.

A Radioactive Ionization Gage Pressure Measurement System[1]

N. W. SPENCER[2] and R. L. BOGGESS[3]

University of Michigan, Ann Arbor, Mich.

ROCKET measurements of upper atmosphere structural parameters have, in large measure, been based upon evaluation of the dynamic air pressure at selected points on the surface of the rocket. Various locations have been chosen for these determinations, but, generally speaking, the nose cone has provided the location for most experiments, as this region permits, usually, the most reliable measurements.

Experiments based upon surface pressure measurement concepts and aerodynamic considerations are limited in altitude capability to heights less than approximately 90 to 100 km, since at this level the mean free path of the gas particles becomes long with respect to sensing device dimensions. Other factors imposing this limit, related to the mean free path concept, are growth of the boundary layer of air surrounding the rocket, reduction of the Reynolds number, and atmospheric composition changes, all resulting in breakdown of aerodynamic concepts based upon the gas law and relatively high air density considerations.

Accordingly, instruments appropriate for measurement under continuum conditions are adequate if they can indicate pressures down to 10^{-3} mm Hg, the approximate value encountered in the 90- to 100-km region. Correspondingly, a high pressure limit is likewise generally accepted in the altitude neighborhood of 30 km, as balloon-borne pressure and temperature measurement experiments are considerably less expensive to carry out up to this level, where the ambient pressure is approximately 10 mm Hg. Rocket-borne equipment, however, at this altitude, can experience much higher (factor of 20 or more) pressures due to the "ram" effect which varies roughly as the square of the Mach number.

Thus instruments suitable in the sense of useful measuring range must be able to measure with the desired precision over the range 100 to 10^{-3} mm Hg, or 5 decades. This large range imposes a severe burden on many instruments, generally being considerably more extensive than their useful range. Some devices, however, do respond adequately throughout this pressure range and have permitted the development of measurement systems which take advantage of their favorable properties.

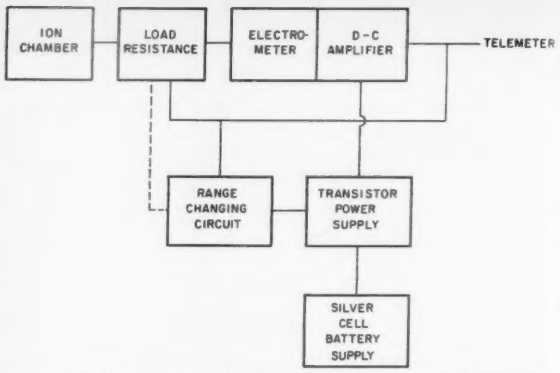

Fig. 1 Block diagram of radioactive pressure measurement system

A radioactive ionization gage is one such instrument which satisfies this requirement. It possesses other desirable characteristics:

It is undamaged by exposure to atmospheric pressure.
It is physically rugged.
It has nearly instantaneous electrical response.
Its construction is relatively simple.

Correspondingly, it exhibits some drawbacks:

It has a very small output current magnitude.
The radioactive source constitutes a potential health hazard.
There is some nonlinearity at very high and very low pressures, generally outside the range indicated above.

The purpose of this paper is to describe briefly a unit, developed and used extensively during the IGY program for pressure measurement, that employs a radioactive ionization gage as its basic sensing element.

Outline of Instrument

Fig. 1 illustrates in block diagram form the system adopted for use with the radioactive ionization chamber. In the arrangement, the small current produced by the chamber is passed through a resistance of sufficient magnitude to cause a voltage drop equivalent to the voltage level desired for presentation to the telemeter. Since large resistances (10^{12} ohms in some cases) are required, and because a telemeter generally imposes relatively low input impedances, a matching circuit

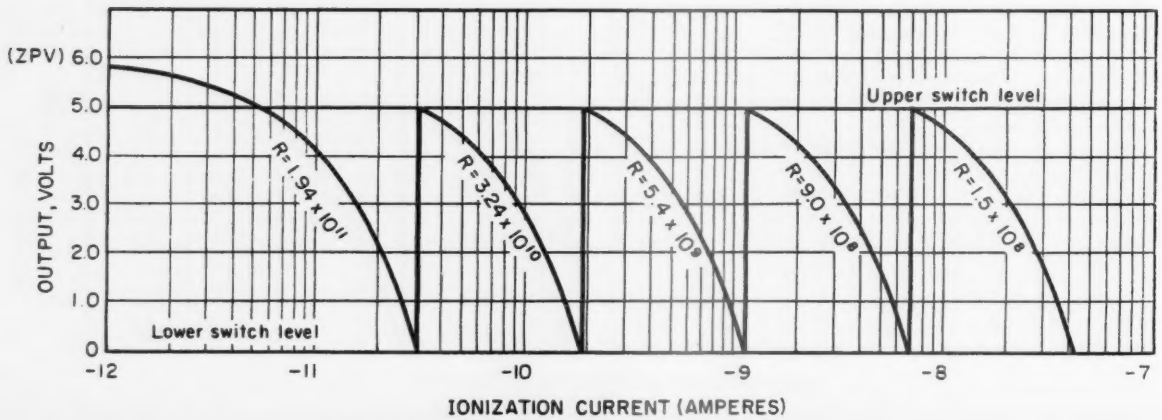

Fig. 2 Output voltage and hi-meg resistor relationships

Received Oct. 9, 1958.

[1] This report was prepared for presentation at the 5th General Assembly of CSAGI, Moscow, July 30–Aug. 9, 1958.

[2] Lecturer, Electrical Engineering Department. Member ARS.

[3] Research Engineer, Research Institute. Member ARS.

in the form of a unity negative feedback amplifier is included. It provides, in effect, current amplification, overcoming one of the drawbacks of a radioactive ion chamber as noted previously.

This circuit arrangement likewise permits realization of the extensive pressure range characteristic exhibited by the chamber, for it is necessary only to alter the magnitude of the chamber load resistance in some fashion to accomplish a sensitivity change.

In the system five different resistances are employed to cover the desired range. Fig. 2 illustrates the complete current-output voltage relationships under conditions where the resistance is changed by a factor of six at appropriate currents.

Fig. 3 illustrates a composite pressure-current relationship for a typical ion chamber corresponding to the Fig. 2 curves. Fig. 4 is a schematic diagram of the amplifier circuit.

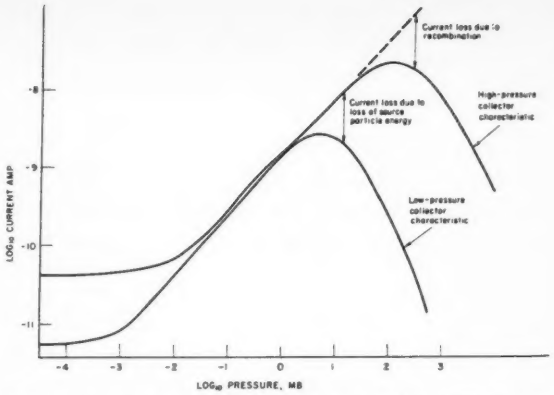

Fig. 3 *i-p* curve of typical ionization chamber showing low-pressure and high-pressure characteristics

Automatic Resistance Change

To fruitfully employ an arrangement that requires resistance change as a function of current or pressure or their equivalent in telemetered signal necessitates, of course, a device which senses that a change is required and then brings about the correct alteration.

A simple d-c servo circuit has been developed for this function. It employs rotary solenoids for effecting the mechanical shift and thyratrons for control of the solenoids. The energy for the solenoids is drawn slowly from the system power supply, and is stored in a capacitance, since functioning of the system is required only every several seconds.

The thyratrons are controlled by transistors which enable rapid thyratron grid-voltage changes and hence more stable control. The output voltage of the d-c amplifier, which constitutes the pressure signal, is applied to the transistors as well as to the telemeter for this control purpose. Thus the total system is able to maintain an on-scale output signal, by self-induced selection of the proper resistance, throughout the useful range of the device. A schematic diagram of the servo circuit appears in Fig. 5.

Power Supply

All power necessary for operation of the pressure measurement system is obtained from a small silver cell battery pack, which supplies approximately 6 v and has a rated capacity of 1 amp-hr. Conversion for the high voltages required is accomplished by a transistor-oscillator system of conventional design.

The primary cells are adequate for about 1 hr of operation of the system.

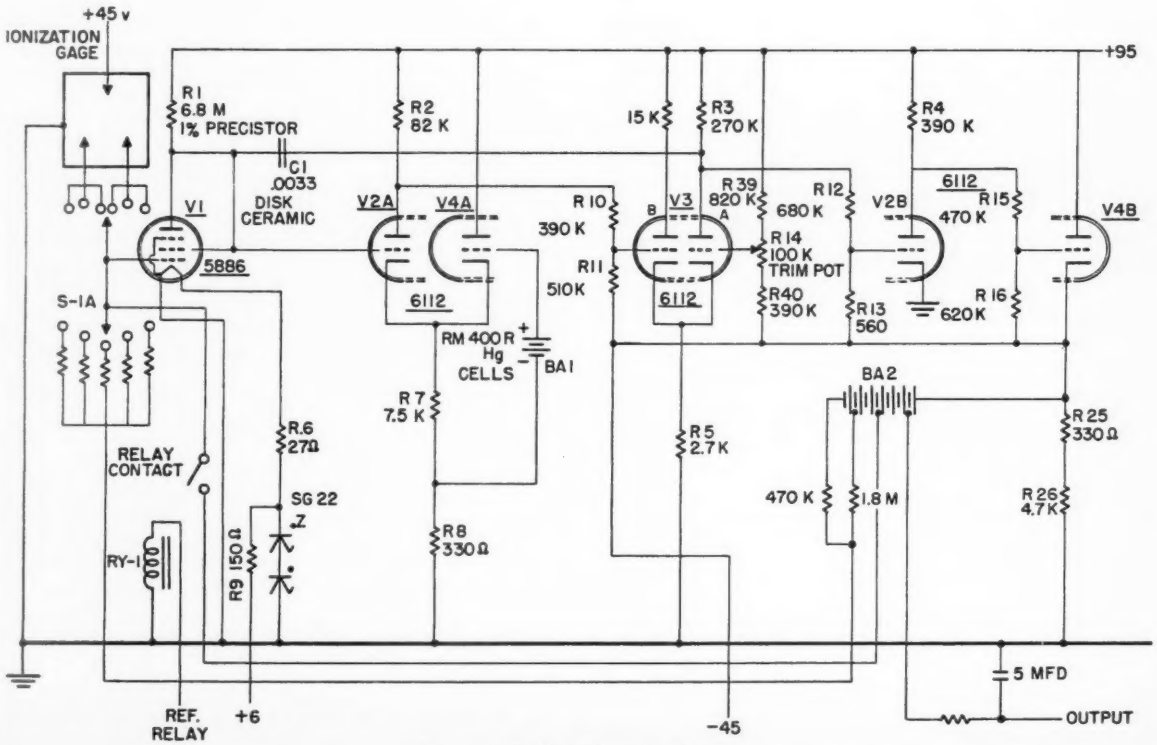

Fig. 4 Amplifier schematic diagram

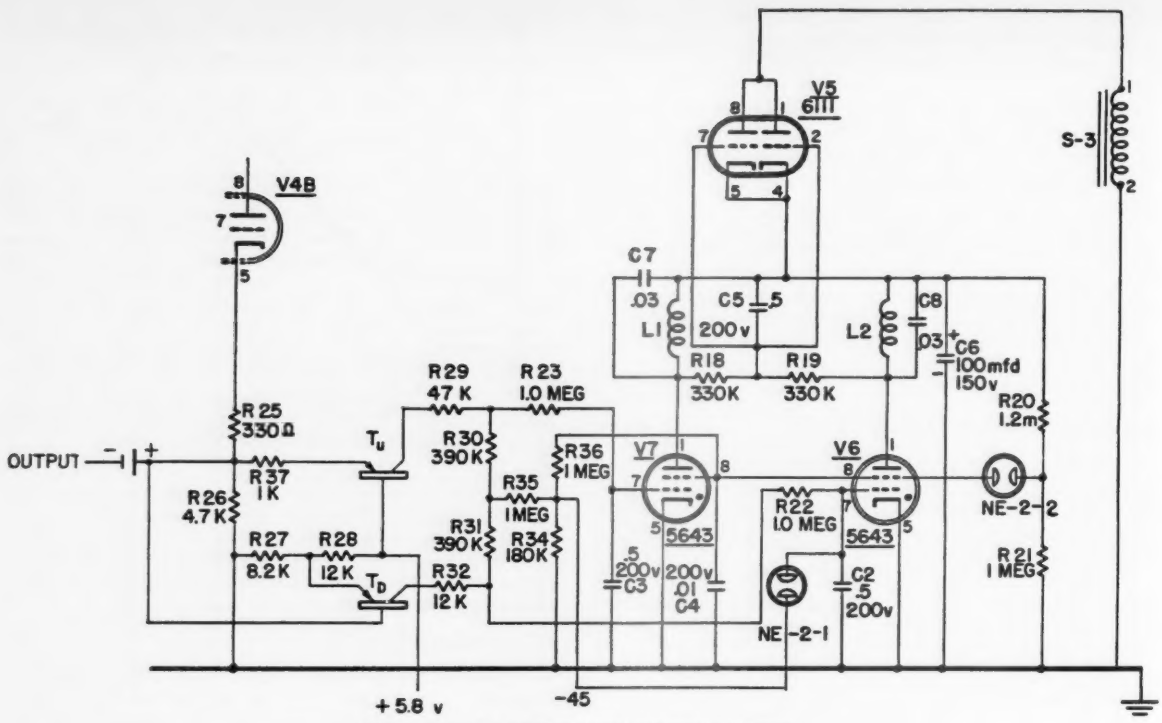

Fig. 5 Range changing circuit schematic diagram

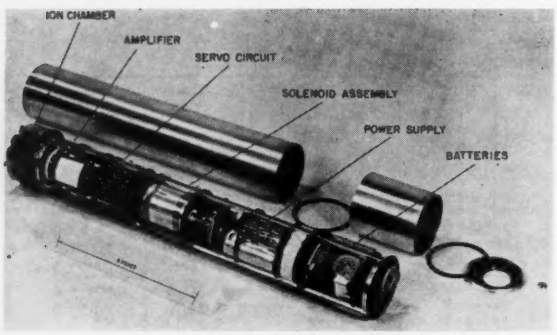

Fig. 6 Complete system out of enclosing tubing

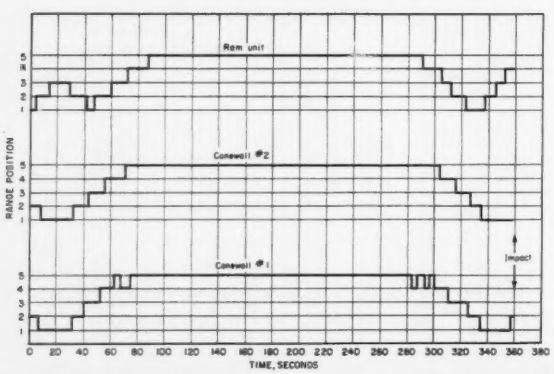

Fig. 7 Range position vs. time for 3 units on Nike-Cajun AM 6.38

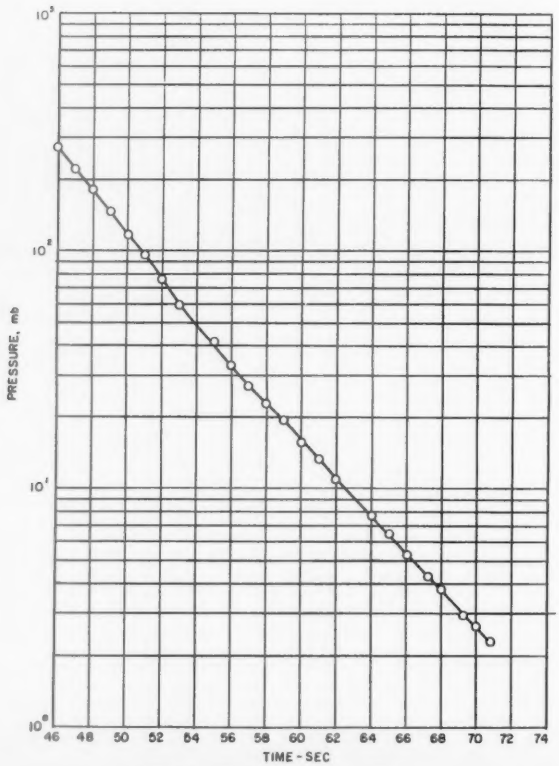

Fig. 8 Ram pressure vs. time

Physical Details and Other Characteristics

The entire system has been constructed in a form readily applicable to rocket instrumentations. It is contained (including power) in a cylinder $2\frac{1}{4}$ in. in diameter, 16 in. long weighing $3\frac{1}{4}$ lb. Fig. 6 is a photograph of a system with cover removed. The various portions of the equipment are indicated.

Fig. 7, which shows the load-resistance changes encountered during a recent rocket application, illustrates the pressure range selection properties of the system.

Finally, Fig. 8 presents a curve of total head pressure vs. time measured with a typical system. The curve is comprised of "raw" pressure data.

Acknowledgment

Many individuals have contributed ideas and effort to the development of this measurement system. M. A. El-Moslimany participated extensively in the area of chamber development, as did L. R. Brace in circuit development. Many others, including W. G. Kartlick, G. Burdette, J. Horvath and T. Miller, contributed to other aspects of the system. Much credit is due all these individuals.

Optimization of Rockets for Maximum Payload Energy

DANDRIDGE M. COLE[1] and MICHAEL A. MARRESE[2]

The Martin Company, Denver, Colo.

THE CLASSICAL criterion for optimizing the design of a mechanical device has been to maximize the output energy for a given input energy. This approach has not been emphasized in design of rockets probably because of the great difficulty involved in making them perform their job at all. However, as rocket capability improves, it can be expected that emphasis will turn toward maximizing the output per dollar expended. This may lead to major changes in design. The purpose of this paper is to give some indication as to the feasibility of the maximum energy approach. The method will be to determine what value of payload will give maximum kinetic energy for a rocket of fixed structural and propellant weights.

Analysis

It is first necessary to develop an equation in which energy or an energy parameter is expressed in terms of rocket configuration ratios. We begin with the definition of kinetic energy

$$KE = \frac{W_L V^2}{2g} \qquad [1]$$

where

KE = kinetic energy
W_L = payload weight
V = velocity at burnout
g = acceleration due to gravity

Then we write the rocket performance equation

$$V = Kg\, I_{sp} \ln \gamma \qquad [2]$$

where

$$\gamma = \frac{W_g}{W_e} = \frac{W_p + W_s + W_L}{W_s + W_L}$$

I_{sp} = specific impulse
W_p = propellant weight
W_s = structural weight
W_g = gross weight
W_e = empty weight
K = correction factor for gravity and atmosphere losses

Let $C = KgI_{sp}$. Then combining Equations [1 and 2] we have

$$KE = \frac{W_L C^2}{2g}\left[\ln \frac{W_p + W_s + W_L}{W_s + W_L}\right]^2 \qquad [3]$$

Dividing both sides of Equation [3] and both the numerator and denominator of the ln factor by W_s, we obtain

$$\frac{KE}{W_s} = \frac{W_L C^2}{2gW_s}\left[\ln \frac{1 + \frac{W_p}{W_s} + \frac{W_L}{W_s}}{1 + \frac{W_L}{W_s}}\right]^2 \qquad [4]$$

Letting

$$\frac{W_p}{W_s} = \beta \qquad \frac{W_L}{W_s} = \alpha$$

results in

$$f(KE) = \frac{2gKE}{C^2 W_s} = \alpha\left[\ln \frac{\beta + \alpha + 1}{\alpha + 1}\right]^2 \qquad [5]$$

In Fig. 1, $f(KE)$ is plotted against α. Care was taken in the computations to isolate the maximum $f(KE)$ on each β curve. Then using these maxima, Fig. 2 was prepared to illustrate the manner in which α depends on β for maximum kinetic energy. Fig. 2 shows, for example, that for a value of $\beta = 9$, which is reasonable for modern rockets, the "optimum" value of α is 4. This value of the payload to structure ratio will give the highest useful output energy and thus the highest mechanical efficiency for the rocket.

When a value of β has been determined by the designer and the value of α selected for maximum efficiency, the burnout velocity will be automatically determined for any given value of I_{sp}. If the resulting burnout velocity or range does not satisfy the mission requirement, the designer should either try to achieve a higher value of I_{sp} or add another stage to the rocket. In the interest of high efficiency, the designer should not increase the velocity by the common expedient of reducing the payload. The "optimization" of a multistage vehicle by this method requires an extensive study which has not yet been undertaken. However, an approach to an optimum multistage vehicle can be made by using standard-stage sizing methods. Thus, for an ideal two-stage vehicle, let $C_1 = C_2$, $\beta_1 = \beta_2$, $\alpha_1 = \alpha_2$, $\gamma_1 = \gamma_2$, and also

$$KE = \frac{W_L(V_1 + V_2)^2}{2g}$$

where V_1 = the increase in velocity during stage 1 burning, and V_2 = the increase in velocity during stage 2 burning.

This leads to

$$KE = \frac{W_L}{2g}\,[2C \ln \gamma]^2 = \frac{2W_L}{g} \ln^2 \gamma \qquad [6]$$

and

$$f_2(KE) = \alpha \ln^2 \gamma \qquad [7]$$

which is of the same form as the function for the one-stage missile. Hence, Figs. 1 and 2 apply to this situation also.

A numerical example of a three-stage vehicle is now provided to clarify and extend the ideas just presented. Let

$$\frac{W_p}{W_p + W_s} = 0.90$$

Received Oct. 10, 1958.

[1] Senior Advanced Planning Specialist, Advanced Planning Dept. Member ARS.

[2] Advanced Planning Dept.

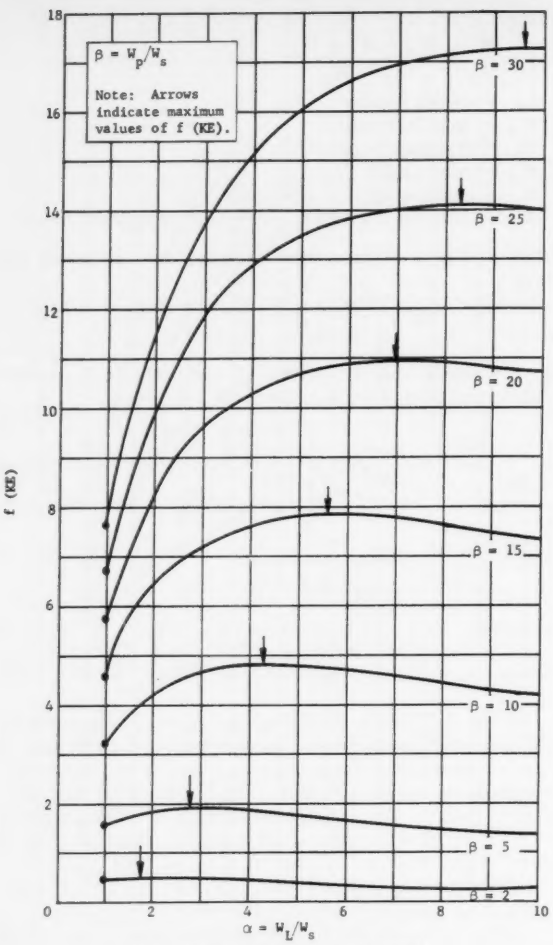

Fig. 1 Maximum values of $f(KE)$

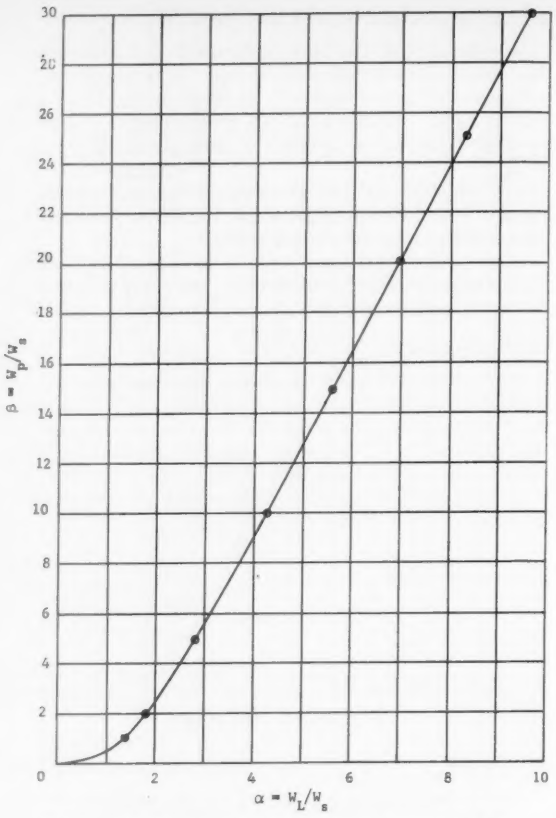

Fig. 2 Relation of α to β for maximum values of KE

Therefore, $\beta = W_p/W_s = 9$; and, by Fig. 2, $\alpha = W_L/W_s = 4$, for all three stages.

If we now assume a payload of 5000 lb, then

W_{s3} = 1250 lb
W_{b3} = 12,500 lb
W_{s2} = 4375 lb
W_{b2} = 43,750 lb
W_{s1} = 15,312.5 lb
W_{b1} = 153,125 lb

where W_{si} = structure weight of ith stage, and W_{bi} = bottle weight of ith stage ($W_b = W_s + W_p$). This gives us W_g = 214,375 lb. With C_s = 10,000 ft/sec (approximately the vacuum value for LOX and RP-1), V = 30,888.6 ft/sec. If an allowance is made of about 4000 ft/sec for gravity and atmosphere loss, it appears that this vehicle could carry a 5000-lb payload to orbit. Actually, this rocket is somewhat idealized, since the β ratio would normally decrease with stage size rather than having the same value for all stages.

Fig. 3 represents a different interpretation of the information pictured in Figs. 1 and 2. For any $\lambda = (W_p)/(W_p + W_s)$ we can obtain the payload to gross weight ratio for maximum payload kinetic energy. From the upper curve, ln γ for the same condition is obtained. The natural log of γ in turn yields the burnout velocity for a known exit velocity C by employing the relation $V = C \ln \gamma$.

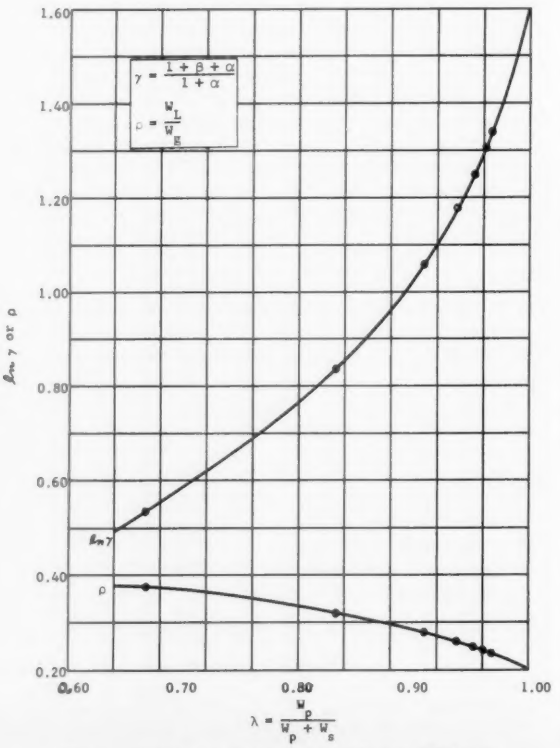

Fig. 3 Design parameters for maximum efficiency

Conclusion

A return to the classical method of machine optimization has been suggested for employement in the design of future rockets. In attempting to maximize output energy it was found that an optimum ratio of payload to structure exists for every value of the propellant ratio.

If a 50,000-lb vehicle with a β of 9 is capable of carrying a 2000-lb payload to 2000 miles, it could be more efficiently employed in carrying a 20,000-lb payload a shorter distance. If the 2000-mile range represents an important mission, then efforts should be made to raise the value of I_{sp} of the rocket, or a stage should be added to bring the performance up to the desired level.

It can be seen from Fig. 3 that the payload to gross weight ratio does not change rapidly with change in the propellant fraction λ. For reasonable values of λ, from 20 to 30 per cent of the rocket should be payload, in order to achieve high efficiency.

Frictional Electricity in Missile Systems

P. MOLMUD[1]

Space Technology Laboratories, Inc., Los Angeles, Calif.

A STUDY of frictional electricity was undertaken some time ago with the purpose of explaining some of the free charges appearing in the rocket exhaust (1).[2] During the course of the literature search many unusual phenomena were brought to light. Some of these were impressive as having some applicability to a rocket propelled missile or as occurring as a complication in the system. It is the purpose of this note to present some of these situations and their consequences. Also, some possible applications of some phenomena are pointed out. Since the theoretical foundations of the subject are not very well developed, very little can be said about the magnitudes of the effects. The answer to any question of this type must depend ultimately on experiment.

Theory

Free charges are produced under many circumstances, some of them quite surprising. For example:

1 The separation of two surfaces (splitting of mica).
2 The rise of gaseous bubbles through liquids.
3 The atomization of liquids.
4 The breaking up of a liquid stream by impact on a solid or dissimilar liquid (ordinary shower bath or waterfall).
5 The passage of a semiconducting liquid (gasoline) through a metallic pipe, and many others.

The most plausible explanation, but certainly not one which has been very well developed, is that there is an electrical double layer at the interface of the two substances. The free charges may arise from the slipping of one layer past another (as in a liquid flowing on a solid) or from the disruption of a double layer (as in a droplet being shattered by a blast of air).

The electrical double layer may form in the following different fashions:

1 Contact difference of potential.
2 Partial solution of one phase into another.
3 Thermionic emission.
4 A surface orientation of permanent dipoles, and possibly many others.

The theory of the double layer has been applied to physical chemistry problems, such as electrophoresis, electro-osmosis, etc. (2, 3), but has only been feebly applied to situations where free charge is produced (4, 5).

Received Oct. 15, 1958.
[1] Member of Technical Staff.
[2] Numbers in parentheses indicate References at end of paper.

The presentation that follows will discuss possible electrostatic effects occurring in a missile system. The discussion will be essentially qualitative and uncertain, since there are usually no a priori means of estimating the magnitudes of the effects.

The Special Situations

THE FLOW OF PROPELLANTS THROUGH PIPES It is a well-established fact that insulated conduits carrying flowing gasoline can establish high potentials with respect to ground. In some instances electrical discharges and gasoline vapor explosions occur (6). One reference (7) states that for turbulent flow of hydrocarbons carrying traces of other materials, such as moisture, tetraethyl lead, etc. through a metal pipe of sufficient length, an equilibrium is reached where the liquid carries 3×10^{-5} coulomb of negative charge per cubic meter, regardless of the rate of flow.

Consider a hypothetical missile expelling 500 lb of hydrocarbon per sec. Let us assume that the liquid is carrying away negative charge at the rate previously specified. This leaves the entire missile with positive charge increasing at the rate of 5×10^{-6} coulomb/sec.

This charge is quite apt to leak off if the missile passes through a conducting atmosphere or if sharp edges and corners of the missile can supply a high enough potential gradient for discharge into the atmosphere. Another possibility for missile charge neutralization occurs in the case where the missile passes through part of the ionosphere.

If the missile operates above the ionosphere, a charge will build up. As an example, suppose the missile operates for 100 sec in a vacuum. The net charge on it will then be of the order of 5×10^{-4} coulomb. If the missile has a surface area of 500 m^2, then the average surface charge density is 0.3 statcoulomb/cm^2 corresponding to an electric field of 1200 v/cm. This field may be considerably larger at corners and regions where the radius of curvature is quite small. If the latter is the case, then upon re-entry into the ionosphere, glow discharges may ensue.

The electrification by hydrocarbons does not always seem to be a reproducible phenomenon. Bruninghaus (8) has shown that upon repeated passage of a sample of liquid hydrocarbon through a conduit, the liquid apparently loses its ability to electrify. There was no difficulty when fresh samples were used. The interpretation was made that there is some essential ingredient in the liquid which is lost to the walls of the conduit upon repeated passage. The electrification is assumed due to the formation of an electrical double layer between the wall and the liquid and a slippage of one of the layers (in the liquid) past the wall. He states that for electrification to be possible the liquid must be very slightly conducting, to facilitate the formation of the double layer, but not too conducting, so that any charge picked up will return to the walls.

THE PASSAGE OF THE MISSILE THROUGH A MIST OR A SUSPENSION OF FINE WATER DROPLETS The violent collision between a metal surface and a liquid and the disruption of the liquid into smaller droplets results in a net charge being deposited on the metal surface. The resulting droplets also have an excesss of charge. This is a well-known phenomenon of electrification. It was made use of in 1842 by Armstrong (9) to construct an electrostatic generator with steam as the generating agent.

Banerji (4) investigated this process quantitatively and found it to be one of the most efficient methods, on an energy basis, for the production of free charges.

The effect, if any, on a missile ought to be small, and any net charge would probably be lost by mechanisms suggested in the first part of this section.

THE SPRAYING OF PROPELLANTS THROUGH THE INJECTOR The propellant is injected into the combustion chamber of the rocket engine through many small orifices usually located in an injector plate. As already suggested, the fluid may al-

ready be charged, but if it issues from the injector orifice in the form of a spray, it may acquire still more charge from this type of disruption. Should the liquid emerge from the orifice as a solid stream, it would nevertheless start to break up into a spray because of its surface tension, friction with the surrounding atmosphere and possibly because of acoustic disturbances. In addition, the presence of an electric charge on the stream or droplets issuing from the plate will cause the effluxing structure, in most cases, to be less stable to external disturbances.

Basset (10) has investigated the oscillations of a jet of viscous liquid, taking into account its surface tension and surface charge. He shows that for disturbances whose wave length is large in comparison with the jet's circumference, the charge tends to produce stability, whereas for shorter wave lengths the charge produces instability.

In a rocket engine we may expect an adequate supply of energy in the form of high frequency acoustic disturbances, so that electrification of jets or streams would enhance their instability and so promote the formation of droplets.

In addition, once droplets are formed, the surface charge they carry acts counter to their surface tension and makes them more liable to rupture. Rayleigh (11) has shown that the natural frequencies of a droplet are dependent upon its charge Q, and that when the charge bears the following relationship to the surface tension T the drop is unstable

$$Q^2 \geqq 16\pi a^3 T$$

where a is the radius of the drop (this relationship is made understandable when one considers the total energy of a drop, $\frac{1}{2} Q^2/a$, electric, and $4\pi a^2 T$, surface tension, before and after "fission").

There is no reason to suppose that sprays and droplets could not be loaded with an excess of charge to promote breakup and thus enhance the mixing of fuel and oxidizer. This type of loading has been accomplished recently in an electrostatic atomizer. The situation is described in an article by Harold Straubel (12). A liquid is held in a nozzle by surface tension. A potential difference of 10,000 v is maintained between the nozzle and a circular, circumscribing ring. The liquid is found to issue spontaneously from the nozzle in the form of a fine spray. Only liquids with permanent dipole moments are found to exhibit this behavior. The resulting droplets are highly charged, and their trajectories can be influenced by electric and magnetic fields.

The mechanism of the spray and the roles of dipole moments, surface tension and viscosity are not elucidated in this reference (12).

Impingement of Fluid Streams In the usual rocket injection system, two or more streams impinge one upon the other, forming a sheet which fluctuates and breaks up into droplets (13). As we have mentioned before, these sheets and droplets are charged (and indeed might become further charged by the impingement mechanism), and their disintegration is somehow modified by this charge. In addition to breaking up, these droplets may collide with each other (or with droplets arising from the breakup of another sheet). This may or may not be a desirable phenomenon. Whether the drops will collide with one another and coalesce may well depend on the nature and magnitude of the charge on each of the droplets.

In the last century, Rayleigh (11) made some remarkable investigations upon slowly moving jets. He found that when a vertical liquid jet breaks up into a spray, the individual drops of the spray are in constant collision, and they rebound from each other like rubber balls. However, under the influence of a weak electric field, these droplets upon colliding, coalesce, and the stream does not break up into a spray. However, upon strengthening the electric field, the droplets start again to rebound, and the stream breaks up again into a spray.

These experiments (done on slowly moving droplets, however) suggest that the mixing of fuel and oxidizer in the combustion chamber might well be influenced by static electric fields.

Since the droplets in the combustion chamber are charged, they will disintegrate as they evaporate and their radius decreases (by Rayleigh's rule and assuming no loss of charge to the surrounding atmosphere).

This disintegration might be hastened by electrical means if the drops could be made to oscillate in their fundamental modes by applied electric fields of the right frequency. However, rough calculations indicate that there is much more acoustic energy available of the right frequencies than could be made readily available by varying electric fields.

The Exhaust Passing Through the Rocket Nozzle Very rarely is there any static electrification produced by only gas impinging on a solid. Perucca (14) has claimed to observe this by using mercury vapor flowing by a copper surface. When there is electrification associated with gaseous jets, it has always been satisfactorily explained on the basis of the gas carrying particles of solids or liquids. It is the impact of these particles which produces the electrification and not the flow of gas.

A current has been observed between a solid propellant motor and ground during running (15). This type of electrification may be due to solid particles of the propellant being carried along in the jet stream and striking the walls of the nozzle.

In addition, should the walls of the exhaust section of the rocket engine get hot enough so that thermionic emission ensues, then an electrical double layer might come into being, extending into the gaseous boundary layer. If this is the case, the exhaust jet may cause slipping of the electrical layer and remove electrons from the wall. The wall would then develop an excess of positive charge.

Conclusion

In this note certain electrostatic phenomena and conjectures as to their appearance and possible utilization in a rocket missile system are pointed out. It appears as if literature research and pure thought will not tell when an effect will be produced and if produced, of what magnitude. Some simple experiments could be performed to determine the magnitude of some of these effects. For example:

1 Determination of average charge on droplets injected into combustion chamber.

2 Varying the conductivity of the propellant to determine concomitant electron density variation in the exhaust stream.

3 Electric field mapping over an insulated missile during static firing.

4 Testing the effects of an applied electric field on combustion.

Some interesting problems arise elsewhere, as: What is the effect of an electrical double layer on the boundary layer in liquid flow? Also, what is the role of the permanent dipole moment in electrostatic atomization?

References

1 Locke, A. S., "Guidance," edited by Grayson Merrill, Van Nostrand, 1955, pp. 119–124.

2 Taylor and Glasstone, "Treatise on Physical Chemistry," vol. II, Van Nostrand, 1951, p. 628.

3 "The Electrical Double Layer," *Trans. Faraday Soc.*, vol. 36, 1940.

4 Banerji, S. K., "On the Interchange of Electricity Between Solids, Liquids and Gases in Mechanical Action," *Indian J. Phys.*, 1938, p. 409.

5 Gilbert, J. W. and Shaw, P. E., "Electrical Charges Arising at a Liquid Gas Interface," *Proc. Phys. Soc.*, London, vol. 37, 1925, pp. 195–212.

6 Guest, P. G., "Static Electricity in Nature and Industry," U.S. Dept. of Commerce, Bureau of Mines Bulletin 368, 1933.

7 Silsbee, F. B., "Static Electricity," U. S. Dept. of Commerce, Nat. Bur. Standards Circular C 438, 1942.

8 Bruninghaus, L., "Electrisation et Conduction Électrique

des Hydrocarbones Liquides," *Revue Générale de L'Electricity*, vol. 26, 1929, p. 787.

9 Armstrong, W. G., "A Hydroelectric Machine," *Philosophical Magazine*, vol. 23, 1843, p. 194.

10 Basset, A. B., "Waves and Jets in a Viscous Fluid," *Amer. J. Math.*, vol. XVI, no. 1, 1892, p. 13.

11 Rayleigh, "Theory of Sound," Dover, 1945, p. 374.

12 Straubel, H., "Die Elektrostatische Zerstaubung Von Flussigkeiten," *Zeitschrift für Angewandte Physik*, vol. 6, no. 6, 1954, p. 264.

13 Heidemann, M. F. and Humphrey, J. C., "Fluctuations in a Spray Formed by Two Impinging Jets," JOURNAL OF THE AMERICAN ROCKET SOCIETY, vol. 22, no. 3, May-June 1952, p. 127.

14 Perucca, Von E., "Elektrisierung durch Reibung Zwischen Festen Körpern und Gasen," *Zeitschrift für Angewandte Physik*, vol. 34, 1925, pp. 120–130.

15 Seifert, Howard, private communication.

Interrelationship of Calculus of Variations and Ordinary Theory of Maxima and Minima for Flight Mechanics Applications

ANGELO MIELE[1]

Purdue University, Lafayette, Ind.

THE ANALYSIS of the optimum conditions of the mechanics of flight has always attracted considerable interest, in view of its implications for both vehicle design and flight operations. Historically speaking, the period ranging from the beginning of aviation up to World War II had been characterized by an extensive use of the Ordinary Theory of Maxima and Minima (5).[2] In more recent times, on the other hand, the methods of the Calculus of Variations have become increasingly familiar to the engineer engaged in the performance analysis of high speed aircraft and missiles.

It is to be noted that the sophisticated variational techniques and the simpler methods of the Ordinary Theory of Maxima and Minima have been developed along parallel, noninteracting lines. Yet, the following questions arise: What, if any, is the relationship between Calculus of Variations and Ordinary Theory of Maxima and Minima with regard to flight mechanics applications? Are there cases where the optimization on a *local* basis (i.e., with the Ordinary Theory of Maxima and Minima) and the optimization on an *integral* basis (i.e., with the Calculus of Variations) lead to identical results?

The answers to the above questions, which are important both academically and practically, is discussed in the present note. A rather general theorem is presented. This theorem, which constitutes a link between Calculus of Variations and Ordinary Theory of Maxima and Minima, has been shown to hold in a variety of particular cases[3] (2 to 5) and can be enunciated as follows: "Consider a certain minimal problem of the nonsteady mechanics of flight and write the equations of motion and the associated set of Euler equations. Next, let the acceleration terms appearing in the equations of motion decrease, tending to zero in the limit. The associated set of Euler equations modifies and, in the limit, yields a new set of Euler equations. Embodied in this limiting set of Euler equations are optimizing conditions which are *identical* with those locally supplied by the Ordinary Theory of Maxima and Minima."

While the exact range of applicability of the above theorem is still unknown to this writer, its practical importance is such that disclosure of the leading ideas is warranted. To this effect, a particular problem, namely, the maximum range problem, is analyzed in the following sections. Two different approaches are considered: The *local* one and the *integral* one.

With regard to the integral approach two alternate roads are possible: (a) to carry out the limiting process *after* writing the Euler equations for the nonsteady case; (b) to carry out the limiting process in the equations of motion *before* writing the Euler equations. These two methods are complementary and lead to *identical* results. Method (b) is shorter and, as a consequence, is adopted in the present paper. This means that, at the onset, a quasi-steady point of view is introduced in the equations of motion.

Equations of Motion

An arbitrary aircraft is considered, traveling at constant altitude over a flat Earth. The aircraft is schematized into a particle, acted upon by aerodynamic forces of symmetric type, i.e., lift (L) and drag (D). The so-called aerodynamic lag is disregarded.

A drag function of the form $D = D(h, V, L)$ is assumed, V being the velocity and h the altitude. Since the altitude is a constant and[4] $L = mg$, the D-function is rewritten as $D = D(V, m)$.

Concerning the thrust (T) and the specific fuel consumption (c), analytical relationships of the type $T = T(h, V, \alpha)$, $c = c(h, V, \alpha)$ are considered, where α is a variable controlling the engine performance and termed engine control parameter (3, 5) or thrust control parameter or power setting. Owing to the constancy of the altitude, the T-function and the c-function are rewritten as $T = T(V, \alpha)$ and $c = c(V, \alpha)$.

Thus, the behavior of the aircraft in *quasi-steady flight* is represented by the set of equations[5]

$$J_1 \equiv \dot{X} - V = 0 \qquad [1]$$

$$J_2 \equiv \dot{m} + \frac{c(V, \alpha)T(V, \alpha)}{g} = 0 \qquad [2]$$

$$J_3 \equiv T(V, \alpha) - D(V, m) = 0 \qquad [3]$$

where X denotes horizontal distance, and the dot sign derivative with respect to time (t).

Approach by the Ordinary Theory of Maxima and Minima

The range flown per unit fuel consumed (Ψ) is given by

$$\Psi = -\frac{\dot{X}}{g\dot{m}} = \frac{V}{c(V, \alpha)T(V, \alpha)} \qquad [4]$$

For a given instantaneous mass m, the *local* problem consists of maximizing $\Psi(V, \alpha)$, subject to the constraint represented by Equation [3]. By the method of the Lagrange multipliers, and within the framework of the Ordinary Theory of Maxima and Minima, the *necessary* conditions for the extremum are stated as[6]

$$\frac{\partial \Psi^*}{\partial V} = \frac{\partial \Psi^*}{\partial \alpha} = 0 \qquad [5]$$

$$\Psi^* = \frac{V}{cT} + \mu(T - D) \qquad [6]$$

Received Oct. 14, 1958.

[1] Professor of Aeronautical Engineering. Member ARS.

[2] Numbers in parentheses indicate References at end of paper.

[3] Among them: Maximum range for a given altitude, maximum endurance for a given altitude, maximum range for a given power setting, maximum endurance for a given power setting.

[4] The symbol m denotes instantaneous mass, while g indicates acceleration of gravity.

[5] For simplicity, no limitation is imposed on the modulus of the thrust.

[6] The symbol μ denotes *constant* Lagrange multiplier.

Elimination of the multiplier μ leads to the following explicit form for the optimizing condition

$$\begin{vmatrix} \frac{\partial}{\partial V}\left(\frac{V}{cT}\right) & \frac{\partial(T-D)}{\partial V} \\ V\frac{\partial}{\partial \alpha}\left(\frac{1}{cT}\right) & \frac{\partial T}{\partial \alpha} \end{vmatrix} = 0 \qquad [7]$$

Variational Approach

In the class of functions $X(t)$, $m(t)$, $V(t)$ and $\alpha(t)$ consistent with Equations [1 to 3], it is required to find the special set such that $\Delta G = G_f - G_i$ is a minimum,[7] where $G = -X$.

To this effect, a set of *variable* Lagrange multipliers $\lambda_1(t)$, $\lambda_2(t)$ and $\lambda_3(t)$ is introduced, and the Euler-Lagrange Equations (1) written as follows

$$\dot{\lambda}_1 = 0 \qquad [8]$$

$$\dot{\lambda}_2 = -\lambda_3 \frac{\partial D}{\partial m} \qquad [9]$$

$$0 = -\lambda_1 + \frac{\lambda_2}{g}\frac{\partial(cT)}{\partial V} + \lambda_3 \frac{\partial(T-D)}{\partial V} \qquad [10]$$

$$0 = \frac{\lambda_2}{g}\frac{\partial(cT)}{\partial \alpha} + \lambda_3 \frac{\partial T}{\partial \alpha} \qquad [11]$$

They admit the first integral

$$\lambda_1 V - \lambda_2 \frac{cT}{g} = C \qquad [12]$$

where C is an integration constant. The latter also appears in the general transversality condition[8]

$$[\delta G + \lambda_1 \delta X + \lambda_2 \delta m - C\delta t]_i^f = 0 \qquad [13]$$

which is to be identically satisfied for all systems of variations $\delta(\ldots.)$ consistent with the prescribed end conditions.

It is now assumed that t_i, X_i, m_i, m_f are specified, while t_f is free of choice. The transversality condition yields $C = 0$. As a consequence, nontrivial solutions exist for the Lagrange multipliers (Eqs. [10 to 12]) if, and only if

$$\begin{vmatrix} -1 & \frac{\partial(cT)}{\partial V} & \frac{\partial(T-D}{\partial V} \\ 0 & \frac{\partial(cT)}{\partial \alpha} & \frac{\partial T}{\partial \alpha} \\ V & -cT & 0 \end{vmatrix} = 0 \qquad [14]$$

Discussion

The first optimizing condition (Eq. [7]) has been deduced from a *local* point of view; the second optimizing condition (Eq. [14]) has been calculated from an *integral* point of view. Nevertheless, they are physically and mathematically *identical:* In the first place, one condition can be transformed into the other; furthermore, *both* conditions can be reduced to the equation

$$\frac{\partial \log T}{\partial \log \alpha}\left[1 - \frac{\partial \log (cD)}{\partial \log V}\right] + \frac{\partial \log c}{\partial \log \alpha}\frac{\partial \log (T/D)}{\partial \log V} = 0 \qquad [15]$$

It is, therefore, concluded that, for the quasi-steady maximum range problem, the Ordinary Theory of Maxima and Minima and the Calculus of Variations lead to *identical* results.

Particular Cases

For an ideal engine, such that $\partial c/\partial \alpha \cong 0$, $\partial T/\partial \alpha \neq 0$, Equation [15] reduces to

$$\frac{\partial \log (cD)}{\partial \log V} = 1 \qquad [16]$$

implying that, for $\partial \log c/\partial \log V = 0$

$$\frac{\partial \log D}{\partial \log V} = 1 \qquad [17]$$

and that, for $\partial \log c/\partial \log V = 1$

$$\frac{\partial \log D}{\partial \log V} = 0 \qquad [18]$$

Equation [17] approximates the behavior of a turbojet aircraft at low subsonic speeds, whereas [18] approximates the behavior of a piston-engined aircraft. Notice that, for a parabolic drag polar with coefficients independent of the Mach number, Equations [17 and 18] respectively yield the well-known solutions[9] $R = 1/3$ and $R = 1$.

Conclusions

The maximum range problem for constant altitude flight is analyzed from a quasi-steady point of view. It is shown that the optimizing condition *locally* computed with the Ordinary Theory of Maxima and Minima is *identical* with the optimizing condition *integrally* derived via Calculus of Variations.

The above result is only a special case of a rather general theorem (see introduction), which also holds in a variety of other minimal problems where the acceleration terms may be neglected, such as: Maximum range for a given power setting, maximum endurance for a given altitude, and maximum endurance for a given power setting (2 to 5). The exact limits of applicability of the above theorem, however, have not yet been established by the writer.

Clearly, the above theorem has little value for a rocket powered vehicle, in view of the importance of the acceleration terms at all points of the flight trajectory. The same theorem, on the contrary, is important for aircraft propelled by air-breathing engines and—in particular—for turbojet powered aircraft which will dominate the next 10 years of commercial air transportation. In fact, for these aircraft, there are several flight conditions (e.g., range, endurance) such that the neglect of the acceleration terms is justifiable on physical grounds. It is, therefore, stressed that the Ordinary Theory of Maxima and Minima is still a valuable (and far from useless) device for flight mechanics applications.

References

1 Bliss, G. A., "Lectures on the Calculus of Variations," The University of Chicago Press, Chicago, 1946.

2 Miele, A., "Variational Approach to the Stratospheric Cruise of a Turbo-jet Powered Aircraft," *Zeitschrift für Flugwissenschaften*, Sept. 1958, vol. 6, no. 9, pp. 253–257.

3 Miele, A., "Lagrange Multipliers and Quasi-Steady Flight Mechanics," Purdue University, School of Aeronautical Engineering, Report no. A-58-4, May 1958.

4 Miele, A., "Minimal Manoeuvres of High Performance Aircraft in a Vertical Plane," Purdue University, School of Aeronautical Engineering, Report no. A-58-3, May 1958.

5 Miele, A., "Some Recent Advances in the Mechanics of Terrestrial Flight," JET PROPULSION, Sept. 1958, vol. 28, no. 9, pp. 581–587.

[7] In the variational terminology, the above problem is called a Mayer problem.

[8] Subscript i denotes initial point; subscript f refers to final point.

[9] The symbol $R = D_i/D_0$ denotes ratio of induced drag (D_i) to zero-lift drag (D_0).

New Patents

George F. McLaughlin, *Contributor*

Vibration testing device (2,851,877). I. L. Joy, Topeka, Kans.

System of sending short time vibrational waves into a body and detecting vibrational energy reflected from discontinuities in the body.

Orientation control for a space vehicle (2,856,142). R. P. Haviland, Schenectady, N. Y., assignor to General Electric Co.

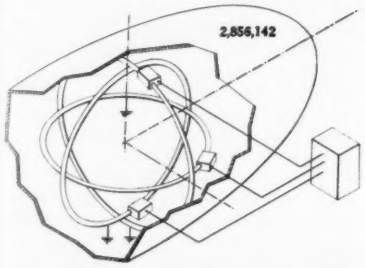

Means for displacing weighted materials at a controllable rate, and in desired directions within a craft to produce control torques. The torques are produced independently of the absence or presence of a fluid medium outside the craft.

Method for telemetering information from a missile in flight (2,852,208). C. H. Schlesman, Washington, D. C.

Signal, generated and transmitted from a rotating missile, which varies in magnitude in accordance with changes in declination angle. Means at the launching point for receiving the signal and firing a steering charge at any desired rotational position of the missile.

Magnetic accelerometer (2,852,243). E. S. Shepard Sr., Phoenix, Ariz., assignor to The Garrett Corp.

Device for sensing acceleration of a body consisting of three magnets each having opposite poles, two fixed to the body, and the third spaced between them. An electrical output from means associated with the magnets is representative of the position of the free magnet in relation to one or the other fixed magnet.

Ramjet fuel control having a main and probe diffuser (2,855,753). G. H. McLafferty, Manchester, Conn., assignor to United Aircraft Corp.

Pair of diffusers with similar fluid flow characteristics and producing similar Mach numbers. The combustion chamber receives air from one of the diffusers, and the other diffuser controls fuel flow.

Gyroscopic apparatus (2,855,782). L. R. Grohe, Hingham, Mass., assignor to Research Corp.

Static weight adjusting member on a shaft projecting through the case. The shaft may be bent to change the relative position of the weight and the gimbal after the device has been assembled.

Vertical velocity meter (2,856,772). L. F. Strihafka, West Hempstead, N. Y., assignor to Sperry Rand Corp.

Gyroscopic rate of climb measuring device including an acceleration responsive means deriving from a signal in accordance with the vertical velocity of the craft.

Liquid contents gaging means for liquid oxygen containers (2,856,773). A. T. Gellos, Flushing, N. Y., assignor to Liquidometer Corp.

Metallic container having an opening for receiving a liquid sensing means A complementary plug is screwed into the opening to effect a pressure-tight seal.

Method and apparatus for telemetering information from a missile in flight (2,852,208). C. H. Schlesman, Washington, D. C.

Means for generating and transmitting a signal which varies in magnitude in accordance with changes in declination angle of the missile. A steering charge in one side of the missile may be fired at any desired rotational position of the missile when the declination angle reaches a predetermined value.

Angle of attack and yaw indicating apparatus (2,855,779). M. Zaid, Levittown, N. Y., assignor to Bulova Research and Development Laboratories, Inc.

Apparatus for indicating the direction of a strain-producing force comprising a sensing sphere surrounding and fixed to one end of a boom. The boom is stressed in accordance with an impinging wind force and coupled to strain gages to measure the differential values of the indications.

Range-height parallel-type radar system (2,859,438). R. H. Reed, Los Angeles, Calif., assignor to Hughes Aircraft Co.

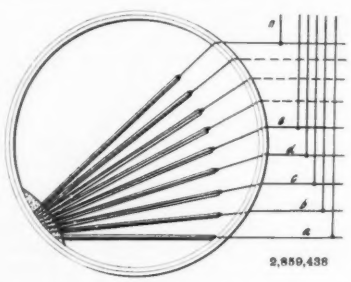

Radar system radiating an exploratory microwave pulse over a broad angle. Electron beams are deflected over fluorescent strips in synchronism with the pulse

Airplane design (183,675). L. F. Begin Jr., W. E. Gasich, G. L. Gluyas, R. B. Katkov, A. Nitikman and A. M. Ogness, Rolling Hills, Calif., assignors to Northop Aircraft, Inc.

Aerodyne (2,859,003). L. Servanty, Paris, France, assignor to Societé Nationale de Constructions Aeronautiques du Sud-Ouest.

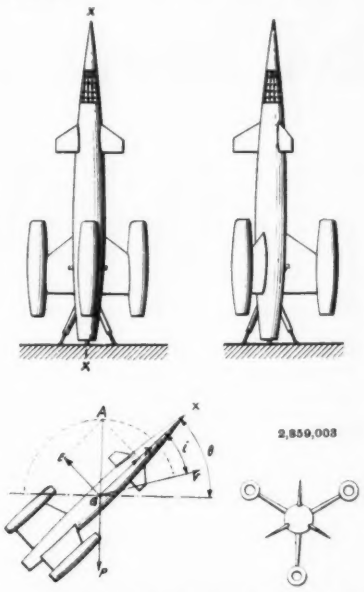

Elongated fuselage with three adjustable airfoils angularly spaced and pivotally mounted about radial axis. A reaction jet is fixed at the tip of each airfoil for orientation of its main axis in a plane parallel to the fuselage longitudinal axis.

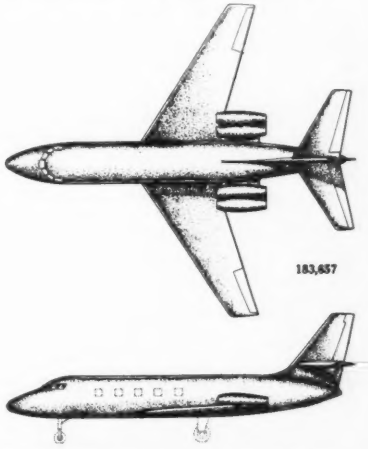

Airplane design (183,657). C. L. Johnson and W. H. Statler, Northridge, Calif., assignors to Lockheed Aircraft Corp.

Missile or mine launcher (2,858,737). A. J. Tolomeo, Stratford, Conn., assignor to the U. S. Navy.

Structure located in an aircraft including a shaft supporting a missile external of the aircraft. The shaft is manually rotatable by means of a worm gear.

Thrust reversing device for jet engines (2,858,669). S. P. Compton, San Diego, Calif., assignor to The Ryan Aeronautical Co.

A diverter cone axially slidable in the

EDITOR'S NOTE: Patents listed above were selected from the Official Gazette of the U.S. Patent Office. Printed copies of patents may be obtained from the Commissioner of Patents, Washington 25, D. C., at a cost of 25 cents each; design patents, 10 cents.

tail pipe and having lateral openings and vanes in each opening. When in forward position, the diverter cone blocks the tail pipe so exhaust gases are diverted through the openings.

Reaction propulsion method (2,857,736). D. R. Carmody and A. Zietz, Park Forest, Ill., assignors to Standard Oil Co. of Indiana.

Method of injecting into the combustion chamber of a rocket motor a nitric acid oxidizer which contains not more than 10 weight per cent of nonacidic materials and a fuel consisting of monoalkylphosphines, dialkylphosphines and trialkylphosphines.

Method of rocket propulsion (2,857,737). D. R. Carmody and A. Zletz, Park Forest, Ill., assignors to Standard Oil Co. of Indiana.

Propulsion method comprising injecting into the combustion chamber a nitric acid oxidizer of white fuming nitric acid and a liquid rocket fuel in an amount and at a rate sufficient to initiate a hypergolic reaction and support fuel combustion. The method is operable at temperatures lower than −100 deg. F.

Book Reviews

Ali Bulent Cambel, Northwestern University, *Associate Editor*

Rocket, by Air Chief Marshall Sir Philip Joubert de la Ferté, Philosophical Library, Inc., New York, 1957, 190 pp. $6.00.

Reviewed by ANDREW G. HALEY
AMERICAN ROCKET SOCIETY

I am amazed that this unique contribution to astronautics has not received wider attention in the American press, and I am even more amazed that the scientists and engineers working in the field of rocketry and other aspects of astronautics have not known of this book. Air Chief Marshal Sir Philip Joubert de la Ferté has made a most honest contribution, and despite his acknowledgments the book is one hundred per cent Joubert and a rare piece of source material for the student of astronautics.

We will pass over the excellent history of rocketry and proceed directly to a few of the Joubert rarities. Among the first of these is his quizzical and not at all unfriendly evaluation of the rise and triumph of Maj. Gen. Walter Dornberger. In typical Joubert style, he reviews the early background of Dornberger with refreshing frankness, and, slowly but surely, he brings the indifferent officer from his undistinguished junior career into final focus as a brilliant rocket engineer and administrator. Many of us in America have known Dornberger in this latter status and capacity. He also shows a cynical admiration for Dr. Wernher von Braun which finally develops into full-blown admiration for von Braun as a capable and successful engineer and scientist who actually was responsible for the success of the V2.

I have just discussed some spectacular personalities in "Rocket" by Joubert, but far more fascinating episodes are centered around the artists of photographic reconnaissance. One can become absolutely fascinated with the advent and growth of Sgt. Laws of the R.E. and R.F.C. Joubert abruptly brings Laws into the chapter, "Photographic Reconnaissance," and on page 29 he states that the first airship survey took place in 1912 by Sgt. Laws and that "this event must be regarded as the birth of photographic reconnaissance from the air." Laws then turned his attention to photography from airplanes and, on a ceremonial occasion, stumbled upon one of the outstanding aspects of his art. It seems that Laws then became enamored of aerial photography. For the next 50 pages we trace the career of Laws up through the ranks—but we never finally discover whether he became an Air Vice Marshal or simply squandered away his military credit in a more junior capacity.

Laws is not the only unheralded hero whose career Joubert immortalizes for the first time. There are others, male and female. Only the true rocketeer will really understand the great spirit of this book.

No other author has so vividly and in such detail described the V1 and V2 launching problems and operational sequences. As these are matters of description and of detail, the book must be read in its entirety to appreciate the fine brush of the author. The author philosophizes and seems to combine in a salty British militarist the less briny characteristics of an essentially kindly person and the realist who appreciates the problems of humanity. This book belongs in the collection of every rocket man.

Mechanical Vibrations, by A. H. Church, John Wiley and Sons, Inc. New York, 1955, 490 pp. $6.75.

Reviewed by RALPH BURTON
University of Missouri

This presents a more rigorous and extensive coverage of mechanical vibration than did the author's earlier book, "Elementary Mechanical Vibrations," (Pitman Publishing Corp.). Nevertheless, it is primarily aimed at the undergraduate engineering student and makes no pretension toward an exhaustive coverage of the field. Such a book is primarily justified by the belief that the student can master basic principles best in a clear and uncluttered form and can later turn to harder books to complete his knowledge—perhaps by self study. In preparing such a book, the author is governed by what he thinks an introductory student can learn well in a semester and selects his material accordingly. Undoubtedly he will omit some people's favorite topics.

Church has built his text around the straightforward analysis of linear mechanical systems. He begins with the concept of harmonic motion, and the representation of this in terms of complex variables. He proceeds to a discussion of undamped free vibration, damped free vibration and forced vibration with one degree of freedom. Following this he deals with two degrees of freedom, multimass torsional systems and multimass transverse systems, introducing the Holzer method, Rayleigh's method and Stodola's method. He then concludes with a chapter on balancing and an introduction to electrical analogs. He has included over 200 problems and has worked a number of examples into the text. Many useful touches, such as the discussion of "commercial isolators" and a chart showing the working range for several instruments add value to the text.

I feel that the student should have no difficulty following the discussion or the derivations, and I think that the coverage chosen for him will go a long way toward filling his needs.

Fluid Mechanics for Engineers, by P. S. Barna, Butterworth and Co., Toronto, Canada, 1957, x + 377 pp. $11.50.

Reviewed by R. C. BINDER
Purdue University

The author is a senior lecturer in mechanical engineering at the New South Wales University of Technology, at Sydney, Australia. The author states that the text was planned primarily to provide in one volume adequate coverage for undergraduates studying for a degree or diploma in mechanical or civil engineering. The author also states that emphasis is laid upon the broad representation of the fundamentals, leaving certain topics not included in the text for the choice of individual teachers.

The book is divided into three parts. Part 1 has chapters on fluid statics, perfect fluids in motion, viscous fluids in motion, flow in closed conduits, flow in open channels, fluid metering, dimensional analysis of fluid flow phenomena, boundary layer theory and elements of wing theory. Part 2 is a single chapter on the fundamentals of the flow of compressible fluids. Part 3 has chapters on centrifugal pumps and fans, axial flow pumps and fans, and hydraulic turbines. A large number of examples with solutions are included. The treatment of the topics follows pretty much the pattern found in various other texts. What looks new is the author's particular sequence or organization of topics and his selection of topics.

Apparently the book was intended solely as an undergraduate text, and not as a reference work. Some teachers may feel that the large number of examples have occupied so much space that there has been a sacrifice of other material. Various teachers may question the author's claim that the book has adequate coverage for undergraduate students. It may be possible that the text serves adequately the needs in some curricula as, for example, one in civil engineering. In various other

undergraduate curricula, however, attention is being devoted to the education of such workers as the scientist-engineer; in such cases, judging by the courses now given and the material covered, many teachers indicate that this book alone would not provide adequate coverage.

1958 Heat Transfer and Fluid Mechanics Institute, A. K. Oppenheim, chairman, Stanford University Press, Stanford, Calif., 1958, viii + 264 pp. $8.50.

Reviewed by JAMES J. KAUZLARICH
Worcester Polytechnic Institute

The "1958 Heat Transfer and Fluid Mechanics Institute" is a preprint of the papers presented at the Institute meeting which was held at the University of California, Berkeley campus on June 19–21, 1958. It is stated in the preface that one of the main purposes of the Institute is to provide an opportunity for authoritative discussion of fundamental ideas at an early stage of their development. Thus, this publication derives its greatest importance in that it is a preprint and was made available before the Institute meeting. The papers to be published subsequent to the meeting will have benefited by the discussions that followed presentation. The contents of the preprint are listed at the end with an alternate publication source where available.

All of the papers in the preprint are highly specialized. Although the papers suffer from abridgment, papers in a particular field well-known to a reader are sufficiently detailed. Unfortunately, a number of typographical errors have crept into the preprint, usually in equations. Also, the legibility of equations is poor in some cases.

At least half of the papers in the preprint are directly or indirectly concerned with aerodynamic heating. The paper by Scala and Sutton on a study of surface melting is particularly interesting. In the discussion following the presentation of the paper at the Institute meeting, it was pointed out that the melted material from the nose area of a blunt nosed hypersonic vehicle will flow in the form of rivulets due to surface tension. Observation of the melting of a blunt nosed body showed that the rivulets of melted material oscillate, so that melting is fairly uniform back of the nose area.

A supplement to the paper by Hartnett and Eckert was presented at the Institute meeting in which the effect of gas injection on laminar boundary layer stability was studied experimentally. The study was under the direction of C. Scott and presented by G. Anderson, both at the University of Minnesota, Rosemount Laboratory. The experimental model was a 16 deg hollow, porous wall cone of 4 in. base diameter and $14^1/_2$ in. slant height. Observed transition Reynolds numbers vs. injection rate showed that, although the transition Reynolds number does decrease with increased injection (more for helium than for air injection), the percentage decreases are not large for injection rates which produce large cooling effects.

Three papers in the relatively new field of magnetohydrodynamics are published

How a creative engineer can grow with IBM

"Certainly my present assignment on the B-70 offers many growth opportunities," says Project Engineer Edward V. Zaucha. Designed to fly farther, faster and higher than any manned aircraft ever has before, the B-70 requires a completely new radar display system. "My responsibility includes the design of new cathode ray tube circuits plus system studies dealing with specific bomb-nav problems. These studies cover related equipment, such as the search radar and circuit indicator devices. In addition, I coordinate the development of storage tubes, high voltage power supplies and other equipment. A job that covers this much territory is a creative challenge. With IBM I have the opportunity to use all of my training; and in addition, I learn new things every day that will advance my engineering career."

Career opportunities in these areas . . .

- **Airborne digital & analog computers**
- **Ground support equipment**
- **Inertial guidance & missile systems**
- **Information and network theory**
- **Magnetic engineering**
- **Maintainability engineering**
- **Optics**
- **Radar electronics & systems**
- **Servomechanism design & analysis**
- **Theoretical design & analysis**
- **Transistor circuits**

Qualifications: B.S., M.S. or Ph.D. in Electrical or Mechanical Engineering, Physics, or Mathematics, and proven ability to assume a high degree of technical responsibility in your sphere of interest.

IBM is a recognized leader in the rapidly expanding electronic computer field. Its products are used for both commercial and military applications. Continuous growth means excellent advancement opportunities. The "small-group" approach assures recognition of individual merit. IBM provides excellent company benefits and salaries are commensurate with your abilities and experience.

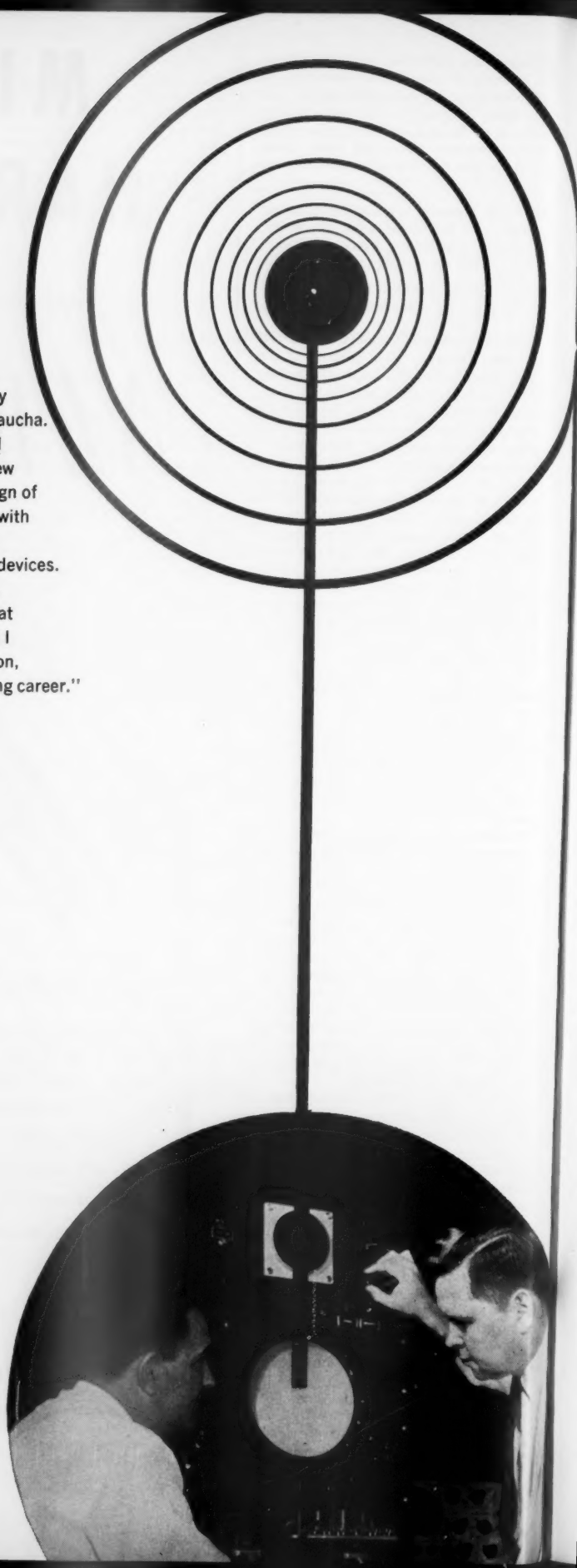

in the preprint. A number of interesting possibilities are discussed in these papers; however, it appears that any significant application to aerodynamics using magnetic fields for beneficial effects where plasma is encountered will depend on some method of substantially increasing the electrical conductivity of the plasma.

In addition to the preprint papers, an invited paper entitled "Combustion" by Wilhelm Jost, University of Göttingen, West Germany, was presented at the Institute meeting, but has not been published as yet.

Contents: 1 "Theoretical Aerothermodynamics,"* Howard W. Emmons; 2 "Effect of a Contraction on Turbulence and Temperature Fluctuations,"* R. R. Mills Jr. and S. Corrsin; 3 "Experimental Investigation of Turbulent Pipe Flow with Coolant Injection,"* S. W. Yuan and A. Barazotti; 4 "An Analysis of the Energy Separation in Laminar and Turbulent Compressible Vortex Flows," Robert G. Deissler and Morris Perlmutter; 5 "Mass Transfer Cooling With Combustion in a Laminar Boundary Layer," J. P. Hartnett and E. R. G. Eckert; 6 "Considerations Related to the Quenching of Flames With Simple Kinetics," Melvin Gerstein and A. E. Potter Jr.; 7 "Wave Propagation in a Reacting Mixture," Boa-Teh Chu; 8 "Criteria for Thermodynamic Equilibrium in Gas Flow," Morton Rudin (Lockheed Aircraft Corp., LMSD 2920); 9 "Compressible Couette Flow With Diffusion of a Reactive Gas From a Decomposing Wall," Eldon L. Knuth (University of California, Report C57-78); 10 "Boundary-Layer Transitions and Heat Transfer in Shock Tubes,"* R. Hartunian, A. Russo and P. Marrone; 11 "Heat Transfer and Friction in Swirling Turbulent Flow,"* Frank Krieth and David Margolis (Thesis of D. Margolis, Lehigh University, 1957); 12 "Turbulent Heat Transfer on Highly Cooled Blunt Nosed Bodies of Revolution in Dissociated Air, "Peter H. Rose, Mac C. Adams and Ronald F. Probstein; 13 "Natural Convection Heat Transfer in Liquids Confined by Two Horizontal Plates and Heated From Below,"* Samuel Globe and David Dropkin; 14 "Drag of a Sphere Moving in a Conducting Fluid in the Presence of a Magnetic Field," K. P. Chopra and S. F. Singer; 15 "On a Class of Magnetic Laminar Boundary Layers,"* Paul S. Lykoudis; 16 "Exploratory Studies of a Spiked Body for Hypersonic Flight," S. M. Bogdonoff and I. E. Vas (Princeton University, Report no. 412); 17 "Results From Aerodynamic Studies of Blunt Bodies in Hypersonic Flows of Partially Dissociated Air," A. J. Vitale, E. M. Kaegi, N. S. Diaconis and W. R. Warren; 18 "The Laminar Hypersonic Heat Transfer on a Blunt Body According to the Integral Method," Paul A. Libby; 19 "The Two-Phase Hypersonic Laminar Boundary Layer—A Study of Surface Melting," S. M. Scala and G. Sutton (*J. Aeron. Sci.*, vol. 25, no. 1, 1958, p. 29); 20 "Thermal Analysis of Stagnation Regions With Emphasis on Heat Sustaining Nose Shapes at Hypersonic Speeds,"* A. J. Hanawalt, A. H. Blessing and C. M. Schmidt; 21 "Magnetohydrodynamics," Rolf K. Landshoff.

* Authors intend to publish elsewhere.

Technical Literature Digest

M. H. Smith, *Associate Editor*, and **M. H. Fisher**, *Contributor*
The James Forrestal Research Center, Princeton University

Heat Transfer and Fluid Flow

Differential Methods for the Calculation of Temperature Equalizing Processes in One-dimensional Heat Flow in Simple and Complex Bodies, by H. Schuk, *VDI-Forschungsheft*, no. 459, 1957.

Heat Transfer to Surfaces in the Neighborhood of Protuberances in Hypersonic Flow, by M. H. Bloom and Adrian Pallone, *USAF WADC TN* 57-95 (*ASTIA AD* 118138), Aug. 1957.

Stationary Wall Temperatures of Bodies Undergoing Aerodynamic Heating at Mach Numbers of 1 to 10 and at Altitudes up to 30 Kilometers, by H. G. L. Krause and M. E. Kubler, *Forschungsinstitut fur Physik der Strahlantriebe Mitteil.* 7, Oct. 1957, 138 pp.

A Simple Model of the Nonequilibrium Dissociation of a Gas in Couette and Boundary Layer Flow, by J. E. B roadwell, *Douglas Aircraft Co., Rep.* SM-22888, Aug. 1957. 62 pp.

Heat Transfer and Recovery Temperatures on a Sphere with Laminar, Transitional and Turbulent Boundary Layers at Mach Numbers of 2.00 and 4.15, by I. E. Beckwith and J. J. Gallagher, *NACA TN* 4125, Dec. 1957, 59 pp.

Heat Transfer in a Laminar Boundary Layer from a Surface Having a Temperature Distribution, by B. N. Pridmore Brown, *J. Aeron. Sci.*, vol. 24, Dec. 1957, pp. 912–913.

The Stability of Binary Boundary Layers, by E. E. Covert, *Mass. Inst. Tech. Nav. Supersonic Lab., TR* 217, June 30, 1957, 30 pp. (*AFOSR TN* 57–200; *AD* 126497).

Effects of Leading-edge Blunting on the Local Heat Transfer and Pressure Distributions over Flat Plates in Supersonic Flow, by M. O. Creager, *NACA TN* 4142, Dec. 1957, 54 pp.

Heat Transfer and Boundary-layer Transition on Two Blunt Bodies at Mach Number 3.12, by N. S. Diaconis, R. J. Wisniewski and J. R. Jack, *NACA TN* 4099, Oct. 1957, 31 pp.

Heat Transfer Measurements on Two Bodies of Revolution at a Mach Number of 3.12, by J. R. Jack and N. S. Diaconis, *NACA TN* 3776, Oct. 1956, 36 pp.

Effects of Extreme Surface Cooling on Boundary-layer Transition, by John R. Jack, Richard J. Wisniewski and N. S. Diaconis, *NACA TN* 4094, Oct. 1957, 19 pp.

Influence of Turbulence on Transfer of Heat from Cylinders, by J. Kestin, and P. F. Maeder, *NACA TN* 4018, Oct. 1957, 78 pp.

Effect of Externally Generated Vorticity on Laminar Heat Transfer, by Richard M. Mark, *J. Aeron. Sci.*, vol 24, Dec. 1957, pp. 923–924.

Equations, Tables and Figures for Use in the Analysis of Helium Flow at Supersonic and Hypersonic Speeds, by James N. Mueller, *NACA TN* 4063, Sept. 1957 178 pp.

An Approximate Solution of the Hypersonic Laminar Boundary-layer Equations and Its Application, by Tosimitu Nagakura and Humio Naruse, *J. Phys. Soc. Japan*, vol. 12, Nov. 1957, pp. 1298–1304.

Laminar Boundary Layer with Heat Transfer on a Cone at Angle of Attack in a Supersonic Stream, by E. Reshotko, *NACA TN* 4152, Dec. 1957, 64 pp.

Approximate Calculation of the Compressible Turbulent Boundary Layer with Heat Transfer and Arbitrary Pressure Gradient, by E. Reshotko and M. Tucker, *NACA TN* 4154, Dec. 1957, 34 pp.

Application of Gortler's Series Method to the Boundary Layer Energy Equation, by E. M. Sparrow, *J. Aeron. Sci.*, vol. 24, Jan. 1958, pp. 71–72.

The Hydrodynamics and Heat Conduction of a Melting Surface, by George W. Sutton, *J. Aeron. Sci.*, vol. 25, Jan. 1958, pp. 29–32.

Experiments on Boundary-layer Transition at Supersonic Speeds, by E. R. Van Driest and J. Christopher Boison, *J. Aeron. Sci.*, vol 24, Dec. 1957, pp 885–889.

The Effects of Molecular Vibration on Recovery Temperature in Plane Couette Flow, by Hsun-Tiao Yang, *J. Aeron. Sci.*, vol. 24, Dec. 1957, pp. 911–912.

Note on "Dissociation Effects in Hypersonic Viscous Flows," by Denis Zigrang, *J. Aeron. Sci.*, vol. 24, Dec. 1957, pp. 916–917.

Film Boiling of Flowing Subcooled Liquids, by E. I. Motte and L. A. Bromley, *Ind. & Engng. Chem.*, vol. 49, Nov. 1957, pp. 1921–1926.

A Rapid Analytical Method for Calculating the Early Transient Temperature in a Composite Slab, by W. F. Campbell, *Trans. Engng. Inst. of Canada*, no. 1, Sept. 1957, pp. 16–21.

On a Problem of Heat Conduction with Time-dependent Boundary Conditions, by T. S. Chow, *Zeitschrift für Angewandte Mathematik und Physik*, vol. 8, 1957, pp. 478–481.

A Method of Computing the Transient Temperature of Thick Walls from Arbitrary Variation of Adiabatic-wall Temperature and Heat-transfer Coefficient, by P. R. Hill, *NACA TN* 4105, Oct. 1957, 54 pp.

Electrical Analogy for Transient Axisymmetrical Heat Flow, by J. S. Przemieniecki, *J. Aeron. Sci.*, vol. 24, Dec. 1957 pp. 922–923.

One-dimensional Transient Heat Conduction into a Double-layer Slab Subjected to a Linear Heat Input for a Small Time Interval, by B. Wassermann, *J. Aeron. Sci.*, vol. 24, Dec. 1957, pp. 924–925.

Optical Pyrometry below Red Heat, by Michael M. Benarie, *J. Optical Soc. Amer.*, vol. 47, Nov. 1957, pp. 1005–1012.

Some Further Results on the Rubber Membrane Theory and Laplace's Equation, by W. Fulop, *J. Sci. Instr.*, vol. 34, Nov. 1957, pp. 453–457.

The Plasma Jet and Its Application, by G. M. Giannini, *Giannini Res. Lab. Rep.*, Aug. 2, 1957, 30 pp. (*ASTIA AD* 136508; *AFOSR TN* 57–520).

EDITOR'S NOTE: Contributions from Professors E. R. G. Eckert, J. P. Hartnett, T. F. Irvine Jr. and P. J. Schneider of the Heat Transfer Laboratory, University of Minnesota, are gratefully acknowledged.

Measurement of Temperature at High Pressure by Radiation and Certain Optical Effects in Gases, by A. Kalashnikov and L. F. Vereshchagin, *Sov. Phys. Tech. Phys.* no. 8, 1957, pp. 1749–1757.

Investigation of Heat Transfer from a Stationary and Rotating Conical Forebody, by Robert S. Ruggeri and James P. Lewis, *NACA TN* 4093, Oct. 1957, 30 pp.

Method for Determining Thermal Conductivity at High Temperatures, by C. L. Longmire, *Rev. Sci. Instr.*, vol. 28, Nov. 1957, pp. 904–906.

On Almost Rigid Rotations, by K. Stewartson, *J. Fluid Mech.*, vol. 2, Oct. 1957, pp. 17–22.

Thermal Conductivity of Technical Materials at Low Temperatures, by N. V. Zavaritskii and A. G. Zel'dovich. *Sov. Phys. Tech. Phys.*, no. 9, 1957, pp. 1970–1978.

Laminar and Turbulent Mixing of Jets of Compressible Fluid—1. Flow Far from Orifice, by L. J. Crane and D. C. Pack, *J. Fluid Mech.*, vol. 2, July 1957, pp. 449–454.

A Modified Pohlhausen Method for Solution of Laminar Boundary Layers, Part II—Compressible Flow with Zero Heat Transfer, by N. Curle, *Natl. Phys. Lab.*, June 17, 1957, 14 pp. (*ARC* 19, 342; *FM* 2554; *NACA* 57640, pt. 2).

Theory of Stagnation Point Heat Transfer in Dissociated Air, by J. A. Fay and F. R. Riddell, *J. Aeron. Sci.*, vol. 25, no. 2, Feb. 1958, pp. 73–81.

Approximate Calculations of the Laminar Boundary Layer with Suction, with Particular Reference to the Suction Requirements for Boundary Layer Stability on Aerofoils of Different Thickness/Chord Ratios, by M. R. Head, *ARC* 19, 519; *FM* 2582, Sept. 10, 1957, 31 pp. (*NACA N*-57724).

A Simple Derivation of Lighthill's Heat Transfer Formula, by H. W. Liepmann, *J. Fluid Mech.*, Pt. 4, Jan. 1958, pp. 357–360.

Stagnation Point Heat-transfer Measurements in Dissociated Air, by P. H. Rose and W. I. Stark, *J. Aeron. Sci.*, vol. 25, no. 2, Feb. 1958, pp. 86–92.

Heat Transfer Between a Flat Plate and a Fluid Containing Heat Sources, by I. R. Whiteman, *Trans. ASME*, vol. 80, no. 2, Feb. 1958, pp. 360–362.

Symposium on High Pressure, *Ind. & Engng. Chem.*, vol. 49, no. 12, Dec. 1957, pp. 1945–2050.

Two-phase Flow in Rough Tubes, by D. Chisholm and A. D. K. Laird. *Trans. ASME*, vol. 80, no. 2, Feb. 1958, pp. 276–286.

Heat Transfer to Subsaturated Water, Dry Air and Hydrogen in Turbulent Flow Inside a Tube, by Irving Granet, *J. American Soc. Naval Engrs.*, vol. 69, Nov. 1957, pp. 787–795.

Flow and Heat Transfer in Falling Films, by H. W. Hahnemann, *VDI-Zeitschr.* 100, 1958, pp. 60–61 (in German).

Some Characteristics of the Flow of a Two-phase Mixture in a Horizontal Pipe, by L. I. Krasiakova, translated by P. Collins from Zhur. Tekh. Fiz. 22, 654–669, 1952, 19 pp., AERE-Lib/Trans-695.

Heat Transfer "Beyond Burnout" for Forced-convection Bulk Boiling, by L. H. McEwen, J. M. Batch, D. J. Foley and M. R. Kreiter, *ASME, Paper* 57-SA-49, June 9–13, 1957, 6 pp.

Film Boiling of Flow Subcooled Liquids, by E. E. Motte and L. A. Bromley, *Ind. & Engng. Chem.*, vol. 49, Nov. 1957. pp. 1921–1928.

On the Correlation of Data in Nucleate Pool Boiling from a Horizontal Surface, by Novak Zuber, *J. AIChE* vol. 3, no. 3, Sept. 1957, pp. 95–103.

A Theoretical Study of Stability in Water Flow through Heated Passages, by H. Chilton, *J. Nuclear Energy*, vol. 5, nos. 3–4, 1957, pp. 273–284.

Heat Transfer in Fully Developed Flow between Parallel Plates with Variable Heat Sources, by Albert L. Loeffler Jr., *Nuclear Sci. & Engng.*, vol. 2, Sept. 1957, pp. 547–567.

The Heat-balance Integral and Its Application to Problems Involving a Change of Phase, by T. R. Goodman, *Trans. ASME*, vol. 80, no. 2, Feb. 1958, pp. 335–342.

Hydrodynamics and Heat Conduction of Melting Surface, by R. W. Sutton, *J. Aeron. Sci.*, vol. 25, no. 1, Jan. 1958, pp. 29–32, 36

Heat Transfer and Fluid Friction During Flow Across Banks of Tubes, VI, by O. P. Bergelin, K. J. Bell and M. D. Deighton, *Trans. ASME*, vol. 80, no. 1, Jan. 1958, pp. 53–60.

Convection Heat Transfer and Pressure Drop of Air Flowing Across In-line Tube Banks, II, by A. J. Gram, C. O. Mackey and E. S. Monroe Jr., *Trans. ASME*, vol. 80, no. 1, Jan. 1958, pp. 25–35.

Pressure Drop for Parallel Flow through Rod Bundles, by B. W. LeTourneau, R. E. Grimble and J. E. Zerbe, *Trans. ASME*, vol. 79, Nov. 1957, pp. 1751–1758.

Measurements of High Temperatures in Strong Shock Waves in Gases, by I. Sh. Model', *Soviet Physics JETP*, vol. 5, no. 4, Nov. 1957, pp. 589–593.

Heat-transfer Characteristics of the Rotational and Axial Flow between Concentric Cylinders, by C. Gazley Jr., *Trans. ASME*, vol. 80, no. 1, Jan. 1958, pp. 79–90.

Heat Transfer from a Rotating Cylinder with and without Crossflow, by W. M. Kays and I. S. Bjorklund, *Trans. ASME*, vol. 80, no. 1, Jan. 1958, pp. 70–78.

Transient Free Convection from a Vertical Flat Plate, by Robert Siegel, *Trans. ASME*, vol. 80, no. 2, Feb. 1958, pp. 347–359.

Measurements of the Total Absorptivity for Solar Radiation of Several Engineering Materials, by E. C. Birkebak and J. P. Hartnett, *Trans. ASME*, vol. 80, no. 2, Feb. 1958, pp. 373–378.

Thermal Radiation from an Anisotropic Medium, by F. V. Bunkin, *Soviet Physics JETP*, vol. 5, no. 4, Nov.1957, pp. 661–668.

Measurement of Heating of Skin during Exposure to Infrared Radiation, by E. Hendler, R. Crosbie and J. D. Hardy, *ASME, Paper* 57-SA-33, June 9–13, 1957, 8 pp.

Heat Transfer by Radiation from Flames, a Summary of the Work of the International Flame Research Foundation, by R. A. Sherman, *Trans. ASME*, vol.79, Nov. 1957. p. 1727–1741.

A Model Method for Determining Geometric Factors in Solid-to-solid Radiation Heat Transfer, by P. L. Tea Jr., and H. D. Baker, *Trans. ASME*, vol. 80, no. 2, Feb. 1958, pp. 367–372.

Effect of Oxygen Recombination on One Dimensional Flow at High Mach Numbers, by Steve P. Heims, *NACA TN* 4144, Jan. 1958, 52 pp.

Thermal and Material Transfer in Turbulent Gas Streams; Local Transport from Spheres, by N. T. Hsu and B. H. Sage, *J. AIChE*, vol. 3, no. 3, Sept. 1957, pp. 405–410.

Influence of Electric Fields on the Heat

Transfer in Fluid Flows, *Zeitschrift für Naturforschung,* vol. 13a, 1958, pp. 99–105 (in German).

Mass and Heat Transfer in Concurrent Liquid-gas Flow, by S. Finzi, R. Renzoni, M. Silvestri and S. Villani, *Energia Nucleare,* vol. 4, no. 3, June 15, 1957, pp. 211–221 (in Italian).

Temperature Gradient and Thermal Stresses in Heat Generating Bodies, by F. A. Field, *Oak Ridge Natl. Lab., Tenn.,* CF-54-5-196, May 21, 1954. Decl. April 2, 1958, 12 pp.

The Supersonic Motion of an Aerofoil through a Temperature Front, by J. W. Craggs, *J. Fluid. Mech.,* vol. 3, part 2, Nov. 1957, pp. 176–184.

Composition and Thermodynamic Properties of Air in Chemical Equilibrium, by W. E. Moeckel and Kenneth C. Weston, *NACA TN* 4265, April 1958, 39 pp.

Heat Transfer to Surfaces in the Neighborhood of Protuberances in Hypersonic Flow, by Martin Bloom and Adrian Pallone, *Wright Air Dev. Center, TN* 57–95 (*ASTIA AD* 118138), Aug. 1957, 32 pp.

Shock Waves in Chemical Kinetics: The Decomposition of N_{205} at High Temperatures, by Garry Schott and Norman Davidson, *J. American Chem. Soc.,* vol. 80, April 20, 1958, pp. 1841–1853.

The Viscosity of Five Gases: A Reevaluation, by J. Kestin and H. E. Wang, *Trans. ASME,* vol. 80, Jan. 1958, pp. 11–17.

How to Find Airframe Material Emissivity, by G. V. Thompson, *Aviation Age,* vol. 29, May 1958, pp. 68–71.

The Evaporation of Sprays, by R. T. Jarman, *Brit. J. Appl. Phys.,* vol. 9, April 1958, pp. 153–154.

Hydrodynamics of a Reacting and Relaxing Fluid, by R. M. Mazo and J. R. Mayer, *J. Appl. Phys.,* vol. 29, April 1958, pp. 735–736.

Statistical Thermodynamics of Quantum Fluids, by R. M. Mazo and J. G. Kirkwood, *J. Chem. Phys.,* vol. 28, April 1958, pp. 644–646.

Heat Transfer and Safe Exposure Time for Man in Extreme Thermal Environment, by K. Buettner, *ASME, Paper* 57-SA-20, June 9–13, 1957, 7 pp.

Dynamic Response of Heat Exchangers Having Internal Heat Sources—I, by J. A. Clark, V. S. Arpaci and K. M. Treadwell, *ASME, Paper* 57-SA-14, June 9–13, 1957, 11 pp.

Some Shock Tube Experiments on the Chemical Kinetics of Air at High Temperatures, by Saul Feldman, *J. Fluid Mech.,* Pt. 3, Dec. 1957, pp. 225–242.

Correlations Relating Heat Transfer and Pressure Drop in Compact Heat Exchangers, by Hilbert Schenck Jr. ,*J. American Soc. Naval Engrs.,* vol. 69, Nov. 1957, pp. 767–770.

Experimental Investigation of Transpiration Cooling for a Turbulent Boundary Layer in Subsonic Flow Using Air as a Coolant, by W. E. Brunk, *NACA TN* 4091, Oct. 1957, 35 pp.

Mass Transfer through Compressible Turbulent Boundary Layers, by T. K. Sherwood and H. S. Bryant Jr., *Canadian J. Chem. Engrs.,* vol. 35, Aug. 1957, pp. 35–48.

Mass Transfer Cooling of a Laminar Boundary Layer by Injection of a Lightweight Foreign Gas, by E. R. G. Eckert, P. J. Schneider, A. A. Hayday and R. M. Larson, *Minn. Univ., Dept. Mech. Engng., Heat Transfer Lab., TN* 14, June 1957, 45 pp.

Evaporative Cooling at High Speeds, by G. Jarre, *Gt. Brit., Roy. Aircr. Estab., Lib. Transl.* 678, July 1957, 25 pp.

Mass Transfer Cooling at Mach Number 4.8, by B. M. Leadon, C. J. Scott and G. E. Anderson, *J. Aeron. Sci.,* vol. 25, Jan. 1958, pp. 67–68.

Mass-transfer Cooling of a 20° Porous Cone at M-5, by B. M. Leadon, C. J. Scott and G. E. Anderson, *Univ. Minn. Inst. Tech. Dept. Aero. Engr., RAL Res. Rep.* 143, July 1957, 48 pp. (*ASTIA AD* 136452; *AFOSR TN* 57–461).

On Harmonic Functions Satisfying Mixed Boundary Condition with Application to Flow Past Porous Wall, by L. C. Woods, *Appl. Sci. Res.,* Sec. A, vol. 6, 1957, pp. 635–642.

Unsteady-state Method of Measuring Thermal Diffusivity and Biot's Modulus for Alumina between 1500 and 1800 C, by A. E. Paladino, E. L. Swarts and W. B. Crandall, *J. Amer. Cer. Soc.,* vol. 40, Oct. 1957, pp. 340–349.

Combustion, Fuels and Propellants

The Structure of a Steady State One Dimensional Detonation Wave Supported by a Reversible Reaction, by B. Linder, C. F. Curtiss, J. O. Hirschfelder and C. Y. Cho, *Univ. Wisconsin, Naval Res. Lab., Tech. Rep.* WIS-AF-8, Nov. 1957, 27 pp. 5 figs.

Introduction to Theory of Detonations, I, by Joseph O. Hirschfelder and Charles F. Curtiss, *Univ. Wisconsin, Naval Res. Lab.,* CM-911a, Dec. 1957, 11 pp.

The Kinetics and Mechanism of Ethylene Oxide Decomposition at High Temperatures, by L. Crocco, I. Glassman and I. E. Smith, *Princeton Univ., Dept. Aeron. Engng., Rep.* 416 (*AFOSR-TN* 58–273; *ASTIA AD* 154174), April 1958, 13 pp., 6 figs.

Dilution of Liquid Oxygen When Nitrogen Is Used for Pressurization, by Thomas J. Walsh, R. R. Hibbard and Paul M. Ordin, *NACA Res. Mem.* E58A03a, April 1958, 17 pp.

Quarterly Periodic Status Report, *Mass. Inst. Tech., Hydrogen Peroxide Labs.,* Dec. 1957, 10 pp.

High Speed Digital Calculations of the Composition and Thermodynamic Properties of Propellant Gases by the Brinkley Method, by Tadeusz Leser, *Aberdeen Proving Ground, Ballistic Res. Labs., Rep.* 1023, Aug. 1957, 78 pp.

Infrared Method for Determining Toluene, O, M, and P Nitrotoluene, 2,4-and 2,6-DNT, and 2,4,6-TNT in Admixtures, by Walter E. Fredericks and Frank Pristera, *Picatinny Arsenal, Samuel Feltman Ammunition Labs., Tech. Rep.* 2485, March 1958, 10 pp.

Static Test Facilities, *Redstone Arsenal, Brochure* 3, Sep. 1957, 23 pp.

Instrumentation for Studies of the Exploding Wire Phenomenon, by W. G. Chace and E. H. Cullington, *Air Force Cambridge Res. Center, Geophysics Res. Directorate, Instrumentation for Geophysical Res.* 7 (*AFCRC-TR-57-235; ASTIA AD* 133842), Aug. 1957, 35 pp.

Model Study of Processes of Burning or Gasification of Solid Fuels, by V.A., Smirnov, *Akademiia Nauk SSSR, Izvestiia, Otdelenie Tekhnicheskikh Nauk,* no. 1, Jan. 1958, pp. 95–99 (in Russian).

Similarities in Explosions in Plastic Compressible Media, by E. E. Lovenkii, *Akademiia Nauk SSSR, Izvestiia, Otdelenie Tekhnicheskikh Nauk,* no. 1, Jan. 1958, pp. 120–122 (in Russian).

A Kinetic Study of the Thermodynamic Properties of the Acetyl Free Radican, by Jack G. Calvert and Jerry T. Cruver, *J. Amer. Chem. Soc.*, vol. 80, March 20, 1958, pp. 1313–1317.

Ballistic Piston for Investigating Gas Phase Reactions, by P. A. Longwell, H. H. Reamer, N. P. Wilburn and B. H. Sage, *Ind. & Engng. Chem.*, vol. 50, April 1958, pp. 603–610.

Combustion of Metals in Oxygen, by A. V. Grosse and J. B. Conway, *Ind. & Engng. Chem.*, vol. 50 April 1958, pp. 663–672.

Heat Transfer to a Gas-phase Chemical Reaction, by William Schotte, *Ind. & Engng. Chem.*, vol. 50, April 1958, pp. 683–690.

Correlation of Vapor-liquid Equilibrium Data, by J. W. Tierney, *Ind. & Engng. Chem.*, vol. 50, April 1958, pp. 707–710.

Kinetic Study of Cyanogen Combustion, by H. James, *Inst. Francais du Petrole, Rev. et Annales des Combustibles Liquides*, vol. 13, Jan. 1958, pp. 83–113, 78 ref. (in French).

Burning-rate Studies, VI, Effect of Chemical Composition on the Consumption-rate of Various Nitric Acid Systems, by A. Greenville Whittaker, *J. Phys. Chem.*, vol. 62, March 1958, pp. 267–271.

Molecular Structure and Properties of Hydrocarbons and Related Compounds, by John B. Greenshields and Frederick D. Rossini, *J. Phys. Chem.*, vol. 62, March 1958, pp. 271–280.

The Explosive Oxidation of Pentaborane, by Harry C. Baden, Walter H. Bauer and Stephen E. Wiberley, *J. Phys. Chem.*, vol. 62, March 1958, pp. 331–334.

Inhibition by Hydrogen Peroxide of the Second Explosion Limit of the Hydrogen-oxygen Reaction, by W. Forst and Paul A. Giguere, *J. Phys. Chem.*, vol. 62, March 1958, pp. 340–343.

I. An Apparatus for Use with Condensed Phases at 10,000°; II. Some Thermodynamic and Rate Considerations at Very High Temperatures, by Tracy Hall, Billings Brown, Bruce Nelson and Lane A. Compton, *J. Phys. Chem.*, vol. 62, March 1958, pp. 346–351.

Stability of Nitric Oxide over a Long Time Interval, by Charles S. Howard and Farrington Daniels, *J. Phys. Chem.*, vol. 62, March 1958, pp. 360–361.

Combustion in the Laminar Boundary Layer of Chemically Active Sublimating Surfaces, by M. R. Denison and D. A. Dooley, *J. Aeron. Sci.*, vol. 25, April 1958 pp. 271–272.

Toxicity of High-energy Fuels Poses Hazards for Handlers, by William H. Schecter, *Missiles and Rockets*, vol. 3, April 1958, pp. 85–86.

Reactions of the Ethyl Radical, I. Metathesis with Unsaturated Hydrocarbons, by D. G. L. James and E. W. R. Steacie, *Proc. Roy. Soc.*, vol. 244A, March 25, 1958, pp. 289–296.

Reactions of the Ethyl Radical, II. Addition to Unsaturated Hydrocarbons, by D. G. L. James and E. W. R. Steacie, *Proc. Roy. Soc.*, vol. 244A. March 25, 1958, pp. 297–311.

Gas-phase Oxidation of Propylene, by J. D. Mullen and G. Skirrow, *Proc. Roy. Soc.*, vol. 244A, March 25, 1958, pp. 331–344.

Gas-phase Oxidation of Hexene-1, by G. Skirrow, *Proc. Roy. Soc.*, vol. 244A, March 25, 1958, pp. 345–354.

Microwave Spectrum of Hydrazine, by Takeshi Kojima, Hiromasa Hirakawa and Takeshi Oka, *J. Phys. Soc. of Japan*, vol. 13, March 1958, p. 321.

Exploratory Study Relating Viscosity and Propellant Stability, by Charles Lenchitz and Marvin Goldstein, *Picatinny Arsenal, Samuel Feltman Ammunition Lab., Tech. Rep.* 2458, Feb. 1958, 25 pp.

Two Gages for the ASROC Cruciform Grain, by Robert G. Field, Robert H. Martin and William C. Shaw, *NAVORD Rep.* 5833 (*NOTS* 1927), Feb. 1958, 9 pp.

The Solubility of Aluminum Nitrate in Red Fuming Nitric Acid, by R. F. Muraca, S. P. Vango and L. L. Taylor, *Calif. Inst. Tech., Jet. Propulsion Lab., Progr. Rep.* 20–338, Jan. 1958, 10 pp.

Tables and Charts for Thermodynamic Calculations Involving Air and Fuels Containing Boron, Carbon, Hydrogen and Oxygen, by Eldon W. Hall and Richard J. Weber, *NACA Res. Mem.* E56B27, July 1956, 82 pp. (Declassified from Confidential by authority of NACA Res. Abstr. 125, p. 23, 3/18/58.)

Thermal Decomposition of Ethylpentaborane in Gas Phase, by Glen E. McDonald, *NACA Res. Mem.* E56D26, July 1956, 20 pp. (Declassified from Confidential by authority of NACA Res. Abstr. 125, p. 23, 3/18/58.)

Theoretical Performance of JP-4 Fuel with a 70-30 Mixture of Fluorine and Oxygen as a Rocket Propellant, II—Equilibrium Composition, by Sanford Gordon and Vearl N. Huff, *NACA Res. Mem.* E56F04, Oct. 1956, 49 pp. (Declassified from Confidential by authority of NACA Res. Abstr. 125, p. 23, 3/18/58.)

The Rate of Decomposition of Liquid Pentaborane from 85° to 202° C, by Glen E. McDonald, *NACA Res. Mem.* E55HOl, Oct. 1955, 22 pp. (Declassified from Confidential by authority of NACA Res. Abstr. 125, p. 22, 3/18/58.)

Theoretical Performance of JP-4 Fuel with a 70-percent-fluorine–30-percent-oxygen Mixture as a Rocket Propellant, I—Frozen Composition, by Sanford Gordon and Vearl N. Huff, *NACA Res. Mem.* E56A13a, April 1956, 38 pp. (Declassified from Confidential by authority of NACA Res. Abstr. 125, p. 22, 3/18/58.)

A Study of Fuel-nitric Acid Reactivity, by Charles E. Feiler and Louis Baker Jr., *NACA Res. Mem.* E56A19, April 1956, 48 pp. (Declassified from Confidential by authority of *NACA Res. Abstr.* 125, p. 22, 3/18/58.)

Temperature Determination on Flames by X-Ray Absorption Using a Radioactive Source, by George J. Mullaney, *Rev. Sci. Instr.*, vol. 29, Feb. 1958, pp. 87–91.

Apparatus for Precision Flash Radiography of Shock and Detonation Waves in Gases, by Herbert T. Knight and Douglas Venable, *Rev. Sci. Instr.*, vol. 29, Feb. 1958, pp. 92–98.

Prandtl-Meyer Expansion of Chemically Reacting Gases in Local Chemical and Thermodynamic Equilibrium, by Steve P. Heims, *NACA TN* 4230, March 1958, 17 pp.

Motion Study of the Combustion of Cyanogen, by H. James, *Inst. Francaise du Petrole, Rev. et Annales des Combustibles Liquides*, vol. 12, Dec. 1957, pp. 1241–1293 (in French).

Determination of Oxygen Atoms in Lean, Flat, Premixed Flames by Reaction with Nitrous Oxide, by C. P. Fenimore and G. W. Jones, *J. Phys. Chem.*, vol. 62, Feb. 1958, pp. 178–182.

How Good are Free Radicals? by Erik Bergaust, *Missiles and Rockets*, vol. 3, March 1958, pp. 78–80.

Combustion—an Aeronautical Science,

by H. W. Emmons, *Inst. of Aeron. Sci., SMF Fund Paper* FF-19, 1958, 36 pp.

Longitudinal Combustion Instability in a Duct with Oblique Flame Front, by Marcel Vinokur, *Lockheed Aircr. Corp., Missiles Systems Div., Rep.* LMSD-2346, March 1958, 118 pp.

Thermodynamic Properties and Calculated Rocket Performance of Hydrogen to 20,000°K, by David Altman, *Calif. Inst. Tech., Jet Propulsion Lab., Rep.* 20-106, Sept. 1956, 28 pp.

High Energy Fuels—Smoke Removal by D. W. Dembrow, *Johns Hopkins Univ. Appl. Phys. Lab.*, CF 2717, Feb. 1958, 22 pp.

Injection and Combustion of Liquid Fuels, *Battelle Memorial Inst., Wright Air Dev. Center, Tech. Rep.* 56-344 (*ASTIA AD* 118142), March 1957. Includes bibliographies.

Chemical "Zip" for the Birdmen, by Roy McLeavy, *Air Power*, vol. 5, Spring 1958, pp. 207–212.

"Aerodynamic" Combustion Ups Afterburner Performance, by Jean Bertin and Benjamin Salmon, *Aviation Age*, vol. 29, May 1958, pp. 46, 48, 50, 53.

Guidance Systems and Components

Guidance and Control, by L. H. Bedford, *J. Roy. Aeron. Soc.*, vol. 62, May 1958, pp. 348–354.

Titan Guidance Reliable, Accurate, by Philip J. Klass, *Aviation Week*, vol. 68, May 12, 1958, pp. 92–93, 95, 97, 99, 101, 103.

Application of Statistical Theory to Beam-rider Guidance in the Presence of Noise, II: Modified Wiener Filter Theory, by Elwood C. Stewart, *NACA TN* 4278, June 1958, 48 pp. (Supersedes RM A55E11a.)

Guidance and Control Problems in the Air Force Ballistic Missile Program, Part II, by J. C. Fletcher, *Aero-Space Engng.* (formerly *Aeron. Engng. Rev.*), vol. 17, June 1958, pp. 65–71.

Scanning the Skies: A Roundup of Tracking Systems, by Norman L. Baker, *Missiles and Rockets*, vol. 3, June 1958, pp. 76–80.

Infra-red Guidance, by Roger Esty, *Missiles and Rockets*, vol. 3, June 1958, pp. 107–108.

Hypersonic Aerodynamic Factors in Performance, Guidance and Control, by William H. Dorrance, *Aero-Space Engng.* (formerly *Aeron. Engng. Rev.*), vol. 17, May 1958, pp. 30–33, 43.

Guidance and Control Problems in the Air Force Ballistic Missiles Program, Part I, by J. C. Fletcher, *Aero-Space Engng.* (formerly *Aeron. Engng. Rev.*), vol. 17, May 1958, pp. 50–54.

Cross Coupling in Inertial Navigation Systems, by Robert E. Wilson and John B. Lewis, *Aero-Space Engng.* (formerly *Aeron. Engng. Rev.*), vol. 17, May 1958, pp. 60–65, 80.

Infrared Application to Guidance and Control, by R. W. Powell and W. M. Kauffman, *Aero-Space Engng.* (formerly *Aeron. Engng. Rev.*), vol. 17, May 1958, pp. 66–71.

Range Finders Using Projected Images, *J. Res., Nat. Bur. Standards*, vol. 60, April 1958, pp. 327–334.

Systematic Examination of Guidance Methods, by Ferdinand Müller, *Raketentechnik und Raumfahrtforschung*, vol. 2, no. 2, April 1958, pp. 38–44 (in German).

Modern Building Blocks for the Control of Remotely Guided Flight Vehicle, by H. Pöschl, *Raketentenchik und Raumfahrtforschung*, vol. 2, no. 2, April 1958, pp. 55–57 (in German).

Space Flight

The Structure of Our Space, by H. Hlavaty, *Aeron. Engng. Rev.*, vol. 17, April 1958, pp. 25–29.

Interrelations of Space Medicine with Other Fields of Science, by Hubertus Strughold, *Aeron. Engng. Rev.*, vol. 17, April 1958, pp. 30–32, 37.

Meteoric Abrasion Studies Proposed for Vanguard, by Martin J. Swetnick, *J. Astronautics*, vol. 4, no. 4, Winter 1957, pp. 69–71.

Plants as a Means of Balancing a Closed Ecological System, by James G. Gaume, *J. Astronautics*, vol. 4, no. 4, Winter 1957, pp. 72–75.

Abstracts and Reviews of the Astronautical Sciences, *J. Astronautics*, vol. 4, no. 4, Winter 1957, pp. 81–86.

Man on the Moon? by Frederick I. Ordway III and Ronald C. Wakeford, *Missiles and Rockets*, vol. 3, April 1958, pp. 69–74.

Problems in Space Navigation, by Louis G. Walters, *Missiles and Rockets*, vol. 3, April 1958, pp. 76–79.

Ground Support: A Must for Space, by Robert J. Laws, *Missiles and Rockets*, vol. 3, April 1958, p. 80–81.

Internal Dangers Threat in Space, by Alfred J. Zachringer, *Missiles and Rockets*, vol. 3, April 1958, pp. 82.

How to Travel Outside Our Solar System, by Franco Fiorio, *Missiles and Rockets*, vol. 3, April 1958, pp. 89–90, 93.

How to Keep Space Crews Content, by Donald N. Michael, *Missiles and Rockets*, vol. 3, April 1958, pp. 110, 112–114.

Interrelations of Space Medicine with Other Fields of Science, by Hubertus Strughold, *Inst. Aeron. Sci., Preprint* 819, Jan. 1958, 12 pp.

Towards Space Flight, by A. R. Weyl, *Aeronautics*, vol. 38, March 1958, pp. 32–35.

New Zealand Visual Observations of the Rocket Accompanying the Russian Artificial Satellite, by R. A. Anderson and C. S. L. Keay, *Astronautica Acta*, vol. 3, no. 4, 1957, pp. 227–230.

On Determining the Orientation of a Cylindrical Artificial Earth-Satellite, by R. J. Davis, R. C. Wells and F. L. Whipple, *Astronautica Acta*, vol. 33, no. 4, 1957, pp. 231–236.

Development of Manned Space Flight, *Aviation Age*, vol. 28, March 1958, pp. 14–20.

Blueprint for Space Research, by Homer E. Newell Jr. and Kurt R. Stehling, *Aviation Age*, vol. 28, March 1958, pp. 28–29, 106.

Getting Man into Space, by W. A. Orr and J. W. Tucker, *Aviation Age*, vol. 28, March 1958, pp. 30–31, 102.

Balloon-Launched Vehicle May Be First on the Moon, by Kurt R. Stehling, *Aviation Age*, vol. 28, March 1958, pp. 32–35.

Orbits, by Samuel Herrick and Robert M. L. Baker, *Aviation Age*, vol. 28, March 1958, pp. 70–77.

Detection of Sputniks I and II by CW

Reflection, by John D. Kraus, *Proc., Inst. Radio Engrs.*, vol. 46, March 1958, pp. 611–612.

The Last Days of Sputnik I, by John D. Kraus, *Proc., Inst. Radio Engrs.*, vol. 46, March 1958, pp. 612–614.

Sputnik Not So Secret, by Dr. Victor P. Petrov, *Missiles and Rockets*, vol. 3, March 1958, p. 82.

Martian Atmosphere Restudied, *Tech. News Bull.* (Nat. Bur. Standards), vol. 42, March 1958, pp. 48–52.

Moon Looks Promising as Manned Space Station, by Kurt R. Stehling, *Aviation Age*, vol. 29, May 1958, pp. 22–23, 180.

An Approximation Method for the Calculation of Rocket Orbits, by H. H. Koelle, *Raketentechnik und Raumfahrtforschung*, vol. 2, no. 1, 1958, pp. 8–12 (in German).

Satellite Carrying Rockets, by R. Enge and U. T. Boedewadt, *Raketentechnik und Raumfahrtforschung*, vol. 2, no. 1, 1958, pp. 23–25 (in German).

The Test Satellites of the U.S.A. and U.S.S.R., by Dietrich E. Kölle, *Raketentechnik und Raumfahrtforschung*, vol. 2, no. 1, 1958, pp. 25–28 (in German).

U. S. Satellites (Failure and Success), Artificial Meteors and Project Farside, by Frank Pollard, *Spaceflight*, vol. 1, no. 7, April 1958, pp. 231–237.

Photographic Observations of Artificial Earth Satellites, by M. J. Smyth, *Spaceflight*, vol. 1, no. 7, April 1958, pp. 247–251.

Astrophysics, Aerophysics

Atmospheric Turbulence Environment with Special Reference to Continuous Turbulence, by Harry Press, *NATO, AGARD, Rep.* 115, April-May 1957, 40 pp.

Charting Physical Properties of the Atmosphere, *Missiles and Rockets*, vol. 3, April 1958, pp. 139–142.

The Role of Manned Balloons in the Exploration of Space, by Malcome D. Ross and M. Lee Lewis, *Inst. Aeron. Sci., Preprint* 834, Jan. 1958, 25 pp., 6 tabs., 6 figs.

The 3 Manned Stratosphere Balloon Ascents of 1957, by Otto C. Winzen, *Inst. Aeron. Sci., Preprint* 833, Jan. 1958, 28 pp., 3 tabs., 33 figs.

Cosmology, by Winston H. Bostick, *Inst. Aeron. Sci., Preprint* 830, Jan. 1958, 10 pp., 9 figs.

Project Far Side Launchings, by John L. Cramer, *Inst. Aeron. Sci., Preprint* 824, Jan. 1958, 10 pp., 9 figs.

The Plastic Balloon as a Geophysical Platform, by Richard H. Braun, *Inst. Aeron. Sci., Preprint* 823, Jan. 1958, 10 pp.

Origin and Dynamics of Cosmic Rays, by E. N. Parker, *Phys. Rev.*, vol. 109, Feb. 15, 1958, pp. 1328–1343.

Primary Cosmic-ray Proton and Alpha Flux Near the Geomagnetic Equator, by Frank B. McDonald, *Phys. Rev.*, vol. 109, Feb. 15, 1958, pp. 1367–1375.

Nuclear Propulsion

Design Study: 60 MW Closed Cycle Gas Turbine Nuclear Power Plant, *American Turbine Corp., Rep.* ATC 54-12, Dec. 1954, 38 pp.

U235 Thermal Fission Product Activities and Emission Powers Plotted Against Irradiation and Decay Times, by E. A. C. Crouch, *Gt. Brit., Atomic Energy Res. Estab.*, C/M 324, 1957, 2 pp., 6 figs.

The Thermal-neutron Fission Cross Section of Pu^{240}, by C. B. Bigham, *Canadian J. Phys.*, vol. 36, April 1958, pp. 503–507.

Chemical Activity of Cooling Agents in Reactors and the Detection of Leaks of Fission Products, by J. Labeyrie, *France, Commissariat a l'Energie Atomique, Bull. d'Informations Scientifiques et Techniques*, no. 14, Feb. 1958, pp. 2–13 (in French).

Some Experiments with Electrostatic Accelerators of Low Energy, by Noel J. Felici, *France, Commissariat a l'Energie Atomique, Bull. d'Informations Scientifiques et Techniques*, no. 14, Feb. 1958, pp. 23–30 (in French).

Neutron Scattering Cross Section of U^{235}, by H. L. Foote Jr., *Phys. Rev.*, vol. 109, March 1, 1958, pp. 1641–1644.

Neutron Scattering Cross Section of U^{233}, by Sophie Oleksa, *Phys. Rev.*, vol. 109, March 1, 1958, pp. 1645.

Yield and Angular Distribution of Fast Photoneutrons from Deuterium and Carbon, by P. S. Baranov, V. I. Gol'danskii and V. S. Roganov, *Phys. Rev.*, vol. 109, March 1, 1958, pp. 1801–1805.

Controlled Thermonuclear Reactions, *Atomic Energy Comm., TID-7536* (Part 1), Sept. 1957, 41 pp.

Progress in Peaceful Uses of Atomic Energy, *Atomic Energy Comm.*, July-Dec. 1957, 463 pp.

The Townsend Discharge in a Coaxial Diode with Axial Magnetic Field, by P. A. Redhead, *Canadian J. Phys.*, vol. 36, March 1958, pp. 255–270.

Correlations in the Charge Density of a Classical Plasma, by S. F. Edwards, *Phil. Mag.*, vol. 3, March 1958, pp. 302–306.

Excitation of Plasma Oscillations and Growing Plasma Waves, by G. D. Boyd, L. M. Field and R. W. Gould, *Phys. Rev.*, vol. 109, Feb. 15, 1958, pp. 1393–1394.

A Variational Calculation of the Equilibrium Properties of a Classical Plasma, by S. F. Edwards, *Phil. Mag.*, vol. 3, Feb. 1958, pp. 119–124.

Fuels Figure in our Future, by Rear Admiral H. G. Rickover, *Ind. Labs.*, vol. 9, March 1958, pp. 22–26.

The Application of Nuclear Power to Logistic Aircraft Systems, by Robert W. Middlewood and Robert B. Ormsby Jr., *SAE Preprint* 206, Oct. 1957, 11 pp., 26 figs.

Atomic Reactors (a Symposium), *Inst. Aeron. Sci., SMF Fund Paper* FF-17, March 1957, 40 pp.

Some Engineering Considerations on the Present Trends of the Aircraft Propulsion with Nuclear Propellants, by M. Medici, *L'Aerotecnica*, vol. 37, no. 5, Oct. 1957, pp. 273–277 (in Italian).

Neutron Production at High Energies, by Walter E. Crandall and George P. Millburn, *J. Appl. Phys.*, vol. 29, April 1958, pp. 698–704.

A New Probe Method for Measuring Ionized Gases, by Takayoshi Okuda and Kenzo Yamamoto, *J. Phys. Soc. Japan*, vol. 13, April 1958, pp. 411–418.

On the Problem of the Applicability of Thermonuclear Reactions to Rockets, Part III, by H. J. Kaeppeler, *Raketentechnik und Raumfahrtforschung*, vol. 2, no. 1, 1958, pp. 13–19 (in German).

The Time and Temperature Dependence of Thermal Stresses in Cylindrical Reactor Fuel Elements, by K. R. Merckx, *Trans. ASME*, vol. 80, no. 2, Feb. 1958, pp. 505–509.

Index to Advertisers